The Dissertation Committee for Yirui Liang Certifies that this is the approved version of the following dissertation:

Novel Methods of Characterizing Phthalate Emissions and Their Fate and Transport in Residential Indoor Environments

Committee:

Ying Xu, Supervisor

Atila Novoselac

Richard Corsi

Kerry Kinney

John Little

Yinping Zhang

Novel Methods of Characterizing Phthalate Emissions and Their Fate and Transport in Residential Indoor Environments

by

Yirui Liang, B.E.; M.S.E.

Dissertation

Presented to the Faculty of the Graduate School of

The University of Texas at Austin

in Partial Fulfillment

of the Requirements

for the Degree of

Doctor of Philosophy

The University of Texas at Austin

December 2014

Dedication

To my parents, LIANG Yuanen and XIANG Runlian, for their constant encouragement, unconditional support, and selfless affection.

Acknowledgements

I would like to acknowledge, first and foremost, my advisor, Dr. Ying Xu, for taking me on as her first student in 2009 and supporting me throughout my graduate studies. Dr. Xu has guided me with her scientific knowledge and countless insightful discussions during these past five years. I am truly grateful to have worked with her since 2009 and hope that this rewarding partnership can continue long into the future.

Along with Dr. Xu, I owe a debt of gratitude to Dr. Richard Corsi, Dr. Atila Novoselac, Dr. Kerry Kinney, Dr. John Little and Dr. Yinping Zhang for serving on my committee. They have provided technical support and valuable suggestions during the completion of this dissertation.

My graduate career would not be as smooth as it was without Ms. Dori Eubank, who is not only a great coordinator of our research group but also an amicable person to go along with.

It was a great pleasure working with Brandon Boor, Jordan Clark, Shichao Liu, Liangchung Lo, and Chenyang Bi at UT over the several years. Their companionship has made my life in Austin, TX colorful and enjoyable.

I would like to thank my major funding sources for supporting me continuously and making this research possible: the National Science Foundation (NSF) and the American Society of Heating, Refrigerating and Air-Conditioning Engineers (ASHRAE).

Finally, I thank my parents for everything they did for me. They respected and understood my choice of leaving them to study abroad back in 2009. I owe my deepest gratitude to them for supporting me in every possible way.

Novel Methods of Characterizing Phthalate Emissions and Their Fate and Transport in Residential Indoor Environments

Yirui Liang, Ph.D.

The University of Texas at Austin, 2014

Supervisor: Ying Xu

Phthalates have been used pervasively as plasticizers in consumer products and building materials. These semi-volatile organic compounds (SVOCs) are ubiquitous in indoor environments, redistributing from their original sources to indoor air, and subsequently to all interior surfaces. Because they partition strongly to surfaces, most phthalates persist for years after the source is removed. Biomonitoring data based on blood and urine testing provide direct evidence of the universal and significant human exposure to phthalates, which may result in serious adverse health effects. However, effective strategies to limit exposures to phthalates remain hamstrung by our poor understanding of their sources and fate and transport in indoor environments. The goal of this research is to explicitly elucidate the fundamental mechanisms governing emission, transport, and human exposure associated with phthalates in indoor environments. The specific research objectives are to 1) develop a novel, rapid, small-chamber method to determine the key parameters that control phthalate emissions and characterize the emissions; 2) investigate the influences of temperature, air flow rate, and surface sorption on phthalate emissions via a series of controlled tests in small and large chambers; 3) develop and validate a new indoor fate and transport model for phthalates with consideration of particle dynamics and its effects on emission and sorption. This

research, which connects emission measurements to chemical transport and exposure assessment, will explicitly elucidate the fundamental mechanisms governing emission, transport, and human exposure associated with phthalates in indoor environments.

Table of Contents

List of Tables

List of Figures

Chapter 1: Introduction

Phthalates have been widely used and produced as plasticizers to enhance the flexibility of polyvinylchloride (PVC) products. These chemicals are classified as semi-volatile organic compounds (SVOCs) because of their low volatility. Phthalates can be found in a wide range of building materials and consumer products such as vinyl flooring, carpet padding, wall coverings, floor tiles, furniture, and electronics (Bornehag et al., 2005), where they may be present at percent to tens-of-percentage levels (Weschler and Nazaroff, 2008). Because phthalate additives are not chemically bound to the polymer matrix, slow emission usually occurs from the products to air or other media (Xu et al. 2012). As a result, phthalates are ubiquitous and among the most abundant SVOCs in indoor environments (Bornehag et al., 2005; Clausen et al., 2012; Bornehag et al., 2004; Rudel and Perovich, 2009).

Exposure to phthalates and their metabolites may result in a number of adverse health effects (Jaakkola and Knight, 2008). Detailed information on the serious health effects can be found in recent studies (Albert and Jegou, 2014; Alcock et al., 2011; Birnbaum et al., 2003; Darnerud, 2003; Engel and Wolff, 2013; Heudorf et al., 2007; Huang et al., 2012; Jaakkola and Knight, 2008; Jurewicz et al., 2013; Kay et al., 2013; Latini et al., 2006; Legler and Brouwer, 2003; Matsumoto et al., 2008; McKee et al., 2004; Meerts et al., 2000; North et al., 2014; Ritter and Arbucklet, 2007; Vonderheide et al., 2008). Collectively, these studies show that exposure to phthalates can cause irreversible changes in the development of the reproductive tract, especially in males. Effects such as increases in prenatal mortality, reduced growth and birth weight, and skeletal, visceral and external malformations, are also associated with exposure to phthalates.

The global production rate of phthalate plasticizers has increased from 2.5 to 6 million tons/year within a decade (Rudel and Perovich, 2009; Cadogan et al., 1996). However, following the restrictions on using certain phthalates in toys and child care products (CPSC, 2008), phthalates used in PVC products are changing rapidly, with a trend toward using phthalates of higher molecular weight and lower volatility (Schossler et al., 2011; Weschler, 2009). The use of alternative plasticizers, such as diisononyl cyclohexane-1,2-dicarboxylate (DINCH) and di(2-ethylhexyl) adipate (DEHA), has also occurred very recently. Because these phthalate alternatives share chemical structures and properties similar to phthalates, similar emissions and environmental fate and transport may be expected (Schossler et al., 2011).

Understanding emission mechanisms of phthalates and the ability to predict their emission rates from various sources are a prerequisite for characterizing their fate and transport in indoor environments. Previous studies (Xu et al., 2012; Cluasen et al., 2004, 2010, and 2012; Schossler et al., 2011; Afshari et al., 2004) revealed the substantial difficulties associated with chamber tests for phthalates resulting from the low gas-phase concentration, strong sorption onto surfaces, and ubiquitous contamination in laboratory facilities. Based on the results of early chamber studies (Clausen et al., 2004), Xu and Little (2006) developed a fundamental mass-transfer model to predict SVOC emissions from polymeric materials. They showed that emissions of these compounds that have very low volatility are subject to "external" control (partitioning from the material into the gas phase, the gas-phase mass-transfer coefficient, and strong sorption onto interior surfaces, including airborne particles).

No methods exist to measure or estimate y_0, the gas-phase concentration of DEHP in equilibrium with the material phase, for phthalates in PVC products. Using DEHP steady-state concentrations in the Field and Laboratory Emission Cell (FLEC) as

approximations of y_0, Clausen et al. (2012) found that the value of y_0 for a vinyl flooring sample is close to the vapor pressure (V_p) of pure DEHP at five temperatures. However, the results showed that there is about three times difference at 23°C between y_0 and estimated V_p values (y_0: 0.9 μg/m^3 versus V_p: 2.4 μg/m^3). The relationship between y_0 and V_p for other phthalates is still unclear. Little et al. (2012) suggested that y_0 cannot be well approximated by V_p in all cases. The material-phase concentration (C_0) of phthalate additives in different products can vary substantially; as a result, development of appropriate methods to determine y_0 for phthalates in PVC products has become a high priority. In addition, the availability of reliable measurements of V_p is limited for phthalates and for other SVOCs (Schossler et al., 2011; Letcher and Naicker, 2004). Therefore, to investigate the relationship between y_0 and V_p, more reliable data of phthalates V_p are needed. Furthermore, an accurate value of V_p at room temperature will help to understand the distribution of phthalates in indoor environments, especially among the gas phase, airborne particles, interior surfaces, and settled dust (Weschler and Nazaroff, 2008; Xu et al., 2009; Weschler et al., 2008; Weschler and Nazaroff, 2010).

Temperature may have a strong influence on the emissions of phthalates in indoor environments, because y_0 is related to vapor pressure, which depends strongly on temperature. Despite its importance for exposure and risk assessment, the influence of temperature on the emission and transport of indoor phthalates have yet to be studied comprehensively. Clausen et al. (2012) measured emissions of DEHP from PVC flooring in the Field and Laboratory Emission Cell (FLEC) at five different temperatures between 23 and 61 ºC. They observed that the steady-state concentrations of DEHP increased considerably as temperature increased, while adsorption to the chamber walls decreased greatly as temperature increases. They also found that y_0, the gas-phase DEHP concentration in equilibrium with vinyl flooring surface, is close to the vapor pressure

(V_p) of pure DEHP liquid. However, because temperature dependence is strongly related to the type of phthalates (Fujii et al., 2003), y_0 might not be well approximated by V_p for other phthalates. To date, no systematic investigations have been conducted to characterize the effect of temperature on the mechanisms governing emissions of major phthalates and their alternatives.

In actual indoor environments, there are various interior surfaces such as furniture, the ceiling, and walls, many of which are not as impenetrable as stainless steel. Therefore, the simple partition relationship often used for surface adsorption may not be good enough to elucidate the mechanisms governing the process of surface absorption. Liu et al. (2014c) developed an experimental method to estimate the solid-phase diffusion coefficient (D_m) and the material/air partition coefficient (K_{ma}) of polychlorinated biphenyl (PCB) congeners for different sink materials such as glass and concrete. The results can be used to predict the absorption of SVOCs in the materials. However, the researchers also acknowledged that D_m and K_{ma} values obtained were rough estimates, because a single data set was used to fit the two parameters simultaneously, which may result in erroneous values. In addition, because SVOCs sorbed strongly to interior surfaces, surface sorption may also have a great impact on the fate and transport of indoor phthalates. To date, no systematic investigations have been conducted to characterize the mechanisms governing absorption of phthalates to interior penetrable surfaces and the influence of surface sorption on emissions of phthalates from building materials.

The effect of increased ventilation on reducing indoor exposure to volatile organic compounds (VOCs) and formaldehyde has been observed in field studies (Hodgson et al., 2004; Zuraimi et al., 2006), but it is difficult to make the same conclusion for SVOCs because they behave quite differently as VOCs whose emissions are generally subject to "internal" control (diffusion within the source material) (Xu and Zhang, 2003). Liu et al.

(2014a) developed a mass balance model incorporating the impacts of ventilation on particle mass concentration, mass transfer, and particle mediation, and found that ventilation affects exposure to SVOCs; but the researchers stated that more experimental studies were needed to further validate the theoretical model.

The emission rate measured in a test chamber may be quite different from the emission rate from the same material in a real indoor environment, because the emissions of SVOCs such as phthalates are controlled by external gas-phase resistance and exterior sinks (Xu and Little, 2006). Environmental conditions (e.g., temperature and air flow rate) may have important impacts on the fate and transport of indoor phthalates. Temperature increases may significantly increase phthalate emission from sources and desorption from interior sink surfaces due to the increase in chemical vapor pressure. In addition, the emission rate of SVOCs may increase greatly with an increase of air flow rate due to the enhanced mass transfer above the surface of the emission source. As a result, recent small-chamber studies have found that, although the increased flow rate of fresh air reduced the residence time of air and introduced more dilution, the enhanced emission compensated for the decrease in the gas phase, and thus the gas-phase concentration of SVOCs did not drop substantially with increasing air-flow rates (Clausen et al., 2010). However, current studies were mostly carried out in small-scale experimental chambers, and there are no comprehensive and systematic investigations on the influence of environmental conditions on the fate and transport of indoor phthalates that have been conducted in large-scale chambers, which are more representative of indoor environments than small chambers.

Particles have a great influence on the fate and transport of indoor phthalates. Because gas-particle sorption and desorption kinetics are sufficiently rapid (Benning et al., 2012; Odum et al., 1994; Weschler et al., 2008), airborne particles become important

carriers that accelerate the transport of phthalates from their original source to other indoor surfaces through deposition, resuspension, and advection of air. Although previous modeling studies (Liu et al., 2010, 2013 and 2014b; Shi and Zhao, 2012) acknowledged the importance of gas-particle partitioning on the fate of indoor SVOCs, the actual role of particles in the transport of indoor SVOCs has not been fully characterized. Particle deposition and resuspension may result in a redistribution of SVOCs among the gas, particle, and surface phases near the source and sink surfaces, and thereby significantly influence the rate of SVOC emission from and sorption to those surfaces. Currently no model exists for accurately characterizing the effect of particle dynamics on SVOC emission and sorption as well as the subsequent impacts on the fate and transport of indoor SVOCs. Furthermore, none of the fate and transport model developed for SVOCs has been strictly validated, though most of them have compared their predicted airborne concentrations with field campaign data. In addition, phthalates (including both gas- and particle-phase phthalates) can accumulate in porous materials such as carpet and subsequently re-emitted into indoor environments. These materials can act as buffers for indoor phthalates, modulating and prolonging their presence in the environment (Zhang et al., 2009). Therefore, to accurately characterize the fate and transport of phthalates in indoor environments, it is necessary to include those porous materials.

To fill the knowledge gap, there is a need to explicitly elucidate the fundamental mechanisms governing emission, transport, and human exposure associated with phthalates in indoor environments. The work in this dissertation is grouped to fulfill three objectives:

1. Develop a novel, rapid, small-chamber method to determine the key parameters that control phthalate emissions and characterize the emissions.

2. Investigate the influences of temperature, air flow rate, and surface sorption on phthalate emissions via a series of controlled tests in small and large chambers.
3. Develop and validate a new indoor fate and transport model for indoor phthalates with consideration of particle dynamics and its effects on emission and sorption.

The dissertation is organized in two major sections: (1) the Summary of Methods and Research Findings (Chapter 3), and (2) Appendices A-E, which include five full-length manuscripts corresponding to the five investigations. The five paper topics are as follows:

Paper 1 Improved Method for Measuring and Characterizing Phthalate Emissions from Building Materials and Its Application to Exposure Assessment (Objective 1; Appendix A).

Paper 2 Emission of Phthalates and Phthalate Alternatives from Vinyl Flooring and Crib Mattress Covers: The Influence of Temperature (Objective 2; Appendix B).

Paper 3 The Influence of Surface Sorption and Air Flow Rate on Phthalate Emissions from Vinyl Flooring: Measurement and Modeling (Objective 2; Appendix C).

Paper 4 Large-Scale Chamber Investigation and Simulation of Phthalate Emissions from Vinyl Flooring (Objective 2; Appendix D).

Paper 5 Indoor Residential Fate Model of Phthalate Plasticizers (Objective 3; Appendix E).

The research represents the first attempt to explicitly elucidate the fundamental mechanisms governing emission, transport, and human exposure associated with phthalates in indoor environments. It developed a rapid small-chamber method for measuring key parameters that control phthalate emissions. The innovative approach can

certainly be generalizable a wide range of SVOC additives that are most harmful to human health and is urgently needed for rapid screening of products for SVOCs. The results of this study will be of value to architects and engineers who wish to specify low-emitting materials for use in green buildings, and allow the use of validated models for developing standards of product environmental performance or green labels.

Chapter 2: Literature Review

2.1 BACKGROUND

Many building materials and consumer products used in indoor environments emit harmful contaminants (Weschler, 2009). Emissions from these sources produce indoor concentrations that are substantially higher than those found outdoors (Rudel and Perovich, 2009). Since the 1950s, levels of some indoor pollutants (formaldehyde, aromatic and chlorinated solvents, chlorinated pesticides, and polychlorinated biphenyls [PCBs]) have increased and then decreased (Weschler, 2009). In contrast, levels of phthalates have increased and remain high (Rudel and Perovich, 2009; Weschler, 2009). Phthalates have been extensively used as plasticizers to enhance the flexibility of polymeric products. Members of this chemical family are classified as SVOCs due to their low vapor pressures at room temperature. Phthalates are found in a wide range of building materials and consumer products such as vinyl flooring, carpet padding, wall coverings, floor tiles, furniture, and electronics (Bornehag et al., 2005), where they may be present at percent to tens-of-percentage levels (Weschler and Nazaroff, 2008). Because phthalate additives are not chemically bound to the polymer matrix, slow emission from the products to air or other media usually occurs (Xu et al., 2012). As a result, phthalates are ubiquitous and among the most abundant SVOCs in indoor environments (Bornehag et al., 2005; Clausen et al., 2012; Bornehag et al., 2004; Rudel and Perovich, 2009).

There are a number of adverse health effects caused by exposure to phthalate esters and their metabolites (Jaakkola and Knight, 2008). The serious adverse effects associated with phthalates have been detailed in several recent reviews (Albert and Jegou, 2014; Alcock et al., 2011; Birnbaum et al., 2003; Darnerud, 2003; Engel and Wolff, 2013; Heudorf et al., 2007; Huang et al., 2012; Jaakkola and Knight, 2008; Jurewicz et

al., 2013; Kay et al., 2013; Latini et al., 2006; Legler and Brouwer, 2003; Matsumoto et al., 2008; McKee et al., 2004; Meerts et al., 2000; North et al., 2014; Ritter and Arbucklet, 2007; Vonderheide et al., 2008). Collectively, these reviews show that exposure to phthalates results in profound and irreversible changes in the development of the reproductive tract, especially in males. Effects such as increases in prenatal mortality, reduced growth and birth weight, and skeletal, visceral, and external malformations, are also associated with exposure to phthalates. In addition, epidemiologic studies in children show associations between phthalates and the risk of asthma and allergies. Experimental studies (Oie et al., 1997; Lagercrantz et al., 2005) have shown that inhalation exposures to even low levels of phthalates may cause lung inflammation through their chemical similarity to prostaglandins, naturally occurring inflammatory agents. Other in vivo and in vitro studies also supported the adjuvant effects on basic mechanisms in allergic sensitization by several phthalates (Larsen et al., 2004 and 2007; Hansen et al., 2007; Yang et al., 2008; Bornehag and Nanberg, 2010). Furthermore, certain phthalates have chemical structures that are similar to those of human hormones and can either mimic or block endocrine activity (Bornehag and Nanberg, 2010). These endocrine disrupters have been suggested as potential contributors to neurodevelopment and behavioral problems ranging from autism to attention deficit disorder (Weschler and Nazaroff, 2008). Heudorf et al. (2007) estimate that effective intake of phthalates is higher in children than in adults, although data are not available for children less than 3 years of age. Exposure during development (in utero, infants and children) is of special concern, because developing tissues are exquisitely sensitive to endocrine signals and disruption of these signaling pathways can result in permanent alterations in tissue structure and function (Rudel and Perovich, 2009).

Concentrations of phthalate metabolites measured in the general population using biomonitoring methods (blood and urine) provide direct evidence of wide-spread human exposure (Calafat and McKee, 2006; Heudorf et al., 2007). Biomonitoring data based on blood suggest that over 75% of the US population is exposed to phthalates (Silva et al., 2004). When urinary concentrations of secondary metabolites are measured, the estimate increases to 95% (Kato et al., 2006). Therefore, an urgent need exists to identify the most important sources and pathways of exposure. However, exposure to phthalates is difficult to evaluate because phthalates are ubiquitous and because phthalate concentration measurements are hampered by contamination (Koch et al., 2003). To complicate matters, phthalates are sorbed strongly to surfaces, as do other SVOCs such as biocides and flame retardants (Weschler and Nazaroff, 2008). A relatively small gas-phase concentration, such as 0.1 ppb, is sufficient for meaningful vapor transport of a phthalate ester and its consequent partitioning between the gas phase and indoor surfaces, including airborne particles and settled dust (Weschler, 2003). Adibi et al. (2008) measured phthalate metabolite concentrations in urine samples from 246 pregnant women and correlated these with indoor air concentrations. They concluded that a single indoor air sample may be sufficient to characterize phthalate exposure in the home. Other recent filed measurements also suggested that indoor environments play an important role in phthalate exposures (Allen et al., 2007; Bornehag et al., 2005; Frederiksen et al., 2009; Harrad et al., 2006; Jaakkola et al., 2004; Meeker et al., 2009).

Despite the nationwide exposure and the negative health impacts, phthalates still dominate the plasticizer market (Schossler et al., 2011). The global production rate of phthalate plasticizers has increased from 2.5 to 6 million tons/yr within a decade (Cadogan and Howick, 1996; Rudel and Perovich, 2009). In 2009, the U.S. Consumer Product Safety Improvement Act (CPSIA) was enacted to restrict the use of phthalates in

toys and child care articles (CPSC, 2009). As a result, phthalates used in polymeric products are changing rapidly, with a shift from low to high molecular phthalates (Weschler, 2009). Alternative plasticizers, such as di(2-ethylhexyl) terephthalate (DEHT) and diisononyl cyclohexane-1,2-dicarboxylate (DINCH) have emerged very recently, but toxicological information on these compounds is lacking. Given that these alternatives share properties similar to those of phthalates, similar levels of emission, environmental fate and transport, and human exposure are expected (Stapleton et al., 2008). Furthermore, because typical lifetimes for some building materials and consumer products may exceed ten years (Stapleton et al., 2006), and these chemicals may continue to be produced in developing countries and exported to the U.S. as additives in finished products, the levels of phthalate in indoor environments are not likely to drop for a long time (Park et al., 2011). Therefore, there is an urgent need to quickly identify the source and accurately characterize phthalate emissions and transport in indoor environments, because it represents the essential first step in investigating subsequent health effects, and developing strategies to limit exposures.

2.2 CHAMBER STUDIES ON PHTHALATE EMISSIONS

Characterizing phthalate emissions in chambers is very difficult. Standard chamber methods designed for measuring volatile organic compounds (VOCs), ozone and particulate matter may not be appropriate for measuring emissions of phthalates (Afshari et al., 2004; Destaillats et al., 2008). There have been very few emission studies with low volatile plasticizers as target compounds, probably due to the difficulties associated with sampling and analysis of SVOCs (Clausen et al., 2004; Wensing et al., 2005). Afshari et al. (2004) tested dibutyl phthalate (DBP) and di(2-ethylhexyl) phthalate (DEHP) emissions from materials such as wallpaper, PVC flooring and electric wire in

the Chamber for Laboratory Investigations of Materials, Pollution and Air Quality (CLIMPAQ) as well as the Field and Laboratory Emission Cell (FLEC), as shown in Figure 2.1 and found that the chamber concentration of DEHP reached steady state after about 150 days and that sorption by chamber surfaces has a strong effect on the rate of increase of gas-phase chamber concentrations. Fujii et al. (2003) developed a passive-type sampler to measure the emission rate of phthalates from synthetic leather, wallpaper and vinyl flooring and found that emission rates of several phthalates increased significantly at higher temperature. Kawamura et al. (2011) estimated the emission rate of DEHP from building materials through small-chamber studies with variable surface area. Schossler et al. (2011) measured air concentration for diisononyl phthalate (DINP), DINCH, and DBP emitted from PVC samples in the FLEC and found that the time it took for DINP and DINCH to reach the steady-state concentration is in the same order of magnitude. Ekelund et al. (2008) studied the aging of PVC plasticized with DEHP by measuring weight loss over time at temperatures from 60°C to 155°C. They concluded that evaporation (diffusion in the boundary layer) controlled emissions below 100°C, and the evaporation has an activation energy which is equal to that for evaporation of pure liquid DEHP. Their experiments were carried out in ventilated ovens with no control of the air change rate, which might be important for the emission of DEHP from PVC. Clausen et al. (2004, 2012, 2010 and 2007) performed a series of tests on emissions of DEHP from vinyl flooring in the FLEC. Their work showed that 1) the emission rate of DEHP was limited by gas-phase mass transfer, 2) strong sorption of DEHP onto the FLEC chamber surface resulted in a very long time period to reach steady state, 3) relative humidity had no impact on the emission rate, 4) increasing the ventilation rate increased the emission rate, and 5) gas-phase DEHP concentration in equilibrium with vinyl flooring surface was close to the vapor pressure of pure DEHP. Recently, Xu et al.

(2012) designed a special stainless steel chamber (Illustration 1) to measure emission of DEHP from vinyl flooring. By increasing the area of vinyl flooring and decreasing that of the stainless steel surface within the chamber, the time to reach steady state was reduced, compared to the previous studies (30 days versus 150 days). Additionally, the adsorption isotherm of DEHP on the stainless steel chamber surfaces was measured independently. These chamber studies provided valuable information on the emission characteristics of phthalates from PVC materials. They also collectively reveal the substantial difficulties associated with chamber tests for SVOCs due to the low gas-phase concentration, strong sorption onto surfaces, and ubiquitous contamination in laboratory facilities.

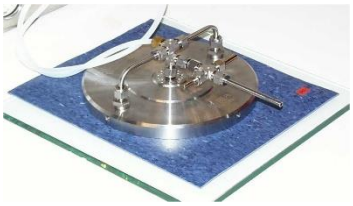

FLEC
(Field and laboratory emission

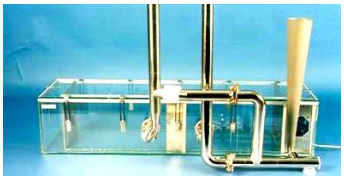

CLIMPAQ
(Chamber for laboratory investigations of materials, pollution, and air quality)

A specially-designed chamber

Figure 2.1: Photos of controlled emission chamber in previous studies.

2.3 SVOC EMISSION MODEL

Building upon previous success in characterizing emissions of volatile organic compounds (VOCs) (Little et al., 1994; Cox et al., 2001 and 2002; Kumar and Little, 2003; Xu and Zhang, 2003 and 2004), Xu and Little (2006) developed the first mechanistic model to predict emission rates of SVOCs from polymer materials. Figure 2.2 depicts a slab of material (e.g., vinyl flooring) in a chamber. The mechanisms affecting emissions of SVOCs are: diffusion within the slab, equilibrium between the

surface of the slab and the air in immediate contact with the slab, mass transfer through the boundary layer into the bulk chamber air, and sorption to airborne particles and interior surfaces. In Figure 2.2, Q is the volumetric flow rate of air through the chamber, V is the chamber volume, A is the exposed surface area of the slab, A_i is the exposed chamber surface area, L is the thickness of the slab, and TSP is the suspended particle concentration. C(x,t) is the material-phase concentration with an initial value of C_0, t is time, x is distance from the base of the slab, y_0 is the gas-phase concentration in equilibrium with $C_{x=L}$, y is the gas-phase concentration in the well-mixed chamber air, q_s is the sorbed surface concentration, y_s is the gas-phase concentration in equilibrium with q_s, and q_p is the sorbed particle-phase concentration. Finally, K represents the material/air equilibrium partition coefficient, K_s is the chamber surface/air partition coefficient, K_p is the particle/air partition coefficient, D is the material-phase diffusion coefficient, and h_m is the gas-phase mass transfer coefficient.

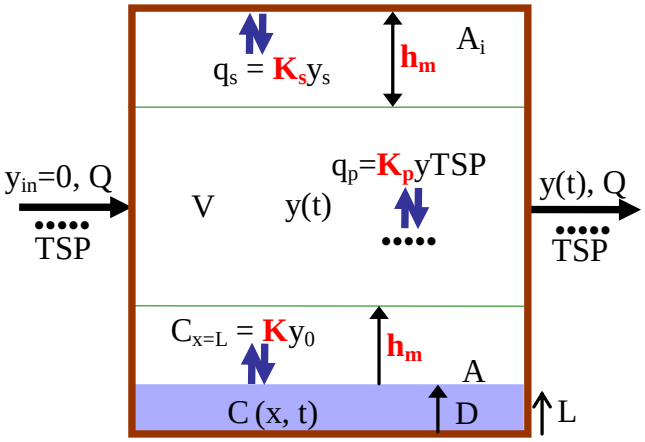

Figure 2.2: Schematic showing emissions of SVOCs from a material in a chamber.

A mass balance for an SVOC in chamber air yields

$$\frac{dy}{dt} \cdot V + \frac{dq_p}{dt} \cdot V = M - M_s - Q \cdot y - Q \cdot q_p \quad (1)$$

where M is the emission rate from the material and M_s is the sorption rate to the chamber surface:

$$M = h_m \cdot (y_0 - y) \cdot A = -D \frac{dC_{x=L}}{dx} \qquad M_s = h_m \cdot (y_0 - y_s) \cdot A_i = \frac{dq_s}{dt} \cdot A_i \quad (2)$$

They (Xu and Little, 2006) showed that emissions of these very low volatility compounds are subject to "external" control (partitioning from the material into the gas phase, convective mass transfer through the boundary layer, and strong sorption onto interior surfaces including airborne particles). Using data collected in a specially-designed stainless steel chamber, Xu et al. (2012) further showed that the emission rate of DEHP from vinyl flooring can be predicted based on a priori knowledge of the gas-phase concentration of DEHP in equilibrium with the material-phase (y_0), the material to air and air to stainless steel surface mass-transfer coefficients (h_m), and the stainless steel/air equilibrium relationship (K_s).

Currently, no methods exist to measure or estimate y_0 for phthalates in PVC products. Using DEHP steady-state concentrations in the FLEC as approximations of y_0, Clausen et al. (2012) found that the value of y_0 for a vinyl flooring sample is close to the vapor pressure (V_p) of pure DEHP at five temperatures. However, the results showed that there is about three times difference at 23°C between y_0 and estimated V_p values (y_0: 0.9 μg/m^3 versus V_p: 2.4 μg/m^3). The relationship between y_0 and V_p for other phthalates is still unclear. Little et al. (2012) suggested that y_0 cannot be well approximated by V_p in all cases. The material-phase concentration (C_0) of phthalate additives in different products can vary substantially; therefore, when their content is low, they may not behave as pure liquid, resulting in the y_0 value being much lower than its V_p. As a result, development of appropriate methods to determine y_0 for phthalates in PVC products and

to study the impacts of temperature on y_0 has become a high priority. In addition, the availability of reliable measurements of V_p is limited for phthalates and for other SVOCs (Schossler et al., 2011; Letcher and Naicker, 2004). Significant discrepancies (by several orders of magnitude) were found in the literature (Schossler et al., 2011; Weschler et al., 2008), probably because of the difficulties associated with SVOC analysis, various measuring methods, and different purities of samples (Schossler et al., 2011; Letcher and Naicker, 2004). For example, the measured V_p (at 25°C) for diisononyl phthalate (DINP) is in the range of 3.6×10^{-7} Pa to 1.0×10^{-4} Pa (Schlssler et al., 2011; Howard et al., 1985). Predictions using some V_p calculators also showed significant deviations, primarily because they follow different approaches in estimating physical parameters of compounds (Schossler et al., 2011). In the case of DINP, the predicted values of V_p (at 25°C), by using SPARC and EPI Suite, are 9×10^{-9} Pa and 3×10^{-6} Pa, respectively. Therefore, to investigate the relationship between y_0 and V_p, more reliable data of phthalates V_p are needed. Furthermore, an accurate value of V_p at room temperature will help to understand the distribution of phthalates in indoor environments, especially among the gas phase, airborne particles, interior surfaces, and settled dust (Weschler and Nazaroff, 2008; Xu et al., 2009; Weschler et al., 2008; Weschler and Nazaroff, 2010).

2.4 THE FATE AND TRANSPORT MODEL FOR INDOOR SVOCS

Multimedia models have been served as useful tools for elucidating the behavior of SVOCs (Gouin and Harner, 2003). Bennett and Furtaw (2004) developed a dynamic mass-balance compartment model based on fugacity principles to predict exposure to pesticides used in residences. They used the model to make predictions about pesticide concentrations in residential air (both gas phase and aerosols) and surfaces (carpet, smooth flooring, and walls) following pesticides application. The model results are of

the same order of magnitude as measurements from an independent study but tend to over-predict the measured data. Zhang et al. (2009) extended the model of Bennett and Furtaw to consider emissions and fate of polybrominated diphenyl ethers (PBDEs) and to understand the variability of indoor concentrations. The model was applied to an office in which an 80% decrease in PBDE air concentration was observed after an old computer was exchanged with a new one. They found that the most sensitive parameters to air concentrations and estimated emission rates are room temperature, particle concentrations and deposition velocity, and air change rates. For phthalates, Xu et al. (2009 and 2010) extended the chamber-based SVOC emission model to predict human exposures to DEHP emitted from vinyl flooring in a realistic residential environment using data collected in a field campaign (Wilson et al., 2004) to establish surfaces/air partition coefficient values for dust and other interior surfaces. Based on Xu et al.'s model, Liu et al. (2010) investigated the influence of aerosol particles on the accumulation of indoor airborne DEHP by incorporating a variable indoor particle source. Little et al. (2012) simplified Xu et al.'s model and proposed rapid methods to obtain screening-level estimates of potential indoor exposure of building occupants to a range of SVOCs.

Particles have a great influence on the fate and transport of indoor phthalates. Because gas-particle sorption and desorption kinetics are sufficiently rapid (Benning et al., 2012; Odum et al., 1994; Weschler et al., 2008), airborne particles become important carriers that accelerate the transport of phthalates from their original source to other indoor surfaces through deposition, resuspension, and advection of air. Liu et al. (2010) investigated the influence of aerosol particles on airborne DEHP concentration by applying a variable particle source to the indoor environment. Shi and Zhao (2012) included gas-particle sorption kinetics to predict indoor concentrations of polycyclic aromatic hydrocarbons (PAHs), and found that the model performed better than use of

the typical assumption of linear instantaneous gas-particle partitioning. Liu et al. (2013) further showed that the size distribution of particles is critical to the timescale that is required for gas-particle partitioning to reach equilibrium. Recently, Liu et al. (2014b) found that indoor concentrations of particle-associated SVOCs are affected by several factors including the gas/particle-partition coefficients of the SVOC, the residence time of the particles and the mass transfer coefficients around particles. Although these modeling studies (Liu et al., 2010, 2013 and 2014b; Shi and Zhao, 2012) acknowledged the importance of gas-particle partitioning on the fate of indoor SVOCs, the actual role of particles in the transport of indoor SVOCs has not been fully characterized. Particle deposition and resuspension may result in a redistribution of SVOCs among the gas, particle, and surface phases near the source and sink surfaces, and thereby significantly influence the rate of SVOC emission from and sorption to those surfaces. Clausen et al. (2004) conducted small chamber studies and discovered that dust layer on a vinyl flooring sample increased the emission rate of DEHP by increasing the external concentration gradient above the surface. Similarly, a recent theoretical study (Liu et al., 2012) found that SVOC flux between air and indoor surfaces was significantly enhanced in the presence of particles. Currently no model exists for accurately characterizing the effect of particle dynamics on SVOC emission and sorption as well as the subsequent impacts on the fate and transport of indoor SVOCs. Furthermore, none of the fate and transport model developed for SVOCs has been strictly validated, though most of them have compared their predicted airborne concentrations with field campaign data. In addition, phthalates (including both gas- and particle-phase phthalates) can accumulate in porous materials such as carpet and subsequently re-emitted into indoor environments. These materials can act as buffers for indoor phthalates, modulating and prolonging their presence in the environment (Zhang et al., 2009). Therefore, to accurately characterize

the fate and transport of phthalates in indoor environments, it is necessary to include those porous materials.

2.5 FIELD STUDIES OF INDOOR PHTHALATES

Recent field studies of indoor phthalates primarily focused on the air and dust levels of phthalates (Bergh et al., 2011; Harrad et al., 2006; Kanazawa et al., 2010; Rudel et al., 2010; Thuresson et al., 2012; Vorkamp et al., 2011). The field studies of gaseous phthalates showed that the most abundant phthalate compounds in indoor air were DEP, DnBP, and DEHP (Table 2.1). In addition to gas-phase concentrations, phthalates were also measured in settled dust samples in field campaigns (Table 2.2), with DEHP as the most abundant phthalate compound in indoor settled dusts. A recent CTEPP study led by EPA (2005) measured the total exposure of 257 preschool children (ages 2 to 5 years) and their primary adult caregivers to more than 50 target compounds in homes and daycare centers. The two phthalates targeted in the CTEPP study (Benzylbutylphthalate and Di-n-butylphthalate) were detected in residential air, house dust, and dermal wipe samples. The measured phthalate concentrations were the highest among the selected pollutants (including pesticides, PAHs, and polychlorinated biphenyls). Collectively, these field studies reveal the presence of phthalates in indoor environments is in large amounts and in a wide range of products. However, what remains unclear is how indoor phthalates are redistributed from their original sources to various interior surfaces, which makes it impossible to identify the most important sources of phthalate exposure. It is therefore critically important to conduct field studies to investigate the fate and transport of phthalates in indoor environments, the sorption kinetics and their equilibrium levels on various interior surfaces.

Recent chamber measurements of phthalate (Fujii et al., 2003; Ekelund et al., 2010; Clausen et al., 2012) revealed the strong influence of temperature on phthalate emissions. Temperature increase due to climate change and/or the use of air conditioning (AC) may increase the emission rate of phthalates from building materials by orders of magnitude, resulting in significant increases of phthalate in air, dust and other various interior surfaces. However, no field studies have been conducted to investigate the temperature effects on the mechanisms controlling the fate and transport of phthalate in indoor environments. There is an urgent need to experimentally investigate the concentration changes of phthalate in air, dust, and various indoor surfaces due to temperature fluctuations and to assess human exposure to indoor phthalates.

Reference	**Country**	**N**	**Building type**	**DMP**	**DEP**	**DnBP**	**BBzP**	**DEHP**	**DnOP**
Wilson et al. (2001)	U.S.	29	Day care	n.a.	n.a.	0.24 (0.11-0.4)	0.1 (0.01-0.58)	n.a.	n.a.
Rudel et a l. (2003)	U.S.	120	Residence	n.a.	0.59[a] (0.13-4.3)	0.22[a] (0.05-1.1)	n.a.	0.08[a] (<d.l.-1.0)	n.a.
Fromme et al. (2004)	Germany	59	Residence	1.2 (n.a.-4.6)	0.81 (n.a.-5.5)	1.2 (n.a.-5.6)	0.04 (n.a.-0.58)	0.19 (n.a.-0.62)	n.a.
Otake et al. (2004)	Japan	27	Residence	n.a.	0.14 (0.01-0.61)	0.75 (0.01-6.2)	0.02 (<d.l.-110)	0.32 (<d.l.-3.2)	n.a.
Fromme et al. (2004)	Germany	74	Day care	1.0 (n.a.-6.3)	0.40 (n.a.-1.3)	2.4 (n.a.-13.3)	<d.l. (n.a.-0.39)	0.60 (n.a.-1.5)	n.a.
Kanazawa et al. (2010)	Japan	40	Residence	0.48[a] (0.01-0.19)	0.06[a] (0.02-0.20)	0.20[a] (0.08-0.74)	<d.l.[a] (<d.l.-0.03)	0.15[a] (0.012-1.7)	n.a.
Rudel et al. (2010)	U.S.	50	Residence	n.a.	0.33[a] (0.11-2.5)	0.14[a] (0.03-1.1)	0.007[a] (<d.l.-0.08)	0.06[a] (<d.l.-0.2)	n.a.
Bergh et al. (2011b)	Sweden	10	Residence	0.02 (0.007-0.05)	1.6 (0.68-3.9)	0.93 (0.30-2.3)	0.03 (0.007-0.097)	0.21 (0.09-0.53)	n.a.
Bergh et al. (2011a)	Sweden	169	Residence	0.03 (<d.l.-0.38)	0.32 (0.04-2.2)	0.27 (0.02-1.6)	0.02 (<d.l.-0.30)	0.23 (0.04-0.89)	0.001 (<d.l.-0.02)
Bergh et al. (2011b)	Sweden	10	Day care	0.006 (0.002-0.014)	1.2 (0.65-2.6)	0.68 (0.33-1.7)	0.02 (0.009-0.03)	0.27 (0.13-0.48)	n.a.
Bergh et al. (2011b)	Sweden	10	Office	0.005 (0.003-0.008)	0.67 (0.42-1.4)	0.60 (0.19-1.2)	0.02 (0.009-0.03)	0.12 (0.02-0.32)	n.a.

(Table 2.1 continues on the next page)

Pei et al. (2013)	China	10	Residence	1.5 (<d.l.-7.9)	2.3 (0.48-5.6)	1.9 (0.35-3.5)	4.0 (<d.l.-7.2)	2.4 (0.3-11.1)	n.a.
Xu et al. (2014)	U.S.	12	Retail store	0.15 (0.008-0.81)	0.15 (0.007-0.44)	0.23 (0.048-1.4)	0.05 (0.003-0.17)	0.13 (0.01-0.44)	0.03 (0.004-0.01)

Table 2.1: Phthalate concentrations ($\mu g/m^3$) in indoor air samples as reported in relevant studies. All values are means with range (minimum – maximum) unless stated otherwise.

Country	Reference	N	Building type	DMP	DEP	DnBP	BBzP	DEHP	DnOP
North America									
U.S.	Wilson et al. (2001)	29	Day care	n.a.	n.a.	18.4 [a] (1.58-46.3)	67.7 [a] (15.1-175)	n.a.	n.a.
U.S.	Rudel et a l. (2003)	120	Residence	n.a.	4.98 (<d.l.-111)	20.1 (<d.l.-352)	45.4 (3.87-1310)	340 (16.7-7700)	n.a.
U.S.	Wilson et al. (2003)	4	Day care	n.a.	n.a.	1.87 [a] (0.06-5.85)	3.72 [a] (0.02-7.43)	n.a.	n.a.
U.S.	Wilson et al. (2003)	9	Residence	n.a.	n.a.	1.21 [a] (0.38-3.03)	5.86 [a] (0.50-15.6)	n.a.	n.a.
U.S.	Hwang et al. (2008)	10	Residence	n.a.	n.a.	n.a.	n.a.	386 (104-2050)	n.a.
U.S.	Guo and Kannan (2011)	33	Residence	0.08 (>d.l.-3.3)	2 (0.7-11.8)	13.1 (4.5-94.5)	21.1 (3.6-393)	304 (37.2-9650)	0.4 (<d.l.-14.1)
U.S.	Xu et al. (2014)	24	Retail store	<d.l. <d.l.	72 (6-591)	258 (8-961)	148.5 (14-3262)	192 (12-4187)	117 (16-343)
Europe									
Norway	Oie et al. (1997)	372	Residence	n.a.	10[a] (<d.l.-110)	100 [a] 10-1030	110 [a] (<d.l.-440)	640 [a] (100-1610)	n.a.
Germany	Butte et al. (2001)	286	Residence	n.a.	n.a.	49 n.a.	49 n.a.	740 n.a.	n.a.
Germany	Becker et al. (2002)	199	Residence	n.a.	3.3 n.a.	42 n.a.	15 n.a.	416 n.a.	n.a.
Demark	Clausen et al. (2003)	15	School	n.a.	n.a.	n.a.	n.a.	3214 [a] (400-8500)	n.a.
Germany	Kersten and Reich (2003)	65	Residence	n.a.	5 n.a.	47 n.a.	19 n.a.	600 n.a.	n.a.
France	Santillo et al. (2003)	31	Residence	<d.l. n.a.	6.87 (<d.l.-49.4)	55.3 (11.6-624)	28.2 (<d.l.-3551)	504.6 (14.9-3289)	n.a.
Germany	Santillo et al. (2003)	5	Residence	1.42 (<d.l.-2.83)	12.9 (1.86-368)	44.1 (22.3-1511)	82.2 (4.4-218)	996 (547-1586)	n.a.
Italy	Santillo et al. (2003)	5	Residence	<d.l. (<d.l.-1.5)	6.78 (1.92-23.6)	42.8 (22.8-46.8)	23.6 (9.0-308)	434 (314-933)	n.a.

(Table 2.2 continues on the next page)

Spain	Santillo et al. (2003)	22	Residence	<d.l. (<d.l.-0.92)	5.33 (1.09-64.6)	79.4 (48.6-201)	4.54 (0.81-153)	317.2 (113-2151)	n.a.
U.K.	Santillo et al. (2003)	29	Residence	<d.l. (<d.l.-1.1)	3.5 (0.6-114.8)	52.8 (0.1-106.4)	24.5 (<d.l.-238.9)	195.4 (0.5-416.4)	n.a.
Germany	Becker et al. (2004)	252	Residence	n.a.	n.a.	n.a.	n.a.	515 (22-5330)	n.a.
Germany	Fromme et al. (2004)	59	Residence	1.5 n.a.	6.1 n.a.	47 n.a.	29.7 n.a.	703.4 n.a.	n.a.
Sweden	Bornehag et al. (2005)	346	Residence	n.a.	<d.l. (<d.l.-2425)	150 (<d.l.-5446)	135 (<d.l.-45549)	770 (<d.l.-40459)	n.a.
Germany	Nagorka et al. (2005)	278	Residence	n.a.	n.a.	29 n.a.	13 n.a.	480 n.a.	n.a.
Germany	Butte et al. (2008)	29	Residence	n.a.	n.a.	28 n.a.	51 n.a.	970 n.a.	n.a.
Bulgaria	Kolarik et al. (2008)	177	Residence	260 [b] (<d.l.-4300)	350 [b] (<d.l.-9070)	7860 [b] (<d.l.-58070)	320 [b] (<d.l.-2730)	960 [b] (<d.l.-29440)	250 [b] (<d.l.-2510)
Germany	Abb et al. (2009)	30	Residence	n.a.	n.a.	87.4 n.a.	15.2 n.a.	604 n.a.	n.a.
Denmark	Langer et al. (2010)	497	Residence	n.a.	1.7 (8.8)[c]	15 (7.2)[c]	3.7 (4.0)[c]	210 (2.4)[c]	n.a.
Denmark	Langer et al. (2010)	151	Day care	n.a.	2.2 (2.6)[c]	38 (4.6)[c]	17 (3.4)[c]	500 (1.9)[c]	n.a.
Sweden	Bergh et al. (2011)	10	Residence	0.04 (0.03-0.1)	3.7 (1.3-63)	130 (17-260)	17 (3.1-110)	680 (130-3200)	n.a.
Sweden	Bergh et al. (2011)	10	Office	0.2 (0.05-1.2)	20 (3.7-180)	100 (20-450)	8.8 (1.4-110)	1100 (57-3700)	n.a.
Sweden	Bergh et al. (2011)	10	Day care	0.1 (0.01-1.5)	4.2 (1.0-23)	150 (38-560)	31 (9.0-120)	1600 (260-5800)	n.a.
Asia									
Japan	Kanazawa et al. (2010)	41	Residence	<d.l. (<d.l.-1.01)	0.35 (<d.l.-6.3)	22.3 (5.1-549)	2.4 (<d.l.-35.8)	1200 (220-10200)	n.a.
China	Guo and Kannan (2011)	75	Residence	0.2 (>d.l.-8.2)	0.4 (0.7-45.5)	20.1 (1.5-1160)	0.2 (<d.l.-12)	228 (9.9-8400)	0.2 (<d.l.-45.7)
Taiwan	Hsu et al. (2012)	101	Residence	0.1 n.a.	1 n.a.	20.2 n.a.	1 n.a.	753 n.a.	n.a.
Kuwait	Gevao et al. (2013)	21	Residence	0.03 (>d.l.-0.1)	1.8 (0.1-16)	45 (8.3-160)	8.6 (<d.l.-160)	2256 (380-7800)	14 (<d.l.-1300)
China	Zhang et al. (2013)	215	Residence	0.1 (<d.l.-24)	0.2 (<d.l.-33.9)	23.7 (<d.l.-2150)	1.6 (<d.l.-38.7)	183 (<d.l.-9950)	0.1 (<d.l.-39.5)

a. Mean value
b. Geometric mean value
c. Geometric standard deviation

Table 2.2: Phthalate concentrations (µg/g) in indoor dust as reported in relevant studies. All values are means with range (minimum – maximum) unless stated otherwise.

Chapter 3: Summary of Methods and Research Findings

This chapter describes the investigations conducted in support of the three research objectives outlined in Chapter 1. Full manuscripts describing each investigation appear in Appendices A-E with complete introduction, methods, results, discussion, and supporting information.

3.1 Characterization of Phthalate Emissions in Specially Designed Small-Chambers (Objective 1)

3.1.1 Emission Chamber

The design of a stainless steel chamber used in previous experiments (Xu et al., 2012) was improved. As shown in Figure 3.1, the thin chamber was positioned between two vinyl flooring sheets. The two flooring sheets and the internal stainless steel chamber wall form a very short semicylindrical cavity. In this way, we maximized the vinyl flooring emission area and minimized the stainless steel sorption area. To enhance air flow mixing inside the chamber, three inlets and six outlets were applied in the design. Simulation of air velocity field by computational fluid dynamics (CFD) suggests that the air flow is reasonably well mixed within the chamber cavity. No bypass flow was detected in measurements. Three of the six outlet ports were constructed specially to fit with sorbent tubes, so that they could be directly inserted into the chamber without any fixtures. Thus, the loss of phthalates to stainless steel tubing and fittings along the sampling pathway was avoided. Another three outlets were made with particular fittings to hold stainless steel rods and allow air flows to pass through. These precision-ground rods (3 mm diameter × 3 cm in length) have similar roughness to the interior stainless steel chamber surface. They were inserted into the chamber in sorption experiments and periodically removed so that the amount of phthalates sorbed to stainless steel surface

could be measured. Because the outlet flow resulted in high velocity around the rods, fast sorption kinetics was achieved. Vinyl flooring itself acts as a good gasket. PTFE sheets (from Fluoro-Plastics Inc.) were used in blank chamber experiments. The air leakage rate was less than 2% of the total flow rate.

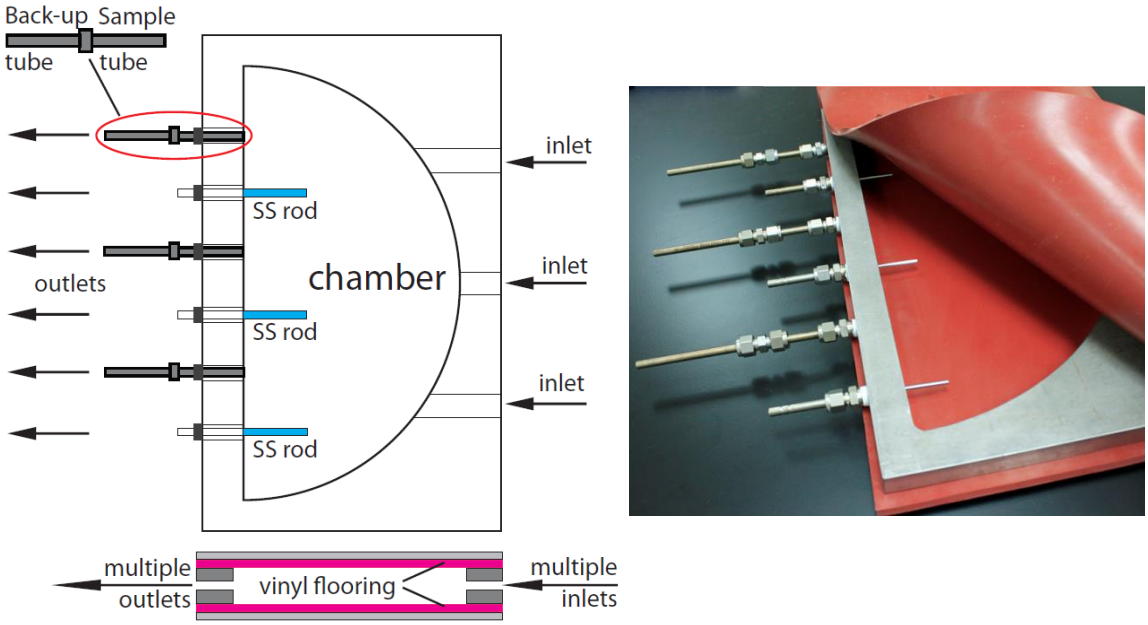

Figure 3.1: Configuration of the chamber. (a) Top and side view, (b) Photo.

3.1.2 Determination of y_0

Xu and Little (Xu and Little, 2006) developed an SVOC emission model, and the model was recently simplified by Xu et al. (Xu et al., 2012). In their analysis, the emission rate is

$$E(t) = h_m \cdot [y_0 - y\,(t)] \tag{3}$$

where y ($\mu g/m^3$) is the bulk gas-phase concentration, and h_m (m/s) is the convective mass-transfer coefficient. The ratio of the concentration of a chemical on sorption surfaces

(such as the chamber wall or the rods) to its concentration in the gas phase is equal to the surface/air partition coefficient, K_s (m), or

$$K_s = q(t)/y_{0s}(t) \quad (4)$$

where q is the surface concentration (μg/m^2) and y_{0s} (μg/m^3) is the gas-phase concentration immediately adjacent to the surface. Assuming a boundary layer exists adjacent to the sorption surfaces, the amount of SVOC accumulated on the surface is equal to the total mass transferred through the boundary layer from the gas phase, or

$$\frac{dq(t)}{dt} = h_s[y(t) - y_{0s}(t)] \quad (5)$$

where h_s (m/s) is the convective mass-transfer coefficient near the sorption surface. The accumulation of SVOCs in the chamber obeys the following mass balance:

$$\frac{dy(t)}{dt} \cdot V = E(t) \cdot A - \frac{dq(t)}{dt} \cdot A_s - y(t) \cdot Q \quad (6)$$

where V is the chamber volume (m^3), A is the area of emission surfaces (m^2), A_s is the internal stainless steel surface area (m^2), and Q is the air flow rate of the chamber. The simplified SVOC emission model is obtained by combing equations (3)-(6).

This section discusses the method to determine y_0 as well as h_m based on the results of vapor pressure and emission experiments. When steady state is reached in vapour pressure experiments, by modifying Equation (6), we obtained

$$V_p = \frac{y_{ss} \cdot Q}{h_m \cdot A} + y_{ss} \quad (7)$$

where V_p is the saturated vapor pressure concentration (μg/m^3) of phthalates and y_{ss} is the steady-state gas phase concentration in the chamber. DMP, a volatile organic compound that has reliably measured vapor pressure (mean ± SD: 0.27±0.04 Pa at 25 °C) reported in the literature (Letcher and Naicker, 2004; Weschler et al., 2008), was selected as a reference chemical. Because the V_p of DMP is known, y_{ss} measured through the vapor

pressure experiment for DMP can be used to obtain the only unknown parameter (h_m) in Equation (7).

With the knowledge of h_m for DMP, the convective mass transfer coefficient for other target phthalates ($h_{m,\ phthalate}$) can be calculated. The traditional method for predicting h_m for volatile organic compounds and SVOCs (Xu and Little, 2006; Axley, 1991; Xu and Zhang, 2003 and 2004) is based on empirical correlations, which can be generally expressed as $Sh = f(Re)\cdot Sc^n$, where Sh is the Sherwood number, h_mL/D_a; Sc is the Schmidt number, υ/D_a; Re is the Reynolds number; n is a parameter that usually taken as 1/3; L (m) is characteristic length; D_a (m^2/s) is the chemical air diffusivity; and υ (m^2/s) is the kinematic viscosity of air. For different chamber configurations and flow conditions, the expression of f(Re) would be different. However, if samples with the same dimensions but emitting different pollutants were tested in the same chamber condition, the expression of f(Re) should be the same because of the similar flow field inside the chamber (Xiong et al., 2012). Therefore, the following formula can be derived:

$$\frac{h_{m,\ ref}}{h_{m,\ phthalate}} = \left(\frac{D_{a,\ ref}}{D_{a,\ phthalate}}\right)^{2/3} \tag{8}$$

where $h_{m,\ ref}$ and $h_{m,\ phthalate}$ are the convective mass transfer coefficients of a reference chemical (i.e., DMP) and a specific phthalate compound, respectively; and $D_{a,\ ref}$ and $D_{a,\ phthalate}$ are their corresponding air diffusivities, which can be estimated based on chemical molecular weight (Schwarzenbach et al., 2003). Therefore, $h_{m,\ phthalate}$ for the chamber condition can be calculated by Equation (8).

Finally, when emission experiments reach steady state, by modifying Equation (6), we obtained

$$y_0 = \frac{y_{ss}\cdot Q}{h_m \cdot A} + y_{ss} \tag{9}$$

Because h_m for phthalates under the test condition has been determined as described previously, based on the measured y_{ss} in the emission experiments, the values of y_0 for each vinyl flooring sample emitting particular phthalates can be determined using Equation (9).

3.1.3 Emission Experiments

As shown in Figure 3.2, phthalate concentrations increased and reached steady state in less than five days for all experiments. In the improved chamber design, the ratio of emission surface to sorption surface was high, the mass loss of phthalates onto sampling pathways was avoided, and the velocity field inside the chamber was optimized to enhance air mixing. Therefore, the build-up of phthalates in the gas phase occurred much faster and the time to reach steady state was significantly reduced, compared to the previous studies of DEHP emission in FLEC and in a special chamber from the same vinyl flooring (sample 1), in which it took about 150 and 30 days, respectively (Xu et al., 2012; Cluasen et al., 2004). In all tests, the phthalate concentration in a blank chamber was more than 10 times lower than the highest measured concentrations in the sample chamber with vinyl flooring. The experimental conditions were constant over the entire test period. In sorption experiments, stainless steel rods were inserted into the chamber after steady state had been reached. The additional sorption surface area (< 10% of the chamber internal surface area) due to the introduction of rods did not change the chamber concentration significantly. The fluctuation of concentration in the chamber tests after steady state had been reached was probably caused by normal measurement errors.

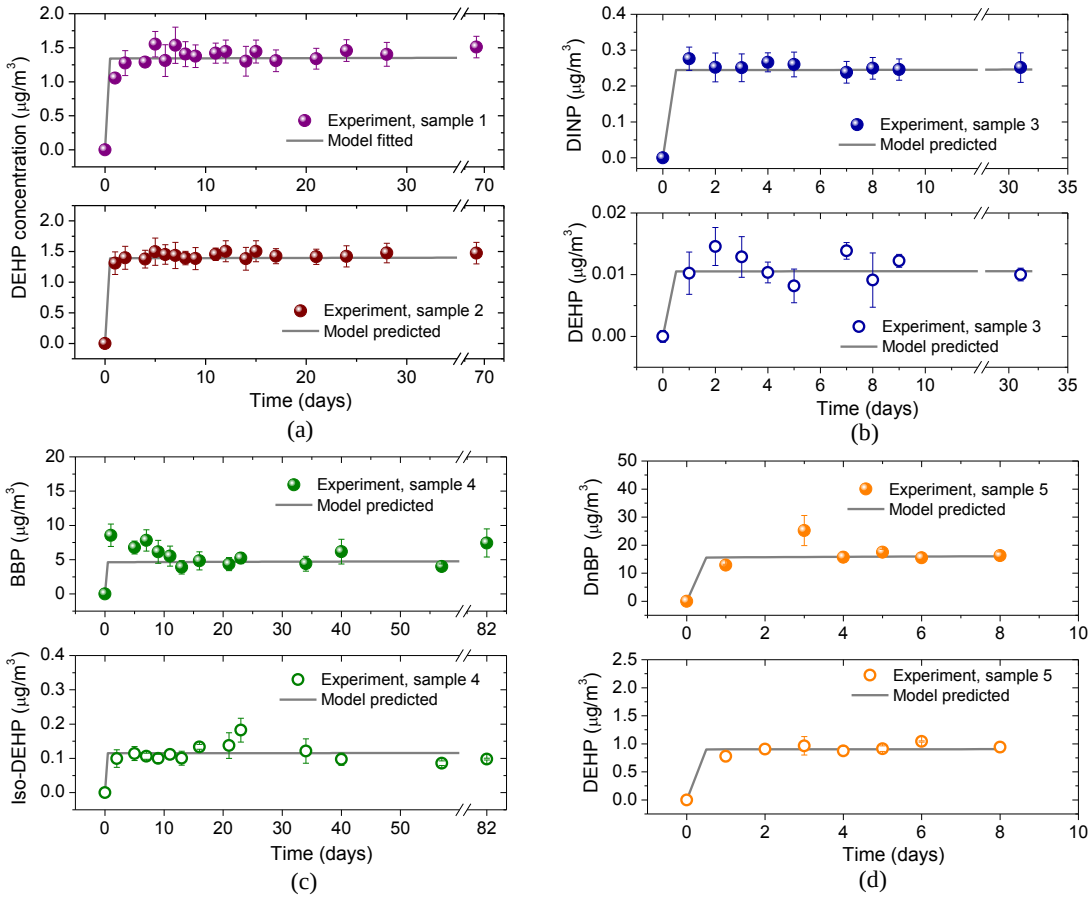

Figure 3.2: Gas-phase chamber concentration of phthalates emitted from vinyl flooring samples. (a) sample 1 and 2, (b) sample 3, (c) sample 4, and (d) sample 5.

Sample ID	Phthalates	Content	C_0 (μg/m^3)	y_0 (μg/m^3)	Vp (μg/m^3) at 25 °C
1	DEHP	13 ± 2 %	1.70×10^{11}	2.30	5.64
2	DEHP	23 ± 3 %	3.26×10^{11}	2.37	5.64
3	DINP DEHP	20 ± 3 % 0.1 ± 0.02 %	3.47×10^{11} 1.73×10^{9}	0.42 0.02	0.52 5.64
4	BBP Iso-DEHP	15 ± 2 % 7 ± 1 %	1.93×10^{11} 9.02×10^{10}	8.47 0.12	12.3 0.88
5	DnBP DEHP	9 ± 1 % 7 ± 1 %	1.42×10^{11} 1.10×10^{11}	24.7 1.54	464 5.64

Table 3.1: The measured values of C_0 and y_0 for tested vinyl floorings and of V_p for pure phthalates at 25 °C.

Based on the steady-state gas phase concentration in the emission chamber (y_{ss}) and h_m calculated previously, the value of y_0 for each vinyl flooring sample emitting particular phthalates was determined using Equation (9) and is listed in Table 3.1. A sensitivity analysis of h_m shows that doubling the mass-transfer coefficient (h_m) decreases the determined y_0 values less than 30%. Sample 1 was the exact same vinyl flooring used in previous studies (Xu et al., 2012; Clausen et al., 2012), but the measured y_0 of DEHP emission from Sample 1 (2.3 $\mu g/m^3$) was higher than previous estimations (~ 1 $\mu g/m^3$). The differences might be associated with approximation of y_0 using y_{ss} value (Clausen et al., 2012) and uncertainties related to fitting parameters (Xu et al., 2012; Xu and Little, 2006). Samples 1, 2, 3, and 5, which contained DEHP in different levels, were used to explore the relationship between y_0 and C_0. As shown in Figure 3.3a, for low concentrations of DEHP in the materials (samples 1, 3, and 5), a simple partition coefficient corresponding to a value of 7×10^{10} can be used to linearly relate y_0 and C_0. Although three data observations might not be enough, the finding is similar as volatile organic compound (VOC) emissions from building materials (Kumar and Little, 2003). For the high weight percentage of DEHP in vinyl flooring (sample 2), however, simple partitioning mechanisms cannot be invoked. Considering that the molecular weight of DEHP is 391 g/mol and that of PVC flooring is from 20,000 to 80,000 g/mol, a weight percentage of ~20% implies that the molar fraction of DEHP in vinyl flooring is approximately 95%. However, the y_0 for sample 2 did not exceed 50% of the pure liquid V_p of DEHP, suggesting that the DEHP/vinyl flooring system is not an ideal solid mixture due to the extremely large size of polymer molecules compared to the size of DEHP molecules (Little et al., 2012; Hawkes et al., 1995; Nicholson, 2006) and thus cannot be described by Raoult's law. Recently, DEHP was found to behave as a thermodynamically separate liquid phase in PVC products at high temperatures (between

35 °C and 100 °C) (Clausen et al., 2012; Little et al., 2012; Ekelund et al., 2010). In contrast, our measurements of y_0 and V_p suggested that y_0 may not be accurately approximated by V_p at room temperatures, even for vinyl floorings containing a relatively high concentration of phthalates (e.g., sample 2 [DEHP], sample 3 [DINP], and sample 4 [BBP]). But, V_p could have important influences on the value of y_0. For example, with samples 4 (Iso-DEHP) and 5 (DnBP and DEHP) having similar material-phase concentrations (C_0), the significant differences in y_0 are possibly related with the different V_p and chemical properties (Table 3.1). Therefore, the relationship among C_0, y_0, and V_p and the critical level of C_0, above which simple linear partition coefficient cannot apply, require further research.

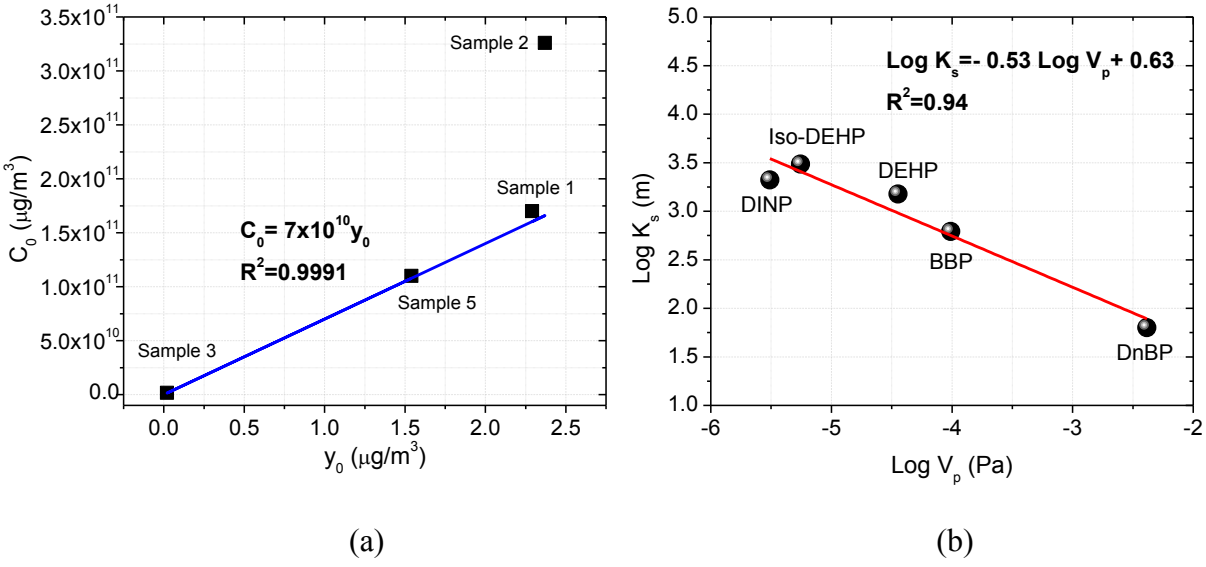

(a) (b)

Figure 3.3: (a) Relationship between C_0 and y_0 for DEHP samples; and (b) Linear regression between K_s and log (V_p).

Although phthalates are present at a very high concentration in vinyl flooring, as SVOCs with low vapor pressures, they emit slowly. The specific emission rate (SER)

can be estimated based on the gas-phase concentration, chamber air change rate, emission surface area and chamber volume (Clausen et al., 2004). After steady state has been reached, the SER was calculated for each vinyl flooring samples (Figure 3.2), falling in the range of 7.8 μg/m^{2}h (DnBP) to 0.06 μg/m^{2}h (Iso-DEHP). In the case of DnBP at this emission rate, calculations show that after five years, only 0.1% of the total mass would have been emitted from the vinyl flooring, although the emission rate measured in these chambers might be somewhat different to that in actual indoor environments. The results indicated that PVC products such as vinyl flooring may behave as permanent indoor sources of phthalates during the product's life time.

3.1.4 Sorption Experiments

Strong sorption occurred on the stainless steel surfaces. Figure 3.4 shows the evolution of phthalate concentrations on the stainless steel rods over time during steady-state conditions, when the gas-phase chamber concentration was constant. The surface concentration of phthalates increased progressively until the sorbed surface concentration reached equilibrium with the chamber air. The time to reach sorption equilibrium was 4 to 25 days, which was significantly reduced compared to a previous study of DEHP sorption (60 days) onto stainless steel (Xu et al., 2012) because of the enhanced mass transfer around the rods caused by the chamber outlet flows. Considering that the values of h_s and A_s are small for the specially designed chamber conditions, sorption onto chamber wall does not have significant influences on the accumulation of gas-phase phthalate concentrations (Equations 5 and 6) and the time to reach chamber steady state (Figure 3.2). Assuming that a linear isotherm (K_s) is appropriate to explain the sorption relationship between stainless steel and gas-phase phthalates, the corresponding K_s values were obtained by dividing the equilibrium concentration on rod surfaces (Figure 3.4) by

the steady-state gas phase concentration within the chamber (Figure 3.2). The difference of K_s for DEHP among samples 2, 3, and 5 is about 40%, which is possibly the result of normal measurement errors of gas- and surface-phase DEHP concentrations. Linear relationship between log (V_p) and log (K_s) were found as shown in Figure 3.3b, with a trend of lower volatility phthalates showing higher K_s values. In addition, phthalates adsorbed on internal stainless steel surface of the chamber were wiped and analyzed at the end of the sorption experiments. The results (Figure 3.4) are comparable to the rod measurements, suggesting that the developed method (rods with air pulling through rod holder) is most likely appropriate to quickly measure phthalate sorption onto indoor sink materials (e.g., wood, cloth, and foam).

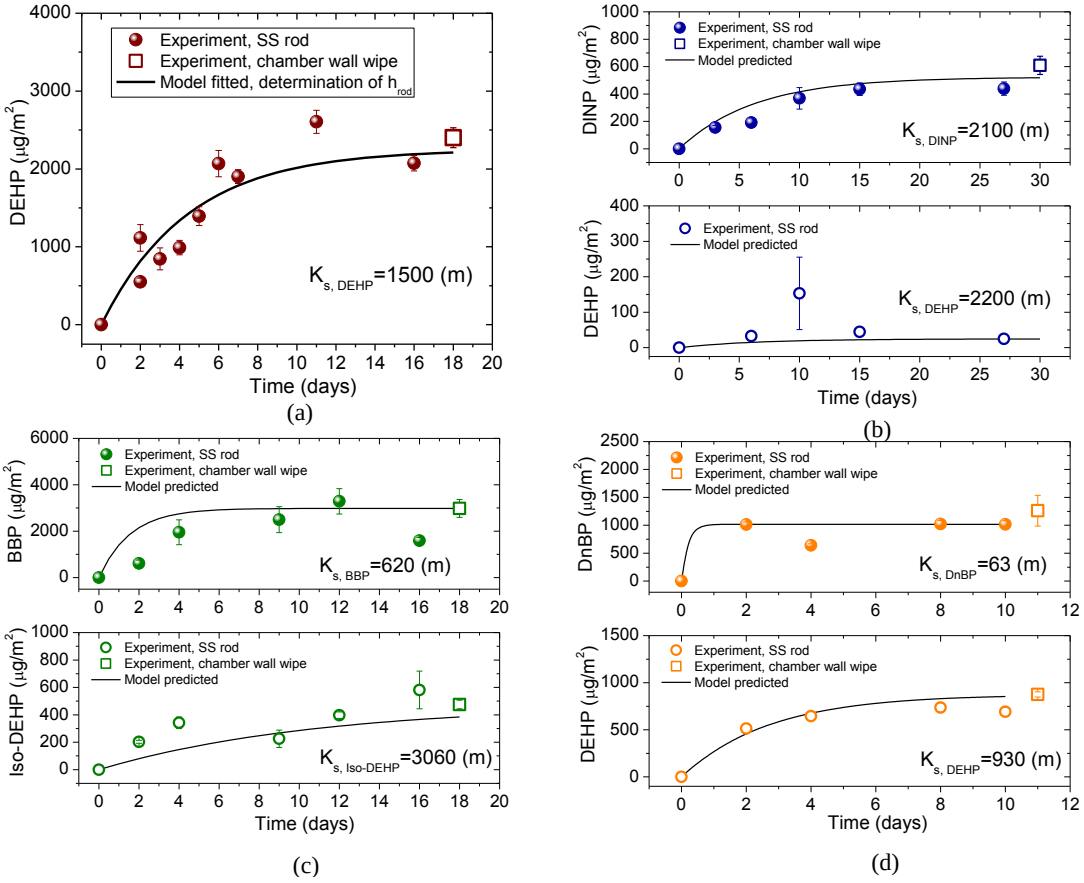

Figure 3.4: Sorption of phthalates on stainless steel surface. (a) Sample 2, (b) sample 3, (c) sample 4, and (d) sample 5.

3.1.5 Estimation of Indoor Exposure to Phthalates

With the knowledge of measured y_0 values, indoor dynamic concentrations resulting from emissions of phthalates can be predicted in multi-phases (e.g., gas, airborne particle, dust, and interior surfaces), using a fate and transport model (Xu et al., 2009; Xu and Liang, 2011). Little et al. (2012) simplified the model and proposed a rapid method to obtain screening-level estimates of indoor exposure to SVOCs. In their simplified model, the steady-state SVOC concentration in indoor air was estimated based on a known y_0:

$$y = \frac{h_m \cdot y_0 \cdot A}{h_m \cdot A + h_s \cdot A_s + (1 + K_p \cdot TSP) \cdot Q} \quad (10)$$

where TSP is the mass concentration of suspended particles in the room and K_p is the equilibrium partitioning of the SVOC between gas phase and particles. The dust-phase concentrations were estimated based on K_{dust} (i.e., the partition coefficients between dust and air). Human indoor exposures to SVOCs can be assessed, with all model parameters that are readily available or that can be easily estimated based on SVOCs chemical properties (Little et al., 2012; Weschler and Nazaroff, 2010). Employing Little et al.'s method, we use the y_0 measured for vinyl flooring samples to assess human exposure to phthalates via inhalation of indoor air, dermal absorption of gas and deposited dust, and oral ingestion of dust when the tested flooring is present in a residential building. The exposure was estimated for five age groups: infants (<1 yr), toddlers (1-3 yrs), children (4-10 yrs), teenagers (11-18 yrs), and adults (≥19 yrs). Equations, exposure factors, and parameters used in the calculation of daily exposure dose can be found in Appendix A (Paper 1). Figure 3.5 shows the contribution of different routes to total exposure of phthalates. The exposure levels of infants, toddlers, and children markedly exceed that of teenagers and adults. A toddler could experience a two to eight times higher exposure than an adult in a home. The findings are similar to those of Guo and Kannan (2011) who measured indoor dust concentrations of phthalates and concluded that children may be more highly exposed than adults. Dermal absorption was the dominant source of DnBP and BBP, whereas ingestion of dust was the dominant pathway of exposure to DEHP, Iso-DEHP, and DINP. For infants, toddlers, and children, exposures to DEHP are higher than the RfD value, which is consistent with observations in previous studies (Little et al., 2012; Nazaroff et al., 2012). Frederiksen et al. (2011) estimated the daily exposure dose of DEHP in Danish people (6-21 yrs) at a median of 4 (μg/kg-bw/day) and

a maximum of 53 (μg/kg-bw/day) based on urinary excretion of DEHP metabolites, which is comparable to the results of this study (12.6-25.3 μg/kg-bw/day).

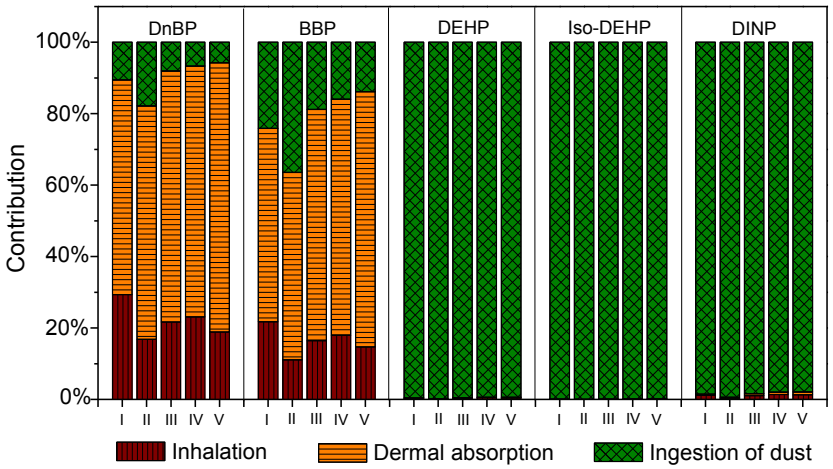

Figure 3.5: Contribution of different routes to total exposure to phthalates.

3.2 THE INFLUENCES OF TEMPERATURE ON PHTHALATE EMISSIONS (OBJECTIVE 2)

3.2.1 Impact of Temperature on Emissions

The concentrations of phthalates and phthalate alternatives were measured periodically in specially designed small chamber, which was operated at an air flow rate of 1000 mL/min, ~0% relative humidity, and four different temperatures (25±0.5, 36±0.5, 45±0.5, and 55±0.5 °C). Figure 3.6 shows that temperature had a strong influence on phthalate emissions. When the temperature was increased from 25 to 36 ºC, the steady-state air concentration of phthalates and their alternatives in the chamber increased up to an order of magnitude for all test samples except sample 5. The specific emission rate (SER) can be estimated based on the gas-phase concentration, chamber air change rate, the surface area of emission source, and the chamber's volume (Clausen et al., 2004). On

average, a 30 ºC increase in temperature (from 25 to 55 ºC) resulted in more than a 300-fold increase in SER, between an increasing factor of 7 (DINCH, sample 5) and as much as a factor of 2000 (DEHP, sample 2). Emission of DnBP from sample 4 showed the highest SER at each temperature. In the case of DnBP emission at 36 ºC (SER ~ 130 $\mu g/m^2h$), calculations show that after five years, only 1% of the total mass would have been emitted from the vinyl flooring sample. Although the SER measured in the chamber might be somewhat different from that in actual indoor environments, the results indicate that PVC products may behave as permanent indoor sources of phthalates during the product's lifetime. But, temperature increase has a strong impact on their emissions from these sources, accelerating off-gassing, elevating their air concentrations, and thereby resulting in significantly greater indoor exposures.

The simplified SVOC emission model (Xu et al., 2012) was used to characterize the emissions of phthalates and phthalate alternatives at different temperatures. Based on the steady-state concentration (y_{ss}) that was measured in the emission chamber, Equation (9) was used to determine the value of y_0 for each vinyl flooring sample emitting specific phthalates at the four different temperatures; the results are listed in Table 3.2. The values of h_m and h_s that were obtained by Liang and Xu (2014a) for the conditions of the test chamber at 25 ºC were corrected to other corresponding temperatures. Because the adsorption of phthalates to chamber wall decreased greatly as temperature increased (Clausen et al., 2012), partitioning between stainless steel and air was ignored at all temperatures except 25 ºC. At 25 ºC, we used the stainless steel/air partition coefficients that were measured in a previous study for phthalates with respect to K_s (Liang and Xu, 2014a). Using the same experimental method, we obtained the K_s values for DINCH (1570 m) and DEHA (1520 m) at 25 ºC in this study. As shown in Figure 3.6, there was reasonable agreement between the gas-phase concentrations of phthalates and phthalate

alternatives predicted by the model and the experimental data that were measured at the different temperatures. When the temperature increased, the value of y_0 increased significantly, and the mass transfer coefficient (h_m) also increased slightly due to the changes in the diffusivity and viscosity of air as a function of temperature. As a result, the steady-state gas phase concentration of phthalates and phthalate alternatives in the chamber increased significantly as the temperature increased. The decrease of partitioning between stainless steel and air at elevated temperatures strengthened the effect, allowing the gas-phase concentration in the chamber to reach steady state more quickly.

Sample ID	**Phthalates**	**Content**	**C_0 ($\mu g/m^3$)**	**y_0 ($\mu g/m^3$)**				**ΔH_{pa} (kJ/mol)**	**ΔH_{vap} (kJ/mol)**
				25 °C	**36 °C**	**45 °C**	**55 °C**		
1 (vinyl flooring)	DEHP	23 ± 3 %	3.26×10^{11}	2.22	13.6	36.9	146	123	116[a]
2 (vinyl flooring)	DINP	20 ± 3 %	3.47×10^{11}	0.43	4.31	16.7	48.3	159	93.8[b]
	DEHP	0.1 ± 0.02 %	1.73×10^{9}	0.02	6.35	14.1	35.5	401	116[a]
3 (vinyl flooring)	BBP	15 ± 2 %	1.93×10^{11}	12.0	14.7	31.7	136	38.7	106 [a]
	Iso-DEHP	7 ± 1 %	9.02×10^{10}	0.17	7.8	25.6	92.7	263	n.a.
4 (vinyl flooring)	DnBP	9 ± 1 %	1.42×10^{11}	27.1	489	1052	4146	196	93.0[a]
	DEHP	7 ± 1 %	1.10×10^{11}	1.44	9.13	15.1	106	125	116[a]
5 (mattress cover)	DINCH	11 ± 1 %	1.88×10^{12}	0.70	2.47	5.15	n.a.	84.3	141[c]
6 (mattress cover)	DEHA	4 ± 0.3 %	1.00×10^{12}	1.05	14.6	36.6	n.a.	179	131[d]

a. (Gobble et al., 2014)
b. Calculated based on measurements in (Cousins et al., 2003).
c. Calculated based on measurements in (BASF, 2013a).
d. Calculated based on measurements in (BASF, 2013b).

Table 3.2: Summary of material-phase concentration (C_0), y_0 values for test samples at different temperatures, enthalpy of phase change between polymeric material and air (ΔH_{pa}), and enthalpy of vaporization for pure chemical liquids (ΔH_{vap}).

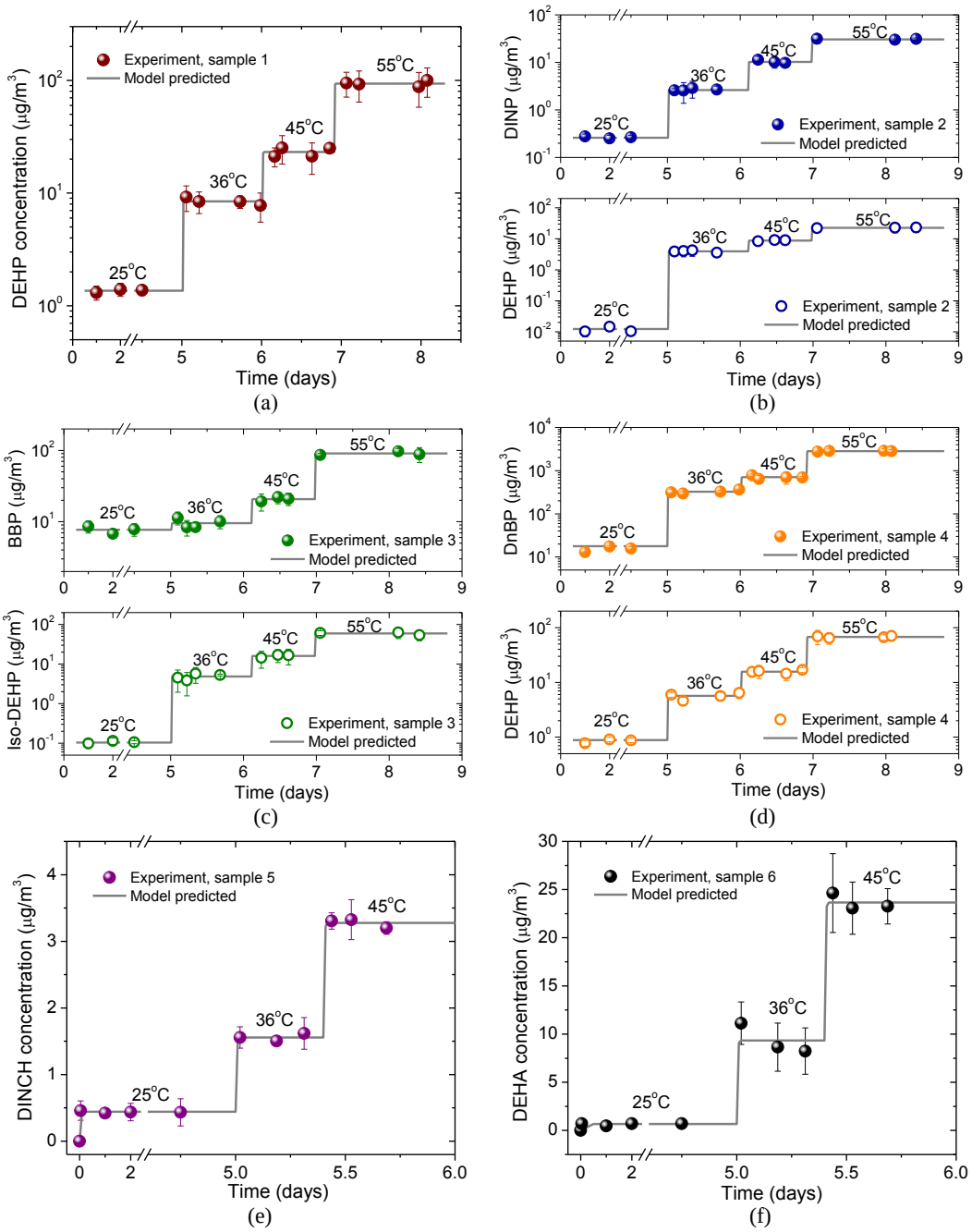

Figure 3.6: Gas-phase chamber concentration of phthalates and phthalate alternatives emitted from tested samples at different temperatures. (a) sample 1, (b) sample 2, (c) sample 3, (d) sample 4, (e) sample 5, and (f) sample 6.

3.2.2 The Relationships between y_0, V_p, C_0, and Temperature

The material-phase concentration (C_0) of phthalate additives in different products can vary substantially, thereby influencing the value of y_0. Samples 1, 2, and 4, which contained different levels of DEHP, were used to explore the relationship between y_0 and C_0. We found that a simple partition coefficient can be used to obtain a linear relationship between y_0 and C_0 at different temperatures. Although only three data observations might not be enough, the finding was consistent with the results of a recent study on phthalate emissions from latex paint (Schripp et al., 2014) and a study of volatile organic compound (VOC) emissions from building materials (Kumar and Little, 2003). Therefore, when the contents of phthalate and phthalate alternatives in the material phase are relatively low, they may not behave as pure liquids, so the values of y_0 would be related to C_0 and would be lower than their V_p values. The critical level of C_0, below which the simple linear partition coefficient can be used, requires further research.

Figure 3.7 shows the ratio of C_0 to y_0 as a function of temperature, allowing us to examine their relationship. The temperature dependence of C_0/y_0 was very strong. The value of C_0/y_0 decreased between a factor of 10 (BBP in sample 3) and by as much as a factor of 2000 (DEHP in sample 2) when the temperature increased from 25 to 55 °C. This also indicates that the C_0/y_0 value is highly variable under environmental conditions as a result of temperature fluctuations. An exponential relationship was observed between C_0/y_0 and the reciprocal temperature (Figure 3.7):

$$\frac{C_0}{y_0} = \exp\left(\frac{A}{T} + B\right) \tag{11}$$

where A and B are constants for a given chemical and polymeric material. Non-linear regression analysis was conducted to avoid any possible errors when fitting a nonlinear

model by transforming to linearity (MathWorks, 2014). The correlations between C_0/y_0 and T were highly significant, with R^2 ranging between 0.85 and 1.

Interestingly, this finding was in agreement with the well-known van't Hoff equation which is generally used to describe the dependence of equilibrium partitioning on temperature (Schwarzenbach et al., 2003). Assuming that the ratio of C_0 to y_0 was approximately equal to the material/air equilibrium partition coefficient, the enthalpy of phase change (polymer/air), ΔH_{pa} (kJ/mol), can be calculated according to the equation:

$$\Delta H_{pa}=1000\times R\times A \quad (12)$$

where R is the ideal gas constant ($Pa\cdot m^3/mol\cdot K$), A is the constant given in Figure 3.7, and the factor of 1000 is a unit converter. Table 3.2 lists the values for ΔH_{pa} along with the calculated enthalpies of vaporization (ΔH_{vap}) for pure phthalates. The enthalpies of vaporization and polymer/air phase change are clearly different, with ΔH_{pa} of DEHP (samples 1 and 4) having the closest values to the ΔH_{vap} of pure DEHP liquid. In general, ΔH_{pa} is somewhat greater than ΔH_{vap}, except for the cases of BBP (sample 3) and DINCH (sample 5). The results indicate that, for most phthalate and phthalate alternatives, the interactions with polymeric materials are stronger than the interactions with pure chemical liquid. Similar results were observed in a previous study of the off-gassing formaldehyde from vinyl flooring (Zhang et al., 2007). Therefore, using V_p to approximate y_0 may lead to misleading results. In addition, no significant dependence of ΔH_{pa} on the molecular weight of phthalates was found. But the values of ΔH_{pa} for phthalates are much greater than that for formaldehyde (37 kJ/mol), which has a lower molecular weight (Zhang et al., 2007). Material-phase concentration (C_0) may also have an impact on the value of ΔH_{pa}. For sample 2, which contained DEHP, the value of ΔH_{pa} is larger than those of samples 1 and 4, which might relate to the sample's low material-phase concentration of DEHP (C_0=0.1%). For ideal solutions, Dobruskin (2014) found

that the enthalpy of evaporation for each component increased as the mole fraction of the component decreased.

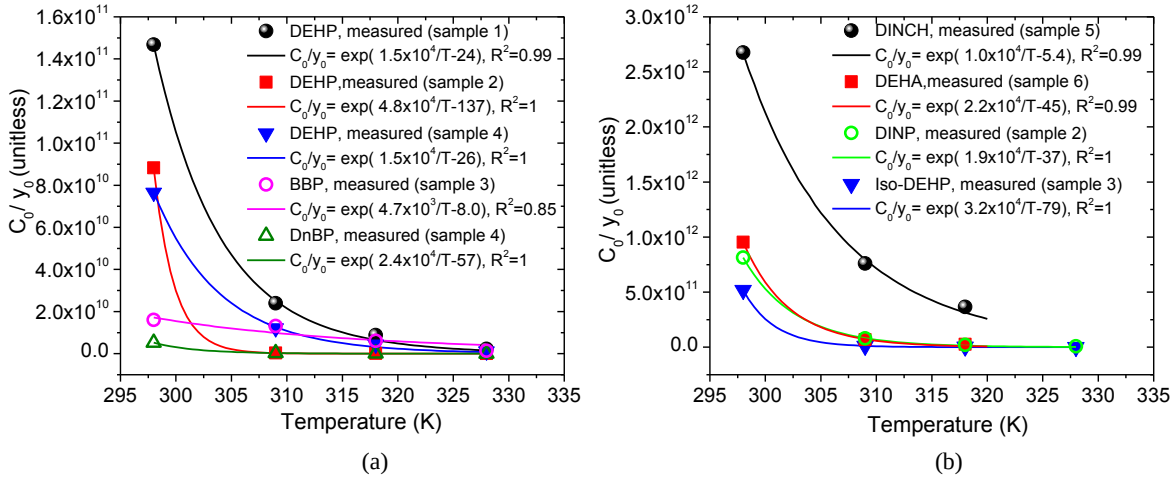

Figure 3.7: The ratio of C_0 to y_0 as a function of temperature. Curved lines are nonlinear regression fits using van't Hoff equation. (a) DnBP, BBP, and DEHP, and (b) DEHA, Iso-DEHP, DINP, and DINCH.

3.3 The Influences of Ventilation and Surface Sorption on Phthalate Emissions (Objective 2)

3.3.1 Wood Chambers

To investigate the mechanisms governing the process of surface absorption and the influence of surface sorption on emission of phthalates, we also made emission chambers out of soft maple wood (Fine Lumber and Plywood, Inc.) in addition to stainless steel. As shown in Figure 3.8, the wood chamber has the same configuration as those made with stainless steel. Similarly, three thin wood strips, matched to the interior wood chamber surface, were inserted into the chamber and then periodically removed to measure the surface absorption on the wood. The air leakage rate for both types of chambers was less than 2% of the total flow rate.

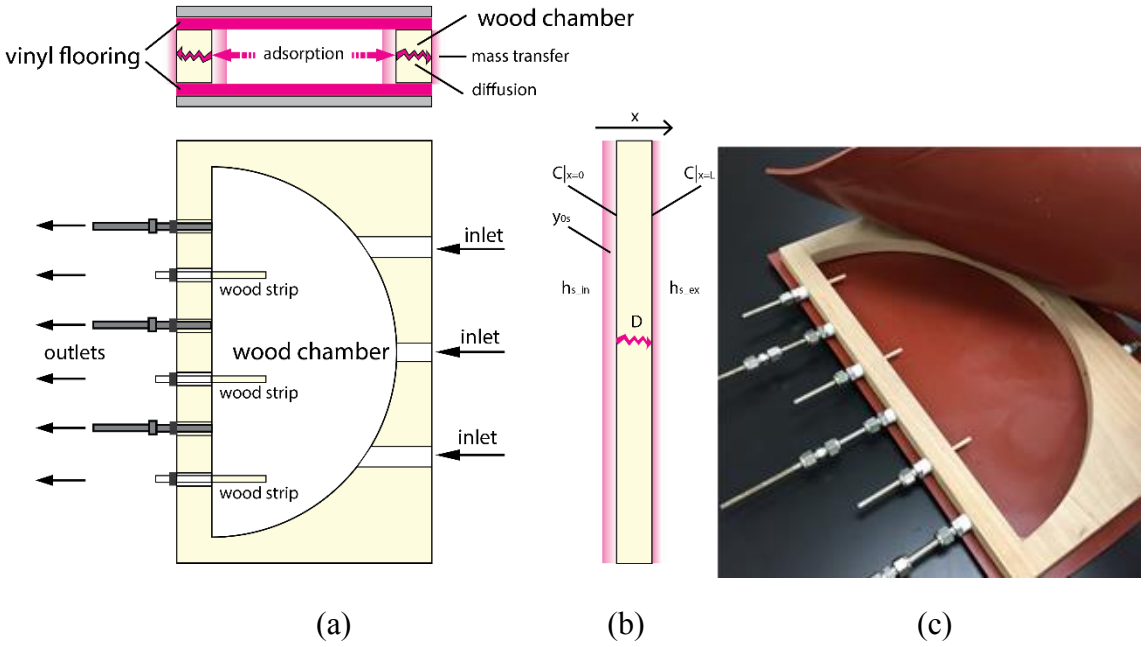

(a) (b) (c)

Figure 3.8: Configuration of the wood chamber. (a) Side and top view, (b) surface absorption at wood chamber wall, and (c) photo.

3.3.2 SVOC Emission Model including Penetrable Absorptive Surfaces

Xu and Little (2006) developed an SVOC emission model that includes adsorption at impenetrable surfaces (e.g., stainless steel chamber wall), and the model was recently simplified by Xu et al. (2012). In their analysis, their simplified SVOC emission model is obtained by combing equations (3)-(6).

To include absorption at penetrable surfaces (e.g., hardwood chamber wall) in the SVOC emission model, partitioning between the gas phase and the sorption surface, molecular diffusion within the material, and mass transfer through the boundary layer that exists adjacent to the sorption surfaces should be considered (Figure 3.8). Using the wood chamber as an example, the governing equation describing transient diffusion through the wood material is

$$\frac{\partial C}{\partial t} = -D\frac{\partial^2 C}{\partial x^2} \tag{13}$$

where C ($\mu g/m^3$) is the material-phase concentration of phthalates in wood, t is the time, and x is the distance from the chamber interior wall. The diffusion coefficient of phthalates in wood, D (m^2/s), is assumed to be independent of material-phase concentration. The initial condition assumes that the wood material contains no phthalates. The boundary condition imposed at the interior chamber wall is

$$-D\frac{\partial C}{\partial x}|_{x=0} = h_{s_{in}}(y - y_{0s}) \tag{14}$$

where h_{s_in} (m/s) is the convective mass-transfer coefficient near the interior chamber wall. Equilibrium exists between concentrations in the surface layer of the interior wall and the air immediately adjacent to the surface, or

$$C|_{x=0} = K_{s\_wd} \cdot y_{0s} \tag{15}$$

where K_{s_wd} (dimensionless) is the wood/air partition coefficient for phthalates. Similarly, the boundary condition imposed at the exterior surface of the wood chamber is

$$-D\frac{\partial C}{\partial x}|_{x=L} = h_{s\_ex}\left(\frac{C|_{x=L}}{K_{s\_wd}} - 0\right) \tag{16}$$

3.3.3 Emission Experiments

Gas-phase concentration of DEHP and DINP was measured for about 20 days in stainless steel and wood chambers, as shown in Figure 3.9. Phthalate concentrations increased and reached steady state in less than five days for all measurements. The steady-state concentration in the stainless steel chamber was about 2–3 times higher than that in the wood chamber for both DEHP and DINP. A simple calculation using Equation (3) indicated that phthalate emission rate from the vinyl floorings increased due to the change in the chamber material from stainless steel to hardwood. This phenomenon may not be simply explained by the possibly larger partition coefficient between wood and air than that between stainless steel and air, because the calculations

using the SVOC emission model showed that stronger surface adsorption (i.e., larger K_s value) increased the time of gas-phase concentration to reach steady state in a chamber but did not influence the level of the concentration at steady state. Therefore, in addition to surface adsorption, diffusion of phthalates within the wood material (i.e., absorption) must be considered. In other words, the gas-phase phthalates in the wood chamber were depleted more than in the stainless steel chamber due to the diffusion mass flow through the chamber wall. To maintain the concentration at steady-state level, the gas-phase DEHP and DINP were resupplied with increased emissions from the vinyl flooring in the wood chamber.

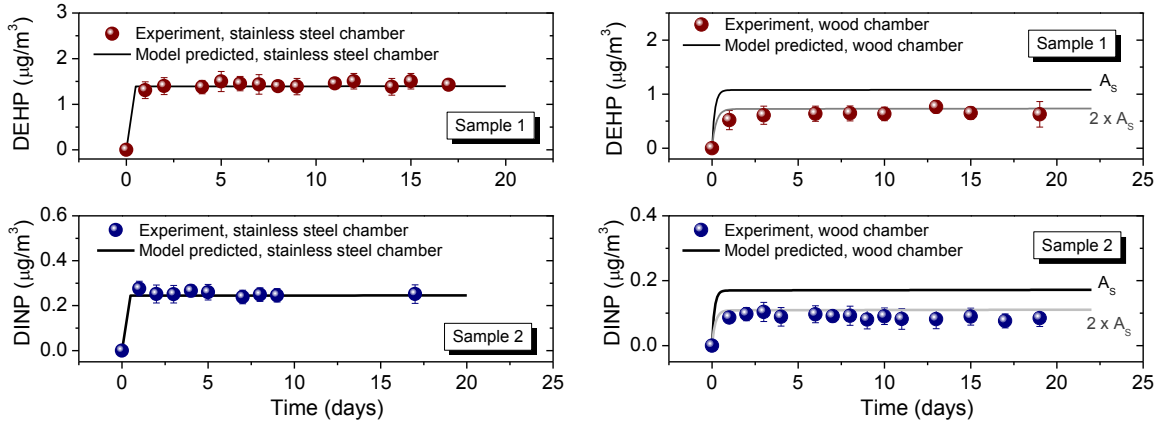

Figure 3.9: Gas-phase chamber concentration of phthalates emitted from vinyl flooring. a) stainless steel chambers, and b) wood chambers.

3.3.4 Characterization of Surface Adsorption and Absorption

To determine the sorption properties of the stainless steel and wood surfaces for phthalates, sorption experiments were conducted using the methods described. Figure 3.10 shows the evolution of phthalate concentrations on the stainless steel rods and the wood strips over time during steady-state conditions, when the gas-phase chamber

concentration was constant. The surface concentration of phthalates increased progressively until sorption equilibrium with the chamber air was reached. The time for DEHP and DINP to reach sorption equilibrium on stainless steel and wood surfaces was no more than 10 days.

For impenetrable surfaces such as stainless steel, assuming that a linear isotherm, K_s (m), is appropriate to explain the adsorption relationship between the surface and the gas-phase phthalates, the corresponding K_s values were obtained by dividing the equilibrium concentration on the rod surfaces (Figure 3.10a) by the steady-state gas phase concentration within the stainless steel chamber (Figure 3.9). DINP has a higher K_s value (2100 m) than DEHP (1500 m) due to its higher molecular weight and lower vapor pressure.

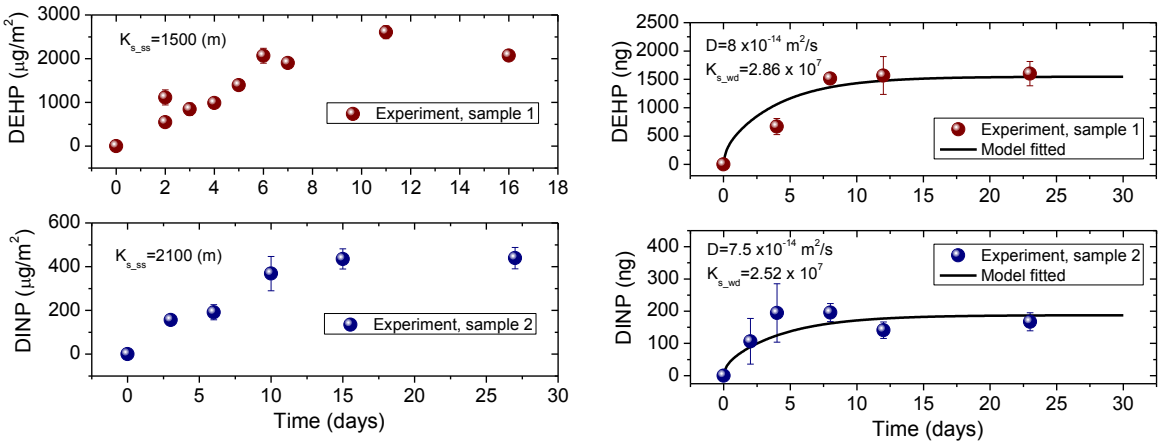

(a) (b)

Figure 3.10: Sorption of phthalates on (a) stainless steel surface and (b) wood surface.

For penetrable surfaces such as maple wood, diffusion within the material must be considered. The wood strip can therefore be envisioned as a very thin symmetric slab capturing phthalates from the chamber outlet air flow at its top and bottom surfaces.

Equation (13) can be used as the governing equation describing transient diffusion through the wood strips. The initial condition assumes that the wood strips contain no phthalates. Because the gas-phase concentration passing across the wood strips was maintained at a constant value, under the experimental conditions, the boundary conditions imposed are

$$\frac{\partial C(x,t)}{\partial x} = 0, \qquad t > 0, \qquad x = 0 \ \ (due\ to\ symmetry) \tag{17}$$

$$-D\frac{\partial C(x,t)}{\partial x} = h_{m\_strip}\left(y_{ss} - \frac{C(x,t)}{K_{s\_wd}}\right), \quad t > 0, \quad x = L/2 \tag{18}$$

where y_{ss} is the steady-state gas-phase concentration of phthalates in chamber air, h_{m_strip} is the convective mass transfer coefficient near the wood strip surface, K_{s_wd} is the equilibrium partition coefficient between the wood surface and the gas phase, and L is the thickness of the strip. For a given value of D and K_{s_wd}, there is a critical value of h_{m_strip}; if h_{m_strip} is larger than the critical value, the impact of convective mass transfer around the strips can be neglected. For the experimental condition, an air flow of 300 mL/min was drawn by a pump through each strip holder. The high air velocity surrounding the strip (about 3.72 m/s) resulted in a large external mass transfer coefficient, which was approximately 0.013 m/s estimated using correlation equations (Axley, 1991), and thus made the impact of h_{m_strip} ignorable. Therefore, the influence of external mass transfer resistance was neglected, and Equation (18) was replaced by

$$C(x,t) = K_{s\_wd} \cdot y_{ss}, \quad t > 0, \quad x = L/2 \tag{19}$$

After sorption equilibrium was reached, phthalates were ultimately uniformly distributed throughout the strip. Similarly as stainless steel rods, the value of K_{s_wd} can be obtained by dividing the equilibrium concentration of phthalate in the strip (Figure

3.10b) by the steady-state gas phase concentration in the wood chamber (Figure 3.9). The diffusion coefficient (D) was then determined by fitting Equations (12), (17), and (19) using the least-squares method, as shown in Figure 3.10b. Liu et al. (2014c) measured the diffusion coefficients and the material/air partition coefficients of PCBs, which also belongs to SVOCs, for different sink materials. The values obtained in the current study for maple wood (DEHP: $D=8\times10^{-14}$ m^2/s; $K_{s\_wd}=2.86\times10^7$ and DINP: $D=7.5\times10^{-14}$ m^2/s; $K_{s\_wd}=2.52\times10^7$) are comparable to those measured for large molecular PCBs absorbed to commonly used laboratory materials such as LDPE sheets ($D=2.2\times10^{-13}$ m^2/s; $K_{s\_LDPE}=3.6\times10^7$) and concrete disks ($D=9.7\times10^{-15}$ m^2/s; $K_{s\_concrete}=4.76\times10^7$), though wood materials were not included in that study. Compared to previous studies of VOCs absorbed by gypsum board (e.g., dodecane: $D=4.6\times10^{-7}$ m^2/s; $K_{s\_gypmsum}=4160$) (Corsi et al., 2007), the diffusion coefficients obtained for phthalates are significantly lower while the partition coefficients (K_{s_wd}) are much higher. This finding is in agreement with theoretical expectations that D decreases when the molecular weight increases (Schwarzenbach et al., 2003) while K_s increases when the chemical vapor pressure decreases (Zhao et al., 2004).

A common problem for estimating sink parameters is to fit D and K_s simultaneously from one single data set, because it may generate different results due to the starting value issue of nonlinear regression (Haghighat et al., 2002; Liu et al., 2014b; Zhang et al., 2001). The current study developed a novel approach for measuring surface absorption, which allowed us to determine the diffusion and partition coefficients independently and accurately, and thus solved this fundamental problem. In addition, the high air flow around the strips allows absorption to reach equilibrium quickly. Therefore,

the proposed approach could be suitable to quickly measure and characterize the SVOC absorption process for a wide range of sink materials.

3.3.5 The Impact of Air Flow Rate

Two stainless steel chambers with the same type of vinyl flooring sample (sample 1) were operated at a temperature of 25 ºC and under the flow rate of 300 mL/min and 3000 mL/min, respectively. The gas-phase concentration of DEHP was directly measured in the experiments, and it reached steady state quickly in both chambers. As shown in Figure 3.11, the steady-state concentration in the chamber with the flow rate of 300 mL/min was about 50% higher than that in the chamber with the flow rate of 3000 mL/min. In a previous study (Clausen et al., 2010), the gas-phase concentration differed only slightly for various flow rates due to unexplained scatters and co-variances in the concentration profile. However, the current measurements showed that the steady-state concentrations decreased when the flow rate increased in the chamber and therefore have a dilution effect for DEHP. After the flow rate was adjusted to 1000 mL/min, the gas-phase concentration changed instantly in both chambers and agreed well with each other, suggesting that DEHP concentration is very sensitive to the chamber air flow rate. The specific emission rate (SER) can be estimated based on the gas-phase concentration at steady state, chamber air change rate, emission surface area, and chamber volume (Clausen et al., 2004). The SER calculated for the three chambers was 0.2 $\mu g/m^2/h$ (300 mL/min), 0.6 $\mu g/m^2/h$ (1000 mL/min), and 1.5 $\mu g/m^2/h$ (3000 mL/min), respectively. Because the DEHP air concentration adjacent to the emission surface was constant (y_0), the vertical air concentration gradient within the boundary layer was therefore larger at the high flow rate due to the lower air concentration in the chamber (y), which in turn increased the driving force of emission. Additionally, the convective mass transfer

coefficient was increased by the higher air velocity above the emission source. As a result, the SER increased greatly with the increasing flow rate. Therefore, although the increased flow rate reduced the residence time of air and introduced more dilution, the increased SER compensated for the decrease in the gas phase, and the gas-phase concentration of DEHP did not drop substantially with the increasing air flow rates.

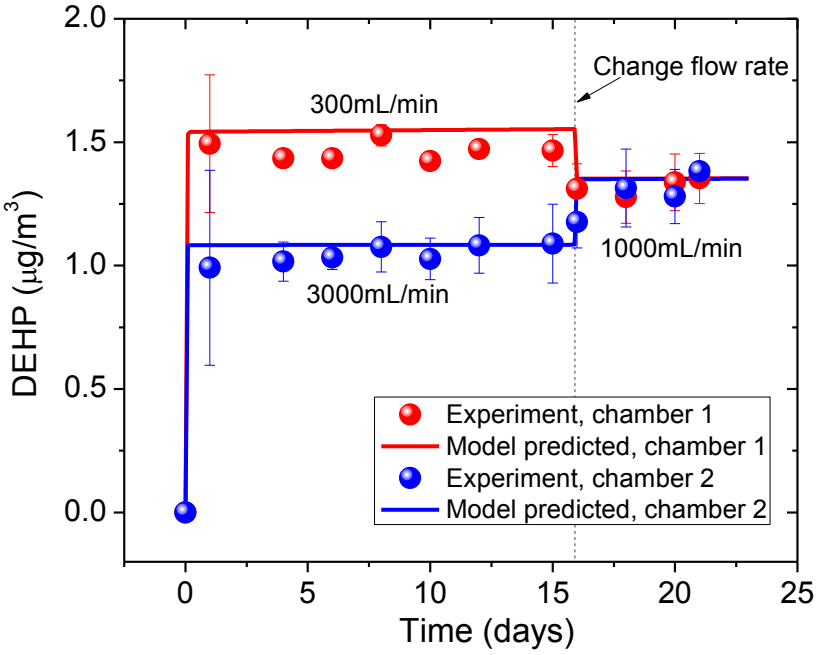

Figure 3.11: Gas-phase chamber concentration of phthalates emitted from vinyl flooring at different flow rates.

3.4 Large-Scale Chamber Investigation and Simulation of Phthalate Emissions from Vinyl Flooring (Objective 2)

3.4.1 Small Chamber Experiment

Small-scale chamber test was conducted to characterize phthalate emissions from the selected vinyl flooring and obtain the dominant emission parameter (y_0). A specially-designed, stainless steel chamber used in previous experiments (Liang and Xu 2014a)

was employed in this study. Figure 3.12 shows the gas-phase concentration of phthalates obtained in the small chamber experiments. The experimental conditions were constant over the entire test period. Each data point in Figure 3.12 represents the mean value of concentrations in triplicate measurements with error bars representing the standard deviation. At the temperature of 25 ºC, the concentration of DINP and DEHP increased and reached steady state in about three days. In addition, the steady-state concentration of DINP is approximately 20 times higher than that of DEHP, primarily related to its high material-phase concentration in vinyl flooring.

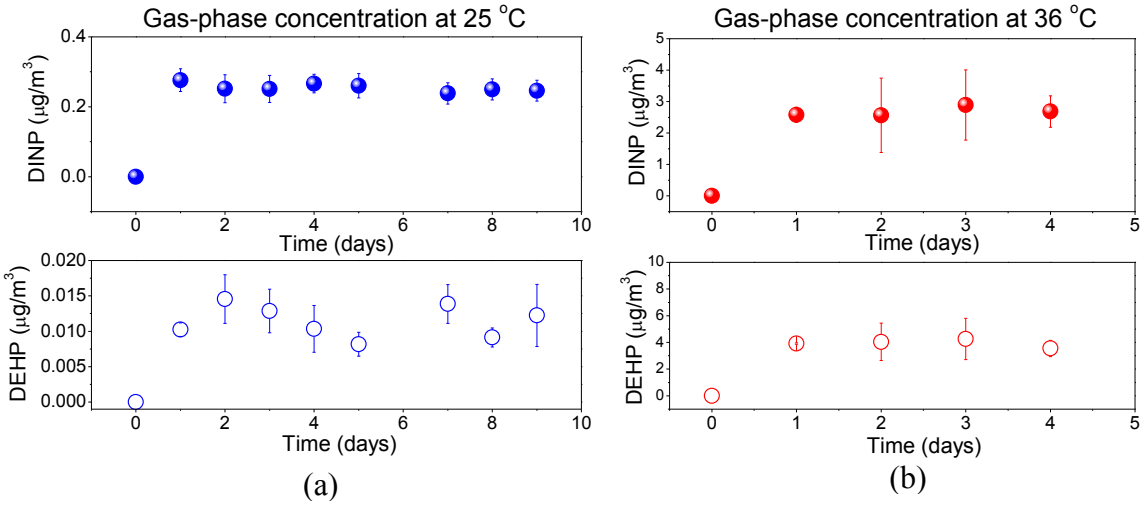

Figure 3.12: Gas-phase concentration of DINP and DEHP measured in the small chamber experiments at two different temperatures. (a) 25 ºC and (b) 36 ºC.

Temperature had a strong influence on phthalate emissions. When the temperature was increased from 25 to 36 ºC, the steady-state air concentration of phthalates in the chamber increased 10 and 80 times for DINP and DEHP, respectively. The specific emission rate (SER) can be estimated based on the gas-phase concentration, chamber air change rate, the surface area of emission source, and the chamber's volume (Clausen et

al. 2004). A 10 ºC increase in temperature (from 25 to 36 ºC) resulted in significant increase in SER. For DINP, the SER increased by 10 times, from 0.11 ± 0.01 to 1.1 ± 0.06 μg/m^2/h, while for DEHP, the value increased from 0.005 ± 0.001 to 1.6 ± 0.1 μg/m^2/h, which is about 300-fold. Based on the steady-state concentration (y_{ss}) that was measured in the small emission chamber, we can determine the value of y_0 (the gas-phase concentration of phthalates in equilibrium with the material phase) for the tested vinyl flooring sample at the two different temperatures based on previous studies (Liang and Xu, 2014a and 2014b). The obtained y_0 values are 0.43 μg/m^3 at 25 ºC and 4.31 μg/m^3 at 36 ºC for DINP and 0.02 μg/m^3 at 25 ºC and 6.35 μg/m^3 at 36 ºC for DEHP.

3.4.2 Large Chamber Experiment

Large-scale chamber measurement was conducted at Syracuse University to investigate the effect of environmental conditions on the emission and transport of phthalates. The full-scale chamber (4.8 m × 3.7 m × 3.0 m) was equipped with a heating ventilation and air-conditioning (HVAC) system, which was automatically controlled to provide precise temperature, RH, and air velocity in the chamber (Figure 3.13). The air-handling unit was equipped with a high efficiency particulate air (HEPA) filter and activated carbon filters to control the pollutant concentration in the supply air. The chamber was operated at a RH of 30%, with a total air flow rate of 270 m^3/h and an air change rate (ACH) of 0.5/h. The vinyl flooring used in the small chamber experiments was installed in the chamber, covering the chamber floor. The large chamber experiment was carried out in three phases. First, the chamber was operated at a high temperature (36 °C) with a large fan on. The temperature of 36 °C was selected to shorten the time for the gas-phase concentration in the chamber to reach steady state, due to the reduced sorption to the chamber surfaces at a relatively high temperature. The large fan with an

air flow rate of 0.9 m^3/s was used to increase the air velocity near the emission source and enhance air mixing in the chamber. In the second phase, the large fan was turned off and a small fan with an air flow rate of 0.2 m^3/s was powered on while the temperature was maintained at 36 °C. In the third phase, the operating temperature was reduced to 25 °C and the large fan was powered back on instead of the small fan.

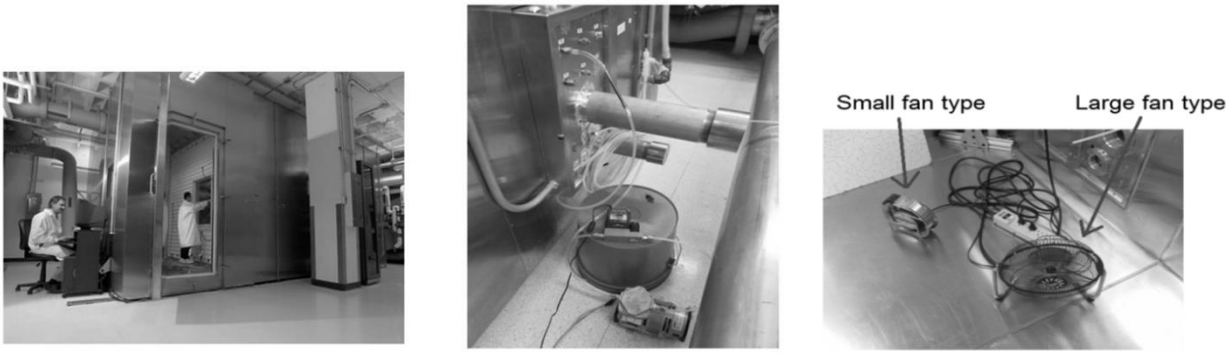

(a) (b) (c)

Figure 3.13: Experimental setup for large chamber experiments. (a) photo of the large environmental chamber; (b) air sampling setup; and (c) mixing fans.

Figure 3.14 shows the measured phthalate concentrations in the large chamber over a period of a month, and the concentration trends for DINP and DEHP are similar. In the first experimental phase, the concentration of DINP and DEHP slowly increased and had not reached steady state at the end of the first phase, although a fast concentration build-up was expected at such a high temperature. The result suggested that surface sorption onto interior surfaces of the chamber (e.g., chamber wall and inner surface of HVAC air duct) could still be strong at 36 ºC for those SVOC compounds, which increased the time for the gas-phase concentration to become stable. Consistent with the lower area/volume ratio, the gas-phase concentrations of DINP and DEHP at 36 ºC were about three times lower in the large chamber experiment than in the small

chamber experiment (Figure 3.12). Nevertheless, the SERs observed in the large chamber (DINP: 2.7 μg/m^2/h and DEHP: 3.2 μg/m^2/h) were consistent at an order of magnitude with those obtained in the small chamber experiment at 36 ºC.

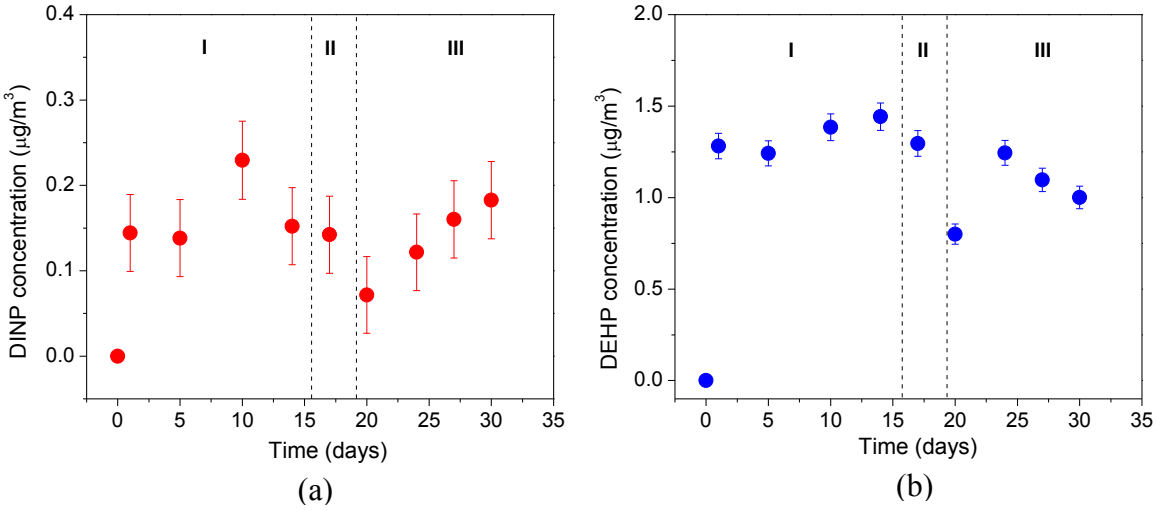

Figure 3.14: Gas-phase concentration phthalates measured in the large chamber experiments with Roman numerals indicating experimental phases. (a) DINP and (b) DEHP.

From the first to the second phase, when a large fan was replaced with a small fan, the velocity across the vinyl flooring sample was reduced by half. As a result, the mass transfer coefficient above the vinyl flooring surface declined, which further caused a decrease of the emission rate, and thus the gas-phase concentrations of DINP and DEHP in the large chamber reduced slightly on day 16. When the third phase was initiated, the temperature of the chamber was reduced to 25 ºC. The concentrations of phthalates dropped instantly and steeply at the beginning, due to the significantly reduced emission from the vinyl flooring (Figure 3.14a). However, the concentration did not decrease as quickly thereafter, which is possibly related to desorption of phthalates from the internal surfaces of the chamber as the gas-phase concentration decreased.

3.4.3 Modeling of Phthalate Emissions in the Large Chamber

To further interpret the experimental results in the large chamber, we extended the SVOC emission model (Xu and Little, 2006; Xu et al., 2012) to predict phthalate concentrations in the large chamber, based on the knowledge of y_0 obtained in small-chamber measurements. Figure 3.15 shows the schematic representation of the model. Phthalates are emitted from the vinyl flooring installed in the large chamber and sorbed onto interior surfaces of the chamber, including chamber walls, ceiling, and the returning duct of the HVAC system. Considering that a high-efficiency particulate air filter was used to precondition the supply air to the chamber, we did not include particle dynamics in the model. We assumed that the air is well-mixed in the chamber with the use of large/small fans; therefore, the gas- and surface-phase concentrations of phthalates were assumed uniformly distributed. The accumulation of the gas-phase concentration of phthalates in the chamber obeys the following mass balance equation:

$$V\frac{dy(t)}{dt} = Q_r y_r(t) + E(t)A - \frac{dq(t)}{dt}A_s - Qy(t) - Q_r y(t) \qquad (20)$$

where y ($\mu g/m^3$) is the bulk gas-phase concentration of phthalates in the chamber, V (m^3) is the interior volume of the chamber, Q_r (m^3/s) is the air flow rate through the return duct, y_r ($\mu g/m^3$) is the gas-phase concentration of phthalates from the return duct, E ($\mu g/m^2/h$) is the emission rate of phthalates from vinyl flooring, A (m^2) is the area of the vinyl flooring, q is the surface concentration ($\mu g/m^2$) of phthalates on interior chamber surfaces (i.e., walls and ceiling), A_s (m^2) is the area of the interior surfaces, and Q (m^3/s) is the fresh air flow rate.

Similarly, in the return duct of the HVAC system, the accumulation of gas-phase concentration of phthalates can be described as

$$V_r \frac{dy_r(t)}{dt} = Q_r y(t) - Q_r y_r(t) - K_s \frac{dy_r}{dt} A_{sr} \quad (21)$$

where V_r (m^3) is the total volume of the return duct, A_{sr} (m^2) is the interior surface area of the duct. Because the air velocity across the interior surface of the return duct is high, we assumed instant sorption equilibrium between the gas- and surface-phase concentrations of phthalates within the duct.

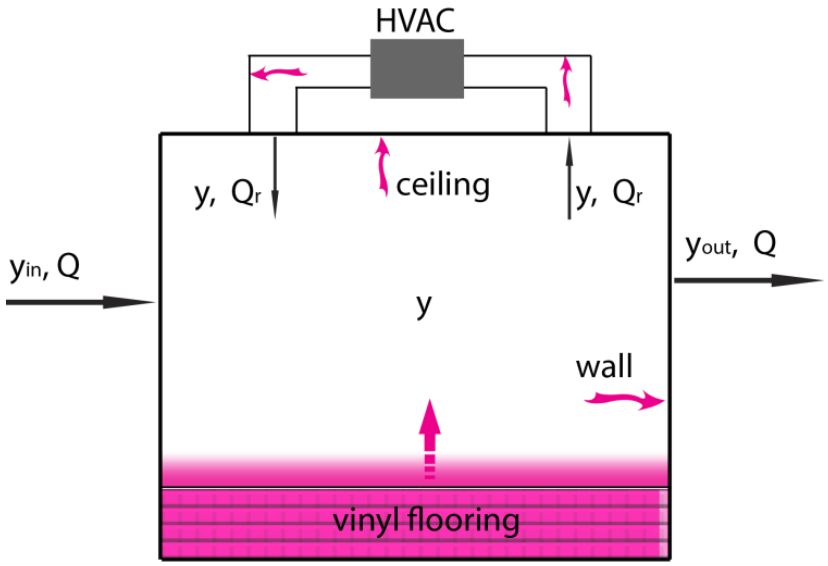

Figure 3.15: Schematic representation of vinyl flooring in the large experimental chamber. HVAC = heating, ventilation and air conditioning system.

As shown in Figure 3.16, reasonable agreement was obtained between the gas-phase concentrations of DEHP and DINP calculated by the model and the experimental data. The difference might be related to uncertainty in the measured chemical concentrations as well as other environmental parameters. For example, we did not collect duplicate samples in the large chamber experiment, which may reduce the reliability of the data. DINP and DEHP showed opposite concentration trends during the third experimental phase. It is difficult to determine whether the slight increase of DINP

concentration was due to the uncertainty of measurements. In addition, air samples in the large chamber experiment were collected by sorbent tubes via long Teflon tubing. The mass loss of phthalates onto sampling pathways might result in underestimations of the real gas-phase concentration in the large chamber. Furthermore, the difference between model calculation and experimental data may also be related to the nonuniform distribution of the gas- and surface-phase phthalates in the large chamber. We measured the air velocity above the vinyl flooring during the experiment to obtain the mass transfer coefficient (h_m) using correlation equations (Axley, 1991). But use of the estimated h_m value resulted in even worse model prediction, indicating that the mass transfer coefficient above the emission surface might not be equal to that above the sorption surfaces. Therefore, we used the concentration data to obtain a lumped parameter, the fitted h_m, which could result in uncertainty in model calculation.

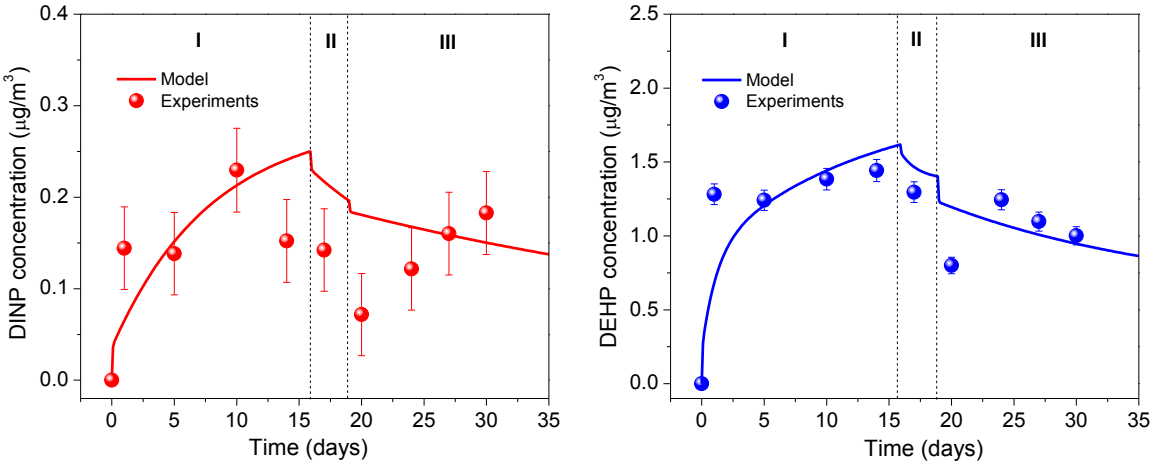

Figure 3.16: Comparison of fitted gas-phase concentration with data measured in the large experimental chamber. (a) DINP and (b) DEHP.

We further investigated the influence of temperature, air mixing, and ACH on the emission of DEHP in the large chamber using the validated model. As shown in Figure

3.17a, it takes over 500 days for the gas-phase concentration of DEHP to reach steady state in the large chamber at the temperature of 25 ºC. In the design of the large chamber experiment, the selection of 36 ºC helped to speed up the concentration build-up. However, the model simulation shows that it still takes about 50 days for the DEHP concentration to become stable at the temperature of 36 ºC. The effect of ACH on reducing DEHP concentration is more obvious at 36 ºC than at 25 ºC, because DEHP behaves more like a VOC compound at a higher temperature. Air mixing (i.e., air velocity) above the emission surface plays an important role on the fate of DEHP in the second phase of the experiment. As shown in Figure 3.17b, the gas-phase concentration of DEHP dropped significantly with a decrease in velocity and h_m close to the vinyl flooring surface. If the third experimental phase was continued, it would take about 1000 days for the gas-phase concentration of DEHP to reach a steady-state level close to that in the small chamber experiment, indicating the persistence of the SVOC compound. During the process, an increase of ACH would only have a limited effect on reducing DEHP concentration; in contrast, the use of all fresh air (ACH=5/h) would result an instant and steep concentration drop, because the amount of DEHP desorbed from the interior surfaces of HVAC duct can be excluded from the chamber system.

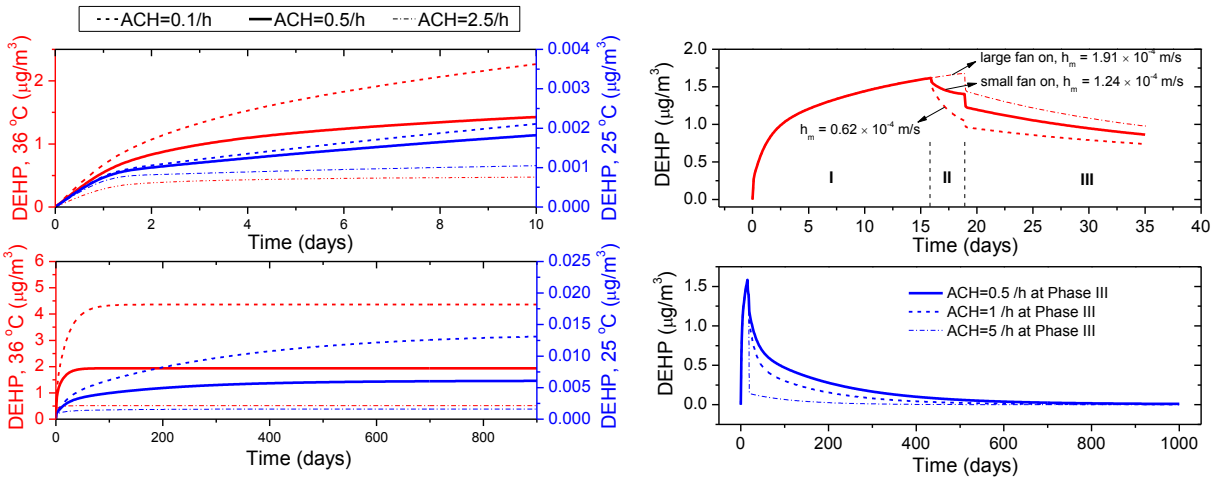

(a) (b)

Figure 3.17: (a) Influence of temperature and air change rate (ACH) on DEHP gas-phase concentration in the large experimental chamber; and (b) influence of air mixing on DEHP emission in Phase II and the effect of ACH on DEHP concentration in Phase III of the large chamber experiments.

3.5 THE FATE AND TRANSPORT MODEL FOR INDOOR PHTHALATES (OBJECTIVE 3)

3.5.1 Model Description

The indoor residential fate model of phthalate plasticizers is a dynamic mass-balance model. This model considers airborne phthalates with input from indoor sources, resuspended particles, and desorption from interior surfaces. Losses occur through air advection, particle deposition, dust removal, and phthalate transport to surfaces. As shown in Figure 3.18, phthalates are emitted from vinyl flooring in a residential environment, the gas-phase phthalate is adsorbed onto interior surfaces, including walls, ceiling, wood floor, furniture, windows, tile, ceramic fixtures, and particles through partitioning mechanisms (Figure 3.19). Particle deposition and resuspension that may further accelerate the mass transfer between sources and sinks are included in this model. In addition to adsorptive partitioning to interior surfaces, phthalates may also diffuse into

porous materials (e.g. carpet) and sorb within the materials (Figure 3.20). Over time, such processes may establish important reservoirs and is thus included in the model.

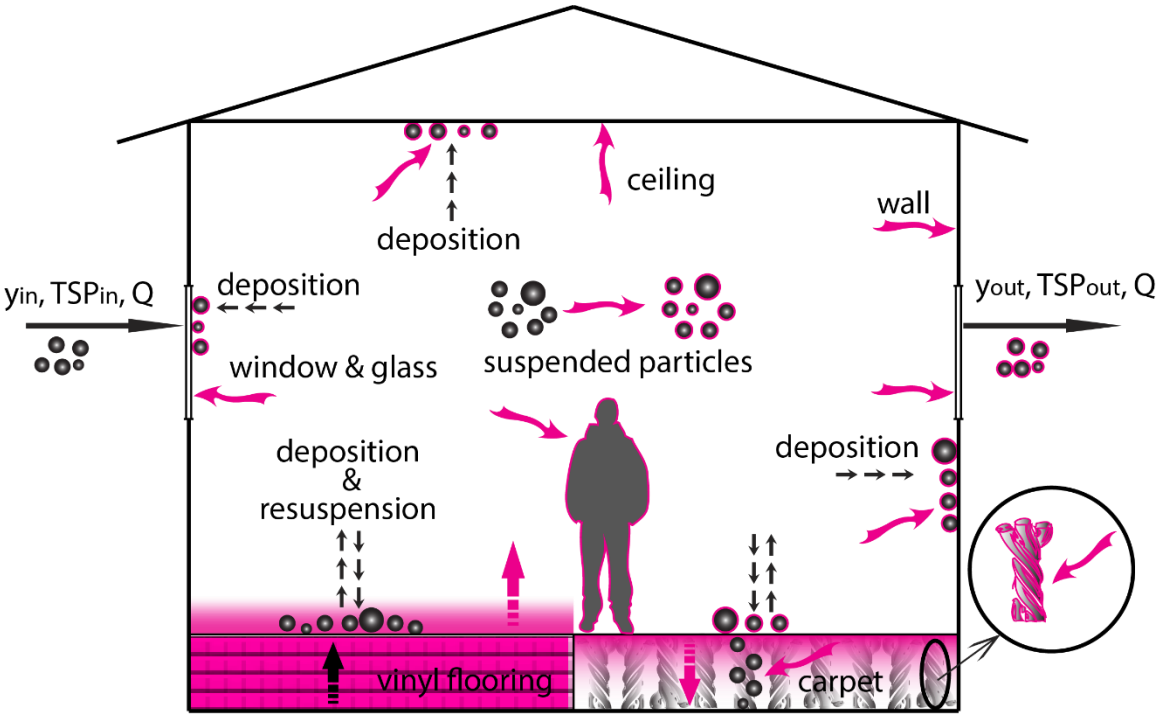

Figure 3.18: Illustration of the residential environment.

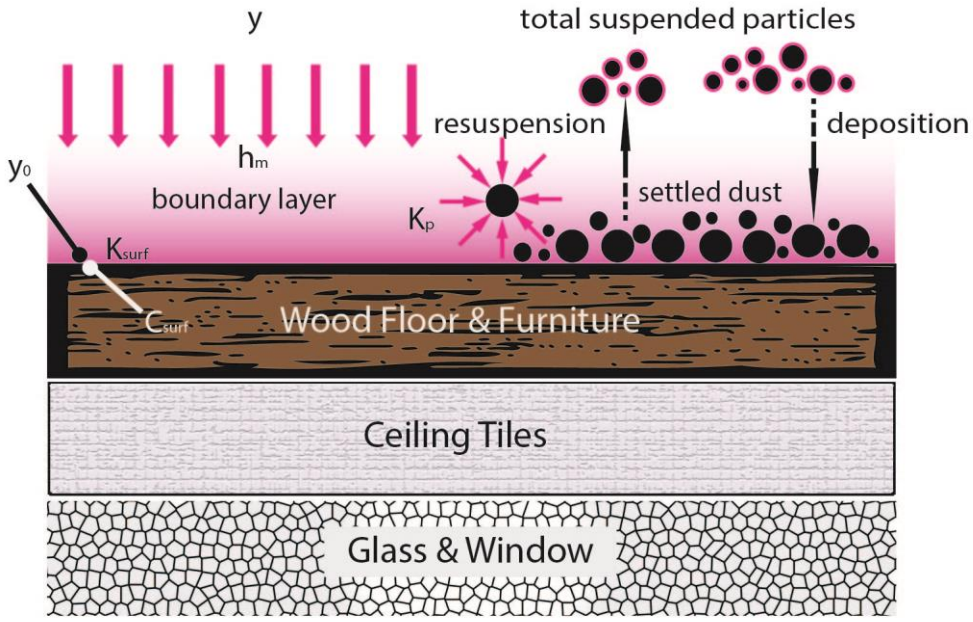

Figure 3.19: Schematic of sorption process of phthalates onto impermeable interior surfaces.

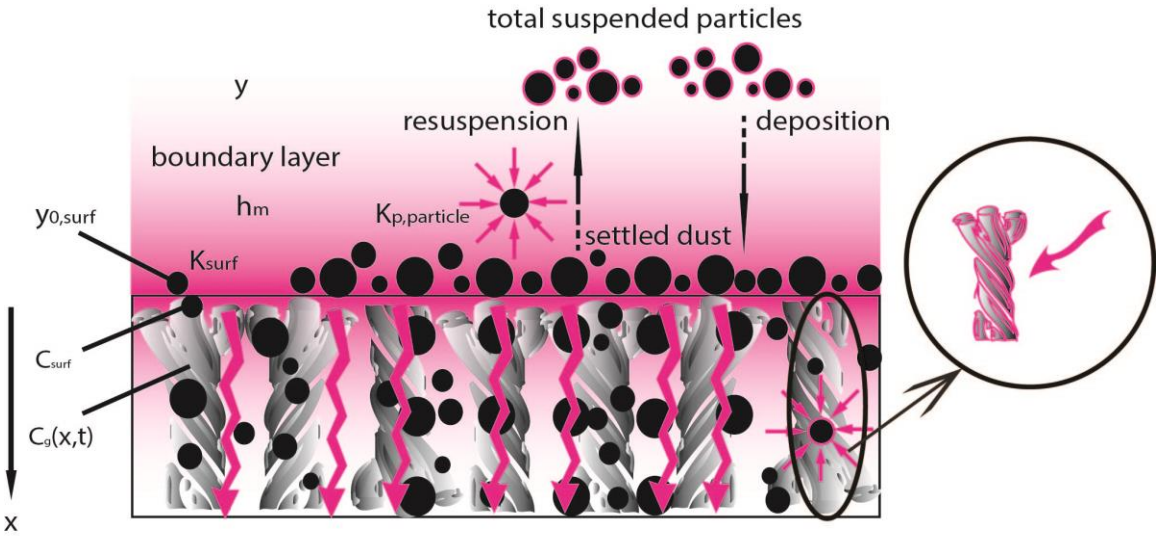

Figure 3.20: Schematic of sorption process of phthalates in carpet.

3.5.2 Model Verification and Uncertainty Analysis

The model was used to estimate BBP emission and transport after vinyl flooring was installed in a residence. The total airborne concentration of BBP reached steady state fast compared to a previous model study of DEHP (Xu et al., 2010). The steep initial rise occurred because the rate at which it is emitted from the vinyl flooring is initially faster than the rate at which it is taken up by the interior surface sinks. The major BBP source identified in the UTest House is the vinyl flooring, which has been in installed in the house for over five years. Therefore, we assumed that the concentrations of BBP in air and dust phases have reached steady state. The measured data were used to perform initial validation of the fate and transport model of phthalates. As shown in Figure 3.21, there are good agreement between model predictions and field measurements. Using the model, we further found that there is no significant difference between the gas and total airborne concentrations of BBP. Because the relatively small gas-particle partition coefficient of BBP, only a small fraction of the airborne mass is bound to particle phase, with the majority present in the gas-phase. The very low TSP concentration (<4 $\mu g/m^3$) in the UTest House strengthened the effect. We also compared the concentration of BBP in floor dust (dust accumulated on vinyl flooring) and non-floor dust (dust accumulated on non-source surfaces). Both model simulation and field measurements showed that the mass of BBP in floor dust (2823 to 3518 μg/g) is approximately 20 times higher than in non-floor dust (140 to 203 μg/g). This significant difference indicated that settled dust on source materials may absorb a great amount of phthalates from the gas layer immediately adjacent to the source. The agreement between predicted dust concentration of BBP and measured data further validated the critical part of the model on simulating phthalate redistribution between gas, particle, and surface phases close to interior source and sink surfaces.

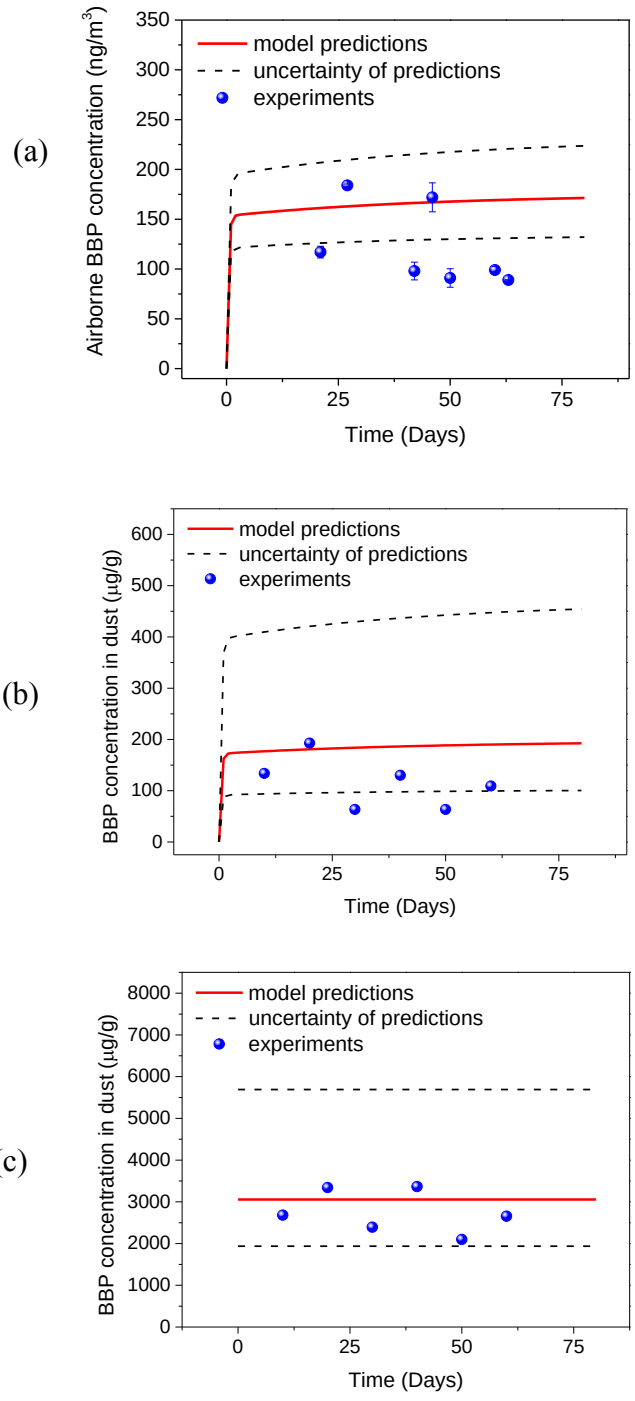

Figure 3.21: (a) Comparison of airborne BBP concentration between model results and experimental data; (b) comparison of BBP mass fraction on floor dust; and (c) non-floor dust between model results and experimental data.

3.5.3 Three-compartment Residential Model

Using DEHP in vinyl flooring as an illustrative example, we extended the one room model to predict DEHP emissions after installation of vinyl flooring in a more realistic family residence and investigate the impacts of environmental conditions on the transport of indoor DEHP. As shown in Figure 3.22, DEHP is emitted from vinyl flooring to the air in a typical residence that we divided into three compartments: kitchen, bathroom and main house. Modeling on emission, sorption, and particle dynamics are similar as the one room model. We obtained the infiltration/exfiltration rates and ventilation rates between rooms from measurements conducted by Wilkes et al. (1992) in a five-room house. We estimated the interior surface area of furnishing and materials using typical surface/volume ratios for American houses established by Hodgson et al. (2005). In this model, we considered typical urban region in the U.S. and the city of Beijing in China as two sites, with the former as the base case. The air velocity across interior surfaces was set to 0.15 m/s (Xu et al., 2009), which was used to estimate the mass transfer coefficients through the boundary layer adjacent to surfaces based on correlation equations (Axley, 1991). Gas-particle partition coefficient (K_p) for DEHP was estimated from its K_{OA} value using the methods discussed in previous studies (Cousins and Mackay, 2000; Weschler et al., 2008). Sorption isotherms for gas-phase DEHP on various indoor surfaces were obtained from estimations in previous studies (Xu et al., 2009).

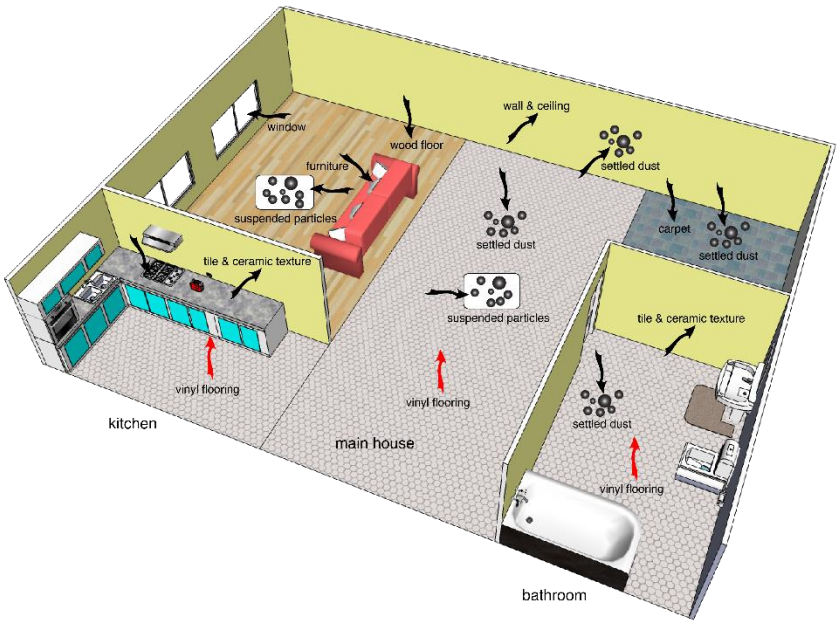

Figure 3.22: Illustration of the three-compartment residential environment.

The gas-phase and total airborne concentrations of DEHP in each compartment were estimated, as shown in Figure 3.23a. The three compartments reached steady state within about two years. Compared with the other two compartments, the main house had the lowest gas-phase concentration because of the larger ratio of sorption surface area to emission surface area. The predicted steady-state total airborne concentration of DEHP in the main house was consistent with measured data in recent field campaigns in the United States and Europe. The gas-phase concentration of DEHP in each compartment was about two times lower than that in the particle phase, due to the large partition coefficient between gas and particle phases (K_p). In addition to the gas-phase concentration, Figure 3.23b shows that DEHP mass fraction in floor dust (dust on source surface) is over an order of magnitude higher compared to that in non-floor dust. The results suggested that particles deposited on source and sink surfaces should be separated when conducting field campaigns to measure SVOC concentrations in dust samples.

Although the predicted steady-state DEHP concentration in non-floor dust agreed well with measured data in the literature, caution should be taken when interpreting this comparison, because the value of K_p may significantly influence the predicted result.

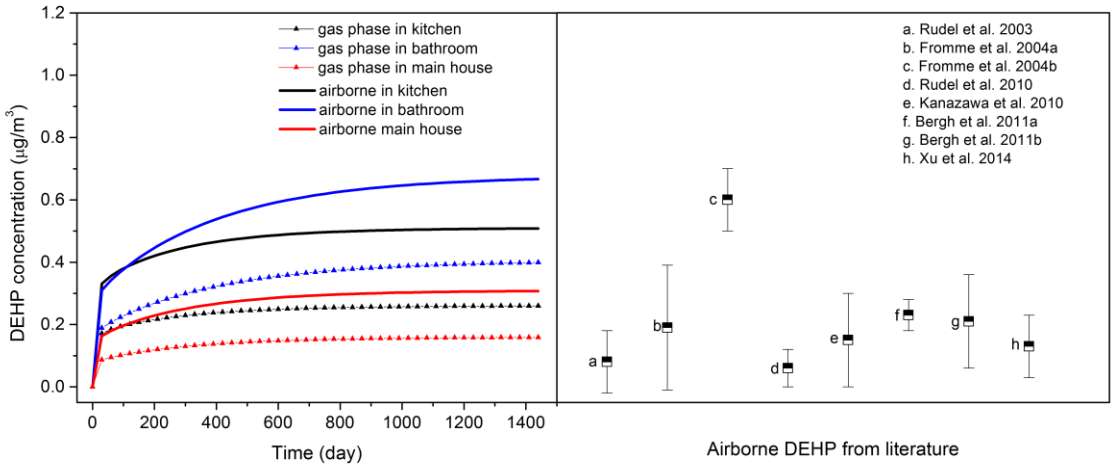

(a)

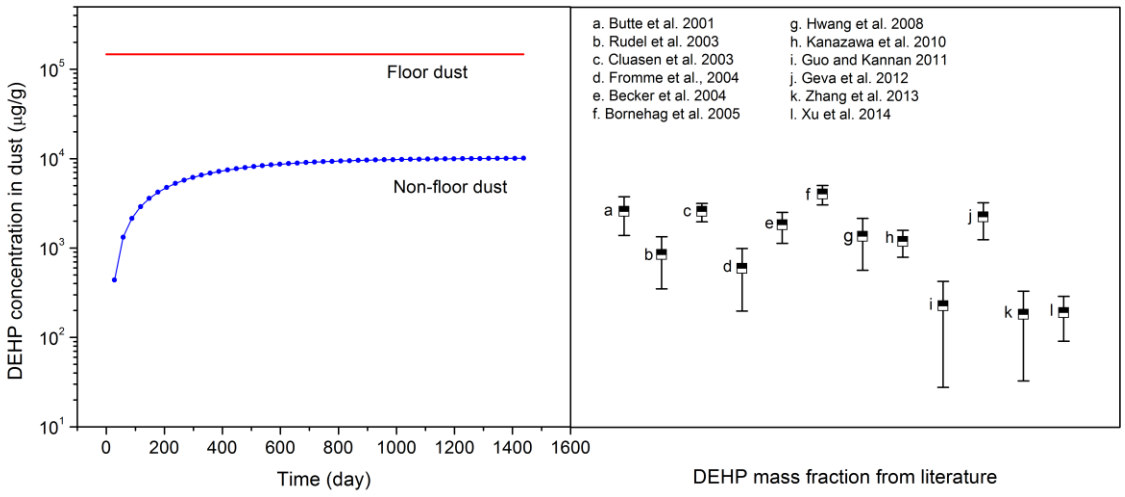

(b)

Figure 3.23: (a) Gas-phase and airborne DEHP in different compartments with comparison to values reported in the literature; and (b) DEHP mass fraction on non-floor dust and floor dust with comparison to values reported in the literature.

3.5.4 The Influences of Environmental Conditions on the Fate of Indoor Phthalates

We investigated the influence of outdoor TSP level on indoor phthalate concentrations by comparing the case of Beijing, China to the base case of typical urban area in the U.S. The outdoor particle concentration in Beijing, China is considerably higher than that in typical urban areas in the U.S., which resulted in a higher indoor TSP level in Beijing. As shown in Figure 3.24a, the predicted airborne DEHP concentration was higher while the gas-phase DEHP concentration was lower in Beijing. We should also note that the difference between airborne and gas-phase DEHP is more prominent in Beijing than that in urban areas in the U.S. With more suspended particles in the environment, more gas-phase DEHP was emitted from the source and then adsorbed to particle phase. Therefore, a lower gas-phase concentration and a higher particle-phase concentration were resulted. Overall, the total airborne DEHP concentration increased with the increase of indoor TSP level. In addition, a high indoor TSP level also means a high dust loading on interior surfaces, and those settled dust on the source surface can resuspend back into the air, increasing the total airborne DEHP concentration.

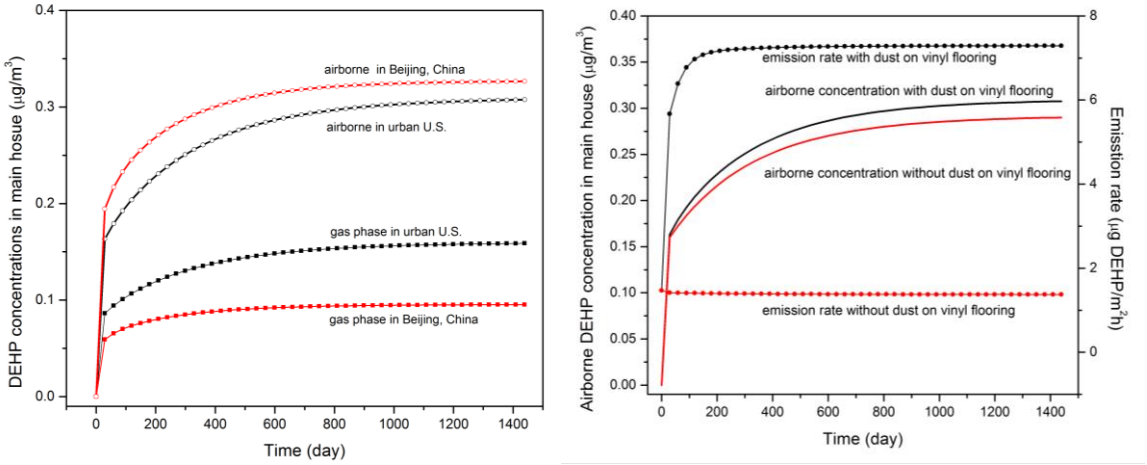

(a) (b)

Figure 3.24: (a) Influence of outdoor TSP level on DEHP concentrations; and (b) Influence of settled dust on DEHP emission rate from vinyl flooring.

To investigate the influence of settled dust on DEHP emission rate, we calculated the emission rate and airborne DEHP concentration under two scenarios: 1) there is settled dust on vinyl flooring, and 2) no dust present on vinyl flooring. As shown in Figure 3.24b, although the airborne DEHP concentrations in two scenarios are close to each other, DEHP emission rate from vinyl flooring with settled dust quadruple the value without dust presence on the source surface. DEHP emission rate is determined by both the gas-phase mass transfer and sorption onto settled dust, the latter is proved to account more for the emissions from the source material. The increase of airborne DEHP concentration is possibly due to particle resuspension from vinyl flooring as an important source. If we look into the increase of emission rate caused by settled dust, we can conclude that approximately 80% of emitted DEHP from the source was captured by settled dust. This increase is subject to change when the dust loading on the source surface varies. Previous study (Liu et al., 2012) on the influence of aerosols on enhancing SVOC flux between air and indoor surfaces showed that DEHP emission rate can be significantly increased with particle mediation, which agreed well with our model results.

Finally, we examined the significance of carpet as in important adsorptive interior surface. In the model simulation, we removed the only source (vinyl flooring) from the main house after a period of time (2 years) and studied the change of concentrations in air and carpet thereafter. Figure 3.25 shows a steep drop on airborne DEHP concentration after the vinyl flooring was removed from the residential home. However, the dramatic drop did not last thereafter and the total airborne concentration of DEHP started to decrease very slowly and was present at the levels above zero for years. We believed that the carpet including settled dust inside, which originally behaved as an indoor sink surface, became secondary source of DEHP after removal of the vinyl flooring.

Furthermore, monthly cleaning activity was found to significantly reduce DEHP concentration of carpet, while its effect on the total airborne concentration is minor. In addition, we investigated the influences of indoor activities such as cooking and cleaning on DEHP concentrations. Indoor TSP concentration increases steeply with a cooking event occurring in the kitchen, which resulted in a sudden increase of total airborne DEHP concentration and a reduction of gas-phase concentration. Change of the cleaning efficiency on different indoor surfaces will have a significant effect on the surface concentration of DEHP. With the increase of cleaning frequency or efficiency, the concentrations of DEHP in air and surfaces decreased greatly.

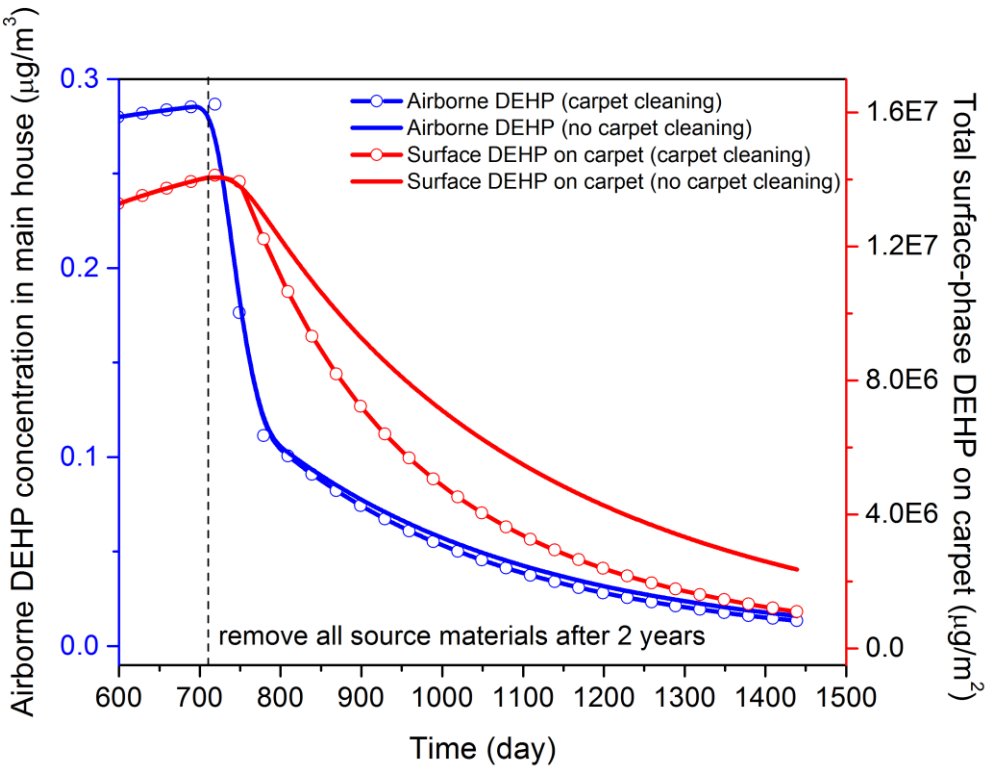

Figure 3.25: Carpet as a secondary source after removing the original source material.

Chapter 4: Conclusions

This dissertation consists of five investigations (Papers 1 to 5), addressing the fundamental mechanisms governing emission, transport, and human exposure associated with phthalates in indoor environments.

One important contribution of this dissertation is that it improved the design of an emission chamber and developed a novel, rapid method to measure y_0, a key parameter that controls phthalate emissions. This effective and economical approach is urgently needed to rapidly identify interior sources of phthalates, as well as the other SVOCs present in building materials and consumer products, which are most harmful to human health. The mechanisms governing emissions of phthalates from polymeric materials were further elucidated through chamber studies. It extended the mechanistic understanding of emissions to an actual indoor environment through the fate and transport model of phthalates and connected the results to exposure assessments. The simple approach proposed will help health professionals estimate screening-level exposure associated with SVOCs present in polymeric materials as additives and conduct risk-based prioritization for a wide range of SVOCs chemicals of concern.

Using the novel, rapid chamber method, this work investigated the influence of temperature on the emission of phthalate from vinyl flooring and crib mattress covers. The gas-phase concentrations versus time were measured at four different temperatures, i.e., 25, 36, 45, and 55 ºC. The key parameter that controls the emissions (y_0, gas-phase concentration in equilibrium with the material phase) was determined, and the emissions were found to increase significantly with increasing temperature. Both the material-phase concentration (C_0) and the chemical vapor pressure (V_p) were found to have great influence on the value of y_0. The measured ratios of C_0 to y_0 were exponentially

proportional to the reciprocal of temperature, in agreement with the van't Hoff equation. An emission model was validated at different temperatures, with excellent agreement between model predictions and chamber observations. In residential homes, an increase in the temperature from 25 to 35 ºC can elevate the gas-phase concentration of phthalates by more than a factor of 10, but the total airborne concentration may not increase that much for less volatile compounds. In infant sleep microenvironments, an increase in the temperature of mattress can cause a significant increase in emission of phthalates from the mattress cover and make the concentration in breathing zone about four times higher than that in the room, resulting in potentially high exposure.

This research further investigated the influences of surface sorption and air flow rate on the emission of phthalates from building materials. Controlled tests were conducted in specially designed stainless steel and wood chambers, and the steady-state concentration in the stainless steel chamber was about 2-3 times higher than that in the wood chamber for DEHP and DINP. The emission rate of phthalates was increased in the wood chamber due to surface absorption. The adsorption isotherm of phthalates on the stainless steel surface and the absorption parameters (i.e., diffusion and partition coefficients) of phthalates on the wood surface were determined experimentally and the values were comparable to those in the literature. The equilibration time scale for phthalates absorbed in the sink reservoir in actual indoor environments was estimated and can be substantial (~ 80 years), indicating that surface absorption may continuously drive phthalates from their indoor sources to various sinks and thus significantly increase the emission rate of phthalates. The gas-phase concentration of DEHP was measured in two stainless steel chambers operated at the flow rates of 300 mL/min and 3000 mL/min, respectively, which were both adjusted to 1000 mL/min after steady state was reached. The gas-phase concentration of DEHP in the chamber was very sensitive to the chamber

air flow rate, and higher air flow rates resulted in lower concentration levels. But, the increased emission rate compensated for the dilution in the gas phase and made DEHP concentration not drop substantially with an increase of air flow rate. Independently measured or calculated parameters were used to validate a semi-volatile organic compounds (SVOCs) emission model that included absorptive surfaces and for a range of air flow rates, with excellent agreement between the model predictions and the observed chamber concentrations of phthalates.

This study also investigated phthalate emissions from vinyl flooring in a large-scale chamber, which is the first study of its kind. Vinyl flooring with high DINP and DEHP content was selected and their emissions were characterized in small chambers at two different temperatures. The values obtained for the dominant emission parameter, gas-phase concentration of phthalates in equilibrium with the material phase (y_0), were 0.43 $\mu g/m^3$ at 25 ºC and 4.31 $\mu g/m^3$ at 36 ºC for DINP and 0.02 $\mu g/m^3$ at 25 ºC and 6.35 $\mu g/m^3$ at 36 ºC for DEHP. Large-scale chamber experiments were then conducted using the same type of vinyl flooring, and the concentrations of DINP and DEHP showed similar trends during three experimental phases. The gas-phase concentrations of DINP and DEHP at 36 ºC were about three times lower in the large chamber than in the small chamber, which is consistent with its lower area/volume ratio. In the second phase, when a large fan was replaced with a small fan, the gas-phase concentrations of DINP and DEHP in the large chamber reduced slightly, due to the decrease in the mass transfer coefficient and emission rate. During the last experimental phase, when the temperature of the chamber was reduced to 25 ºC, phthalate concentrations dropped instantly and steeply due to the significantly reduced y_0 values and emissions. However, they did not decrease as quickly thereafter because of the desorption of phthalates from the internal surfaces of the chamber. A fundamental mechanistic model was developed, with data on

emission characteristics obtained in small chamber measurements, to interpret the experimental results in the large chamber. Reasonable agreement between model prediction and experimental data was obtained. Further model simulations show that temperature and air mixing above the source material have important effects on the fate of phthalates, while the impact of the air change rate (ACH) is not significant.

Finally, a residential fate model was developed to elucidate the mechanisms of phthalates transport and their distribution among the gas phase, airborne particles, interior surfaces and settled dust in indoor environment. This dynamic mass-balance model considers various environmental media (air, particulate matter, settled dust, vinyl flooring, wood floor, carpet, furniture, ceiling and walls) and associates particle dynamics as a core part of transporting phthalates from source to sink. Three size fractions of particles with different transport properties and indoor activities (vacuuming and cooking) were included. This model was validated through independent field experiments in a test house preinstalled with vinyl flooring that contains benzyl butyl phthalate (BBP). BBP concentrations in air, dust and interior surfaces were monitored and the model predictions of BBP were of the same order of magnitude as measured values. The model was further extended to a three-compartment environment for DEHP with different outdoor particle levels and the model results show significant difference of DEHP concentrations and emission rates, indicating the importance of particles and/or dust for enhancing the transport of indoor phthalates.

Overall, this dissertation explicitly elucidates the fundamental mechanisms governing emission, transport, and human exposure associated with phthalates in residential indoor environments. A novel, rapid, small-chamber method to characterize emissions of phthalates from building materials was developed. The influences of environmental conditions (temperature, ventilation rate, and sorption surface) on

phthalate emissions were studied through a series of controlled tests in small-chambers and a large-scale stainless steel chamber. The validated fate and transport model that include the processes of emission, sorption, desorption, and particle transport will help to evaluate human exposures to phthalates in indoor environments.

Appendix A

Paper 1. Improved Method for Measuring and Characterizing Phthalate Emissions from Building Materials and Its Application to Exposure Assessment

Yirui Liang and Ying Xu
(Published in *Environmental Science & Technology*[1])

ABSTRACT

Phthalate emission from vinyl floorings was measured in specially-designed stainless steel chambers. Phthalate concentrations increased and reached steady state after 2 to 5 days for all experiments. By having a high ratio of emission surface to sorption surface, avoiding mass loss of phthalates onto sampling pathways, and improving air mixing inside the chamber, the time to reach steady state was significantly reduced, compared to previous studies (1 to 5 months). An innovative approach was developed to determine y_0, the gas-phase concentration of phthalates in equilibrium with the material phase, which is the key parameter controlling phthalate emissions. Target phthalate material-phase concentration (C_0) and vapor pressure were explicitly measured and found to have great influences on the y_0 value. For low phthalate concentrations in materials, a simple partitioning mechanism may linearly relate y_0 and C_0, but cannot be evoked for high-weight phthalate percentages. In addition, the sorption kinetics and adsorption isotherm of phthalates on stainless steel chamber surfaces were determined experimentally. Independently measured or calculated parameters were used to validate a semi-volatile organic compounds (SVOCs) emission model, with excellent agreement between model predictions and the observed chamber concentrations in gas and stainless steel phases. With the knowledge of y_0 and emission mechanisms, human exposure to

[1]Liang, Y., Xu, Y., 2014. Improved Method for Measuring and Characterizing Phthalate Emissions from Building Materials and Its Application to Exposure Assessment. Environmental Science & Technology 48, 4475-4484. Dr. Ying Xu is the second and corresponding author of this paper.

phthalates from tested floorings was assessed; the levels were comparable to previous studies. This paper developed a rapid, novel method to measure phthalate emissions; emission measurement results can be connected to exposure assessment and help health professionals estimate screening-level exposures associated with SVOCs and conduct risk-based prioritization for SVOC chemicals of concern.

INTRODUCTION

Phthalates have been used as plasticizers to enhance the flexibility of polyvinylchloride (PVC) products. These semi-volatile organic compounds (SVOCs) are found in a wide range of building materials and consumer products such as vinyl flooring, carpet padding, wall coverings, floor tiles, furniture, and electronics (Bornehag et al., 2005), where they may be present at percent to tens-of-percentage levels (Weschler and Nazaroff, 2008). Because phthalate additives are not chemically bound to the polymer matrix, slow emission from the products to air or other media usually occurs (Xu et al., 2012). As a result, phthalates are ubiquitous and among the most abundant SVOCs in indoor environments (Bornehag et al., 2005; Clausen et al., 2012; Bornehag et al., 2004; Rudel and Perovich, 2009). Recent studies suggest that exposure to some phthalates may result in irreversible changes in development of the human reproductive tract (Heudorf et al., 2007; Jaakkola and Knight, 2008; Latini et al., 2006; Matsumoto et al, 2008; McKee et al., 2004; Ritter and Arbuckle, 2007); increase the risk of asthma, rhinitis, and allergies (Bornehag et al., 2005; Jaakkola et al., 2006 and 1999; Kolarik et al., 2008; Øie et al., 1997); and affect endogenous hormones (Rudel and Perovich, 2009). Despite the negative health impacts, phthalates still dominate the plasticizer market (Schossler et al., 2011). The global production rate of phthalate plasticizers has increased from 2.5 to 6 million tons/yr within a decade (Rudel and Perovich, 2009; Cadogan and

Howick, 1996). However, following the restrictions on using certain phthalates in toys and child care products (CPSC, 2008), phthalates used in PVC products are changing rapidly, with a trend toward using phthalates of higher molecular weight and lower volatility (Schossler et al., 2011; Weschler, 2009). Using alternative plasticizers, such as diisononyl cyclohexane-1,2-dicarboxylate (DINCH) and di(2-ethylhexyl) adipate(DEHA), has also occured, but because they share chemical structures and properties similar to phthalates, similar emissions and environmental fate and transport may be expected (Schossler et al., 2011).

Understanding emission mechanisms of phthalates and the ability to predict their emission rates from various sources are a prerequisite for characterizing their fate and transport and developing suitable approaches to reduce their concentrations in indoor environments. However, standard chamber methods designed for measuring volatile organic compounds, ozone, and particulate matter may not be appropriate for measuring SVOC emissions (Afshari et al., 2004; Destaillats et al., 2008). Recent chamber studies on emission of phthalates from PVC materials are briefly reviewed in the Supporting Information (SI). Overall, these studies revealed the substantial difficulties associated with chamber tests for SVOCs resulting from the low gas-phase concentration, strong sorption onto surfaces, and ubiquitous contamination in laboratory facilities.

Informed by the early chamber studies, Xu and Little (2006) developed a fundamental mass-transfer model to predict SVOC emissions from polymeric materials. Using data collected in chamber studies, Xu et al. (2012) showed that the emission rate of di(2-ethylhexyl) phthalate (DEHP) from vinyl flooring can be predicted based on a priori knowledge of y_0, the gas-phase concentration of DEHP in equilibrium with the material phase, the material to air and air to stainless steel surface mass-transfer coefficients (h_m), and the stainless steel/air equilibrium relationship (K_s). The chamber-based model was

extended to predict human exposure to DEHP emitted from vinyl flooring in a realistic residential environment (Xu et al., 2009 and 2010) using field data to establish K_s values for dust and other interior surfaces. Sensitivity and uncertainty analyses revealed that the rather complex steady-state exposure predictions are almost entirely determined by y_0, h_m and A, the surface area of the flooring (Xu et al., 2010). Little et al. (2012) simplified the model and proposed rapid methods to obtain screening-level estimates of potential indoor exposure of building occupants to a range of SVOCs. Their results indicated that y_0 is one of the most important parameters required to estimate the indoor gas-phase concentration resulting from emissions of SVOCs that are present in materials and products as additives.

No methods exist to measure or estimate y_0 for phthalates in PVC products. Using DEHP steady-state concentrations in the Field and Laboratory Emission Cell (FLEC) as approximations of y_0, Clausen et al. (2012) found that the value of y_0 for a vinyl flooring sample is close to the vapor pressure (V_p) of pure DEHP at five temperatures. However, the results showed that there is about three times difference at 23°C between y_0 and estimated V_p values (y_0: 0.9 μg/m^3 versus V_p: 2.4 μg/m^3). The relationship between y_0 and V_p for other phthalates is still unclear. Little et al. (2012) suggested that y_0 cannot be well approximated by V_p in all cases. The material-phase concentration (C_0) of phthalate additives in different products can vary substantially; therefore, when their content is low, they may not behave as pure liquid, resulting in the y_0 value being much lower than its V_p. As a result, development of appropriate methods to determine y_0 for phthalates in PVC products has become a high priority. In addition, the availability of reliable measurements of V_p is limited for phthalates and for other SVOCs (Schossler et al., 2011; Letcher and Naicker, 2004). Significant discrepancies (by several orders of magnitude) were found in the literature (Schossler et al., 2011;

Weschler et al., 2008), probably because of the difficulties associated with SVOC analysis, various measuring methods, and different purities of samples (Schossler et al., 2011; Letcher and Naicker, 2004). For example, the measured V_p (at 25°C) for diisononyl phthalate (DINP) is in the range of 3.6×10^{-7} Pa to 1.0×10^{-4} Pa (Schossler et al., 2011; Howard et al., 1985). Predictions using some V_p calculators also showed significant deviations, primarily because they follow different approaches in estimating physical parameters of compounds (Schossler et al., 2011). In the case of DINP, the predicted values of V_p (at 25°C), by using SPARC and EPI Suite, are 9×10^{-9} Pa and 3×10^{-6} Pa, respectively. Therefore, to investigate the relationship between y_0 and V_p, more reliable data of phthalates V_p are needed. Furthermore, an accurate value of V_p at room temperature will help to understand the distribution of phthalates in indoor environments, especially among the gas phase, airborne particles, interior surfaces, and settled dust (Weschler and Nazaroff, 2008; Xu et al., 2009; Weschler et al., 2008; Weschler and Nazaroff, 2010).

The aim of this study is to develop a new method for measuring and characterizing emissions of phthalates from building materials. The specific objectives are to: (1) develop a novel, rapid chamber method to determine y_0, the gas-phase concentration in equilibrium with the material phase, for a range of phthalates in a variety of vinyl floorings; (2) measure V_p of target phthalates at room temperature in the experimental chambers and combine these measurements with those for y_0 and C_0 to investigate the nature of their relationships; (3) quickly measure the stainless steel/air equilibrium relationship (K_s) for the target phthalates; (4) more completely characterize the mechanisms governing the release of phthalates from vinyl flooring by comparing experimental chamber observations with predicted concentrations of an SVOC emission

model; and (5) to demonstrate the use of obtained y_0 in assessing human exposures to phthalates in residential indoor environment.

METHODS AND MATERIALS

Chemicals. Pure chemicals (anhydrous, >99%) were applied in chamber studies to measure phthalate vapor pressures, in which dimethyl phthalate (DMP), di-n-butyl phthalate (DnBP), butyl benzyl phthalate (BBP), and di(2-ethylhexyl) phthalate (DEHP) were obtained from Acros Organics, di(2-ethylhexyl) isophthalate (iso-DEHP) was purchased from Scientific Polymer Products Inc., and diisononyl phthalate (DINP) was from MP Biomedicals LLC. Standard solutions were used for chemical calibration and identification, including DMP, DnBP, BBP, and DEHP (Absolute Standards Inc.), iso-DEHP (SPEX CertiPrep), and DINP (Accustandards, Inc.). Tetradeuterium ring labeled DEHP (D_4-DEHP) was used as internal standard, and its standard solution was obtained Accustandards, Inc. Hexane, methanol, and dichloromethane (Sigma-Aldrich Co. LLC., anhydrous, >99%) were used as solvent in extraction and cleaning without further purification. The solvents were regularly analyzed to monitor potential phthalate contamination.

Test Pieces. Sixteen types of vinyl floorings were purchased primarily in a home improvement store in the United States according to their popularity. The content of phthalates in each flooring sample was quantified experimentally. Among them, four products with different phthalates at relatively high concentration were selected. Another PVC flooring that had been used in previous experiments (Xu et al., 2012; Clausen et al., 2012 and 2004) was also included in this study. Each flooring sample was cut into two 0.45 m × 0.25 m sheets, wrapped in aluminum foil, and stored at room temperature.

Before a measurement, the test pieces were unwrapped and placed in the emission chamber.

The content of phthalates in vinyl flooring was measured by liquid extraction in duplicate. Ten small pieces of samples (approximately 4 mg in total) were cut out of each type of flooring with a pair of scissors at randomly chosen positions. The samples were ultrasonically extracted for 40 min with dichloromethane for three times. Extractions were conducted in an ultrasonicator filled with clean water and ice bags to maintain a low temperature and avoid evaporation loss of sample during the process. The volume of extracts was reduced using a rotary evaporator (IKA RV-10) and a high purity N_2 stream. After concentrating to about 5 mL, the samples were cleaned up with preassembled filtration devices (Whatman AutovialTM syringless PTFE filters with 0.2 μm pore). Finally, a nitrogen purge was used to further reduce the sample volume to approximately 800 μL. 2 μL of the extracts were then injected with a solution of D_4-DEHP as internal standard into Tenax TA tubes and analyzed by thermal desorption combined with gas chromatography and mass spectrometry (TD-GC-MS). Chemical analysis of phthalates was described in detail in the SI.

Emission Chamber. The design of a stainless steel chamber used in previous experiments (Xu et al., 2012) was improved. As shown in Figure A.1, the thin chamber was positioned between two vinyl flooring sheets. The two flooring sheets and the internal stainless steel chamber wall form a very short semicylindrical cavity. In this way, we maximized the vinyl flooring emission area and minimized the stainless steel sorption area. To enhance air flow mixing inside the chamber, three inlets and six outlets were applied in the design. Simulation of air velocity field by computational fluid dynamics (CFD) suggests that the air flow is reasonably well mixed within the chamber cavity (Figure A.S1) (Table and Figure numbers preceded by an "S" are in the

Supporting Information). No bypass flow was detected in measurements. Three of the six outlet ports were constructed specially to fit with sorbent tubes, so that they could be directly inserted into the chamber without any fixtures. Thus, the loss of phthalates to stainless steel tubing and fittings along the sampling pathway was avoided. Another three outlets were made with particular fittings to hold stainless steel rods and allow air flows to pass through. These precision-ground rods (3 mm diameter × 3 cm in length) have similar roughness to the interior stainless steel chamber surface. They were inserted into the chamber in sorption experiments and periodically removed so that the amount of phthalates sorbed to stainless steel surface could be measured. Because the outlet flow resulted in high velocity around the rods, fast sorption kinetics was achieved. The volume of the chamber is 1 L with other properties shown in Table A.S1. Vinyl flooring itself acts as a good gasket. PTFE sheets (from Fluoro-Plastics Inc.) were used in blank chamber experiments. The air leakage rate was less than 2% of the total flow rate.

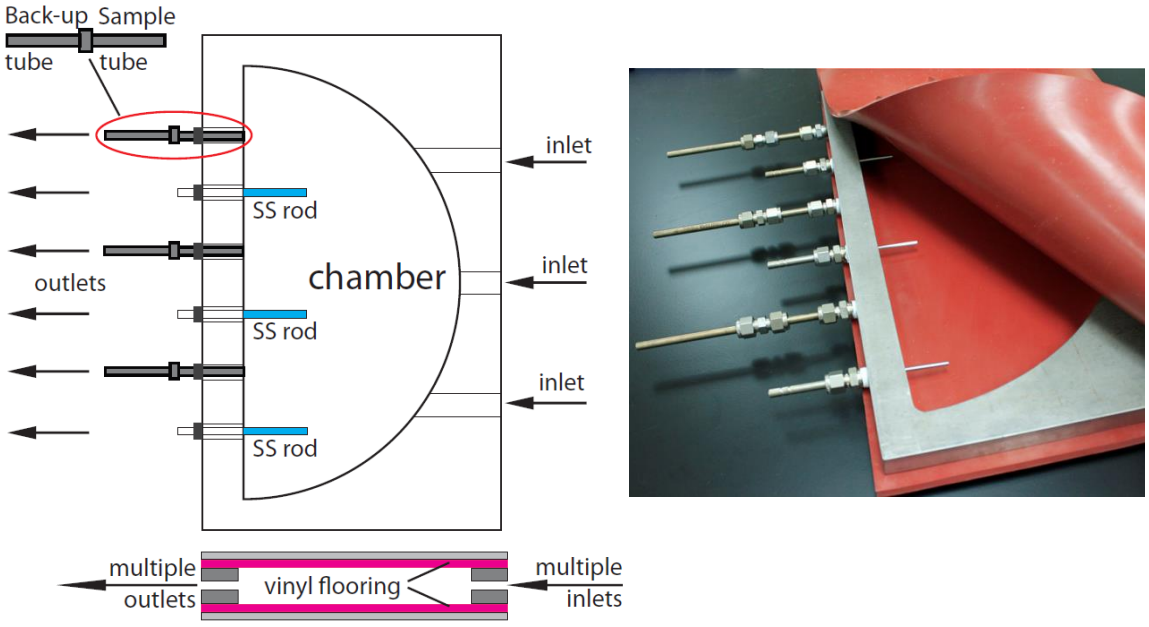

Figure A.1: Configuration of the chamber. a) Top and side view, b) Photo.

Emission Experiments. The emission chambers were placed in a temperature-controlled cabinet (Lunaire CEO-932) and operated at 25±0.5°C. The concentrations of phthalates versus time were measured in the emission chamber at an air flow rate of 1000mL/min. Phthalates was sampled directly on Tenax-TA tubes with a pump (SKC 224-PCXR4) calibrated to a nominal flow rate of 150 ml/min. The sampling time was approximately 24 hours. Backup tubes were connected to each primary sample tube to check for breakthrough (Figure A.1). No breakthrough was observed in any of the tests. Because the sampling system was supplied with high purity air from cylinders, we assumed that no particles were present. Before each emission test, the stainless steel plates and especially the internal chamber surfaces were cleaned with an alkali detergent, hot tap water and Nanopure® water, and then finally rinsed several times with methanol. Background measurements were performed before each test for around a week. In addition, a separate blank chamber was employed to monitor possible contamination during emission tests. Because humidity does not significantly influence phthalate emissions (Clausen et al., 2007) in stainless steel chambers, only temperature and air flow rate through the chamber were checked before and after samples were taken for analysis.

Sorption Experiments. Sorption measurements were conducted at a relatively constant chamber concentration after steady state had been reached, allowing the sorption kinetics and equilibrium end-point to be carefully examined. Three stainless steel rods were inserted into the chamber (Figure A.1) with chamber outlet air flows passing through the rod holders. Because the air flows were drawn by pumps calibrated to a nominal flow rate of 100 ml/min, the high velocity around the rods allow sorption to reach equilibrium quickly. As the surface of the rods is almost identical to the surface of the internal chamber walls, they provide a means to measure the sorption characteristics of the chamber surface. Before use, the rods were cleaned with methanol. After

sampling, the rods were taken out of the chamber, quickly put into stainless steel tubes, and then analysed with TD-GC-MS. The stainless steel tubes were cleaned with methanol and background concentration of the tubes was checked before use. In addition, gas-phase concentration of phthalates was also periodically measured to ensure that steady-state concentration was maintained in the chamber during sorption experiments.

When the sorption experiments of stainless steel rods were completed, the emission chambers that had been at steady state for approximately one month were terminated and disconnected. The internal surface of the chambers was then wiped with wet gauze pads to obtain the surface concentration of phthalates on chamber walls and compare it to that on the rods. The gauze pads were pre-cleaned with dichloromethane, dried, and wetted with 99% hexane. A total of 15 wipes were applied for each chamber. The wipe samples were ultrasonically extracted for 30 min with hexane for three times. The volume of the extract was reduced to approximately 150 μL, after rotary evaporation, clean-up, and nitrogen purge. 5 μL of the extract was then injected with a solution of D_4-DEHP as internal standard into Tenax TA tubes and analysed by TD-GC-MS. Additionally, the recovery of the method for wiping the chamber internal surface was tested. 50 μL methanol containing 20 ng of DnBP, BBP, DEHP, iso-DEHP, and DINP was applied onto the chamber wall. After allowing the surface to dry, the emission chamber was wiped, and the extract was analysed using the method described above. The recovery check was conducted two times, and the mean recovery ratios were 69%, 120%, 95%, 85%, and 113% for DnBP, BBP, DEHP, iso-DEHP, and DINP, respectively.

Vapour Pressure Experiments. Special petri dishes were made of aluminium sheet coated with PTFE (McMaster-Carr Inc.) to fit with the chamber cavity shape (Figure A.S2). Pure phthalate liquid (approximately 300 mL) was delivered to the petri

dish, which covered the bottom of the chamber and formed the emission surface for vapour pressure experiments. PTFE sheets were used as gasket in the experiments and the air leakage rate was less than 2% of the total flow rate. In order to shorten the test duration, the chamber internal sink surfaces (top PTFE surface and stainless steel wall) were coated with a very thin layer of phthalates to saturate the surface. Air samples was collected and analysed periodically from the outlet of the chamber until steady state was reached. Vapour pressure of phthalates, including DMP, DnBP, BBP, DEHP, Iso-DEHP, and DINP, was tested individually, and a total of six experiments were conducted.

Determination of y_0. Xu and Little (2006) developed an SVOC emission model, and the model was recently simplified by Xu et al. (2012). Figure A.S4 provides a schematic representation of the simplified model that predicts the emissions of SVOCs (such as phthalates) from a polymeric material slab in a chamber. In their analysis, the emission rate is

$$E(t) = h_m \cdot [y_0 - y\,(t)] \tag{1}$$

where y ($\mu g/m^3$) is the bulk gas-phase concentration, and h_m (m/s) is the convective mass-transfer coefficient. The ratio of the concentration of a chemical on sorption surfaces (such as the chamber wall or the rods) to its concentration in the gas phase is equal to the surface/air partition coefficient, K_s (m), or

$$K_s = q(t)/y_{0s}(t) \tag{2}$$

where q is the surface concentration ($\mu g/m^2$) and y_{0s} ($\mu g/m^3$) is the gas-phase concentration immediately adjacent to the surface. Assuming a boundary layer exists adjacent to the sorption surfaces, the amount of SVOC accumulated on the surface is equal to the total mass transferred through the boundary layer from the gas phase, or

$$\frac{dq(t)}{dt} = h_s[y(t) - y_{0s}(t)] \quad (3)$$

where h_s (m/s) is the convective mass-transfer coefficient near the sorption surface. With reference to Figure A.S4, the accumulation of SVOCs in the chamber obeys the following mass balance:

$$\frac{dy(t)}{dt} \cdot V = E(t) \cdot A - \frac{dq(t)}{dt} \cdot A_s - y(t) \cdot Q \quad (4)$$

where V is the chamber volume (m^3), A is the area of emission surfaces (m^2), A_s is the internal stainless steel surface area (m^2), and Q is the air flow rate of the chamber. The simplified SVOC emission model is obtained by combing equations (1)-(4).

This section discusses the method to determine y_0 as well as h_m based on the results of vapor pressure and emission experiments. When steady state is reached in vapour pressure experiments, by modifying Equation (4) (see the SI for details), we obtained

$$V_p = \frac{y_{ss} \cdot Q}{h_m \cdot A} + y_{ss} \quad (5)$$

where V_p is the saturated vapor pressure concentration ($\mu g/m^3$) of phthalates and y_{ss} is the steady-state gas phase concentration in the chamber. DMP, a volatile organic compound that has reliably measured vapor pressure (mean ± SD: 0.27±0.04 Pa at 25 °C) reported in the literature (Letcher and Naicker, 2004; Weschler et al., 2008), was selected as a reference chemical. Because the V_p of DMP is known, y_{ss} measured through the vapor pressure experiment for DMP can be used to obtain the only unknown parameter (h_m) in Equation (5).

With the knowledge of h_m for DMP, the convective mass transfer coefficient for other target phthalates ($h_{m,\ phthalate}$) can be calculated. The traditional method for predicting h_m for volatile organic compounds and SVOCs (Xu and Little, 2006; Axley, 1991; Xu and Zhang, 2003 and 2004) is based on empirical correlations, which can be

generally expressed as $Sh=f(Re)\cdot Sc^n$, where Sh is the Sherwood number, h_mL/D_a; Sc is the Schmidt number, υ/D_a; Re is the Reynolds number; n is a parameter that usually taken as 1/3; L (m) is characteristic length; D_a (m^2/s) is the chemical air diffusivity; and υ (m^2/s) is the kinematic viscosity of air. For different chamber configurations and flow conditions, the expression of $f(Re)$ would be different. However, if samples with the same dimensions but emitting different pollutants were tested in the same chamber condition, the expression of $f(Re)$ should be the same because of the similar flow field inside the chamber (Xiong et al., 2012). Therefore, the following formula can be derived:

$$\frac{h_{m,\ ref}}{h_{m,\ phthalate}} = \left(\frac{D_{a,\ ref}}{D_{a,\ phthalate}}\right)^{2/3} \quad (6)$$

where $h_{m,\ ref}$ and $h_{m,\ phthalate}$ are the convective mass transfer coefficients of a reference chemical (i.e., DMP) and a specific phthalate compound, respectively; and $D_{a,\ ref}$ and $D_{a,\ phthalate}$ are their corresponding air diffusivities, which can be estimated based on chemical molecular weight (Schwarzenbach et al., 2003). Therefore, $h_{m,\ phthalate}$ for the chamber condition (Table A.S1) can be calculated by Equation (6).

Finally, when emission experiments reach steady state, by modifying Equation (4), we obtained

$$y_0 = \frac{y_{ss}\cdot Q}{h_m\cdot A} + y_{ss} \quad (7)$$

Because h_m for phthalates under the test condition has been determined as described previously, based on the measured y_{ss} in the emission experiments, the values of y_0 for each vinyl flooring sample emitting particular phthalates can be determined using Equation (7).

RESULTS AND DISCUSSION

Measurements of Phthalate in Vinyl Flooring. The content of phthalates in selected vinyl flooring samples was measured and is listed in Table A.1. The background level of phthalates in blank was less than 0.2 % of the content of the samples. The observed variation may be due to some inhomogeneity of phthalate distribution in vinyl floorings.

Sample ID	Phthalates	Content	C_0 (μg/m^3)	y_0 (μg/m^3)	Vp (μg/m^3) at 25 °C
1	DEHP	13 ± 2 %	1.70×10^{11}	2.30	5.64
2	DEHP	23 ± 3 %	3.26×10^{11}	2.37	5.64
3	DINP DEHP	20 ± 3 % 0.1 ± 0.02 %	3.47×10^{11} 1.73×10^{9}	0.42 0.02	0.52 5.64
4	BBP Iso-DEHP	15 ± 2 % 7 ± 1 %	1.93×10^{11} 9.02×10^{10}	8.47 0.12	12.3 0.88
5	DnBP DEHP	9 ± 1 % 7 ± 1 %	1.42×10^{11} 1.10×10^{11}	24.7 1.54	464 5.64

Table A.1: The measured values of C_0 and y_0 for tested vinyl floorings and of V_p for pure phthalates at 25 °C.

Vapor Pressure Experiments. The measurement of DMP (Figure A.S5) was used to obtain h_m for the emission chamber based on Equation (5); the h_m was then corrected for different phthalates (Table A.S3). Based on the experiment results of DnBP, BBP, DEHP, Iso-DEHP, and DINP (Figure A.S5) and the known h_m values, the vapor pressure of phthalates was obtained using Equation (5) and is reported in Table A.S4. Most of the values in this study are higher than the SPARC estimation and lower than the EPI Suite results. The measured vapor pressures fall into the range of previous experimental studies, although there are significant deviations for some phthalates in the literature (Schossler et al., 2011; Weschler et al., 2008).

Emission Experiments. As shown in Figure A.2, phthalate concentrations increased and reached steady state in less than 5 days for all experiments. In the improved chamber design, the ratio of emission surface to sorption surface was high, the mass loss of phthalates onto sampling pathways was avoided, and the velocity field inside the chamber was optimized to enhance air mixing. Therefore, the build-up of phthalates in the gas phase occurred much faster and the time to reach steady state was significantly reduced, compared to the previous studies of DEHP emission in FLEC and in a special chamber from the same vinyl flooring (sample 1), in which it took about 150 and 30 days, respectively (Xu et al., 2012; Clausen et al., 2004). In all tests, the phthalate concentration in a blank chamber was more than 10 times lower than the highest measured concentrations in the sample chamber with vinyl flooring. The experimental conditions were constant over the entire test period (Table A.S1). In sorption experiments, stainless steel rods were inserted into the chamber after steady state had been reached. The additional sorption surface area (< 10% of the chamber internal surface area) due to the introduction of rods did not change the chamber concentration significantly. The fluctuation of concentration in the chamber tests after steady state had been reached was probably caused by normal measurement errors.

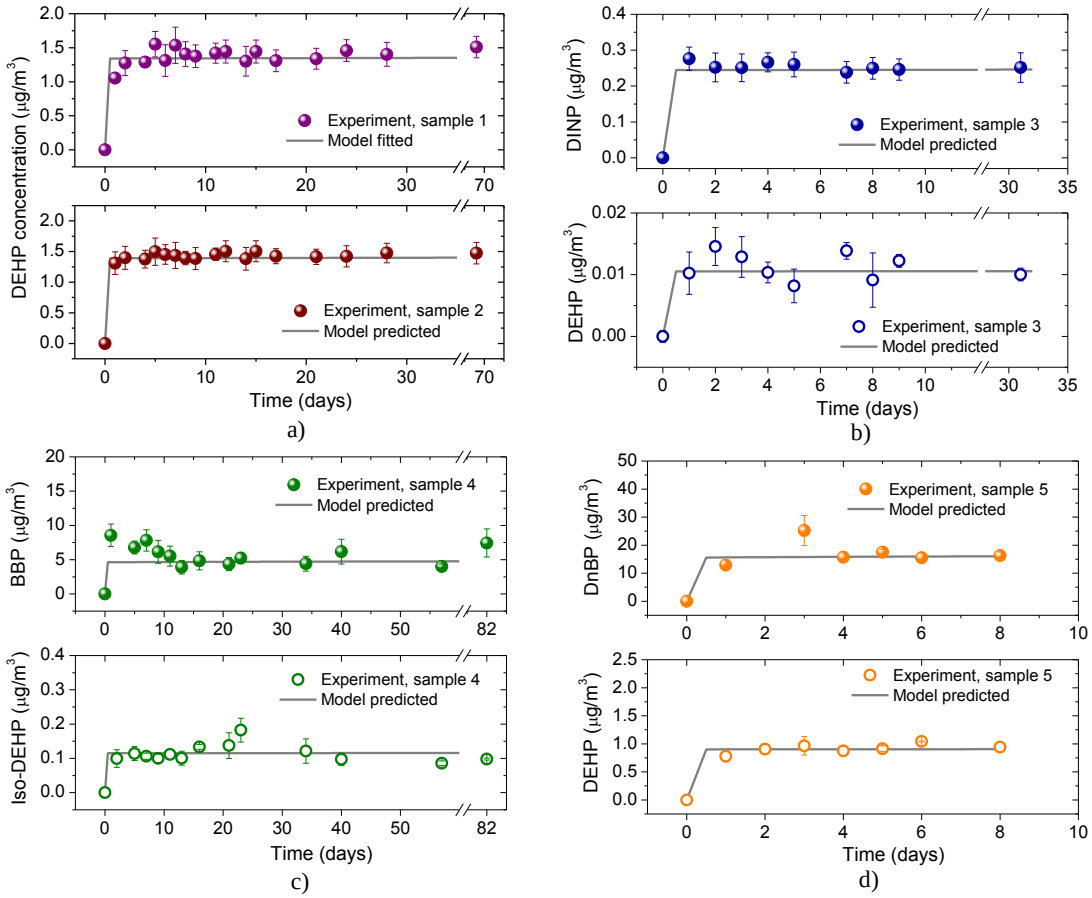

Figure A.2: Gas-phase chamber concentration of phthalates emitted from vinyl flooring samples. a) sample 1 and 2, b) sample 3, c) sample 4, and d) sample 5.

Based on the steady-state gas phase concentration in the emission chamber (y_{ss}) and h_m calculated previously, the value of y_0 for each vinyl flooring sample emitting particular phthalates was determined using Equation (7) and is listed in Table A.1. A sensitivity analysis of h_m is briefly discussed in the SI and the results show that doubling the mass-transfer coefficient (h_m) decreases the determined y_0 values less than 30%. Sample 1 was the exact same vinyl flooring used in previous studies (Xu et al., 2012; Clausen et al., 2012), but the measured y_0 of DEHP emission from Sample 1 (2.3 μg/m^3) was higher than previous estimations (~ 1 μg/m^3). The differences might be associated

with approximation of y_0 using y_{ss} value (Cluasen et al., 2012) and uncertainties related to fitting parameters (Xu et al., 2012; Xu and Little, 2006). Samples 1, 2, 3, and 5, which contained DEHP in different levels, were used to explore the relationship between y_0 and C_0. As shown in Figure A.3a, for low concentrations of DEHP in the materials (samples 1, 3, and 5), a simple partition coefficient corresponding to a value of 7×10^{10} can be used to linearly relate y_0 and C_0. Although three data observations might not be enough, the finding is similar as volatile organic compound (VOC) emissions from building materials (Kumar and Little, 2003). For the high weight percentage of DEHP in vinyl flooring (sample 2), however, simple partitioning mechanisms cannot be invoked. Considering that the molecular weight of DEHP is 391 g/mol and that of PVC flooring is from 20,000 to 80,000 g/mol, a weight percentage of ~20% implies that the molar fraction of DEHP in vinyl flooring is approximately 95%. However, the y_0 for sample 2 did not exceed 50% of the pure liquid V_p of DEHP (Table A.1), suggesting that the DEHP/vinyl flooring system is not an ideal solid mixture due to the extremely large size of polymer molecules compared to the size of DEHP molecules (Little, et al., 2012; Hawkes, 1995; Nicholson, 2006) and thus cannot be described by Raoult's law. Recently, DEHP was found to behave as a thermodynamically separate liquid phase in PVC products at high temperatures (between 35 °C and 100 °C) (Clausen et al., 2012; Little et al., 2012; Ekelund et al., 2010). In contrast, our measurements of y_0 and V_p suggested that y_0 may not be accurately approximated by V_p at room temperatures, even for vinyl floorings containing a relatively high concentration of phthalates (e.g., sample 2 [DEHP], sample 3 [DINP], and sample 4 [BBP]). But, V_p could have important influences on the value of y_0. For example, with samples 4 (Iso-DEHP) and 5 (DnBP and DEHP) having similar material-phase concentrations (C_0), the significant differences in y_0 are possibly related with the different V_p and chemical properties (Table A.1).

Therefore, the relationship among C_0, y_0, and V_p and the critical level of C_0, above which simple linear partition coefficient cannot apply, require further research.

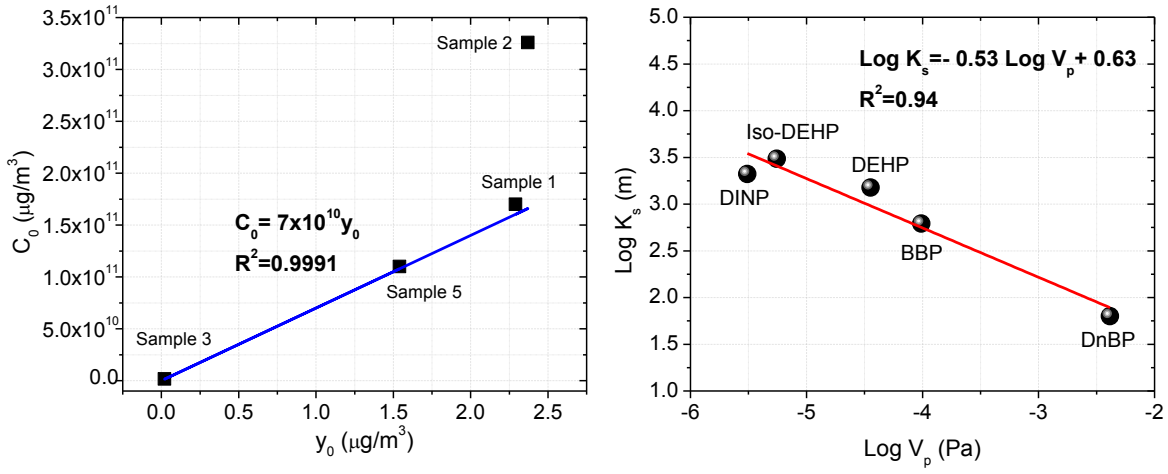

Figure A.3: (a) Relationship between C_0 and y_0 for DEHP samples; (b) Linear regression between K_s and log (V_p).

Although phthalates are present at a very high concentration in vinyl floorings, as SVOCs with low vapor pressures, they emit slowly. The specific emission rate (SER) can be estimated based on the gas-phase concentration, chamber air change rate, emission surface area and chamber volume (Clausen et al., 2004). After steady state has been reached, the SER was calculated for each vinyl flooring samples (Figure A.2), falling in the range of 7.8 μg/m^{2}h (DnBP) to 0.06 μg/m^{2}h (Iso-DEHP). In the case of DnBP at this emission rate, calculations show that after 5 years, only 0.1% of the total mass would have been emitted from the vinyl flooring, although the emission rate measured in these chambers might be somewhat different to that in actual indoor environments. The results indicated that PVC products such as vinyl flooring may behave as permanent indoor sources of phthalates during the product's life time.

Sorption Experiments. Strong sorption occurred on the stainless steel surfaces. Figure A.4 shows the evolution of phthalate concentrations on the stainless steel rods over time during steady-state conditions, when the gas-phase chamber concentration was constant. The surface concentration of phthalates increased progressively until the sorbed surface concentration reached equilibrium with the chamber air. The time to reach sorption equilibrium was 4 to 25 days, which was significantly reduced compared to a previous study of DEHP sorption (60 days) onto stainless steel (Xu et al., 2012) because of the enhanced mass transfer around the rods caused by the chamber outlet flows. Considering that the values of h_s (see the following section) and A_s are small for the specially designed chamber conditions, sorption onto chamber wall does not have significant influences on the accumulation of gas-phase phthalate concentrations (Equation 3 and 4) and the time to reach chamber steady state (Figure A.2). Assuming that a linear isotherm (K_s) is appropriate to explain the sorption relationship between stainless steel and gas-phase phthalates, the corresponding K_s values were obtained by dividing the equilibrium concentration on rod surfaces (Figure A.4) by the steady-state gas phase concentration within the chamber (Figure A.2). The difference of K_s for DEHP among samples 2, 3, and 5 is about 40%, which is possibly the result of normal measurement errors of gas- and surface-phase DEHP concentrations. Linear relationship between log (V_p) and log (K_s) were found as shown in Figure A.3b, with a trend of lower volatility phthalates showing higher K_s values. In addition, phthalates adsorbed on internal stainless steel surface of the chamber were wiped and analyzed at the end of the sorption experiments. The results (Figure A.4) are comparable to the rod measurements, suggesting that the developed method (rods with air pulling through rod holder) is most likely appropriate to quickly measure phthalate sorption onto indoor sink materials (e.g., wood, cloth, and foam).

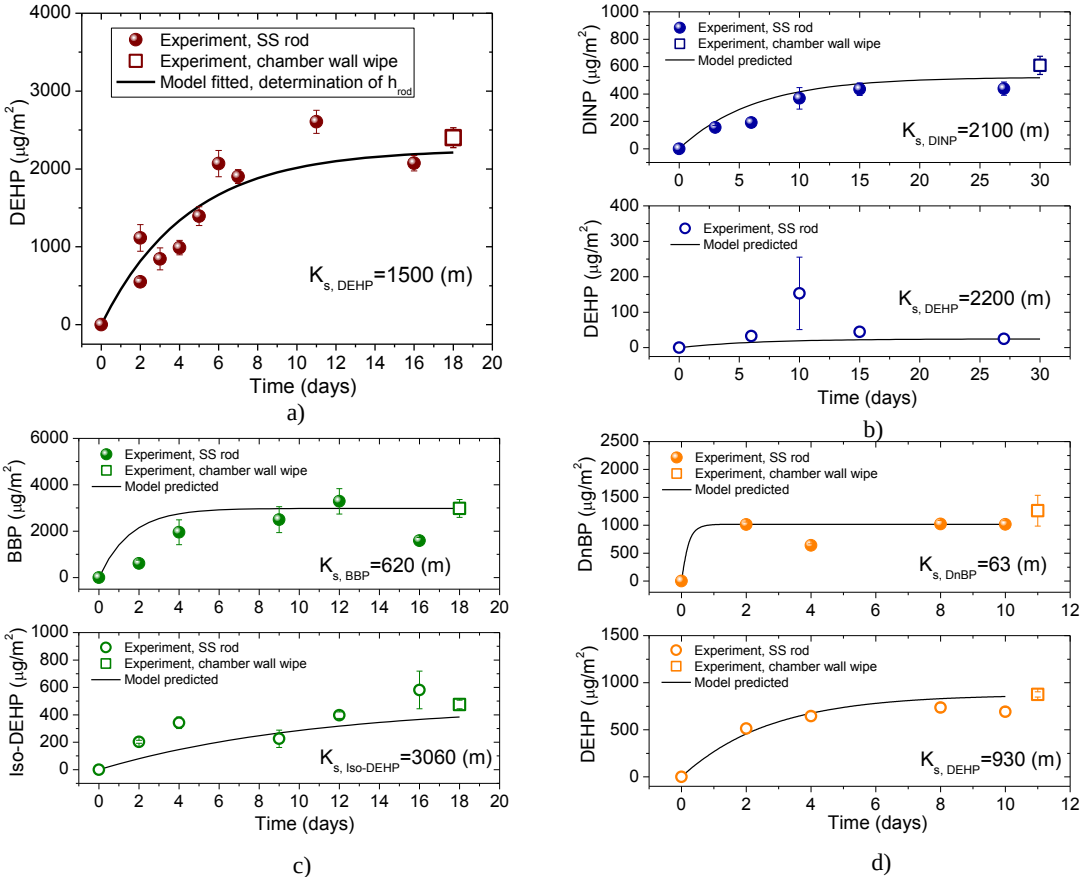

Figure A.4: Sorption of phthalates on stainless steel surface. a) sample 2, b) sample 3, c) sample 4, and d) sample 5.

Characterization of Phthalate Emissions and Sorptions. The simplified SVOC emission model (Xu et al., 2012) reveals that y_0, K_s, h_m, and h_s are important parameters that control phthalate emission rates. The values of y_0, K_s, and h_m were directly measured as described above. The model can therefore be used to obtain the unknown parameter (h_s) from the measured emission profile. Only the data obtained for DEHP emitted from sample 1 (Figure A.2a) were used to obtain this parameter and with the best-fit h_s value of 1.0×10^{-4} m/s. The h_s for other phthalates was then calculated using Equation (6), as shown in Table A.S3. Reassuringly, based on the velocity field

calculated by CFD, h_s was estimated using correlation equations (Axley, 1991), which express h_s as a function of Re and Sc numbers, and the estimated values are comparable to those obtained. Table A.S5 summarizes the model parameters for the experimental chamber conditions. The seven sets of data collected for the remaining experiments carried out in the emission chamber (samples 2 to 5) were used to test the predictive ability of the model, as shown in Figure A.2. Reasonable agreement between the gas-phase phthalate concentrations predicted by the model and the experimental data is obtained. The likely reason for the sharp curve of model prediction is the small h_s values, compared to the previous study (Xu et al., 2012). During the initial period of emission, most emitted phthalates cannot be instantly adsorbed to the chamber wall because of the existence of a relatively large convective mass-transfer resistant layer and are therefore accumulated in the gas phase. Figure A.S6 shows that the convective mass-transfer coefficient near the sorption surface, h_s (m/s), controls the initial emission period and influences the time to reach steady state strongly.

Rearranging Equation (3) to investigate the sorption kinetics of phthalates, the surface concentration on the rod can be expressed as

$$q_{rod}(t) = y_{ss}K_s\left(1 - e^{-\frac{h_{rod}}{K_s}t}\right) \tag{8}$$

where h_{rod} is the convective mass transfer coefficient near the rod surface, and y_{ss} is the steady-state gas phase concentration in the chamber. As shown in Figure A.4a, numerical simulation was used to obtain the only unknown parameter in Equation (8), h_{rod}, for DEHP. The best-fit h_{rod} value for DEHP (4.0×10^{-3} m/s) was then used to calculate h_{rod} for other phthalates (Table A.S3). Finally, the sorption kinetics and the equilibrium concentration on the rod surface can be predicted with the obtained h_{rod}. The variation in

approach to equilibrium is probably due to the different time periods for which the rods were exposed to the chamber air, with sampling intervals shown in Figure A.4. Overall, the results suggest that a linear isotherm (K_s) is most likely appropriate to explain the sorption relationship between stainless steel and gas-phase phthalates.

Estimation of Indoor Exposure to Phthalates. With the knowledge of measured y_0 values, indoor dynamic concentrations resulting from emissions of phthalates can be predicted in multi-phases (e.g., gas, airborne particle, dust, and interior surfaces), using a fate and transport model (Xu et al., 2009; Xu and Liang, 2011). Little et al. (2012) simplified the model and proposed a rapid method to obtain screening-level estimates of indoor exposure to SVOCs. In their simplified model, the steady-state SVOC concentration in indoor air was estimated based on a known y_0:

$$y = \frac{h_m \cdot y_0 \cdot A}{h_m \cdot A + h_s \cdot A_s + (1 + K_p \cdot TSP) \cdot Q} \quad (9)$$

where TSP is the mass concentration of suspended particles in the room and K_p is the equilibrium partitioning of the SVOC between gas phase and particles. The dust-phase concentrations were estimated based on K_{dust} (i.e., the partition coefficients between dust and air). Human indoor exposures to SVOCs can be assessed, with all model parameters that are readily available or that can be easily estimated based on SVOCs chemical properties (Little et al., 2012; Weschler and Nazaroff, 2010). Employing Little et al.'s method, we use the y_0 measured for vinyl flooring samples to assess human exposure to phthalates via inhalation of indoor air, dermal absorption of gas and deposited dust, and oral ingestion of dust when the tested flooring is present in a residential building. The exposure was estimated for five age groups: infants (<1 yr), toddlers (1-3 yrs), children (4-10 yrs), teenagers (11-18 yrs), and adults (≥19 yrs). Equations, exposure factors, and

parameters used in the calculation of daily exposure dose are listed in Table A.S6. Table A.S7 summarizes these exposure estimates along with the reference dose (RfD) values recommended by U.S. EPA (EPA IRIS, 2014), and Figure A.S7 shows the contribution of different routes to total exposure of phthalates. The exposure levels of infants, toddlers, and children markedly exceed that of teenagers and adults. A toddler could experience a two to eight times higher exposure than an adult in a home. The findings are similar to those of Guo and Kannan (2011) who measured indoor dust concentrations of phthalates and concluded that children may be more highly exposed than adults. Dermal absorption was the dominant source of DnBP and BBP, whereas ingestion of dust was the dominant pathway of exposure to DEHP, Iso-DEHP, and DINP. For infants, toddlers, and children, exposures to DEHP are higher than the RfD value, which is consistent with observations in previous studies (Little et al., 2012; Nazaroff et al., 2012). Frederiksen et al. (2011) estimated the daily exposure dose of DEHP in Danish people (6-21 yrs) at a median of 4 (μg/kg-bw/day) and a maximum of 53 (μg/kg-bw/day) based on urinary excretion of DEHP metabolites, which is comparable to the results of this study (12.6-25.3 μg/kg-bw/day). However, vinyl flooring was considered the only source of phthalates for this exposure assessment; therefore the values shown in Table A.S7 are possibly high. The reason might be due to the uncertainty associated with estimation of parameters (e.g., K_{dust} and dust ingestion rate) used in the exposure model.

In this study, we improved the design of an emission chamber and developed a novel, rapid method to measure y_0, a key parameter that controls phthalate emissions. This effective and economical approach is urgently needed to rapidly identify interior sources of phthalates, as well as the other SVOCs present in building materials and consumer products, which are most harmful to human health. The mechanisms governing emissions of phthalates from polymeric materials were further elucidated

through chamber studies. We extended the mechanistic understanding of emissions to an actual indoor environment through the fate and transport model of phthalates (Xu et al., 2009; Little et al., 2012; Xu and Liang, 2011) and connected the results to exposure assessments. The simple approach proposed will help health professionals estimate screening-level exposure associated with SVOCs present in polymeric materials as additives and conduct risk-based prioritization for a wide range of SVOCs chemicals of concern.

ACKNOWLEDGEMENTS

Financial support was provided by the National Science Foundation (NSF) (CBET-1150713 and CBET- 1066642).

SUPPORTING INFORMATION

Review of recent chamber studies on phthalate emissions. Understandings of emission mechanisms of phthalates and the ability to predict their emission rates from various sources are prerequisite for characterizing their fate and transport and developing suitable approaches to reduce their concentrations in indoor environments. However, standard chamber methods designed for measuring volatile organic compounds (VOCs), ozone and particulate matter may not be appropriate for measuring emissions of SVOCs (Afshari et al., 2004; Destaillats et al., 2008). There have been very few emission studies with low volatile plasticizers as target compounds, probably due to the difficulties associated with sampling and analysis of SVOCs (Clausen et al., 2004; Wensing et al., 2005). Afshari et al. (2004) tested dibutyl phthalate (DBP) and di(2-ethylhexyl) phthalate (DEHP) emissions from materials such as wallpaper, PVC flooring and electric wire in the Chamber for Laboratory Investigations of Materials, Pollution and Air Quality (CLIMPAQ) as well as the Field and Laboratory Emission Cell (FLEC) and found that the chamber concentration of DEHP reached steady state after about 150 days and that sorption by chamber surfaces has a strong effect on the rate of increase of gas-phase chamber concentrations. Schossler et al. (2011) measured air concentration for diisononyl phthalate (DINP), DINCH, and DBP emitted from PVC samples in the FLEC and found that the time it took for DINP and DINCH to reach the steady-state concentration is in the same order of magnitude. Clausen et al. (2004, 2012, 2010 and 2007) performed a series of tests on emissions of DEHP from vinyl flooring in the FLEC. Their work showed that (1) the emission rate of DEHP was limited by gas-phase mass transfer, (2) strong sorption of DEHP onto the FLEC chamber surface resulted in a very long time period to reach steady state, (3) relative humidity had no impact on the emission rate, (4) increasing the ventilation rate increased the emission rate, and (5) gas-

phase DEHP concentration in equilibrium with vinyl flooring surface was close to the vapor pressure of pure DEHP. Recently, Xu et al. (2012) designed a special stainless steel chamber to measure emission of DEHP from vinyl flooring. By increasing the area of vinyl flooring and decreasing that of the stainless steel surface within the chamber, the time to reach steady state was reduced, compared to the previous studies (30 days versus 150 days). Additionally, the adsorption isotherm of DEHP on the stainless steel chamber surfaces was measured independently. These chamber studies provided valuable information about the emission characteristics of phthalates from PVC materials. They also collectively reveal the substantial difficulties associated with chamber tests for SVOCs due to the low gas-phase concentration, strong sorption onto surfaces, and ubiquitous contamination in laboratory facilities.

Analysis of Phthalates. Phthalates collected by the Tenax TA sorbent tubes were desorbed by a thermal desorber (TD) (Turbomatrix 650 ATD) and analyzed by a GC-MS system (Agilent 7890A GC- 5975MS). Before analysis, 5 μL solution of D_4-DEHP (2 μg/mL) in methanol was injected into the Tenax tubes as internal standard. The sorbent tubes were then desorbed for 30 min at 300 °C, with a He flow of 50 ml/min, and a cold trap temperature of minus 30 °C. Flash heating of the cold trap to 350 °C transferred the analyte through the valves at 250 °C and the transfer line at 250 °C to the GC. The GC-MS had a constant pressure resulting in a flow rate of 1.6 ml/min at 80 °C, and was equipped with a 30 m × 0.25 mm DB-5MS column and operated at a 5:1 split injection. The temperature program was 80 °C, hold for 0.5 min, ramp 20 °C/min for 8.5 min, then ramp 30 °C/min for 2 min, and finally hold for 9 min. All analyses were performed in full scan mode and the extracted ions used for identification and quantification are summarized in Table A.S2. It should be noted that DINP is mixtures of many isomers, and was detected as correspondingly broad peaks, which took about 1 min to elute

(Figure A.S3). All tubes were analyzed in two successive desorptions to ensure complete desorption of both the tube and the TD-GC-MS system. The second desorption showed concentrations below the detection limit in all cases. A calibration standard was regularly run prior to each GC injection, and the variance was always below 5% for all injections.

Determination of V_p. With reference to Figure A.S4, the accumulation of SVOCs in the chamber obeys the following mass balance:

$$\frac{dy(t)}{dt} \cdot V = E(t) \cdot A - \frac{dq(t)}{dt} \cdot A_s - y(t) \cdot Q \quad (4)$$

At steady state:

$$E(t) \cdot A - y_{ss} \cdot Q = 0 \quad (4')$$

In Equation 1 we know that the emission rate is

$$E(t) = h_m \cdot [y_0 - y(t)] \quad (1)$$

Substitute Equation 1 into Equation 4', we obtain

$$h_m \cdot (y_0 - y_{ss}) \cdot A - y_{ss} \cdot Q = 0 \quad (5')$$

In vapour pressure experiments (Figure A.S2), y_0 is equivalent to V_p, by modifying Equation 5', we obtain

$$V_p = \frac{y_{ss} \cdot Q}{h_m \cdot A} + y_{ss} \quad (5)$$

Sensitivity Analysis of h_m on the Determined Parameters. We conducted a sensitivity analysis of h_m on the determined parameters y_0 and V_p. Here, we computed y_0 and V_p values using Equations 7 and 5, respectively. The sensitivity was assessed by computing the percentage change in y_0 and V_p values per unit increase of h_m. The baseline conditions are those used for the results shown in Table A.1 and Figure A.2. The following table shows the results of the sensitivity analysis. Increasing the mass-transfer coefficient (h_m) decreases y_0 and V_p within 30%.

Sample ID	Phthalates	Baseline value of h_m (m/s)	y_0 sensitivity	V_p sensitivity
1	DEHP	2.10E-04	-0.17	-0.28
2	DEHP	2.10E-04	-0.22	-0.28
3	DINP	2.01E-04	-0.19	-0.28
	DEHP	2.10E-04	-0.28	-0.28
4	BBP	2.38E-04	-0.18	-0.26
	Iso-DEHP	2.10E-04	-0.19	-0.28
5	DnBP	2.54E-04	-0.17	-0.26
	DEHP	2.10E-04	-0.20	-0.28

Parameter	Value
Temperature (°C)	25 ± 0.5
Chamber volume (L), V	1
Air flow rate (mL/min), Q	1000
Air change rate (1/h)	53
Area of test pieces (m^2), A	0.13
Internal stainless steel surface area (m^2), A_s	0.02
Chamber diameter (cm)	40
Chamber height (cm)	1.8
Loading (m^2/m^3), A_s/V	16

Table A.S1: Chamber properties and test conditions.

Phthalate compounds	Abbrev.	CAS no.	MW (g/mol)	t_R (min)	Quantifying ion	Qualifier ions
Dimethyl phthalate	DMP	131-11-3	194.2	6.25	163	194
Di-n-butyl phthalate	DnBP	84-74-2	278.4	9.02	149	205, 223
Butyl benzyl phthalate	BBP	85-68-7	312.4	10.8	149	91, 206
Di(2-ethylhexyl) phthalate	DEHP	117-81-7	390.6	11.44	149	167, 279
Di(2-ethylhexyl) isophthalate	Iso-DEHP	137-89-3	390.6	12.50	149	261
Diisononyl phthalate	DINP	28553-12-0	418.6	11~12	293	149, 167
Di(2-ethylhexyl) phthalate-3,4,5,6-d_4	D_4-DEHP	93951-87-2	394.6	11.44	153	171, 283

Table A.S2: GC-MS retention times (t_R), quantifying and qualifier ions for phthalates.

Phthalates	h_m (m/s)	h_{rod} (m/s)	h_s (m/s)
DMP	3.12×10^{-4} [a]	--	--
DnBP	2.54×10^{-4} [b]	4.85×10^{-3} [b]	1.2×10^{-4} [b], 0.4×10^{-4} [e]
BBP	2.38×10^{-4} [b]	4.54×10^{-3} [b]	1.1×10^{-4} [b], 0.4×10^{-4} [e]
DEHP	2.10×10^{-4} [b]	4.00×10^{-3} [c]	1.0×10^{-4} [d], 0.3×10^{-4} [e]
Iso-DEHP	2.10×10^{-4} [b]	4.00×10^{-3} [b]	1.0×10^{-4} [b], 0.3×10^{-4} [e]
DINP	2.01×10^{-4} [b]	3.85×10^{-3} [b]	0.96×10^{-4} [b], 0.3×10^{-4} [e]

a. Measured in DMP vapor pressure experiment.
b. Calculated using Equation (6).
c. Fitted using sorption experimental data of sample 2.
d. Fitted using emission experimental data of sample 1.
e. Estimated based on velocity calculated by computational fluid dynamic (CFD) simulation.

Table A.S3: Mass transfer coefficients (h_m, h_s, and h_{rod}) for emission and sorption in the chamber.

Phthalates	This study	Estimation using SPARC and EPI Suite	Experimental data in literature
DMP	3.6×10^{-1} [a]	5.6×10^{-2} [b]; 5.4×10^{-1} [c]; 6.2×10^{-1} [d]; 1.1×10^{0} [e].	4.1×10^{-1} [f]; 2.6×10^{-1} [g]; 2.2×10^{-1} [g]; 3.0×10^{-1} [g]; 2.7×10^{-1} [g].
DnBP	4.1×10^{-3} [i]	3.4×10^{-4} [b]; 1.6×10^{-2} [c]; 3.0×10^{-2} [d]; 5.6×10^{-2} [e].	2.7×10^{-3} [f]; 4.7×10^{-3} [g]; 9.7×10^{-3} [g]; 3.6×10^{-3} [g].
BBP	1.0×10^{-4} [i]	3.6×10^{-6} [b]; 2.1×10^{-3} [c]; 5.9×10^{-3} [d]; 1.2×10^{-2} [e].	1.1×10^{-3} [f]; 2.5×10^{-3} [g]; 1.2×10^{-3} [g]; 6.7×10^{-4} [g].
DEHP	3.6×10^{-5} [i]	1.4×10^{-7} [b]; 7.6×10^{-4} [c]; 2.7×10^{-3} [d]; 5.5×10^{-3} [e].	1.9×10^{-5} [f]; 1.7×10^{-5} [f]; 5.1×10^{-5} [f]; 2.1×10^{-5} [g]; 2.5×10^{-5} [g]; 8.6×10^{-4} [g].
Iso-DEHP	5.6×10^{-6} [i]	2.8×10^{-5} [c]; 1.9×10^{-4} [d]; 3.7×10^{-4} [e].	n.a.
DINP	3.1×10^{-6} [i]	8.9×10^{-9} [b]; 2.7×10^{-6} [c]; 3.1×10^{-5} [d]; 6.2×10^{-5} [e].	6.0×10^{-5} [f]; 7.2×10^{-5} [f]; 3.6×10^{-7} [h].

a. Mean value of data reported in literature used to determine $h_{m,\,DMP}$ using equation (5).
b. Estimated using SPARC v4.5.
c. Estimated using EPI Suite v4.1, Antoine Method.
d. Estimated using EPI Suite v4.1, Modified Grain Method.
e. Estimated using EPI Suite v4.1, Mackay Method.
f. Experimental data provided in EPI Suite v4.1.
g. Data reported in (Weschler and Nazaroff, 2008).
h. Data reported in (Schossler et al., 2011).
i. Measured in the vapor pressure experiments.

Table A.S4: Vapor pressure of phthalates (Pa) at 25 °C.

Parameter	Value	Comments
Sample 1		
DEHP		
Concentration in equilibrium with vinyl flooring (μg/m^3), y_0	2.3	Measured
Convective mass-transfer coefficient (m/s), h_m	2.10×10^{-4}	Measured
Convective mass-transfer coefficient near sorption surface (m/s), h_s	1.0×10^{-4}	Model fitted
Sorption surface/air partition coefficient (m), K_s	1500	Measured
Sample 2		
DEHP		
Concentration in equilibrium with vinyl flooring (μg/m^3), y_0	2.37	Measured
Convective mass-transfer coefficient (m/s), h_m	2.10×10^{-4}	Measured
Convective mass-transfer coefficient near sorption surface (m/s), h_s	1.0×10^{-4}	Calculated
Sorption surface/air partition coefficient (m), K_s	1500	Measured

(Table A.S5 continues on the next page)

Sample 3		
DINP		
Concentration in equilibrium with vinyl flooring (μg/m^3), y_0	0.42	Measured
Convective mass-transfer coefficient (m/s), h_m	2.01×10^{-4}	Measured
Convective mass-transfer coefficient near sorption surface (m/s), h_s	0.96×10^{-4}	Calculated
Sorption surface/air partition coefficient (m), K_s	2100	Measured
DEHP		
Concentration in equilibrium with vinyl flooring (μg/m^3), y_0	0.02	Measured
Convective mass-transfer coefficient (m/s), h_m	2.10×10^{-4}	Measured
Convective mass-transfer coefficient near sorption surface (m/s), h_s	1.0×10^{-4}	Calculated
Sorption surface/air partition coefficient (m), K_s	2200	Measured
Sample 4		
BBP		
Concentration in equilibrium with vinyl flooring (μg/m^3), y_0	8.47	Measured
Convective mass-transfer coefficient (m/s), h_m	2.38×10^{-4}	Measured
Convective mass-transfer coefficient near sorption surface (m/s), h_s	1.1×10^{-4}	Calculated
Sorption surface/air partition coefficient (m), K_s	620	Measured
Iso-DEHP		
Concentration in equilibrium with vinyl flooring (μg/m^3), y_0	0.12	Measured
Convective mass-transfer coefficient (m/s), h_m	2.1×10^{-4}	Measured
Convective mass-transfer coefficient near sorption surface (m/s), h_s	1.0×10^{-4}	Calculated
Sorption surface/air partition coefficient (m), K_s	3060	Measured
Sample 4		
DnBP		
Concentration in equilibrium with vinyl flooring (μg/m^3), y_0	24.7	Measured
Convective mass-transfer coefficient (m/s), h_m	2.54×10^{-4}	Measured
Convective mass-transfer coefficient near sorption surface (m/s), h_s	1.2×10^{-4}	Calculated
Sorption surface/air partition coefficient (m), K_s	63	Measured
DEHP		
Concentration in equilibrium with vinyl flooring (μg/m^3), y_0	1.54	Measured
Convective mass-transfer coefficient (m/s), h_m	2.10×10^{-4}	Measured
Convective mass-transfer coefficient near sorption surface (m/s), h_s	1.0×10^{-4}	Calculated
Sorption surface/air partition coefficient (m), K_s	930	Measured

Table A.S5: Model parameters.

Exposure pathways	**Daily exposure dose to phthalates (μg/kg-bw/day)**	**Explanation**	**Exposure factor and parameters used in model**
Indoor air inhalation	$Exposure\ dose = \frac{C \times IR \times IEF}{BW}$	*C* = total air borne concentration of phthalates (μg/m^3) *IR* = inhalation rate (m^3/day) *IEF* = indoor exposure fraction (hours spent over a day in an indoor environment)	*C* (μg/m^3) C = (1+K_p × TSP) × y, where K_p (m^3/μg) [a] is the particle/air partition coefficient, TSP (μg/m^3) [b] is the total suspended particle concentration and y (μg/m^3) [c] is the gas-phase concentration of phthalates. *BW* (kg) [d] infants: 5; toddlers: 16; children: 29;

(Table A.S6 continues on the next page)

		BW = body weight (kg)	teenagers: 52; adult: 80.9 *IR* (m^3/d) [d] infants: 4.5; toddler: 7.6; children: 10.9; teenagers: 14; adult: 15.1 *IEF* [d] infants: 0.88; toddlers: 0.79; children: 0.79; teenagers: 0.88; adults: 0.88
Dust dermal absorption	$Exposure\ dose = \frac{C_d \times BSA \times SAS \times AF \times IEF}{BW \times 1000 mg/g}$	C_d = dust concentration of phthalates (μg/g) *BSA* = body surface area (cm^2/day) *SAS* = soil or dust adhered to skin (mg/cm^2) *AF* = fraction of compounds absorbed in the skin	C_d (μg/g) $C_d = K_{dust} \times y$, where K_{dust} (m^3/μg) [a] is the dust/air partition coefficient and y (μg/m^3) [c] is the gas-phase concentration of phthalates. *BSA* (cm^2/d) [e] infants: 801; toddlers: 2564; children: 3067; teenagers: 3692; adults: 4615 *SAS* (mg/cm^2) [d] 0.096 *AF* [f] for infants, toddlers, children, teenagers and adults: DnBP: 0.001556; BBzP: 0.000707; DEHP: 0.000106; isoDEHP: 0.000106; DiNP: 0.0000636. The values for adults are half.
Gas dermal absorption	$Exposure\ dose = \frac{y \times BSA \times P \times IEF \times 24\ h/d}{BW \times 10000 cm^2/m^2}$	*y* = gas-phase concentration of phthalates (μg/m^3) *BSA* = body surface area (cm^2/day) *P* =overall skin permeability coefficient of gases (m/h)	*y* (μg/m^3) [c] *P* for Phthalates (m/h) [g] DnBP: 4.8; BBzP: 5.9; DEHP: 5.8; isoDEHP: 5.8 *P* for DiNP (m/h) [h]: 1.126
Dust ingestion	$Exposure\ dose = \frac{C_d \times SIR \times IEF}{BW}$	C_d = dust concentration of phthalates (μg/g) *SIR* = soil or dust ingestion rate (g/day)	*SIR* (g/d) [d] infants: 0.02; toddlers: 0.1; children: 0.05; teenagers: 0.05; adults: 0.05

a. The values were estimated utilizing Equation (3.10) and (3.11) in (Weschler and Nazaroff, 2008).
b. The value was 20 μg/m^3 as the average indoor TSP level in US.
c. The values were estimated utilizing Equation (2) and (3) in (Little et al., 2012), where the values of y_0 (μg/m3) were directly measured from experiments in this study.
d. (US EPA Exposure Factors Handbook, 2011).
e. Skin area exposed includes hands, legs, and arms representing 25% of the total skin area (US EPA Exposure Factors Handbook, 2011; Johnson-Restrepo et al., 2009).
f. The values were obtained from (Wormuth et al., 2006). AF values for infants, toddlers, children and teenagers are the mean value of child, which is two times to the value of adult.
g. The values were obtained from (Weschler and Nazaroff, 2012).
h. The values were estimated utilizing Equation (24) and (31) in (Weschler and Nazaroff, 2012).

Table A.S6: Equations and exposure factors used in calculation of daily indoor exposure dose.

Phthalates	Infants	Toddlers	Children	Teenagers	Adults	Exposure guidelines (RfD)
DnBP (sample 5)	25.7	21.2	13.0	9.7	9.1	100
BBP (sample 4)	10.2	9.4	5.1	3.7	3.4	200
DEHP (sample 2)	65.4	91.5	25.3	15.8	12.6	20
Iso-DEHP (sample 4)	22.9	32.1	8.9	5.5	4.4	n.a.
DINP (sample 3)	5.7	7.9	2.2	1.4	1.1	n.a.

Table A.S7: Estimated phthalate indoor exposures (µg/kg-body weight/day).

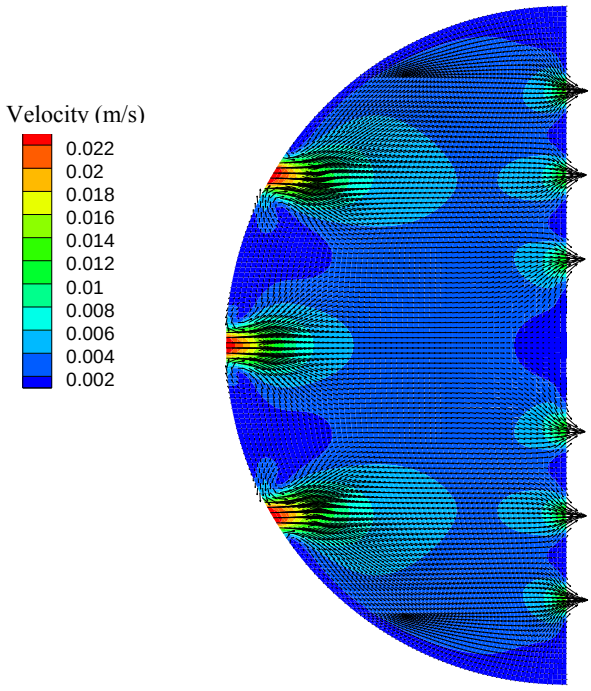

Figure A.S1: Simulation of air velocity field in the emission chamber.

Figure A.S2: Photo of the special petri dish fitted within the chamber.

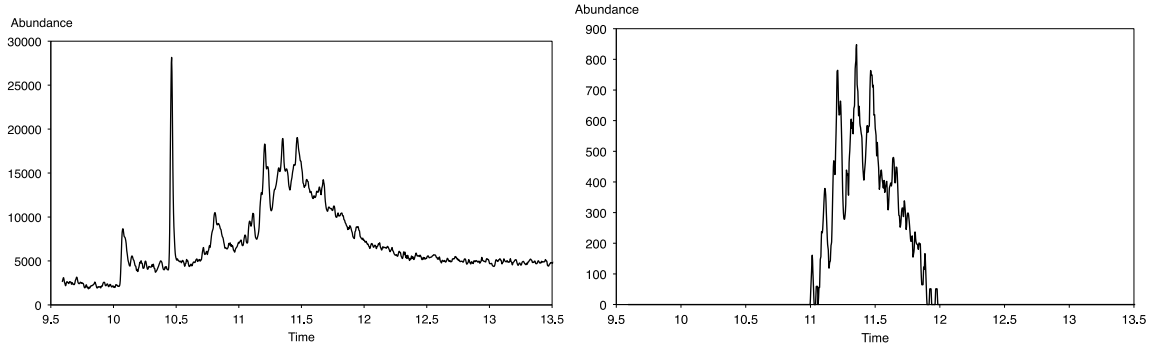

a) Full scan mode. b) Selected ion monitoring.

Figure A.S3: Ion chromatogram of DINP.

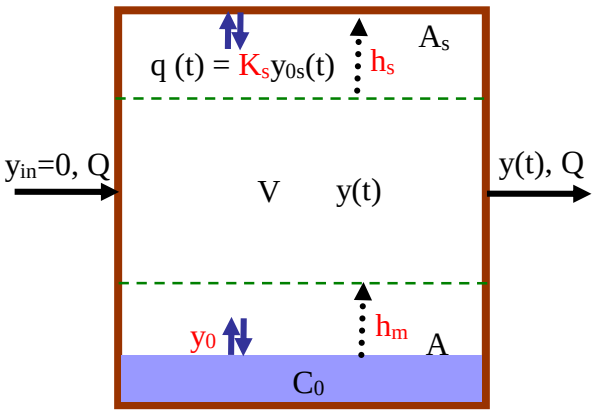

Figure A.S4: Schematic representation of SVOCs emissions in an experimental chamber.

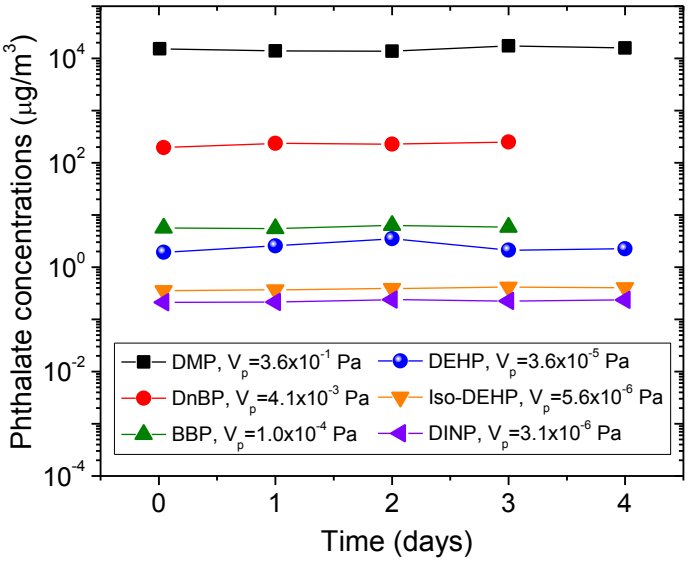

Figure A.S5: Vapor pressure measurements.

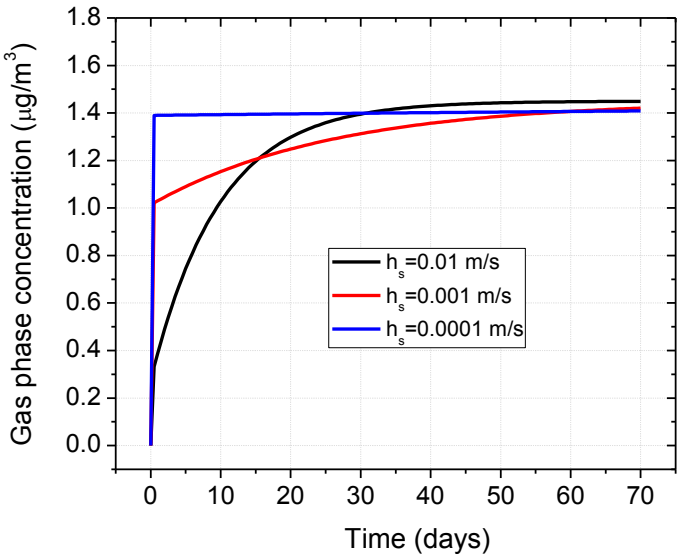

Figure A.S6: The influence of h_s on emission of DEHP from sample 2.

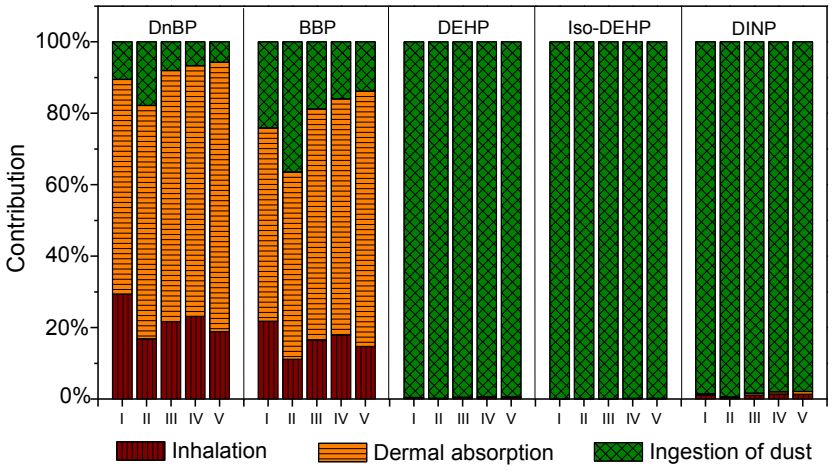

I Infants, **II** Toddlers, **III** Children, **IV** Teenagers, **V** Adults

Figure A.S7: Contribution of different routes to total exposure to phthalates.

Appendix B

Paper 2. Emissions of Phthalates and Phthalate Alternatives from Vinyl Flooring and Crib Mattress Covers: The Influence of Temperature

Yirui Liang and Ying Xu
(Accepted by *Environmental Science & Technology*)

ABSTRACT

Emissions of phthalates and phthalate alternatives from vinyl flooring and crib mattress covers were measured in a specially-designed chamber. The gas-phase concentrations versus time were measured at four different temperatures, i.e., 25, 36, 45, and 55 ºC. The key parameter that controls the emissions (y_0, gas-phase concentration in equilibrium with the material phase) was determined, and the emissions were found to increase significantly with increasing temperature. Both the material-phase concentration (C_0) and the chemical vapor pressure (V_p) were found to have great influence on the value of y_0. The measured ratios of C_0 to y_0 were exponentially proportional to the reciprocal of temperature, in agreement with the van't Hoff equation. An emission model was validated at different temperatures, with excellent agreement between model predictions and chamber observations. In residential homes, an increase in the temperature from 25 to 35 ºC can elevate the gas-phase concentration of phthalates by more than a factor of 10, but the total airborne concentration may not increase that much for less volatile compounds. In infant sleep microenvironments, an increase in the temperature of mattress can cause a significant increase in emission of phthalates from the mattress cover and make the concentration in breathing zone about four times higher than that in the room, resulting in potentially high exposure.

INTRODUCTION

Phthalates have been used as plasticizers to enhance the flexibility of polyvinyl chloride (PVC) products. These semi-volatile organic compounds (SVOCs) are found in

a wide range of building materials and consumer products (Bornehag et al., 2005), and they are present at various levels, with some as high as 10% level or even greater (Weschler and Nazaroff, 2008). Because phthalate additives are not chemically bound to the polymer matrix, they usually are emitted slowly from the products into the air or other media (Xu et al., 2012). As a result, phthalates are ubiquitous and among the most abundant SVOCs in indoor environments (Bornehag et al., 2005 and 2004; Clausen et al., 2012; Rudel and Perovich, 2009). Recent studies have suggested that exposure to some phthalates may cause irreversible changes in the development of the human reproductive tract (Heudorf et al., 2007; Jaakkola and Knight, 2008; Latini et al., 2006; Matsumoto et al., 2008; McKee et al., 2004; Ritter and Arbuckle, 2007); increase the risk of asthma, rhinitis, and allergies (Bornehag et al., 2005; Jaakkola et al., 2006 and 1999; Kolarik et al., 2008; Øie et al., 1997); and affect endogenous hormones (Rudel and Perovich, 2009). As a result, rapid changes are occurring in phthalates used in PVC products, with a trend toward using phthalates that have higher molecular weight and lower volatility (Schossler et al., 2011; Weschler, 2009). Also, alternative plasticizers, such as diisononyl cyclohexane-1,2-dicarboxylate (DINCH), di(2-ethylhexyl) adipate (DEHA), and di(2-ethylhexyl) terephthalate (DEHT), have emerged very recently, but currently there is a lack of toxicological information for these compounds (Schossler et al., 2011). Given that these alternatives have properties that are similar to those of phthalates, similar levels of emissions and environmental fates may be expected.

We must understand the mechanisms by which phthalates and their alternatives are emitted from various sources in order to characterize their fate and develop suitable approaches for reducing their concentrations in indoor environments. However, very few emission studies have targeted low volatility plasticizers (Xu et al., 2012; Clausen et al., 2012; Schossler et al., 2011; Afshari et al., 2004; Clausen et al., 2004, 2010 and 2007),

possibly due to the substantial difficulties associated with chamber tests for SVOCs, including the long duration of tests (months to years), the low gas-phase concentrations in test chambers, strong sorption onto surfaces, and ubiquitous contamination in laboratory facilities. Based on the results of early chamber studies (Clausen et al., 2004), Xu and Little (2006) developed a fundamental mass-transfer model to predict SVOC emissions from polymeric materials. They showed that emissions of these compounds that have very low volatility are subject to "external" control (partitioning from the material into the gas phase, the gas-phase mass-transfer coefficient, and strong sorption onto interior surfaces, including airborne particles). Using data collected in a specially-designed stainless steel chamber, Xu et al. (2012) showed that the emission rate of di(2-ethylhexyl) phthalate (DEHP) from vinyl flooring can be predicted based on a priori knowledge of y_0, the gas-phase concentration of DEHP in equilibrium with the material phase, the material to air and air to stainless steel-surface mass-transfer coefficients (h_m), and the stainless steel/air equilibrium relationship. Liang and Xu (2014a) recently improved the design of the earlier emission chamber and developed a novel, rapid method to measure y_0 for a range of phthalate compounds released from building materials. The mechanisms that govern emissions of phthalates from polymeric materials were also elucidated further by their study.

Temperature may have a strong influence on the emissions of phthalates in indoor environments, because y_0 is related to vapor pressure, which depends strongly on temperature. When sunlight radiates directly onto a surface of plasticized vinyl products in a room, the surface temperature can increase by more than 10 ºC (Figure B.S1) (Table and Figure numbers preceded by an "S: are in the Supporting Information), and the higher temperatures may increase the emission rate significantly because increases in both y_0 and h_m drive faster emissions. Climate change may result in increased indoor

temperatures as outdoor temperatures increase; in addition there may be failures of air-conditioning systems during heat waves and power interruptions. These factors could greatly increase the emissions of various indoor air pollutants including phthalates. In addition to the building environments, people in modern societies spend a significant fraction of their time in automobiles, where air temperatures as high as 89 °C and dashboard temperatures up to 120 °C have been reported (Gearhart and Posselt, 2014). These temperatures likely result in extraordinarily high emission rates from materials, such as the fabric used in the seats, cable insulation, and interior trim. Crib mattresses are a pollutant source of special concern because they commonly have a vinyl cover for waterproofing and anti-bacterial purposes. Various phthalate plasticizers and their alternatives have been found in crib mattress covers (Boor et al., 2014a and 2014b). Temperature dependence is particularly relevant in this case, because phthalate emissions from crib mattresses may be increased due to temperature increases that occur as the result of heat transfer from the infant's body. Thus, infants can be exposed to high concentrations of phthalates while they are in close contact with the mattress, with their breathing zone and skin in immediate proximity to the source.

Despite its importance for exposure and risk assessment, the influence of temperature on the emission and transport of indoor phthalates have yet to be studied comprehensively. Fujii et al. (2003) studied the emission of phthalates from plastic materials using a passive flux sampler. They found that the maximum emissions of DEHP increased 100-fold when the temperature increased from 20 to 80 ºC. Because the concentration of phthalates at the surface of the sampler was assumed to be zero and there was no air exchange inside the sampler, the measured high emission rate, which was caused by a precipitous concentration gradient inside the passive flux sampler, may not represent the actual emission rates in indoor environment. Ekelund et al. (2010 and

2008) investigated the migration of DEHP from the insulation of PVC cables by measuring weight loss over time in ventilated ovens at temperatures between 80 and 155 ºC. They showed that the transport of DEHP to the surrounding air was controlled by diffusion in the boundary layer at temperatures of 80 and 100 ºC with activation energy of 98 kJ/mol, which was equal to that for the evaporation of pure liquid DEHP. With more strict control of air flow, Clausen et al. (2012) measured emissions of DEHP from PVC flooring in the Field and Laboratory Emission Cell (FLEC) at five different temperatures between 23 and 61 ºC. They observed that the steady-state concentrations of DEHP increased considerably as temperature increased, while adsorption to the chamber walls decreased greatly as temperature increases. They also found that y_0, the gas-phase DEHP concentration in equilibrium with vinyl flooring surface, is close to the vapor pressure (V_p) of pure DEHP liquid. However, because temperature dependence is strongly related to the type of phthalates (Fujii et al., 2003), y_0 might not be well approximated by V_p for other phthalates. To date, no systematic investigations have been conducted to characterize the effect of temperature on the mechanisms governing emissions of major phthalates and their alternatives.

The aim of this study is to investigate the influence of temperature on emission of phthalates and their alternatives from building materials and consumer products. The specific objectives are to: (1) conduct a series of controlled tests in specially designed stainless steel chambers to characterize phthalate emissions from vinyl flooring and crib mattress cover at four different temperatures; (2) measure y_0 (the gas-phase concentration in equilibrium with material phase) and C_0 (the concentration of phthalates present in materials), and investigate the nature of their relationship as a function of temperature; (3) validate the SVOC emission model in chamber experiments over a range of temperatures; and (4) use the obtained data to demonstrate the impact of temperature on

phthalate concentrations in residential indoor environments and infant sleep microenvironments.

METHODS AND MATERIALS

Chemicals. Standard solutions were used for chemical calibration and identification, in which di-n-butyl phthalate (DnBP), butyl benzyl phthalate (BBP), and di(2-ethylhexyl) phthalate (DEHP) were obtained from Absolute Standards Inc., iso-DEHP from SPEX CertiPrep, diisononyl phthalate (DINP) and di(2-ethylhexyl) adipate (DEHA) from Accustandards, Inc., and diisononyl cyclohexane-1,2-dicarboxylate (DINCH) from BOC Sciences. Tetradeuterium ring labeled DEHP (D_4-DEHP) was used as internal standard, and its standard solution was obtained Accustandards, Inc. Hexane, methanol, and dichloromethane (Sigma-Aldrich Co. LLC., anhydrous, >99%) were used as solvent in extraction and cleaning without further purification. The solvents were regularly analyzed to monitor potential phthalate contamination.

Test Materials. Sixteen types of vinyl floorings and ten crib mattresses were purchased primarily in the United States. The contents of phthalates and their alternatives in each sample were quantified experimentally. Among them, we selected four floorings and two mattress covers that contained different phthalates at relatively high concentrations. Each material was cut into two 0.45 m × 0.25 m sheets, wrapped in aluminum foil, and stored at room temperature. Before a measurement, the test pieces were unwrapped and placed in the emission chamber.

The content of phthalates and their alternatives in vinyl floorings and crib mattress covers was measured in duplicate by liquid extraction. Ten small pieces of samples (approximately 1~4 mg in total) were cut out of each type of material with a pair of scissors at randomly chosen positions. The samples were ultrasonically extracted for

40 min with dichloromethane for three times. The extractions were conducted in an ultrasonicator filled with clean water and ice bags to maintain a low temperature and avoid evaporation loss of sample during the process. The volume of extracts was reduced using a rotary evaporator (IKA RV-10) and a high purity N_2 stream. After concentrating to about 5 mL, the samples were cleaned up with preassembled filtration devices (Whatman AutovialTM syringless PTFE filters with 0.2 μm pore). Finally, a nitrogen purge was used to further reduce the sample volume to approximately 800 μL. The extracts (2 μL) were then injected with a solution of D_4-DEHP as internal standard into Tenax TA tubes and analyzed by thermal desorption combined with gas chromatography and mass spectrometry (TD-GC-MS). Chemical analysis of phthalates and their alternatives was described in detail in the Supporting Information (SI).

Emission Experiments. A specially-designed, stainless steel chamber used in previous experiments (Liang and Xu, 2014a) was employed in this study. The chamber that was used for SVOC emission testing maximized the surface area of emission source and minimized the surface area of internal sink thereby substantially reducing the time required to reach steady state. In addition, three precision-ground stainless steel rods, matched to the interior stainless steel chamber surface, were inserted into the chamber and then periodically removed so that the concentration of SVOCs sorbed on the surface could be measured. This method allowed us to relate gas-phase concentration to the concentration sorbed on the surface of the chamber and quickly establish the sorption equilibrium relationship. The specific design of the chamber was described in greater detail by Liang and Xu (2014a). The chamber's properties and the test conditions of the current study are listed in Table B.S2.

The concentrations of phthalates and phthalate alternatives were measured periodically in the chamber, which was operated at an air flow rate of 1000 mL/min, ~0%

relative humidity, and four different temperatures (25±0.5, 36±0.5, 45±0.5, and 55±0.5 °C). Before each emission test, the stainless steel plates and the internal surfaces of the chamber were cleaned with an alkali detergent, hot water and Nanopure® water, after which they were rinsed several times with methanol. Background measurements were performed before each test for a week. Then, the emission chambers containing the test samples were placed in a temperature-controlled cabinet (Lunaire CEO-932). Once the gas-phase concentration in the chamber reached steady state, the controlled temperature was elevated to the next target temperature degree. For the two mattress cover samples, the tests at the temperature of 55±0.5 °C were not successful because the material melted. Phthalates and phthalate alternatives were sampled in triplicate on Tenax-TA sorbent tubes with a pump (SKC 224-PCXR4) calibrated approximately to a nominal flow rate of 100 ml/min using a flow calibrator (mini-BUCK™ Model M-5). The sampling time was usually 24 hours for the low concentrations at 25 °C, and approximately 10–80 min for concentrations at the other temperatures. Backup tubes were connected to each primary sample tube to check for breakthrough, and none was observed in any of the tests. As the sampling system was supplied with high purity air from cylinders, we assumed that no particles were present. Because humidity does not significantly influence phthalate emissions (Clausen et al., 2007) in stainless steel chambers, only temperature and air flow rate through the chamber were checked before and after samples were taken for analysis.

SVOC Emission Model. Xu and Little (2006) developed an SVOC emission model, and the model was recently simplified by Xu et al. (2012). In their analysis, the emission rate is:

$$E(t) = h_m \cdot [y_0 - y\,(t)] \quad (1)$$

where y ($\mu g/m^3$) is the bulk gas-phase concentration, and h_m (m/s) is the convective mass-transfer coefficient. The ratio of the concentration of a chemical on sorption surfaces to

its concentration in the gas phase is equal to the surface/air partition coefficient, K_s (m), or

$$K_s = q(t)/y_{0s}(t) \quad (2)$$

where q is the surface concentration (μg/m^2) and y_{0s} (μg/m^3) is the gas-phase concentration immediately adjacent to the surface. Assuming a boundary layer exists adjacent to the sorption surfaces, the amount of SVOC accumulated on the surface is equal to the total mass transferred through the boundary layer from the gas phase, or

$$\frac{dq(t)}{dt} = h_s[y(t) - y_{0s}(t)] \quad (3)$$

where h_s (m/s) is the convective mass-transfer coefficient near the sorption surface. The accumulation of SVOCs in the chamber obeys the following mass balance:

$$\frac{dy(t)}{dt} \cdot V = E(t) \cdot A - \frac{dq(t)}{dt} \cdot A_s - y(t) \cdot Q \quad (4)$$

where V is the chamber volume (m^3), A is the area of emission surfaces (m^2), A_s is the internal stainless steel surface area (m^2), and Q is the air flow rate of the chamber. The simplified SVOC emission model is obtained by combing equations (1)-(4).

Liang and Xu (2014a) developed a novel method to determine y_0 for a range of phthalates emitted from various building materials. They measured h_m independently for phthalates under the chamber test condition. With the knowledge of steady-state gas phase concentration in the emission chamber (y_{ss}), the value of y_0 for each test sample emitting particular phthalates can be determined using the following equation:

$$y_0 = \frac{y_{ss} \cdot Q}{h_m \cdot A} + y_{ss} \quad (5)$$

RESULTS

Phthalates and Phthalate Alternatives in Vinyl Floorings and Crib Mattress Covers. The content of phthalates and their alternatives in material samples was measured. The background level of target compounds in the blank was less than 0.2 % of the content of the samples. Table B.S3 shows that most of the 16 samples of vinyl flooring contained more than 10% phthalates in the material, and DINP was the dominant plasticizer used. The results of crib mattress covers were discussed in more detail by Boor et al. (2014b). Among these samples, four flooring products and two mattress covers were selected for emission measurements in the test chamber, and their material-phase concentrations are listed in Table B.1. The observed variation may be due to some inhomogeneity of phthalate distribution in material samples.

Sample ID	Phthalates	Content	C_0	y_0 ($\mu g/m^3$)				ΔH_{pa}	ΔH_{vap}
			($\mu g/m^3$)	25 °C	36 °C	45 °C	55 °C	(kJ/mol)	(kJ/mol)
1 (vinyl flooring)	DEHP	23 ± 3 %	3.26×10^{11}	2.22	13.6	36.9	146	123	116[a]
2 (vinyl flooring)	DINP	20 ± 3 %	3.47×10^{11}	0.43	4.31	16.7	48.3	159	93.8[b]
	DEHP	0.1 ± 0.02 %	1.73×10^{9}	0.02	6.35	14.1	35.5	401	116[a]
3 (vinyl flooring)	BBP	15 ± 2 %	1.93×10^{11}	12.0	14.7	31.7	136	38.7	106 [a]
	Iso-DEHP	7 ± 1 %	9.02×10^{10}	0.17	7.8	25.6	92.7	263	n.a.
4 (vinyl flooring)	DnBP	9 ± 1 %	1.42×10^{11}	27.1	489	1052	4146	196	93.0[a]
	DEHP	7 ± 1 %	1.10×10^{11}	1.44	9.13	15.1	106	125	116[a]
5 (mattress cover)	DINCH	11 ± 1 %	1.88×10^{12}	0.70	2.47	5.15	n.a.	84.3	141[c]
6 (mattress cover)	DEHA	4 ± 0.3 %	1.00×10^{12}	1.05	14.6	36.6	n.a.	179	131[d]

e. (Gobble et al., 2014)
f. Calculated based on measurements in (Cousins et al., 2003).
g. Calculated based on measurements in (BASF, 2013a).
h. Calculated based on measurements in (BASF, 2013b).

Table B.1: Summary of material-phase concentration (C_0), y_0 values for test samples at different temperatures, enthalpy of phase change between polymeric material and air (ΔH_{pa}), and enthalpy of vaporization for pure chemical liquids (ΔH_{vap}).

Impact of Temperature on Emissions. Figure B.1 shows that temperature had a strong influence on phthalate emissions. When the temperature was increased from 25 to

36 ºC, the steady-state air concentration of phthalates and their alternatives in the chamber increased up to an order of magnitude for all test samples except sample 5. The specific emission rate (SER) can be estimated based on the gas-phase concentration, chamber air change rate, the surface area of emission source, and the chamber's volume (Clausen et al., 2004). On average, a 30 ºC increase in temperature (from 25 to 55 ºC) resulted in more than a 300-fold increase in SER, between an increasing factor of 7 (DINCH, sample 5) and as much as a factor of 2000 (DEHP, sample 2). Emission of DnBP from sample 4 showed the highest SER at each temperature. In the case of DnBP emission at 36 ºC (SER~ 130 $\mu g/m^2h$), calculations show that after five years, only 1% of the total mass would have been emitted from the vinyl flooring sample. Although the SER measured in the chamber might be somewhat different from that in actual indoor environments, the results indicate that PVC products may behave as permanent indoor sources of phthalates during the product's lifetime. But, temperature increase has a strong impact on their emissions from these sources, accelerating off-gassing, elevating their air concentrations, and thereby resulting in significantly greater indoor exposures.

The simplified SVOC emission model (Xu et al., 2012) was used to characterize the emissions of phthalates and phthalate alternatives at different temperatures. Based on the steady-state concentration (y_{ss}) that was measured in the emission chamber, Equation (5) was used to determine the value of y_0 for each vinyl flooring sample emitting specific phthalates at the four different temperatures; the results are listed in Table B.1. The values of h_m and h_s that were obtained by Liang and Xu (2014a) for the conditions of the test chamber at 25 ºC were corrected to other corresponding temperatures, as shown in Tables B.S4 and B.S5. Because the adsorption of phthalates to chamber wall decreased greatly as temperature increased (Clausen et al., 2012), partitioning between stainless steel and air was ignored at all temperatures except 25 ºC. At 25 ºC, we used the stainless

steel/air partition coefficients that were measured in a previous study for phthalates with respect to K_s (Liang and Xu, 2014a). Using the same experimental method, we obtained the K_s values for DINCH (1570 m) and DEHA (1520 m) at 25 ºC in this study. As shown in Figure B.1, there was reasonable agreement between the gas-phase concentrations of phthalates and phthalate alternatives predicted by the model and the experimental data that were measured at the different temperatures. When the temperature increased, the value of y_0 increased significantly (Table B.1), and the mass transfer coefficient (h_m) also increased slightly due to the changes in the diffusivity and viscosity of air as a function of temperature (Tables B.S4 and B.S5). As a result, the steady-state gas phase concentration of phthalates and phthalate alternatives in the chamber increased significantly as the temperature increased. The decrease of partitioning between stainless steel and air at elevated temperatures strengthened the effect, allowing the gas-phase concentration in the chamber to reach steady state more quickly.

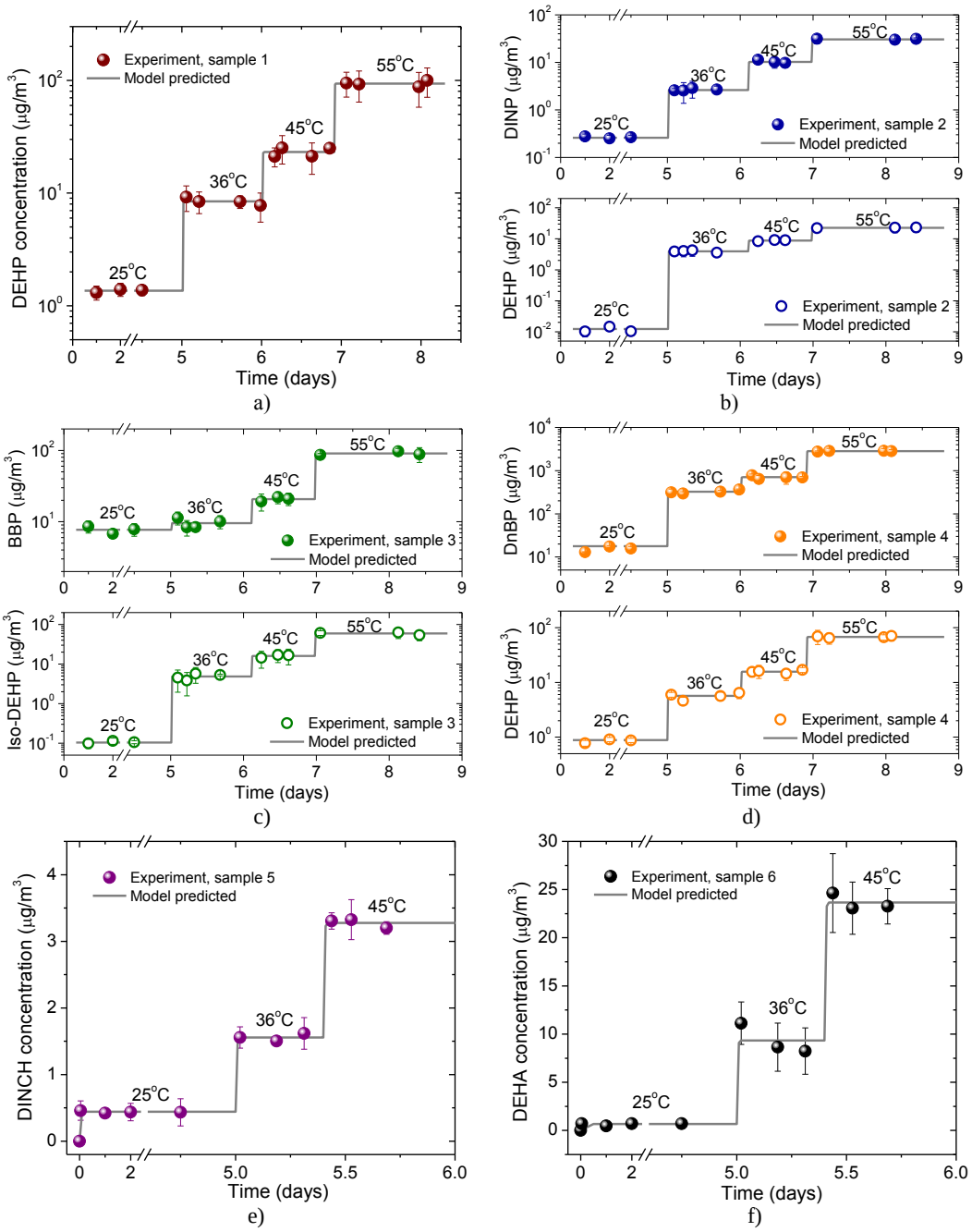

Figure B.1: Gas-phase chamber concentration of phthalates and phthalate alternatives emitted from tested samples at different temperatures. a) sample 1, b) sample 2, c) sample 3, d) sample 4, e) sample 5, and f) sample 6.

The Relationships between y_0, V_p, C_0, and Temperature. Figure B.S2 shows the measured y_0 values and the calculated V_p as a function of temperature. The result for iso-DEHP was not included in the figure because its V_p information was not available in the literature. The y_0 values for DEHP, DEHA, and DINCH were relatively close to V_p. The results for samples 1 and 4, which contained high levels of DEHP compared to sample 2, were consistent with previous findings that DEHP in PVC products evaporated at a rate that was similar to the rate of pure DEHP liquid and that the value of y_0 was close to its V_p (Clausen et al., 2012; Ekelund et al., 2010). In contrast, there are significant differences between the values of y_0 and V_p for DnBP, BBP, and DINP at the four temperatures, and the differences ranged up to an order of magnitude. However, the differences must be considered and explained very carefully, because V_p was estimated using correlation equations from the literature rather than being measured directly, and this could have resulted in erroneous values.

The material-phase concentration (C_0) of phthalate additives in different products can vary substantially, thereby influencing the value of y_0. Samples 1, 2, and 4, which contained different levels of DEHP, were used to explore the relationship between y_0 and C_0. Figure B.S3 shows that a simple partition coefficient can be used to obtain a linear relationship between y_0 and C_0 at different temperatures. Although only three data observations might not be enough, the finding was consistent with the results of a recent study on phthalate emissions from latex paint (Schripp et al., 2014) and a study of volatile organic compound (VOC) emissions from building materials (Kumar and Little, 2003). Therefore, when the contents of phthalate and phthalate alternatives in the material phase are relatively low, they may not behave as pure liquids, so the values of y_0 would be related to C_0 and would be lower than their V_p values. The critical level of C_0, below which the simple linear partition coefficient can be used, requires further research.

Figure B.2 shows the ratio of C_0 to y_0 as a function of temperature, allowing us to examine their relationship. The temperature dependence of C_0/y_0 was very strong. The value of C_0/y_0 decreased between a factor of 10 (BBP in sample 3) and by as much as a factor of 2000 (DEHP in sample 2) when the temperature increased from 25 to 55 °C. This also indicates that the C_0/y_0 value is highly variable under environmental conditions as a result of temperature fluctuations. An exponential relationship was observed between C_0/y_0 and the reciprocal temperature (Figure B.2):

$$\frac{C_0}{y_0} = \exp\left(\frac{A}{T} + B\right) \tag{6}$$

where A and B are constants for a given chemical and polymeric material. Non-linear regression analysis was conducted to avoid any possible errors when fitting a nonlinear model by transforming to linearity (Mathworks, 2014). The correlations between C_0/y_0 and T were highly significant, with R^2 ranging between 0.85 and 1.

Interestingly, this finding was in agreement with the well-known van't Hoff equation which is generally used to describe the dependence of equilibrium partitioning on temperature (Schwarzenbach et al., 2003). Assuming that the ratio of C_0 to y_0 was approximately equal to the material/air equilibrium partition coefficient, the enthalpy of phase change (polymer/air), ΔH_{pa} (kJ/mol), can be calculated according to the equation:

$$\Delta H_{pa} = 1000 \times R \times A \tag{7}$$

where R is the ideal gas constant ($Pa \cdot m^3/mol \cdot K$), A is the constant given in Figure B.2, and the factor of 1000 is a unit converter. Table B.1 lists the values for ΔH_{pa} along with the calculated enthalpies of vaporization (ΔH_{vap}) for pure phthalates. The enthalpies of vaporization and polymer/air phase change are clearly different, with ΔH_{pa} of DEHP (samples 1 and 4) having the closest values to the ΔH_{vap} of pure DEHP liquid. In general,

ΔH_{pa} is somewhat greater than ΔH_{vap}, except for the cases of BBP (sample 3) and DINCH (sample 5). The results indicate that, for most phthalate and phthalate alternatives, the interactions with polymeric materials are stronger than the interactions with pure chemical liquid. Similar results were observed in a previous study of the off-gassing formaldehyde from vinyl flooring (Zhang et al., 2007). Therefore, using V_p to approximate y_0 may lead to misleading results. In addition, no significant dependence of ΔH_{pa} on the molecular weight of phthalates was found. But the values of ΔH_{pa} for phthalates are much greater than that for formaldehyde (37 kJ/mol), which has a lower molecular weight (Zhang et al., 2007). Material-phase concentration (C_0) may also have an impact on the value of ΔH_{pa}. For sample 2, which contained DEHP, the value of ΔH_{pa} is larger than those of samples 1 and 4, which might relate to the sample's low material-phase concentration of DEHP (C_0=0.1%). For ideal solutions, Dobruskin (2014) found that the enthalpy of evaporation for each component increased as the mole fraction of the component decreased.

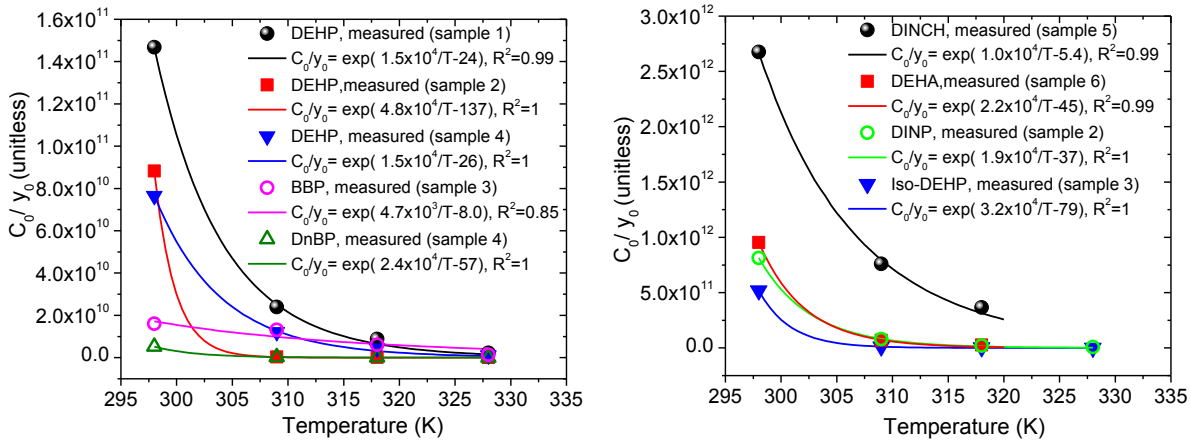

Figure B.2: The ratio of C_0 to y_0 as a function of temperature. Curved lines are nonlinear regression fits using van't Hoff equation. a) DnBP, BBP, and DEHP, and b) DEHA, Iso-DEHP, DINP, and DINCH.

DISCUSSION

Phthalate Concentrations in a Residential Home with an Increase of Temperature. Many building energy models specify that the preferred household winter and summer temperatures are 20 and 26 ºC, respectively (Xu et al., 2014). Field measurements of temperatures in buildings reported that the average temperature in buildings ranges from 16 to 24 ºC, with the maximum temperatures in the range of 29 – 34 ºC (Clausen et al., 2012; Adunola, 2014; Hunt and Gidman, 1982; Raja et al., 2001; French et al., 2007). Therefore, the temperatures of 25 and 36 ºC were selected to investigate phthalate concentrations in residential indoor environments. Also, temperature increases in this range are reasonable and relevant, given that solar radiation through glazing and the indirect effects of climate change can result in such temperature elevations in indoor environments, as discussed above. Temperature increases may greatly increase emissions of phthalates and thus become critical to evaluate indoor exposures and risks that occur in buildings.

Based on the values of y_0 measured at different temperatures for the vinyl flooring samples, the steady-state, gas-phase concentrations of phthalates in residential indoor environments after installation of the flooring can be estimated by the following equation (Little et al., 2012; Xu et al., 2009; Xu et al., 2010):

$$y_{ss,indoor} = \frac{h_m \cdot y_0 \cdot A}{h_m \cdot A + h_s \cdot A_s + (1 + K_p \cdot TSP) \cdot Q} \quad (8)$$

where TSP ($\mu g/m^3$) is the mass concentration of suspended particles in the room and K_p ($m^3/\mu g$) is the equilibrium partitioning of phthalates between gas phase and particles. As an example, we used sample 4 of vinyl flooring, which contained DnBP and DEHP, and estimated the steady-state, gas-phase concentrations of phthalates in a family residence at the temperatures of 25 and 36 ºC. We assumed that the residential home had a volume of 128 m^3 and an air change rate of 0.5/h, and the parameters used in the calculation and the

results that were obtained are shown in Table B.2. At both temperatures, the estimated gas-phase concentrations of phthalates in the home ($y_{ss,\ indoor}$) were significantly lower than those observed in the study that was conducted in the chamber (Figure B.1); we concluded that the discrepancy was due, for the most part, to the presence of suspended particles (TSP) and the large area of interior surfaces (A_s) in actual indoor environment. The ratios of $y_{ss,\ indoor}$ at 36 ºC to that at 25 ºC were about 18.2 and 7.7 for DnBP and DEHP, respectively. The dramatic increase of $y_{ss,\ indoor}$ with temperature occurred primarily because of the change in the value of y_0, which increased by factors of 18 and 6.3 for DnBP and DEHP, respectively, resulting in stronger emissions from the source. In addition, less sorption of phthalates onto particles due to lower K_p at the higher temperature also contributed to the elevation of $y_{ss,\ indoor}$, especially for DEHP.

The total airborne concentration of phthalates, i.e., the combination of gas-phase and particle-phase phthalates, can be obtained by

$$Total\ airborn\ concentration\ = y_{ss,indoor} + (y_{ss,indoor} \times K_p \times TSP) \quad (9)$$

where ($y_{ss,indoor} \times K_p \times TSP$) represents the concentration of particle-phase phthalates. The decrease of K_p due to temperature increase compensated for the dramatic increase of the gas phase. As a result, the particle-phase concentration of phthalates does not elevate as great as $y_{ss,indoor}$. For example, although the indoor gas-phase concentration of DEHP increased by as much as a factor of 7.7 as temperature increased, the particle-phase DEHP level only increased by a factor of 2.8. Furthermore, because DEHP has relatively low volatility, the majority of the airborne mass is bound to the particle phase, with only a small fraction present in the gas phase. Thus, the increase in the total airborne concentration with temperature was limited (e.g., it increased by a factor of 4.1 rather than 7.7 of $y_{ss,\ indoor}$). Therefore, even though temperature increases can significantly enhance emissions and elevate indoor gas-phase concentrations of phthalates, the

increase of the total airborne concentration may not be as great as the increase in the gas-phase for compounds that have very low volatility, such as DEHP. Generally, however, human exposure increases as temperature increases, but the extent of the increase depends upon specific chemical properties (e.g., V_p and K_p), the source's characteristics (e.g., y_0), and other environmental factors (e.g., temperature and TSP).

Parameters	**DnBP**			**DEHP**		
	25 ºC	**36 ºC**	***Ratio***	**25 ºC**	**36 ºC**	***Ratio***
y_0 (µg/m^3)	27.1	489	*18.0*	1.44	9.13	*6.3*
h_m and h_s (m/s)	4.80×10^{-4} [b]	4.95×10^{-4} [c]	*1.03*	4.11×10^{-4} [a]	4.24×10^{-4} [c]	*1.03*
K_p (m^3/µg)	2.42×10^{-3} [d]	8.1×10^{-4} [d]	*0.33*	1.42×10^{-1} [d]	5.3×10^{-2} [d]	*0.37*
A (m^2)	19.2[e]	19.2[e]	-	19.2[e]	19.2[e]	-
A_s (m^2)	263.4[e]	263.4[e]	-	263.4[e]	263.4[e]	-
TSP (µg/m^3)	20[f]	20[f]	-	20[f]	20[f]	-
Q (m^3/h)	64	64	-	64	64	-
Gas phase (µg/m^3) $y_{ss,\ indoor}$	**1.62**	**29.4**	***18.2***	**0.062**	**0.48**	***7.7***
Particle phase (µg/m^3) $y_{ss,\ indoor} \times K_p \times TSP$	**0.08**	**0.48**	***6***	**0.18**	**0.5**	***2.8***
Total airborne (µg/m^3) $y_{ss,\ indoor} \times (1+ K_p \times TSP)$	**1.70**	**29.9**	***17.6***	**0.24**	**0.98**	***4.1***

a. The value used in (Clausen et al., 2012).
b. Corrected based on air diffusivity (Liang and Xu, 2014a).
c. Corrected based on the diffusivity and viscosity of air at different temperatures (Table B.S5).
d. K_p (m^3/µg) can be estimated by the following formula using vapor pressure: log (K_p) =-0.86×log (V_p) (Pa)-4.67 (Xu et al., 2009). The measured vapor pressures (at 25 ºC) of DnBP and DEHP are 4.1×10^{-3} (Pa) and 3.6×10^{-5} (Pa), respectively (Liang and Xu, 2014a). The vapor pressures (at 36 ºC) are calculated using Equation 8 and 9 in (Gobble et al., 2014).
e. The area of emission source (A) and sorption surfaces (A_s) used in a previous study (Xu et al., 2010) were employed here, based on typical surface/volume ratios for American houses.
f. Typical TSP in residential environment (Weschler, 2003).

Table B.2: DnBP and DEHP concentrations in residential house at 25 ºC and 36 ºC and the parameters used in calculation.

Exposure to Phthalates by Infants in Their Sleep Microenvironment. Phthalate plasticizers and their alternatives were found in crib mattress covers (Boor et al., 2014a and 2014b). To make a screening-level estimate of phthalate concentrations around an infant, the SVOC emission model (Equation 1-5) was extended to a two-zone model. As shown in Figure B.3, the breathing zone (BZ) consists of the air space surrounding a sleeping infant, with a bottom cross-sectional area that covers the mattress. It was assumed that the inner BZ air space is well mixed and that air flows freely between the two zones, driven by the thermal plume due to the buoyancy effect of heat from the infant's body. The velocities of air in buildings are commonly less than 0.2 m/s in order to satisfy the thermal comfort requirements of the occupants (ASHREA, 2004), and therefore they do not affect the thermal plume (Rim and Novoselac, 2009). It was also assumed that the outer zone of bulk room air (RA) was well mixed and allowed to exchange with outdoor air. The model is described in detail in the SI, and the model parameters are provided in Table B.S6. In a previous experimental study, we investigated infant exposure to emissions of volatile organic compounds from crib mattresses with a room-scale stainless steel chamber and a thermal manikin of an infant (Boor et al., 2014a). The experimental conditions were used to set up some of the model parameters related to air velocity, flow rate, and sorption property in the RA zone.

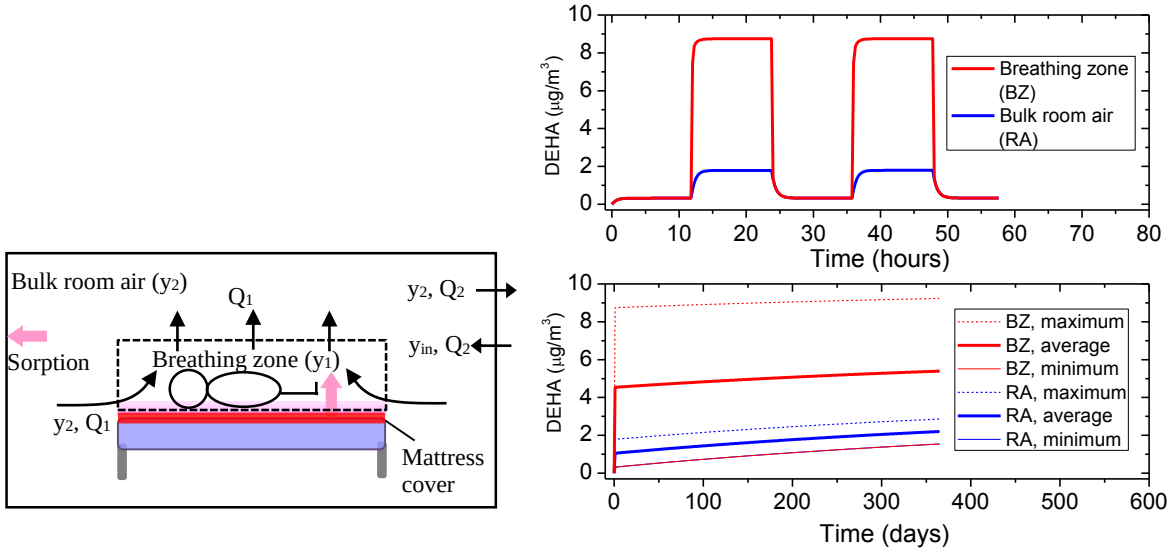

Figure B.3: a). Schematic representation of the two-zone model, and
b) Model prediction of DEHA concentrations in BZ and RA zones.

Using the crib mattress cover that we tested (sample 5, which contains DEHA) as an example, Figure B.3 shows the gas-phase concentrations in the BZ and RA zones versus time. Assuming that infants sleep 12 hours/day, both short- and long-term simulations were conducted. The concentrations in the BZ and RA were higher during the sleeping period than when the child was not on the mattress. This finding indicates that the emission of DEHA from the crib mattress cover increased significantly due to the increase in the temperature of the mattress surface caused by heat transfer from the sleeping infant. When the infant was on the mattress, the DEHA concentration in the infant's BZ was several times higher than that in the bulk room air. It suggests that, due to their close contact with the mattress, infants are likely to be exposed to higher phthalate concentrations than other occupants of the room. Recent large-chamber studies (Boor et al., 2014a; Laverge et al., 2013) also found a similar source-proximity effect for VOCs, showing that pollutant concentrations near mattresses ranged from 1.5 to 24 times

greater than the bulk room air, depending on sleeping positions and bedding arrangements. Considering that infants inhale nearly an order of magnitude more air per body mass than adults, their inhalation dose of phthalates that originate from their mattress covers can be significant. DEHA concentrations in the BZ and RA were observed to increase slowly and continuously over a long period of time (Figure B.3). The result indicates that crib mattress covers may behave as a permanent source of phthalates and other SVOC additives during the lifetime of the covers. This observation is in contrary to the findings for VOCs, since their emission levels tend to decay as their concentrations in the source material are depleted over time (Boor et al., 2014a).

Although simulation using the two-zone model is a first-of-a-kind study of sleep microenvironments, it still served only as a screening-level analysis. We recognize that there are several limitations associated with the current model simulation. Only the gas-phase concentration was included in the two-zone model. Because SVOCs partition strongly to particles, the airborne particles and the particles that are re-suspended by body movement during sleep may have important impacts on the fate of phthalates and infant exposures to them. In addition, real indoor environments are more complicated than the experimental conditions in that they have various interior sorption surfaces other than the stainless steel surface that was in the chamber. Also, the results predicted by the model are sensitive to Q_1, the air flow rate between the BZ and RA zones, i.e., the higher the value of Q_1, the less difference there is between the concentrations in the BZ and the RA. Thus, the actual total airborne concentration may not be as high as the gas-phase concentration predicted by the model. However, since infants spend most of their time sleeping with their breathing zone and skin in immediate proximity to the source, they are likely to be exposed to a significant amount of phthalates through inhalation of air (gas and particles), dermal transfer as a result of contact with the source, and direct air-to-skin

uptake (Weschler and Nazaroff, 2012 and 2013). Therefore, systematic chamber studies should be conducted and theoretical models should be developed to improve our understanding of the fate and transport of phthalates as well as other SVOCs (e.g., flame retardants emitted from mattresses) in infants' sleep microenvironments. These developments represent the essential first step in allowing the accurate evaluation of infant exposures, better investigation of subsequent health effects, and improved strategies to limit exposures.

ACKNOWLEDGEMENT

Financial support was provided by the National Science Foundation (NSF) (CBET-1150713 and CBET- 1066642).

SUPPORTING INFORMATION

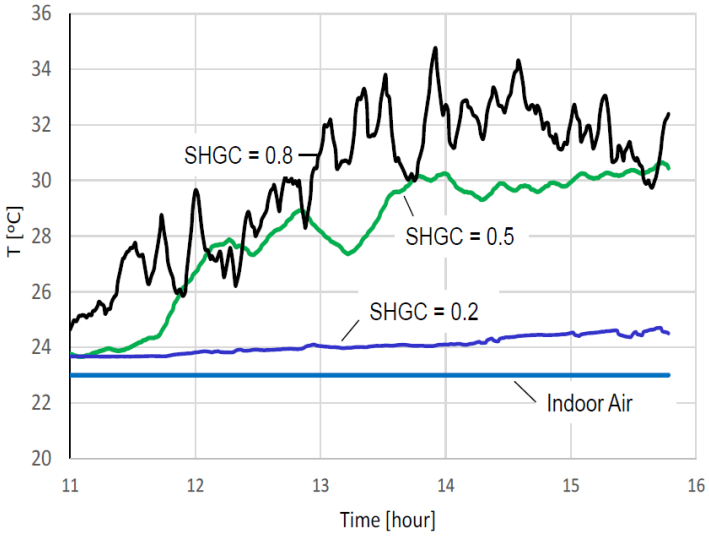

Figure B.S1: Measurements (courtesy of Dr. Atila Novoselac from The University of Texas at Austin) showing the effect of window solar heat gain coefficient (SHGC) on surface temperature in the vicinity of a window.

Chemical Analysis. Phthalates and phthalate alternatives collected by the Tenax TA sorbent tubes were desorbed by a thermal desorber (TD) (Turbomatrix 650 ATD) and analyzed by a GC-MS system (Agilent 7890A GC- 5975MS). Before analysis, 5 µL solution of D_4-DEHP (2 µg/mL) in methanol was injected into the Tenax tubes as internal standard. The sorbent tubes were then desorbed for 30 min at 300 °C, with a He flow of 50 ml/min, and a cold trap temperature of minus 30 °C. Flash heating of the cold trap to 350 °C transferred the analyte through the valves at 250 °C and the transfer line at 250 °C to the GC. The GC-MS had a constant pressure resulting in a flow rate of 1.6 ml/min at 80 °C, and was equipped with a 30 m × 0.25 mm DB-5MS column and operated at a 5:1 split injection. The temperature program was 80 °C, hold for 0.5 min, ramp 20 °C/min for 8.5 min, then ramp 30 °C/min for 2 min, and finally hold for 9 min. All analyses were performed in full scan mode and the extracted ions used for identification and

quantification are summarized in Table B.S1. All tubes were analyzed in two successive desorptions to ensure complete desorption of both the tube and the TD-GC-MS system. The second desorption showed concentrations below the detection limit in all cases. A calibration standard was regularly run prior to each GC injection, and the variance was always below 5% for all injections.

Phthalate compounds	Abbrev.	CAS no.	MW (g/mol)	t_R (min)	Quantifying ion	Qualifier ions
Dimethyl phthalate	DMP	131-11-3	194.2	6.25	163	194
Di-n-butyl phthalate	DnBP	84-74-2	278.4	9.02	149	205, 223
Butyl benzyl phthalate	BBP	85-68-7	312.4	10.8	149	91, 206
Di(2-ethylhexyl) phthalate	DEHP	117-81-7	390.6	11.44	149	167, 279
Di(2-ethylhexyl) isophthalate	Iso-DEHP	137-89-3	390.6	12.50	149	261
Diisononyl phthalate	DINP	28553-12-0	418.6	11~12	293	149, 167
Di(2-ethylhexyl) adipate	DEHA	103-23-1	370.6	9.83	129	112
Di (isononyl)cyclohexane-1,2-dicarboxylate	DINCH	166412-78-8	424.7	10.6~11.6	155	299
Di(2-ethylhexyl) phthalate-3,4,5,6-d_4	D_4-DEHP	93951-87-2	394.6	11.44	153	171, 283

Table B.S1: GC-MS retention times (t_R), with quantifying and qualifier ions for phthalates and phthalate alternatives.

Parameter	Value
Temperature (°C)	25 ± 0.5, 36 ± 0.5, 45 ± 0.5, 55 ± 0.5
Chamber volume (L), V	1
Air flow rate (mL/min), Q	1000
Air change rate (1/h)	53
Area of test pieces (m^2), A	0.13
Internal stainless steel surface area (m^2), A_s	0.02
Chamber diameter (cm)	40
Chamber height (cm)	1.8
Loading (m^2/m^3), A_s/V	16

Table B.S2: Chamber properties and test conditions.

Samples	Phthalates	Content	C_0 ($\mu g/m^3$)	Samples	Phthalates	Content	C_0 ($\mu g/m^3$)
1	DEHP	22.9%	3.2×10^{11}	**9**	DINP	6.3%	8.1×10^{10}
2	BBP	15.2%	2.2×10^{11}		DEHP	0.11%	1.4×10^{9}
	Iso-DEHP	7.3%	9.4×10^{10}	**10**	DINP	24.0%	2.8×10^{11}
3	DINP	20.2%	2.3×10^{11}	**11**	DINP	26.5%	3.1×10^{11}
	DEHP	0.1%	9.4×10^{8}		DEHP	0.3%	3.2×10^{9}
4	DnBP	9.2%	1.5×10^{11}	**12**	DINP	22.1%	2.3×10^{11}
	DEHP	7.1%	4.9×10^{10}	**13**	DINP	14.2%	1.4×10^{11}
5	DINP	19.0%	3.3×10^{11}		DEHP	0.06%	5.9×10^{8}
	DEHP	0.03%	4.7×10^{8}	**14**	DINP	0.1%	1.3×10^{9}
6	DINP	14.5%	1.5×10^{11}		DEHP	23.0%	3.0×10^{11}
	DEHP	0.21%	2.1×10^{9}	**15**	DINP	25.2%	3.0×10^{11}
7	DINP	19.8%	2.3×10^{11}		DEHP	0.1%	1.2×10^{9}
	DEHP	0.7%	8.6×10^{9}	**16**	DINP	16.28%	2.1×10^{11}
8	DINP	12.6%	2.0×10^{11}		DEHP	0.1%	9.0×10^{8}
	DEHP	0.8%	1.4×10^{10}				

Table B.S3: The content and concentration of phthalates in vinyl flooring products.

Temperature (°C)	Air diffusivity of phthalates and phthalate alternatives ($\times 10^2$ cm^2/s)[a]								Air viscosity[b] (kg/m/s)	Air density[c] (kg/m^3)
	DMP	DnBP	BBP	DEHP	Iso-DEHP	DINP	DEHA	DINCH		
25	5.99	4.64	4.45	3.73	3.73	3.57	3.75	3.53	1.86×10^{-5}	1.18
36	6.38	4.95	4.74	3.97	3.97	3.80	4.00	3.76	1.91×10^{-5}	1.14
45	6.71	5.20	4.98	4.17	4.17	4.00	4.20	3.95	1.95×10^{-5}	1.11
55	7.08	5.49	5.26	4.41	4.41	4.22	4.44	4.17	2.00×10^{-5}	1.07

a. Calculated use the method in (Lyman et al., 1990).
b. Calculated use the method in (Smits and Dussauge, 2006).
c. Calculated based on ideal gas law.

Table B.S4: Physical properties of air at different temperatures.

Phthalates	h_m measured at 25°C[a]	h_m calculated at 25°C[b]	h_m calculated at 36°C[c]	h_m calculated at 45°C[c]	h_m calculated at 55°C[c]
DMP	3.12×10^{-4}	1.10×10^{-4}	3.22×10^{-4}	3.30×10^{-4}	3.50×10^{-4}
DnBP	2.54×10^{-4}	0.93×10^{-4}	2.62×10^{-4}	2.69×10^{-4}	2.85×10^{-4}
BBP	2.38×10^{-4}	0.90×10^{-4}	2.46×10^{-4}	2.52×10^{-4}	2.67×10^{-4}
DEHP	2.10×10^{-4}	0.80×10^{-4}	2.17×10^{-4}	2.22×10^{-4}	2.36×10^{-4}
Iso-DEHP	2.10×10^{-4}	0.80×10^{-4}	2.17×10^{-4}	2.22×10^{-4}	2.36×10^{-4}
DINP	2.01×10^{-4}	0.78×10^{-4}	2.07×10^{-4}	2.13×10^{-4}	2.26×10^{-4}
DEHA	2.28×10^{-4}	0.80×10^{-4}	2.36×10^{-4}	2.42×10^{-4}	2.56×10^{-4}
DINCH	2.19×10^{-4}	0.77×10^{-4}	2.26×10^{-4}	2.32×10^{-4}	2.46×10^{-4}

a. See details in (Liang and Xu, 2014a).
b. Calculated using correlation equations (Axley, 1991), which express h_m as a function of Renolds number and Schmidt number. The air velocity required for the Reynolds number was estimated using computational fluid dynamic analysis.
c. Estimated using equation $\frac{h_T}{h_{25^oC}} = \left(\frac{v_T}{v_{25^oC}}\right)^{1/3-n} \times \left(\frac{D_T}{D_{25^oC}}\right)^{2/3}$ that was rearranged based on correlation equations (Axley, 1991), where v is kinematic air viscosity and D is air diffusivity at different temperatures. The results were not sensitive to the value of n; less than 15% uncertainties were observed when changing n from 0.1 to 1. Therefore, n=0.5, which is the same as that employed in the correlation equations (Axley, 1991), was used here.

Table B.S5: Estimation of mass transfer coefficients (h_m, m/s) at different temperatures.

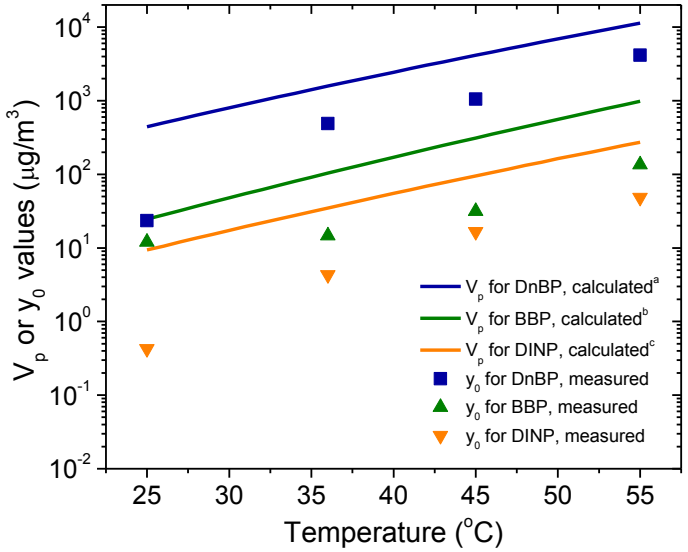

a)

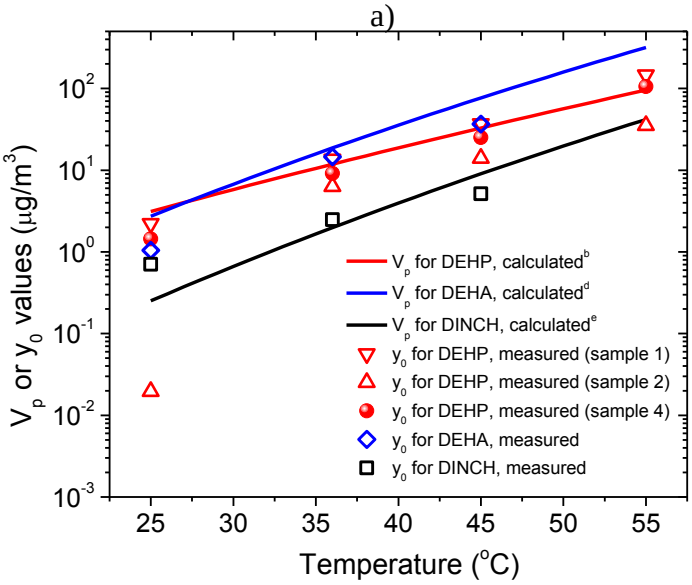

b)

a. Calculated using Equation 8 in (Gobble et al., 2014) (temperature range: 20 to 100 °C).
b. Calculated using Equation 9 in (Gobble et al., 2014) (temperature range: 20 to 327 °C).
c. Calculated using Clausius-Clapeyron equation, with equation constants in (Cousins et al., 2003) (temperature range: 50 to 400 °C).
d. Calculated using Antoine constants measured in (BASF, DEHA) (temperature range: 50 to 270 °C).
e. Calculated using Antoine constants measured in (BASF, DINCH) (temperature range: 50 to 270 °C).

Figure B.S2: Comparison between y_0 and V_p at different temperatures. a) DnBP, BBP, and DINP and b) DEHA, DEHP, and DINCH.

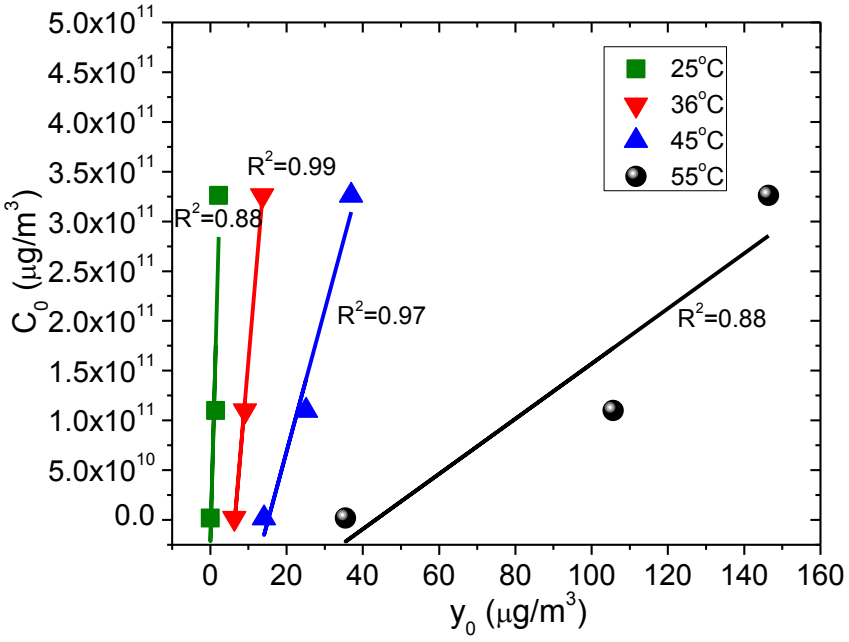

Figure B.S3: Relationship between C_0 and y_0 for samples containing DEHP at different temperature.

Two-Zone Model. The mass balance equation for gas phase concentration in the inner breathing zone (BZ) is

$$V_1 \frac{dy_1}{dt} = Q_1 y_2 - Q_1 y_1 + h_m A(y_0 - y_1)$$

where y_1 (μg/m^3) is the gas-phase phthalate concentration in the BZ zone, y_2 (μg/m^3) is the gas-phase concentration in the bulk room air (RA), V_1 (m^3) is the volume of the BZ, Q_1 (m^3/h) is the air flow rate from the BZ to RA, h_m (m/h) is the mass transfer coefficient near the crib mattress cover, A (m^2) is the area of source material, and y_0 (μg/m^3) is the gas-phase concentration of phthalates in equilibrium with the material phase. Assuming a boundary layer exists adjacent to the sorption surfaces, the amount of phthalates

accumulated on the surface is equal to the total mass transferred through the boundary layer from the gas phase, or

$$K_s \frac{dy_s}{dt} = h_s(y_2 - y_s)$$

where K_s (m) is the surface/air partition coefficient, and h_s (m/h) is the mass transfer coefficient near the adsorptive surfaces (e.g., stainless steel chamber wall). The accumulation of phthalates in the RA zone obeys the following mass balance:

$$V_2 \frac{dy_2}{dt} = Q_2 y_{in} + Q_1 y_1 - Q_2 y_2 - h_s A_s (y_2 - y_s)$$

where V_2 (m^3) is the volume of the large chamber, Q_2 (m^3/h) is the ventilation rate between the large chamber and outside, A_s (m^2) is the area of sorption surface, and y_s ($\mu g/m^3$) is the gas phase concentration immediately adjacent to the sorption surface.

parameters	unit	value	comments
V_1	m^3	0.3	assume the height of BZ is 20cm
Q_1	m^3/h	2.25	assume it is the same as Q_2
A_0	m^2	1.49	crib mattress surface area
A_s	m^2	18.23	area of sorption surface. In the simulation, it is the stainless steel chamber wall area calculated based on the chamber geometry
V_2	m^3	4.5	full scale stainless steel chamber volume (RA)
Q_2	m^3/h	2.25	chamber volumetric flow rate
K_s	m	1520	measured partition coefficient (25 ºC) between stainless steel and air for DEHA. It was set to zero at the temperature of 36 ºC
h_m	m/s	5.02E-04	mass transfer coefficient over the source surface, estimated using correlation equations (Axley, 1991) based on measured air velocity of 0.1 m/s
h_s	m/s	1.00E-04	mass transfer coefficient over the adsorptive surface, estimated using correlation equations based on estimated air velocity
y_{in}	$\mu g/m^3$	0	assume clean air comes from outside

Table B.S6: Parameters used in the two-zone model.

Appendix C

Paper 3. The Influence of Surface Sorption and Air Flow Rate on Phthalate Emissions from Vinyl Flooring: Measurement and Modeling

Yirui Liang and Ying Xu
(Accepted by *Atmospheric Environment*)

ABSTRACT

This study investigated the influences of surface sorption and air flow rate on the emission of phthalates from building materials. Controlled tests were conducted in specially designed stainless steel and wood chambers, and the steady-state concentration in the stainless steel chamber was about 2-3 times higher than that in the wood chamber for di(2-ethylhexyl) phthalate (DEHP) and diisononyl phthalate (DINP). The emission rate of phthalates increased in the wood chamber due to the diffusion mass flow through the chamber wall (i.e., surface absorption). The adsorption isotherm of phthalates on the stainless steel surface and the absorption parameters (i.e., diffusion and partition coefficients) of phthalates on the wood surface were determined experimentally, and the values were comparable to those in the literature. The equilibration time scale for phthalates absorbed to the sink reservoir in actual indoor environments was estimated and can be substantial (approximately 80 years), indicating that surface absorption may continuously drive phthalates from their indoor sources to various sinks and thus significantly increase the emission rate of phthalates. The gas-phase concentration of DEHP was measured in two stainless steel chambers operated at flow rates of 300 mL/min and 3000 mL/min, respectively, which were both adjusted to 1000 mL/min after steady state was reached. The gas-phase concentration of DEHP in the chamber was very sensitive to the chamber air flow rate, and higher air flow rates resulted in lower concentration levels. However, the increased emission rate compensated for the dilution in the gas phase and made the DEHP concentration not drop substantially with an

increase in the air flow rate. Independently measured or calculated parameters were used to validate a semi-volatile organic compounds (SVOCs) emission model that included absorptive surfaces and for a range of air flow rates, with excellent agreement between the model predictions and the observed chamber concentrations of phthalates.

INTRODUCTION

Phthalates have been used as plasticizers to enhance the flexibility of polyvinylchloride (PVC) products. These semi-volatile organic compounds (SVOCs) are found in a wide range of building materials and consumer products (Bornehag et al., 2005), and are present at percent to tens-of-percentage levels (Weschler and Nazaroff, 2008). Because phthalate additives are not chemically bound to the polymer matrix, slow emission from the products to air or other media usually occurs (Xu et al., 2012). As a result, phthalates are ubiquitous and among the most abundant SVOCs in indoor environments (Bornehag et al., 2005; Bornehag et al., 2004; Clausen et al., 2012; Rudel and Perovich, 2009). Recent studies suggested that exposure to some phthalates may result in irreversible changes in the development of the human reproductive tract (Heudorf et al., 2007; Jaakkola and Knight, 2008; Latini et al., 2006; Matsumoto et al., 2008; McKee et al., 2004; Ritter and Arbuckle, 2007); increase the risk of asthma, rhinitis, and allergies (Bornehag et al., 2005; Jaakkola et al., 2006; Jaakkola et al., 1999; Kolarik et al., 2008; Øie et al., 1997); and affect endogenous hormones (Rudel and Perovich, 2009).

Understanding of the emission mechanisms of phthalates and their alternatives from various sources is a prerequisite for characterizing their fate and developing suitable approaches to reduce their concentrations in indoor environments. However, very few emission studies have been conducted with low volatile plasticizers as target compounds

(Afshari et al., 2004; Clausen et al., 2004; Clausen et al., 2012; Clausen et al., 2010; Clausen et al., 2007; Schossler et al., 2011; Xu et al., 2012), possibly due to the substantial difficulties associated with chamber tests for SVOCs including the long test duration (over months to years), low gas-phase concentration, strong sorption onto surfaces, and ubiquitous contamination in laboratory facilities. Informed by the early chamber studies (Clausen et al., 2004), Xu and Little (2006) developed a fundamental mass-transfer model to predict SVOC emissions from polymeric materials. They showed that emissions of these very low volatility compounds are subject to "external" control (partitioning from the material into the gas phase, the gas-phase mass-transfer coefficient, and strong sorption onto interior surfaces including airborne particles). Using data collected in a specially-designed stainless steel chamber, Xu et al. (2012) showed that the emission rate of di(2-ethylhexyl) phthalate (DEHP) from vinyl flooring can be predicted based on a priori knowledge of y_0, the gas-phase concentration of DEHP in equilibrium with the material phase, the material to air and air to stainless steel surface mass-transfer coefficients (h_m), and the stainless steel/air equilibrium relationship (K_s). Liang and Xu (2014a) improved the design of the previous emission chamber and developed a novel, rapid method for measuring y_0 for a range of phthalate compounds released from building materials.

In actual indoor environments, there are various interior surfaces such as furniture, the ceiling, and walls, many of which are not as impenetrable as stainless steel. Therefore, the simple partition relationship often used for surface adsorption may not be good enough to elucidate the mechanisms governing the process of surface absorption. Liu et al. (2014c) developed an experimental method to estimate the solid-phase diffusion coefficient (D_m) and the material/air partition coefficient (K_{ma}) of polychlorinated biphenyl (PCB) congeners for different sink materials such as glass and concrete. The

results can be used to predict the absorption of SVOCs in the materials. However, the researchers also acknowledged that D_m and K_{ma} values obtained were rough estimates, because a single data set was used to fit the two parameters simultaneously, which may result in erroneous values. In addition, because SVOCs sorbed strongly to interior surfaces, surface sorption may also have a great impact on the fate and transport of indoor phthalates. Benning et al. (2013) observed that the total (gas + particle) DEHP concentrations increased by a factor of 3 to 8 when particles were introduced to a stainless steel chamber. The particles rapidly captured DEHP from the gas phase, substantially enhancing the emission rate of DEHP from the source. To date, no systematic investigations have been conducted to characterize the mechanisms governing absorption of phthalates to interior penetrable surfaces and the influence of surface sorption on emissions of phthalates from building materials.

The effect of increased ventilation on reducing indoor exposure to volatile organic compounds (VOCs) and formaldehyde has been observed in field studies (Hodgson et al., 2004; Zuraimi et al., 2006), but it is difficult to make the same conclusion for SVOCs because they behave quite differently as VOCs whose emissions are generally subject to "internal" control (diffusion within the source material) (Xu and Zhang, 2003). Clausen et al. (2010) measured the emission of DEHP from vinyl flooring at five different flow rates in the Field and Laboratory Emission Cell (FLEC) and found that the emission rate strongly depended on the air change rate (ACH). However, the gas-phase DEHP concentrations in FLEC differed only slightly for the various flow rates and thus were not suitable for use in comparing model prediction and experiment data. Xu et al. (2014) studied the influence of the ACH on indoor concentrations of phthalates and polybrominated diphenyl ethers (PBDEs) in retail stores. The researchers observed that the concentrations of phthalate slightly increased but that of PBDEs decreased

significantly when the ACH increased. Liu et al. (2014a) developed a mass balance model incorporating the impacts of ventilation on particle mass concentration, mass transfer, and particle mediation, and found that ventilation affects exposure to SVOCs; but the researchers stated that more experimental studies were needed to further validate the theoretical model.

The aim of this study is to investigate the influence of surface sorption and air flow rate on the emission of phthalates from building materials. The specific objectives are to: (1) conduct controlled tests in specially designed stainless steel and wood chambers, respectively, to examine the effect of surface adsorption/absorption on the emission of phthalates from vinyl flooring; (2) measure the stainless steel/air equilibrium relationship ($K_{s,\ steel}$), wood-phase diffusion coefficient (D_{wood}), and wood/air partition coefficient ($K_{s,wood}$) for the target phthalates, and characterize the mechanisms governing surface adsorption/absorption of phthalates; (3) measure emission of phthalates in the stainless steel chamber over a range of air flow rates; and (4) more completely validate the SVOC emission model with existence of adsorptive/absorptive surfaces and for a range of air flow rates.

METHODS AND MATERIALS

Chemicals

Standard solutions were used for chemical calibration and identification, in which dimethyl phthalate (DMP), di(2-ethylhexyl) phthalate (DEHP) was obtained from Absolute Standards Inc. and diisononyl phthalate (DINP) from Accustandards, Inc. Standard solutions were used for chemical calibration and identification, including DMP and DEHP (Absolute Standards Inc.), and DINP (Accustandards, Inc.). Tetradeuterium ring labeled DEHP (D_4-DEHP) was used as internal standard, and its standard solution

was obtained Accustandards, Inc. Hexane, methanol, and dichloromethane (Sigma-Aldrich Co. LLC., anhydrous, >99%) were used as solvent in extraction and cleaning without further purification. The solvents were regularly analyzed to monitor potential phthalate contamination.

Test Materials

Two vinyl flooring samples containing DEHP (23%) and DINP (20%), respectively, were used in this study. The method applied to measure the material-phase concentration of phthalates in vinyl flooring was described in detail in (Liang and Xu, 2014a). Each material sample was cut into two 0.45 m × 0.25 m sheets, wrapped in aluminum foil, and stored at room temperature. Before a measurement, the test pieces were unwrapped and placed in the emission chamber.

Emission Chambers

A specially-designed stainless steel chamber used in previous experiments (Liang and Xu, 2014a) was employed in this study. The chamber used for SVOC emission testing maximized the surface area of the emission source and minimized the surface area of the internal sink, thus substantially reducing the time to reach steady state. In addition, three precision-ground stainless steel rods, matched to the interior stainless steel chamber surface, were inserted into the chamber and then periodically removed so that the adsorbed surface concentration could be measured. This method allowed us to relate the gas-phase concentration to the adsorbed surface concentration in the chamber and quickly establish the partition equilibrium relationship. The specific chamber design was described in greater detail in (Liang and Xu, 2014a).

To investigate the mechanisms governing the process of surface absorption and the influence of surface sorption on emission of phthalates, we also made emission

chambers out of soft maple wood (Fine Lumber and Plywood, Inc.) in addition to stainless steel. As shown in Figure C.1, the wood chamber has the same configuration as those made with stainless steel. Similarly, three thin wood strips, matched to the interior wood chamber surface, were inserted into the chamber and then periodically removed to measure the surface absorption on the wood. The air leakage rate for both types of chambers was less than 2% of the total flow rate. Other chamber properties and experimental conditions are summarized in Table C.1.

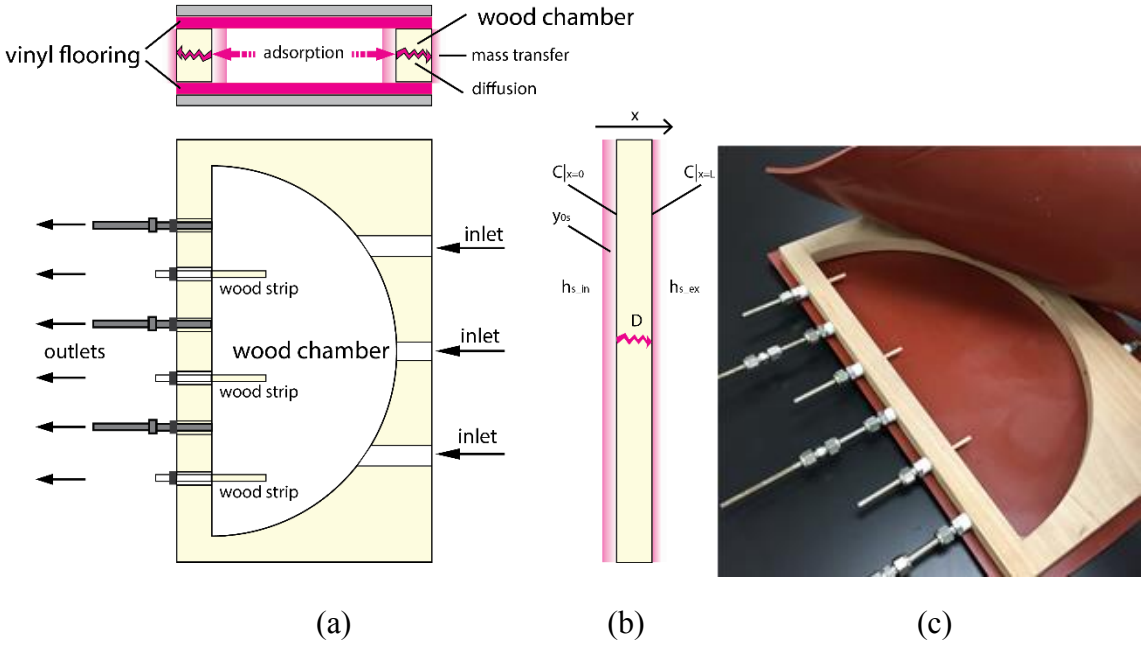

Figure C.1: Configuration of the wood chamber. a) Side and top view, b) surface absorption at wood chamber wall, and c) photo.

Parameter	The influence of surface sorption		The influence of air flow rate		
	Stainless steel chamber	Wood chamber	Stainless steel chamber		
Temperature (°C)	25 ± 0.5	25 ± 0.5	25 ± 0.5		
Chamber volume (L), V	1	1	1		
Air flow rate (mL/min), Q	1000	1000	300	1000	3000
Air change rate (1/h)	53	53	16	53	159
Area of test pieces (m^2), A	0.13	0.13	0.13		
Internal surface area (m^2), A_s	0.02 (stainless steel)	0.02 (wood)	0.02		
Chamber diameter (cm)	40	40	40		
Chamber height (cm)	1.8	1.8	1.8		
Loading (m^2/m^3), A_s/V	16	16	16		
Concentration adjacent to vinyl flooring ($\mu g/m^3$), y_0	DEHP (sample 1): 2.4 DINP (sample 2): 0.4		DEHP (sample 1): 2.4		
Convective mass-transfer coefficient (m/s), h_m	DEHP: 2.10×10^{-4} DINP: 2.01×10^{-4}		DEHP: 2.0×10^{-4}	DEHP: 2.1×10^{-4}	DEHP: 5.4×10^{-4}
Convective mass-transfer coefficient near sorption surface (m/s), h_s	DEHP: 1.0×10^{-4} DINP: 0.96×10^{-4}		DEHP: 1.0×10^{-4}		
Convective mass-transfer coefficient near the exterior surface of the wood chamber (m/s), h_{s_ex}	n.a.	DEHP: 4.5×10^{-3} DINP: 4.4×10^{-3}	n.a.		
Sorption surface/air partition coefficient, K_s	DEHP: 1500 (m) DINP: 2100 (m)	DEHP: 2.86×10^{7} DINP: 2.52×10^{7}	DEHP: 1500 (m)		
Diffusion coefficient (m^2/s), D	n.a.	DEHP: 8.0×10^{-14} DINP: 7.5×10^{-14}	n.a.		

Table C.1: Chamber properties, test conditions, and model parameters.

Emission Experiments

The stainless steel and wood chambers containing the test samples were placed in a temperature-controlled cabinet (Lunaire CEO-932) and operated at an air flow rate of 1000 mL/min, about 0% relative humidity, and a temperature of 25±0.5°C. To study the impact of air flow rate on phthalate emissions, the flow rate of two stainless steel emission chambers were set up to 300 mL/min and 3000 mL/min, respectively, and then adjusted to 1000 mL/min after steady-state concentrations had been reached. The gas-

phase concentrations of phthalates versus time were measured at regular intervals in the emission chambers. Phthalates was sampled directly on Tenax-TA tubes with a pump (SKC 224-PCXR4) calibrated to a nominal flow rate of 150 ml/min. The sampling time was approximately 24 hours. Backup tubes were connected to each primary sample tube to check for breakthrough (Figure C.1). No breakthrough was observed in any of the tests. Because the sampling system was supplied with high purity air from cylinders, we assumed that no particles were present. Before each emission test, the stainless steel plates and especially the internal chamber surfaces were cleaned with an alkali detergent, hot tap water and Nanopure® water, and then finally rinsed several times with methanol. Before use, the wood chambers were baked in a bench-top oven at 80 °C for 24 hours, and then the surfaces of internal chamber wall was wiped several times with methanol. Background measurements were performed before each test for around a week. Temperature and air flow rate through the chambers were checked before and after samples were taken for analysis.

Sorption Experiments

Sorption measurements were conducted at a relatively constant chamber concentration after steady state had been reached, allowing the sorption kinetics and equilibrium end-point to be carefully examined. Three stainless steel rods (3 mm diameter × 3 cm in length) and three wood strips (3.8 cm × 3.9 mm × 0.58mm) were inserted into the stainless steel and wood chambers (Figure C.1), respectively, with the chamber outlet air flows passing through the rod or strip holders. Because the air flows were drawn by pumps calibrated to a nominal flow rate of 100 and 300 ml/min for the stainless steel rods and wood strips, respectively, the high velocity around the rods or strips allowed the sorption to reach equilibrium quickly. Since the surface of the rods and

the strips was almost identical to the surface of the internal chamber walls of the stainless steel chamber and the wood chamber, respectively, they provided a means to measure the sorption characteristics of the chamber surface.

Before use, the stainless steel rods and the wood strips were cleaned with hexane and their background levels were examined. After sampling, the stainless steel rods were taken out of the chamber, quickly put into stainless steel tubes, and then analysed with thermal desorption combined with gas chromatography and mass spectrometry (TD-GC-MS). The wood strips were taken out of the chamber, quickly put into beakers and ultrasonically extracted for 30 min with hexane for three times. The volume of the extract was reduced to approximately 150 μL, after rotary evaporation, clean-up, and nitrogen purge. About 5 μL of the extract was then injected with a solution of D_4-DEHP as the internal standard into the Tenax TA tubes and analysed with TD-GC-MS. In addition, the gas-phase concentration of phthalates was also periodically measured in the stainless steel and wood chambers to ensure that the steady-state concentration was maintained in the chamber during sorption experiments.

Chemical Analysis of Phthalates

Phthalates collected by the Tenax TA sorbent tubes were desorbed by a thermal desorber (TD) (Turbomatrix 650 ATD) and analyzed by a GC-MS system (Agilent 7890A GC- 5975MS). Before analysis, 5 μL solution of D_4-DEHP (2 μg/mL) in methanol was injected into the Tenax tubes as internal standard. The sorbent tubes were then desorbed for 30 min at 300 °C, with a He flow of 50 ml/min, and a cold trap temperature of minus 30 °C. Flash heating of the cold trap to 350 °C transferred the analyte through the valves at 250 °C and the transfer line at 250 °C to the GC. The GC-MS had a constant pressure resulting in a flow rate of 1.6 ml/min at 80 °C, and was

equipped with a 30 m × 0.25 mm DB-5MS column and operated at a 5:1 split injection. The temperature program was 80 °C, hold for 0.5 min, ramp 20 °C/min for 8.5 min, then ramp 30 °C/min for 2 min, and finally hold for 9 min. All analyses were performed in full scan mode. All tubes were analyzed in two successive desorption to ensure complete desorption of both the tube and the TD-GC-MS system. The second desorption showed concentrations below the detection limit in all cases. A calibration standard was regularly run prior to each GC injection, and the variance was always below 5% for all injections.

SVOC Emission Model Including Penetrable Absorptive Surfaces

Xu and Little (2006) developed an SVOC emission model that includes adsorption at impenetrable surfaces (e.g., stainless steel chamber wall), and the model was recently simplified by Xu et al.(2012). In their analysis, the emission rate is

$$E(t) = h_m \cdot [y_0 - y\,(t)] \tag{1}$$

where y (μg/m^3) is the bulk gas-phase concentration, and h_m (m/s) is the convective mass-transfer coefficient. The ratio of the concentration of a chemical on sorption surfaces to its concentration in the gas phase is equal to the surface/air partition coefficient, K_s (m), or

$$K_s = q(t)/y_{0s}(t) \tag{2}$$

where q is the surface concentration (μg/m^2) and y_{0s} (μg/m^3) is the gas-phase concentration immediately adjacent to the surface. Assuming a boundary layer exists adjacent to the sorption surfaces, the amount of SVOC accumulated on the surface is equal to the total mass transferred through the boundary layer from the gas phase, or

$$\frac{dq(t)}{dt} = h_s[y(t) - y_{0s}(t)] \tag{3}$$

where h_s (m/s) is the convective mass-transfer coefficient near the sorption surface. The accumulation of SVOCs in the chamber obeys the following mass balance:

$$\frac{dy(t)}{dt} \cdot V = E(t) \cdot A - \frac{dq(t)}{dt} \cdot A_s - y(t) \cdot Q \quad (4)$$

where V is the chamber volume (m^3), A is the area of emission surfaces (m^2), A_s is the internal stainless steel surface area (m^2), and Q is the air flow rate of the chamber. The simplified SVOC emission model is obtained by combining Equations (1)-(4). Liang and Xu (2014a) developed a novel method to determine y_0 for a range of phthalates emitted from various building materials, with the h_m values measured independently.

To include absorption at penetrable surfaces (e.g., hardwood chamber wall) in the SVOC emission model, partitioning between the gas phase and the sorption surface, molecular diffusion within the material, and mass transfer through the boundary layer that exists adjacent to the sorption surfaces should be considered (Figure C.1). Using the wood chamber as an example, the governing equation describing transient diffusion through the wood material is

$$\frac{\partial C}{\partial t} = -D\frac{\partial^2 C}{\partial x^2} \quad (5)$$

where C ($\mu g/m^3$) is the material-phase concentration of phthalates in wood, t is the time, and x is the distance from the chamber interior wall. The diffusion coefficient of phthalates in wood, D (m^2/s), is assumed to be independent of material-phase concentration. The initial condition assumes that the wood material contains no phthalates. The boundary condition imposed at the interior chamber wall is

$$-D\frac{\partial C}{\partial x}|_{x=0} = h_{s_{in}}(y - y_{0s}) \quad (6)$$

where h_{s_in} (m/s) is the convective mass-transfer coefficient near the interior chamber wall. Equilibrium exists between concentrations in the surface layer of the interior wall and the air immediately adjacent to the surface, or

$$C|_{x=0} = K_{s\_wd} \cdot y_{0s} \tag{7}$$

where K_{s_wd} (dimensionless) is the wood/air partition coefficient for phthalates. Similarly, the boundary condition imposed at the exterior surface of the wood chamber is

$$-D\frac{\partial C}{\partial x}|_{x=L} = h_{s\_ex}\left(\frac{C|_{x=L}}{K_{s\_wd}} - 0\right) \tag{8}$$

where h_{s_ex} (m/s) is the convective mass-transfer coefficient near the exterior surface of the wood chamber and L is the average thickness of the chamber wall. The measured air concentration of phthalates in the temperature-controlled cabinet, where the emission chambers were placed, was much lower than that inside the emission chamber, and thus was assumed to be zero in Equation (8).

Determination of h_m for Different Air Flow Rates

Special petri dishes were made of an aluminium sheet coated with PTFE (McMaster-Carr Inc.) to fit with the chamber cavity shape (Figure C.S1, Table and Figure numbers preceded by an "S" are in the Supporting Information). Pure DMP liquid (approximately 300 mL) was delivered to the petri dish, which covered the bottom of the chamber and formed the emission surface for the measurements. PTFE sheets were used as gasket in the experiments, and the air leakage rate was less than 2% of the total flow rate. In order to shorten the test duration, the chamber internal sink surfaces (top PTFE surface and stainless steel wall) were coated with a very thin layer of DMP to saturate the surface. Air samples were collected and analysed periodically from the outlet of the chamber until steady state was reached.

When steady state was reached in the experiments, by modifying Equation (4), the unknown mass transfer coefficient (h_m) under different air flow rates was obtained with

$$h_m = \frac{y_{ss,DMP} \cdot Q}{(y_0 - y_{ss,DMP}) \cdot A} \quad (9)$$

where $y_{ss,DMP}$ is the steady-state gas phase concentration of DMP in the chamber. Because pure DMP liquid was used in the experiments, y_0 is equivalent to the vapor pressure of DMP (about 27.8 mg/m^3, at 25 °C) (Weschler et al., 2008).

RESULTS AND DISCUSSION

Emission Experiments

Gas-phase concentration of DEHP and DINP was measured for about 20 days in stainless steel and wood chambers, as shown in Figure C.2. Phthalate concentrations increased and reached steady state in less than 5 days for all measurements. The steady-state concentration in the stainless steel chamber was about 2–3 times higher than that in the wood chamber for both DEHP and DINP. A simple calculation using Equation (1) indicated that phthalate emission rate from the vinyl floorings increased due to the change in the chamber material from stainless steel to hardwood. This phenomenon may not be simply explained by the possibly larger partition coefficient between wood and air than that between stainless steel and air, because the calculations using the SVOC emission model showed that stronger surface adsorption (i.e., larger K_s value) increased the time of gas-phase concentration to reach steady state in a chamber but did not influence the level of the concentration at steady state (Figure C.S2). Therefore, in addition to surface adsorption, diffusion of phthalates within the wood material (i.e., absorption) must be considered. In other words, the gas-phase phthalates in the wood chamber were depleted more than in the stainless steel chamber due to the diffusion mass

flow through the chamber wall. To maintain the concentration at steady-state level, the gas-phase DEHP and DINP were resupplied with increased emissions from the vinyl flooring in the wood chamber.

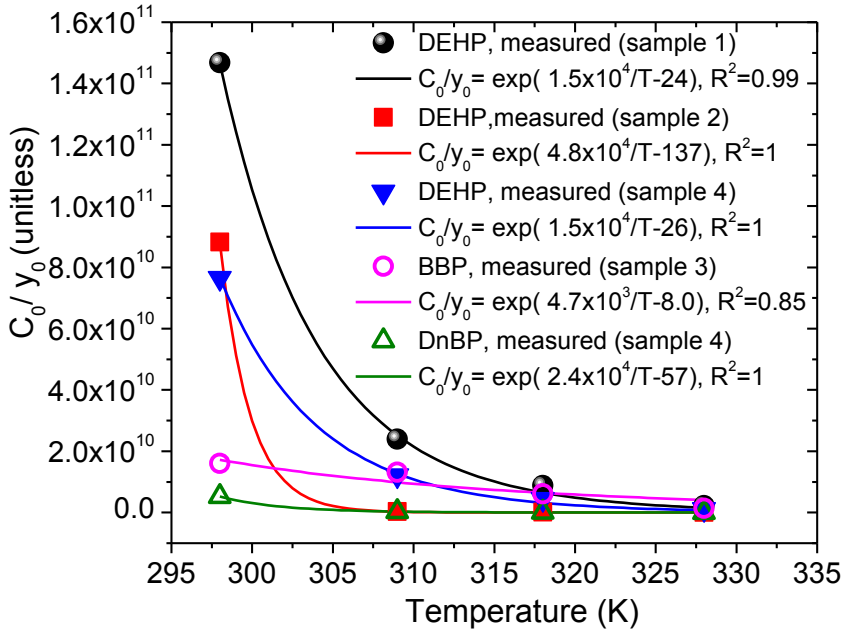

Figure C.2: Gas-phase chamber concentration of phthalates emitted from vinyl flooring samples in stainless steel chambers and wood chambers.

Characterization of Surface Adsorption and Absorption

To determine the sorption properties of the stainless steel and wood surfaces for phthalates, sorption experiments were conducted using the methods described. Figure C.3 shows the evolution of phthalate concentrations on the stainless steel rods and the wood strips over time during steady-state conditions, when the gas-phase chamber concentration was constant. The surface concentration of phthalates increased progressively until sorption equilibrium with the chamber air was reached. The time for

DEHP and DINP to reach sorption equilibrium on stainless steel and wood surfaces was no more than 10 days.

For impenetrable surfaces such as stainless steel, assuming that a linear isotherm, K_s (m), is appropriate to explain the adsorption relationship between the surface and the gas-phase phthalates, the corresponding K_s values were obtained by dividing the equilibrium concentration on the rod surfaces (Figure C.3a) by the steady-state gas phase concentration within the stainless steel chamber (Figure C.2). DINP has a higher K_s value (2100 m) than DEHP (1500 m) due to its higher molecular weight and lower vapor pressure.

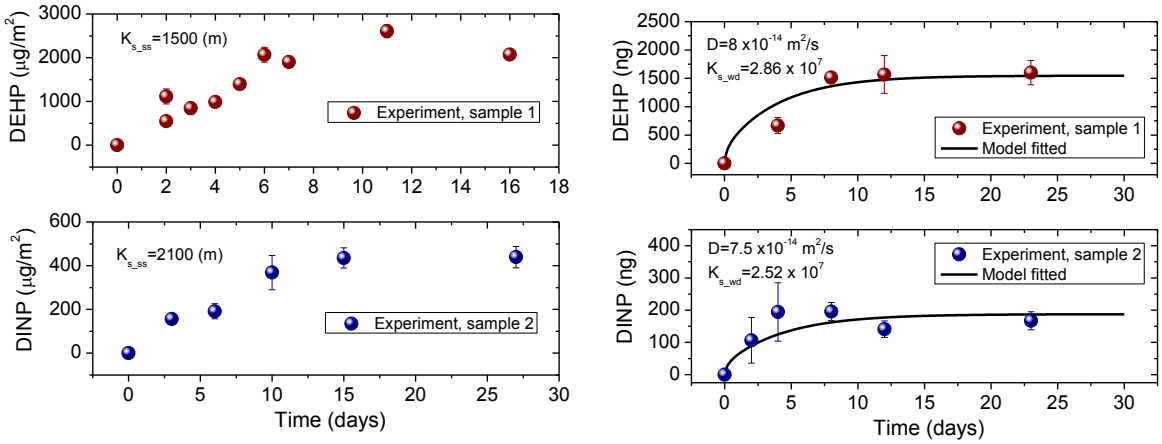

a) b)

Figure C.3: Sorption of phthalates on (a) stainless steel surface and (b) wood surface.

For penetrable surfaces such as maple wood, diffusion within the material must be considered. The wood strip can therefore be envisioned as a very thin symmetric slab capturing phthalates from the chamber outlet air flow at its top and bottom surfaces (Figure C.S3). Equation (5) can be used as the governing equation describing transient

diffusion through the wood strips. The initial condition assumes that the wood strips contain no phthalates. Because the gas-phase concentration passing across the wood strips was maintained at a constant value, under the experimental conditions, the boundary conditions imposed are

$$\frac{\partial C(x,t)}{\partial x} = 0, \qquad t > 0, \qquad x = 0 \ \ (due\ to\ symmetry) \tag{10}$$

$$-D\frac{\partial C(x,t)}{\partial x} = h_{m\_strip}\left(y_{ss} - \frac{C(x,t)}{K_{s\_wd}}\right), \quad t > 0, \quad x = L/2 \tag{11}$$

where y_{ss} is the steady-state gas-phase concentration of phthalates in chamber air, h_{m_strip} is the convective mass transfer coefficient near the wood strip surface, K_{s_wd} is the equilibrium partition coefficient between the wood surface and the gas phase, and L is the thickness of the strip. The influence of h_{m_strip} on the absorption of phthalates in the wood strips is analyzed in Figure C.S4. For a given value of D and K_{s_wd}, there is a critical value of h_{m_strip}; if h_{m_strip} is larger than the critical value, the impact of convective mass transfer around the strips can be neglected. For the experimental condition, an air flow of 300 mL/min was drawn by a pump through each strip holder. The high air velocity surrounding the strip (about 3.72 m/s) resulted in a large external mass transfer coefficient, which was approximately 0.013 m/s estimated using correlation equations (Axley, 1991), and thus made the impact of h_{m_strip} ignorable. Therefore, the influence of external mass transfer resistance was neglected, and Equation (11) was replaced by

$$C(x,t) = K_{s\_wd} \cdot y_{ss}, \quad t > 0, \quad x = L/2 \tag{12}$$

After sorption equilibrium was reached, phthalates were ultimately uniformly distributed throughout the strip. Similarly as stainless steel rods, the value of K_{s_wd} can be obtained by dividing the equilibrium concentration of phthalate in the strip (Figure C.3b) by the steady-state gas phase concentration in the wood chamber (Figure C.2). The

diffusion coefficient (D) was then determined by fitting Equations (5), (10), and (12) using the least-squares method, as shown in Figure C.3b. Liu et al. (2014c) measured the diffusion coefficients and the material/air partition coefficients of PCBs, which also belongs to SVOCs, for different sink materials. The values obtained in the current study for maple wood (DEHP: $D=8\times10^{-14}$ m^2/s; $K_{s\_wd}=2.86\times10^7$ and DINP: $D=7.5\times10^{-14}$ m^2/s; $K_{s\_wd}=2.52\times10^7$) are comparable to those measured for large molecular PCBs absorbed to commonly used laboratory materials such as LDPE sheets ($D=2.2\times10^{-13}$ m^2/s; $K_{s\_LDPE}=3.6\times10^7$) and concrete disks ($D=9.7\times10^{-15}$ m^2/s; $K_{s\_concrete}=4.76\times10^7$), though wood materials were not included in that study. Compared to previous studies of VOCs absorbed by gypsum board (e.g., dodecane: $D=4.6\times10^{-7}$ m^2/s; $K_{s\_gypmsum}=4160$) (Corsi et al., 2007), the diffusion coefficients obtained for phthalates are significantly lower while the partition coefficients (K_{s_wd}) are much higher. This finding is in agreement with theoretical expectations that D decreases when the molecular weight increases (Schwarzenbach et al., 2003) while K_s increases when the chemical vapor pressure decreases (Zhao et al., 2004).

A common problem for estimating sink parameters is to fit D and K_s simultaneously from one single data set, because it may generate different results due to the starting value issue of nonlinear regression (Haghighat et al., 2002; Liu et al., 2014b; Zhang et al., 2001). The current study developed a novel approach for measuring surface absorption, which allowed us to determine the diffusion and partition coefficients independently and accurately, and thus solved this fundamental problem. In addition, the high air flow around the strips allows absorption to reach equilibrium quickly. Therefore, the proposed approach could be suitable to quickly measure and characterize the SVOC absorption process for a wide range of sink materials.

Characterization of Phthalate Emissions

In stainless steel chambers, the SVOC emission model (Equations 1-4) reveals that y_0, K_s, h_m, and h_s are important parameters that control phthalate emission rates. The y_0 values (DEHP: 2.4 μg/m^3 and DINP: 0.4 μg/m^3) were calculated based on the measurement results (Figure C.2) using the method described in Liang and Xu (2014a). The values of K_s were obtained by sorption experiments, the mass transfer coefficient (h_m) was directly measured (Figure C.S5), and h_s was estimated in a previous study (Liang and Xu, 2014a). Table C.1 summarizes the model parameters for the experimental chamber conditions. The model can therefore be used to predict the gas phase concentration of DEHP and DINP in the experimental chambers, with reasonable agreement between model prediction and experimental data being obtained.

In the wood chambers, diffusion flux through the wood chamber wall was incorporated into the SVOC emission model (Equations 5–8). The diffusion and partition coefficients (D and K_{s_wd}) obtained from the sorption experiments were used in the model to predict the gas-phase concentrations of DEHP and DINP in the emission measurements in the wood chambers. The convective mass-transfer coefficient near the exterior surface of the wood chamber (h_{s_ex}) can be estimated using correlation equations (Axley, 1991) based on the measured air velocity surrounding the exterior wall of the chamber, approximately 3.96 m/s. The average thickness of the chamber wall (L) was calculated based on the geometry of the chamber, which was about 4 cm (see details in the Supporting Information). As shown in Figure C.4, the model prediction overestimated the concentration by about 50%. The reason may be related to the sorption area and the estimated average chamber wall thickness (i.e., diffusion depth) used in the model. A surface area calculated based on the geometry of the chamber may not represent the actual sorption area, considering the surface roughness of wood. When the

sorption surface area of the wood chamber was doubled, we found that the gas-phase concentrations of DEHP and DINP decreased, and a better agreement with the experimental measurements resulted.

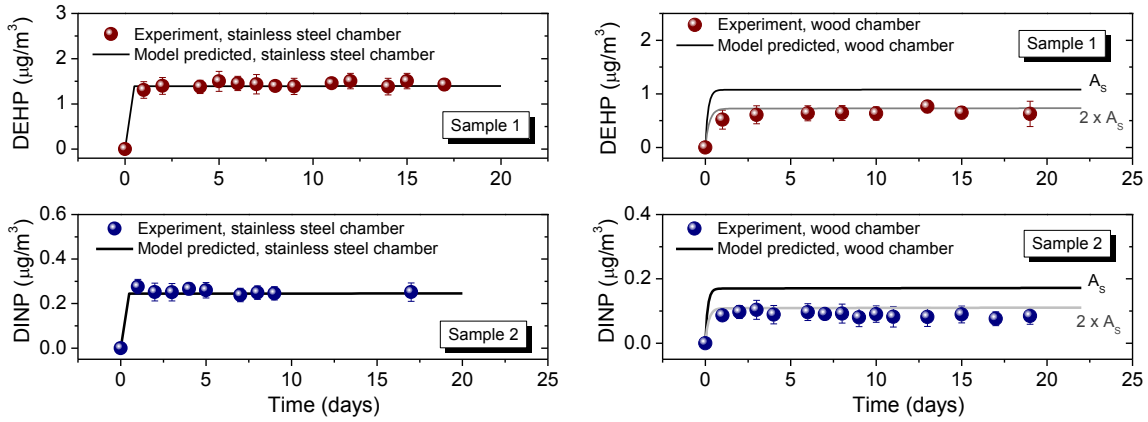

a) b)

Figure C.4: Gas-phase chamber concentration of phthalates emitted from vinyl flooring. a) stainless steel chambers, and b) wood chambers.

Time Scales for Uptake of Phthalates in Wood Compartments

The time scale for molecular diffusion of the sorbed phthalates through wood to produce uniform concentrations within the material was approximated by (Weschler and Nazaroff, 2008)

$$\tau_i \sim \frac{X^2}{2D} \tag{13}$$

where D is the diffusion coefficient of phthalates in the sorption reservoir and X is the thickness of the reservoir. Using $D \sim 8\times10^{-14}$ m^2/s, based on the sorption measurements of DEHP and DINP in maple wood, the internal diffusion transport time scale was about 6 days for the wood strips. The τ_j value agreed very well with observations in the sorption equilibrium measurements (Figure C.3b).

In actual indoor environments, the external mass transfer resistance may not be ignorable because the air velocity was slower than that for the wood strips in the sorption experiments. If the rate-limiting process for sorptive partitioning is external mass transfer, the time scale required to achieve sorption equilibrium by overcoming the external resistance (τ_e) can be calculated:

$$\tau_e \sim \frac{K_{s\_wd} X}{h_m} \tag{14}$$

We assumed the surface mass transfer coefficient (h_m) ranged from 2.5 to 3.9 m/h (Weschler and Nazaroff, 2008) in real indoor environments. The thickness of the indoor sorptive reservoirs (e.g., wood furniture) is always larger than the 0.58 mm wood strip. At the fast end, we had X ~ 2 mm, yielding τ_i ~ 0.8 years and τ_e ~ 2 years for DEHP or DINP, with the external mass transfer being the rate-limiting process for absorption. On the other hand, with a larger thickness, X ~ 2 cm, the equilibration time scale can be substantial (~ 80 years) and the rate-limiting process for sorptive partitioning changed from external mass transfer to internal diffusion (τ_i ~ 80 years vs. τ_e ~ 24 years). Therefore, with a strongly sorbing compound (e.g., DEHP and DINP) and a thick sink reservoir (e.g., common wood furniture), equilibrium partition might never be achieved in actual indoor environments. The absorption within the material reservoirs continuously and slowly drives phthalates from their indoor sources to the sinks and may thus significantly enhance phthalate emissions from the sources in indoor environments.

The Impact of Air Flow Rate

Two stainless steel chambers with the same type of vinyl flooring sample (sample 1) were operated at a temperature of 25 ºC and under the flow rate of 300 mL/min and 3000 mL/min, respectively. The gas-phase concentration of DEHP was directly

measured in the experiments, and it reached steady state quickly in both chambers. As shown in Figure C.5, the steady-state concentration in the chamber with the flow rate of 300 mL/min was about 50% higher than that in the chamber with the flow rate of 3000 mL/min. In a previous study (Clausen et al., 2010), the gas-phase concentration differed only slightly for various flow rates due to unexplained scatters and co-variances in the concentration profile. However, the current measurements showed that the steady-state concentrations decreased when the flow rate increased in the chamber and therefore have a dilution effect for DEHP. After the flow rate was adjusted to 1000 mL/min, the gas-phase concentration changed instantly in both chambers and agreed well with each other, suggesting that DEHP concentration is very sensitive to the chamber air flow rate. The specific emission rate (SER) can be estimated based on the gas-phase concentration at steady state, chamber air change rate, emission surface area, and chamber volume (Clausen et al., 2004). The SER calculated for the three chambers was 0.2 $\mu g/m^2/h$ (300 mL/min), 0.6 $\mu g/m^2/h$ (1000 mL/min), and 1.5 $\mu g/m^2/h$ (3000 mL/min), respectively. Because the DEHP air concentration adjacent to the emission surface was constant (y_0), the vertical air concentration gradient within the boundary layer was therefore larger at the high flow rate due to the lower air concentration in the chamber (y), which in turn increased the driving force of emission. Additionally, the convective mass transfer coefficient was increased by the higher air velocity above the emission source. As a result, the SER increased greatly with the increasing flow rate. Therefore, although the increased flow rate reduced the residence time of air and introduced more dilution, the increased SER compensated for the decrease in the gas phase, and the gas-phase concentration of DEHP did not drop substantially with the increasing air flow rates.

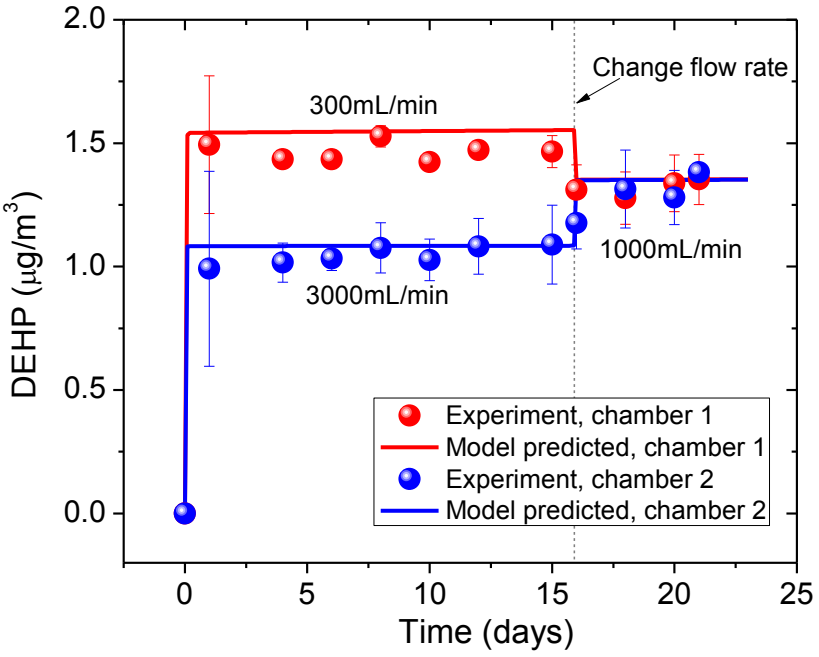

Figure C.5: Gas-phase chamber concentration of phthalates emitted from vinyl flooring at different flow rates.

The experimental results were used to further validate the SVOC emission model under different flow rates. The measurements of the emissions of DMP pure liquid (Figure C.S5) were used to obtain the mass transfer coefficient (h_m) at air flow rates of 300, 1000, and 3000 mL/min using Equation (9). The values of h_m obtained were then corrected for DEHP based on the air diffusivities of DEHP and DMP (Table C.S1). The air velocity near the chamber interior wall was estimated with computational fluid dynamic (CFD) simulation. The values were then used to estimate the mass transfer coefficient near sorption surface (h_s). Because h_s at different flow rates (Table C.S1) did not vary greatly, the fitted value (Table C.1) in the previous study (Liang and Xu, 2014a) at 1000 mL/min air flow rate, which we believe more accurately represents the

experimental conditions, was used. As shown in Figure C.5, reasonable agreement between the gas-phase DEHP concentration predicted by the model and the experimental data was obtained. The comparisons showed that the SVOC emission model can follow the dynamic change in the gas concentration when the air flow rate changes and is suitable to predict emission behaviors of phthalates over a wide range of air flow rates in experimental chambers.

Although the effect of increased ventilation on reducing indoor exposure to VOCs and formaldehyde has been observed (Hodgson et al., 2004; Zuraimi et al., 2006), no significant conclusion can be made about SVOCs indoor air concentrations as a function of ACH through recent field studies (Xu et al., 2014). Real indoor environments are more complicated than experimental chambers, where suspended particles, dust, and various interior surfaces are present. Airborne particles can enhance the flux of gas-phase SVOCs from indoor sources and influence SVOC transport (Liu et al., 2012; Liu et al., 2014b; Xu and Little, 2006). The concentration of total suspended particles is also closely linked to ventilation (Alshitawi et al., 2009). Therefore, the observation in strictly controlled experimental chambers may not be true in actual indoor environments. Further field measurements and theoretical analysis are needed to examine the influence of ventilation on indoor exposure to SVOCs.

CONCLUSIONS

This study investigated the influence of surface sorption and air flow rate on the emission of phthalates from building materials. Controlled tests were conducted in specially designed stainless steel and wood chambers, and the steady-state concentration in the stainless steel chamber was about 2-3 times higher than that in the wood chamber for DEHP and DINP. The emission rate of phthalates was increased in the wood

chamber due to surface absorption. The adsorption isotherm of phthalates on the stainless steel surface and the absorption parameters (i.e., diffusion and partition coefficients) of phthalates on the wood surface were determined experimentally and the values were comparable to those in the literature. The equilibration time scale for phthalates absorbed in the sink reservoir in actual indoor environments was estimated and can be substantial (~ 80 years), indicating that surface absorption may continuously drive phthalates from their indoor sources to various sinks and thus significantly increase the emission rate of phthalates. The gas-phase concentration of DEHP was measured in two stainless steel chambers operated at the flow rates of 300 mL/min and 3000 mL/min, respectively, which were both adjusted to 1000 mL/min after steady state was reached. The gas-phase concentration of DEHP in the chamber was very sensitive to the chamber air flow rate, and higher air flow rates resulted in lower concentration levels. But, the increased emission rate compensated for the dilution in the gas phase and made DEHP concentration not drop substantially with an increase of air flow rate. Independently measured or calculated parameters were used to validate a semi-volatile organic compounds (SVOCs) emission model that included absorptive surfaces and for a range of air flow rates, with excellent agreement between the model predictions and the observed chamber concentrations of phthalates.

ACKNOWLEDGEMENTS

Financial support was provided by the National Science Foundation (NSF) (CBET-1150713 and CBET- 1066642) and American Society of Heating, Refrigerating and Air Conditioning Engineers (ASHRAE) (Grant-In-Aid and NIA Awards).

SUPPORTING INFORMATION

Ventilation rate	h_m (DMP) [a]	h_m (DEHP) [b]	Air velocity near interior chamber wall [c]	h_s (DEHP) [d]
ml/min	m/s	m/s	m/s	m/s
300	2.92×10^{-4}	1.24×10^{-4}	0.0013	5.1×10^{-5}
1000	3.12×10^{-4}	2.27×10^{-4}	0.0025	7.2×10^{-5}
3000	7.44×10^{-4}	3.93×10^{-4}	0.005	2.3×10^{-4}

a. Measured in experiments (Figure C.S5).
b. Corrected from h_m value of DMP based on air diffusivity (see details in Liang and Xu 2014a).
c. Calculated by computational fluid dynamic (CFD) simulation.
d. Estimated using correlations (Axley 1991) based on the air velocity calculated by CFD

Table C.S1: The measured h_m values at different flow rates.

Figure C.S1: Photo of the special petri dish fitted within the chamber.

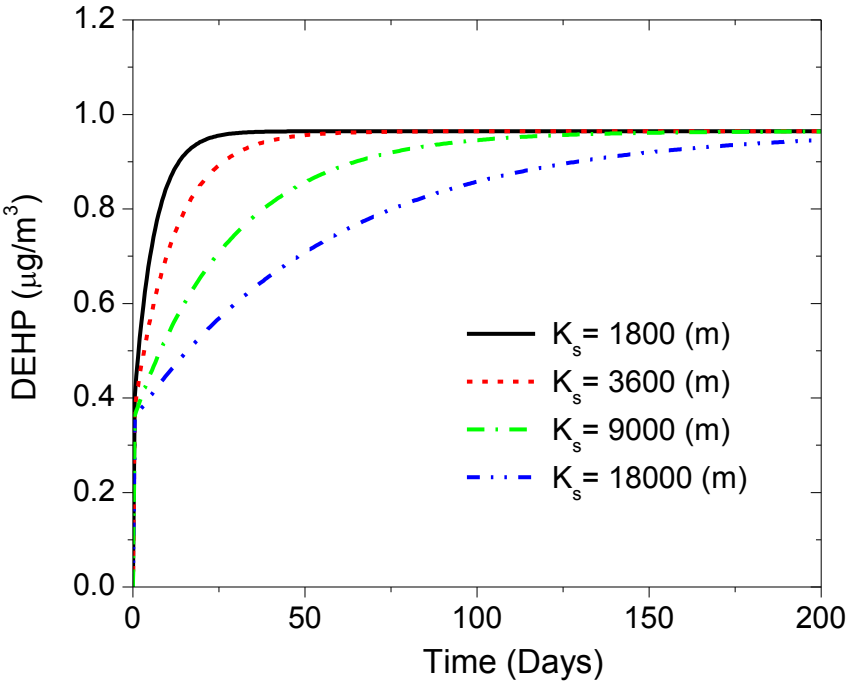

Figure C.S2: Influence of partition coefficient (K_s) on DEHP gas-phase concentration in stainless steel chamber. Experimental parameters in Xu et al. (2012) were used in simulating the baseline condition.

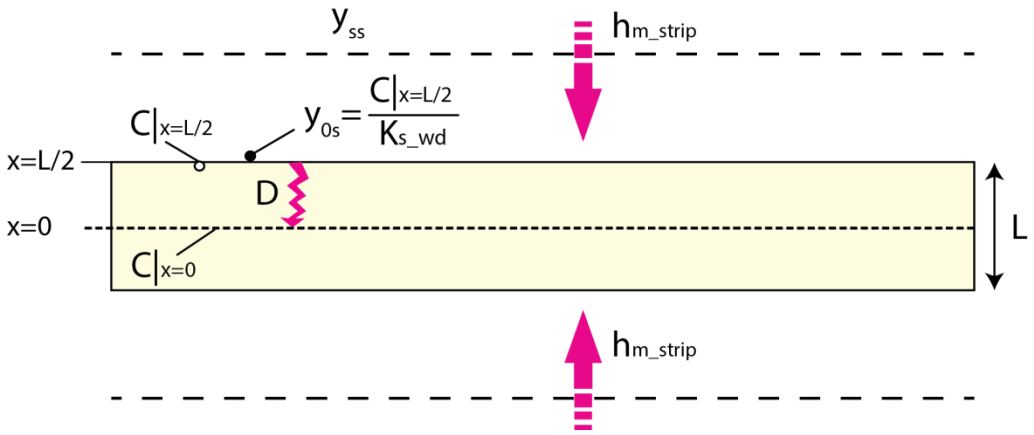

Figure C.S3: Schematic representation of phthalate absorption to wood strips.

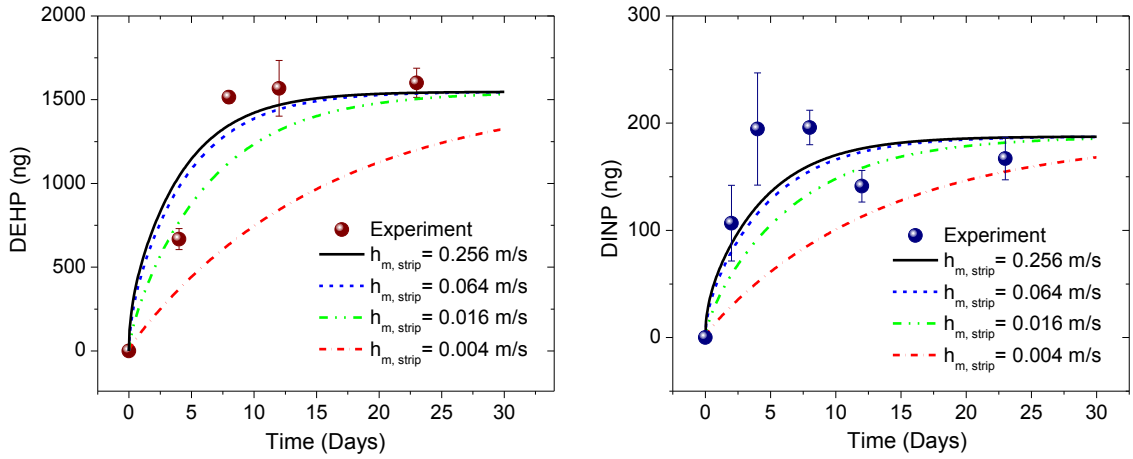

Figure C.S4: Influence of mass transfer coefficient ($h_{m,\ strip}$) on phthalate absorption to wood strips.

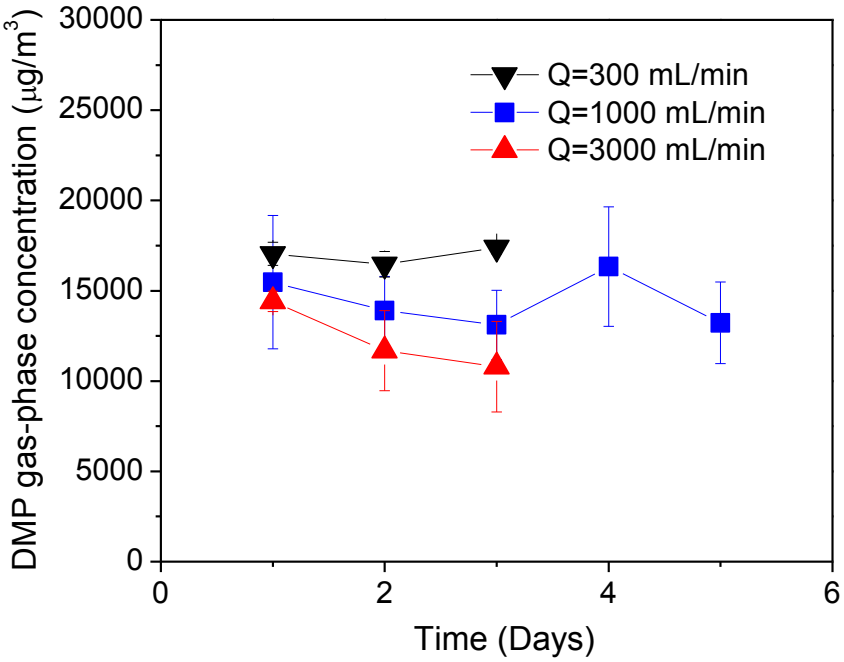

Figure C.S5: Measurements of h_m at different flow rates using pure DMP liquid.

Estimation of the Average Thickness of the Wood Chamber

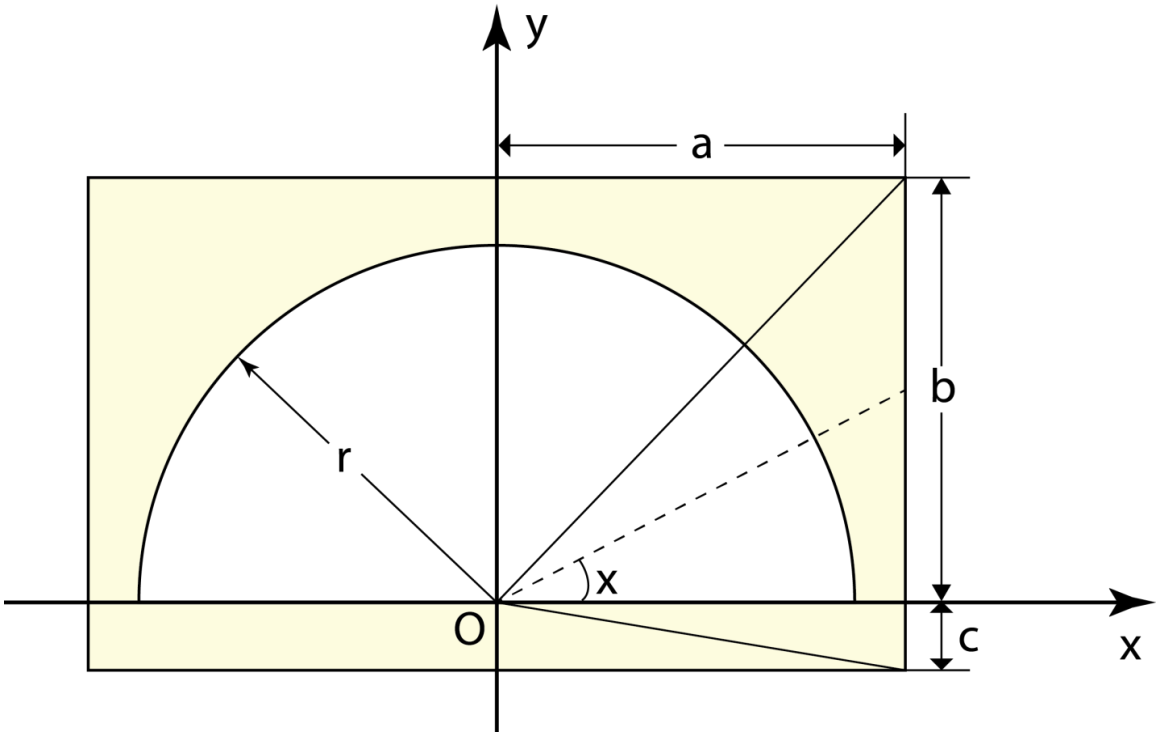

In order to determine the average thickness of the wood chamber wall, the dimensions of the chamber were explicitly measured. As shown in the illustration, a = b = 228.6 mm, c = 25.4 mm, r = 200 mm.

$$\bar{y} = \frac{1}{2\pi - 0}\left[4\int_0^{\frac{\pi}{4}}\left(\frac{a}{\cos x} - r\right)dx + \int_0^{0.1}\frac{a}{\cos x}dx + \int_{0.1}^{1.47}\frac{c}{\sin x}dx\right]$$

Considering the two equations

$$\int \frac{1}{sinx}dx = \ln\left(\tan\frac{x}{2}\right) + const.$$

$$\int \frac{1}{cosx}dx = \ln\left(\frac{sin\frac{x}{2} + cos\frac{x}{2}}{cos\frac{x}{2} - sin\frac{x}{2}}\right) + const.$$

The average thickness of the wood chamber is y = 43.61 mm = 0.04361 m.

Appendix D

Paper 4. Large-Scale Chamber Investigation and Simulation of Phthalate Emissions from Vinyl Flooring

Yirui Liang, Olivier Caillot, Jianshun Zhang, Jiping Zhu and Ying Xu
(Submitted to *Building and Environment*)

ABSTRACT

This study investigated phthalate emissions from vinyl flooring in a large-scale chamber, which is the first study of its kind. Vinyl flooring with high DINP and DEHP content was selected and their emissions were characterized in small chambers at two different temperatures. The values obtained for the dominant emission parameter, gas-phase concentration of phthalates in equilibrium with the material phase (y_0), were 0.43 $\mu g/m^3$ at 25 ºC and 4.31 $\mu g/m^3$ at 36 ºC for DINP and 0.02 $\mu g/m^3$ at 25 ºC and 6.35 $\mu g/m^3$ at 36 ºC for DEHP. Large-scale chamber experiments were then conducted using the same type of vinyl flooring, and the concentrations of DINP and DEHP showed similar trends during three experimental phases. In the first phase, the gas-phase concentrations of DINP and DEHP in the large chamber at 36 ºC were about three times lower than those in the small chamber, which is consistent with its lower area/volume ratio. In the second phase, when a large fan was replaced with a small fan, the gas-phase concentrations of DINP and DEHP in the large chamber were reduced slightly, due to the decease of mass transfer coefficient and emission rate. During the last experimental phase, when the temperature of the chamber was reduced to 25 ºC, phthalate concentrations dropped instantly and steeply due to the significantly reduced emissions. However, they did not decrease as quickly thereafter because of desorption of phthalates from the internal surfaces of the large chamber. A fundamental mechanistic model was developed to interpret the experimental results in the large chamber based on the emission characteristics obtained in the small chamber measurements. Reasonable

agreement was obtained between model prediction and experimental data. Further model simulations show that temperature and air mixing above the source material have important effects on the fate of phthalates, while the impact of air change rate (ACH) is not significant.

HIGHLIGHTS

- Large-scale controlled chamber tests were conducted to measure phthalate emissions
- Dominant emission parameter was determined in small chamber experiments
- A mechanistic model was developed to interpret the experimental results
- Reasonable agreement between model prediction and experimental data is obtained
- Temperature and air mixing have important effects on the fate of phthalates

KEYWORDS

Phthalates, Large-scale chamber, Emission, Sorption, Modeling

INTRODUCTION

Phthalates have been used as plasticizers to enhance the flexibility of polyvinyl chloride (PVC) products. These semi-volatile organic compounds (SVOCs) can be found in a wide range of building materials and consumer products including vinyl flooring, wall coverings, carpet padding, ceiling and floor tiles, furniture, and electronics (Bornehag et al., 2005). They are abundant in source materials and usually are present at percent to tens-of-percentage levels (Weschler and Nazaroff, 2008). Because phthalate additives are not chemically bound to the polymer matrix, emissions from source products usually occur (Xu et al., 2012); as a result, phthalates are ubiquitous in indoor environments (Bornehag et al., 2005; Clausen et al., 2012; Bornehag et al., 2004; Rudel

and Perovich, 2009). Biomonitoring data based on blood testing suggest that over 75% of the US population has been exposed to phthalates (Silva et al. 2004). When urinary concentrations of secondary metabolites are measured, the estimate increases to 95% (Kato et al. 2004).

Exposure to phthalates and their metabolites may result in a number of adverse health effects (Jaakkola and Knight 2008). Detailed information on the serious health effects can be found in recent studies (Albert and Jegou 2014; Alcock et al., 2011; Birnbaum et al., 2003; Darnerud, 2003; Engel and Wolff 2013; Heudorf et al., 2007; Huang et al. 2012; Jaakkola and Knight, 2008; Jurewicz et al. 2013; Kay et al. 2013; Latini et al., 2006; Legler and Brouwer, 2003; Matsumoto et al., 2008; McKee et al., 2004; Meerts et al., 2000; North et al. 2014; Ritter and Arbucklet, 2007; Vonderheide et al., 2008). Collectively, these studies show that exposure to phthalates can cause irreversible changes in the development of the reproductive tract, especially in males. Effects such as increases in prenatal mortality, reduced growth and birth weight, and skeletal, visceral and external malformations, are also associated with exposure to phthalates.

Despite nationwide exposure and adverse health effects, phthalates are still dominant in the current market of plasticizers (Schossler et al., 2011). Within a decade the global production rate of phthalates increased from 3.5 to 6 million tons/yr (Cadogan and Howick, 1996; Rudel and Perovich, 2009). Recently, the U.S. Consumer Product Safety Improvement Act was enacted to restrict the use of phthalates in toys and child care articles (CPSC, 2008). As a result, phthalates used in polymeric products are changing rapidly, with a shift from low to high molecular phthalates (Weschler, 2009). In addition, alternative plasticizers, such as di(2-ethylhexyl) terephthalate (DEHT) and diisononyl cyclohexane-1,2-dicarboxylate (DINCH) have emerged very recently. Given

that these alternatives share properties similar to those of phthalates, similar emissions, environmental fate and transport, and human exposure are expected (Schossler et al. 2011).

It is important to understand the mechanisms by which phthalates are emitted and transported in indoor environments, because it is the essential first step for investigating subsequent exposure and health effects and developing strategies to limit exposure. However, very few emission studies have targeted on these low volatility plasticizers (Xu et al., 2012; Clausen et al., 2012, 2004, 2010 and 2007; Schossler et al., 2011; Afshari et al., 2004), possibly due to the substantial difficulties associated with chamber tests for SVOCs, including the long duration of tests (months to years), the low gas-phase concentrations in test chambers, strong sorption onto surfaces, and ubiquitous contamination in laboratory facilities. Clausen et al. (2004) measured emissions of di-2-ethylhexyl phthalate (DEHP) from vinyl flooring for about 500 days in both the Field and Laboratory Emission Cell (FLEC) and Chamber for Laboratory Investigations of Materials, Pollution, and Air Quality (CLIMPAQ). Based on the measurements, Xu and Little (2006) developed a fundamental mass-transfer model to predict SVOC emissions from polymeric materials. They showed that emissions of these compounds that have very low volatility are subject to "external" control (partitioning from the material into the gas phase, the gas-phase mass-transfer coefficient, and strong sorption onto interior surfaces, including airborne particles). Using data collected in a specially-designed stainless steel chamber, Xu et al. (2012) showed that the emission rate of di(2-ethylhexyl) phthalate (DEHP) from vinyl flooring can be predicted based on a priori knowledge of y_0, the gas-phase concentration of DEHP in equilibrium with the material phase, the material to air and air to stainless steel surface mass transfer coefficients (h_m), and the stainless steel/air equilibrium relationship. Liang and Xu (2014a) recently improved the design of

the previous small chamber and developed a novel, rapid method to measure y_0 for a range of phthalate compounds released from building materials. The mechanisms that govern emissions of phthalates from polymeric materials were also elucidated further by their small-chamber study.

The emission rate measured in a small-scale emission chamber can be quite different from those associated with the same material in a real indoor environment, because the emissions of SVOCs such as phthalates are controlled by external gas-phase resistance and exterior sinks (Xu and Little 2006). However, the SVOC emission model (Xu and Little 2006) is based on mass-transfer mechanisms with model parameters that have clear physical meaning. Therefore, it can predict emissions for various conditions if the requisite model parameters are known. Xu et al. (2009; 2010) extended this chamber-based model to a fate and transport model to predict human exposure to DEHP emitted from vinyl flooring in a realistic residential environment and conducted sensitivity and uncertainty analyses. Based on the research, Liu et al. (2010) further investigated the influence of aerosol particles on the accumulation of indoor airborne DEHP with consideration of a variable particle concentration. Although the predicted phthalate concentrations in indoor air were orders of magnitude consistent with data in literature, application of these transport models without validation of measurements may result in high uncertainty. Therefore, validation of the mechanisms governing the fate and transport of phthalates via large-scale chamber experiments or field measurements has become a high research priority.

Environmental conditions (e.g., temperature and air flow rate) may have important impacts on the fate and transport of indoor phthalates. Temperature increases may significantly increase phthalate emission from sources and desorption from interior sink surfaces due to the increase in chemical vapor pressure. Fujii et al. (2003) studied

the emission of phthalates from plastic materials using a passive flux sampler. They found that the maximum emissions of DEHP increased 100-fold when the temperature increased from 20 to 80 ºC. Clausen et al. (2012) measured emissions of DEHP from PVC flooring in the FLEC at different temperatures. They observed that the steady-state concentrations of DEHP increased considerably as temperature increased, while adsorption to the chamber walls decreased greatly as temperature increases. Liang and Xu (2014b) measured emissions of phthalates and phthalate alternatives from vinyl flooring and crib mattress covers in a specially-designed small chamber at four different temperatures between 25 and 55 ºC and obtained y_0 values using the method they developed (Liang and Xu 2014a). They found that the ratio of phthalate material-phase concentration to y_0 was exponentially proportional to the reciprocal of temperature. In addition, an increase in ventilation to reduce indoor exposure to SVOCs may not be as effective as for volatile organic compounds (VOCs) whose emissions are generally subject to "internal" control (diffusion within the source material) (Xu and Zhang, 2003). For SVOCs, the emission rate may increase greatly with an increase of air flow rate due to the enhanced mass transfer above the surface of the emission source. As a result, recent small-chamber studies have found that, although the increased flow rate of fresh air reduced the residence time of air and introduced more dilution, the enhanced emission compensated for the decrease in the gas phase, and thus the gas-phase concentration of SVOCs did not drop substantially with the increasing air flow rates (Clausen 2010; Liang and Xu 2014c). However, current studies were mostly carried out in small-scale experimental chambers, and there are no comprehensive and systematic investigations on the influence of environmental conditions on the fate and transport of indoor phthalates that have been conducted in large-scale chambers, which are more representative of indoor environments than small chambers.

The aim of this study is to measure and predict emission of phthalates from vinyl flooring in large-scale chambers. The specific objectives are to: (1) conduct small-chamber tests to characterize phthalate emissions from vinyl flooring and obtain the dominant emission parameter (y_0); (2) conduct controlled tests in a room-sized chamber to measure phthalate emissions from the same type of vinyl flooring at different environmental conditions (i.e., temperature and air velocity); and (3) extend the SVOC emission model to predict phthalate concentrations in the large chamber, based on the y_0 obtained in small-chamber measurements, and investigate the effect of environmental condition changes on the fate and transport of phthalates.

METHODS AND MATERIALS

Chemicals. Standard solutions were used for chemical calibration and identification, in which butyl benzyl phthalate (BBP) and di(2-ethylhexyl) phthalate (DEHP) were obtained from Absolute Standards Inc., bis(2-ethylhexyl) isophthalate (iso-DEHP) from SPEX CertiPrep, and diisononyl phthalate (DINP) from Accustandards, Inc. Tetradeuterium ring labeled DEHP (D_4-DEHP) was used as internal standard, and its standard solution was obtained Accustandards, Inc. Hexane, methanol, sodium sulfate, and dichloromethane (DCM) (Sigma-Aldrich Co. LLC., anhydrous, >99%) were used as solvent in extraction and cleaning without further purification. The solvents were regularly analyzed to monitor potential phthalate contamination.

Test Materials. Six types of vinyl floorings were purchased primarily in the United States, and the contents of phthalates in each sample were quantified experimentally at the laboratory of Health Canada. Among them, we selected one vinyl flooring sample that contained phthalates at relatively high concentration. The selected flooring was wrapped in aluminum foil, and stored at room temperature. Before

measurements, the test pieces were unwrapped, cut, and placed in a small- and a large-scale emission chambers.

The content of phthalates in vinyl floorings was measured by solvent extraction. Small pieces of samples (approximately 100 mg in total) were cut out of each type of the flooring material. The samples were then transferred to a 15 mL vial, where 400 mg of anhydrous sodium sulfate was added with an injection of 5 mL hexane/DCM (1:1) mixture. The samples were ultrasonically extracted for 30 min. The extractions were conducted in an ultrasonicator filled with clean water and ice bags to maintain a low temperature and avoid evaporation loss of sample during the process. After centrifuged for 5 minutes, the clear solution was transferred to vials that were sealed properly. Finally the extracts were diluted (1:50) and injected to gas chromatography and mass spectrometry (GC-MS) for further analysis.

Small Chamber Experiment. Small-scale chamber test was conducted at the University of Texas at Austin to characterize phthalate emissions from the selected vinyl flooring and obtain the dominant emission parameter (y_0). A specially-designed, stainless steel chamber used in previous experiments (Liang and Xu 2014a) was employed in this study. As shown in Figure D.1, the chamber maximized the surface area of emission source and minimized the surface area of internal sink thereby substantially reducing the time required to reach steady state. In addition, three precision-ground stainless steel rods, matched to the interior stainless steel chamber surface, were inserted into the chamber and then periodically removed so that the concentration of SVOCs sorbed on the surface could be measured. This method allowed us to relate gas-phase concentration to the concentration sorbed on the surface of the chamber and quickly establish the sorption equilibrium relationship. The specific design

of the chamber was described in greater detail by Liang and Xu (2014a). The chamber's properties and the test conditions of the current study are listed in Table D.1.

The emission chamber was placed in a temperature-controlled cabinet (Lunaire CEO-932) and operated at 25±0.5°C. The concentrations of phthalates versus time were measured in the emission chamber at an air flow rate of 1000mL/min. Phthalates was sampled directly on Tenax-TA tubes with a pump (SKC 224-PCXR4) calibrated to a nominal flow rate of 100 ml/min. The sampling time was approximately 24 hours. Backup tubes were connected to each primary sample tube to check for breakthrough (Figure D.1). No breakthrough was observed in any of the tests. Because the sampling system was supplied with high purity air from cylinders, we assumed that no particles were present. Before emission test, the stainless steel plates and especially the internal chamber surfaces were cleaned with an alkali detergent, hot tap water and Nanopure® water, and then finally rinsed several times with methanol. Background measurement was performed before the test for around a week. Because relative humidity (RH) does not significantly influence phthalate emissions (Clausen et al. 2007), only temperature and air flow rate through the chamber were checked before and after samples were taken for analysis.

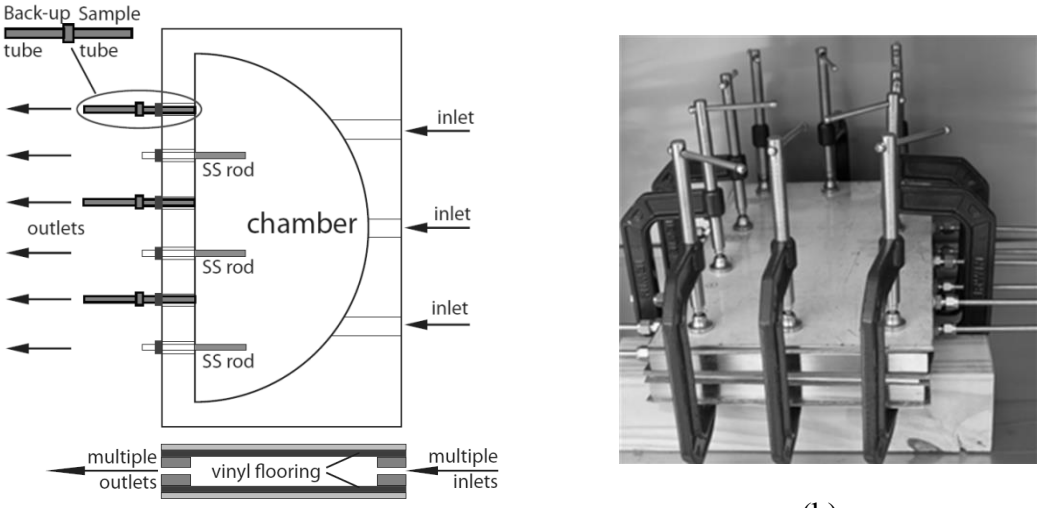

Figure D.1: (a) Schematic and (b) photo of the experimental setup for small chamber experiments.

Parameter	Unit	Value
Small chamber		
Temperature	°C	25 ± 0.5 and 36 ± 0.5
Chamber volume	L	1
Air flow rate (Q)	mL/min	1000
Air change rate	1/h	53
Area of test pieces (A)	m^2	0.13
Internal stainless steel surface area (A_s)	m^2	0.02
Area/volume ratio	m^2/m^3	130
Large chamber		
Temperature	°C	25 ± 0.5 and 36 ± 0.5
Chamber volume (V)	m^3	54.4
Air flow rate (Q)	m^3/h	270
Air change rate	1/h	0.5
Emission area (A)	m^2	17.8
Internal stainless steel surface area (A_s)	m^2	52
Area/volume ratio	m^2/m^3	0.33
Velocity across the flooring (large fan)	m/s	2.4
Velocity across the flooring (small fan)	m/s	1.0

Table D.1: Chamber properties and test conditions.

Large Chamber Experiment. Large-scale chamber measurement was conducted at Syracuse University to investigate the effect of environmental conditions on the emission and transport of phthalates. The full-scale chamber (4.8 m × 3.7 m × 3.0 m) was equipped with a heating ventilation and air-conditioning (HVAC) system, which was automatically controlled to provide precise temperature, RH, and air velocity in the chamber (Figure D.2). The air-handling unit was equipped with a high efficiency particulate air (HEPA) filter and activated carbon filters to control the pollutant concentration in the supply air. The chamber was operated at a RH of 30%, with a total air flow rate of 270 m^3/h and an air change rate (ACH) of 0.5/h. The selected vinyl flooring (4.8 m × 3.7 m) was installed in the chamber, covering the chamber floor. The large chamber experiment was carried out in three phases. First, the chamber was operated at a high temperature (36 °C) with a large fan on. The temperature of 36 °C was selected to shorten the time for the gas-phase concentration in the chamber to reach steady state, due to the reduced sorption to the chamber surfaces at a relatively high temperature. The large fan with an air flow rate of 0.9 m^3/s was used to increase the air velocity near the emission source and enhance air mixing in the chamber. In the second phase, the large fan was turned off and a small fan with an air flow rate of 0.2 m^3/s was powered on while the temperature was maintained at 36 °C. In the third phase, the operating temperature was reduced to 25 °C and the large fan was powered back on instead of the small fan. During the experiment, the gas-phase concentration of phthalates was sampled periodically using Tenax-TA sorbent tubes with a sampling flow rate of 100 ml/min and sampling time of approximately 24 hours. After sample collection, the sample tubes were sealed with brass storage end caps, wrapped with aluminum foil, and stored in a refrigerator to maintain a storage temperature below 4 °C. The sample tubes were eventually shipped to the University of Texas at Austin within an

icebox with gel packs and analyzed within two days of receipt. Before the test was initiated, the large chamber was conditioned at a temperature of 36 °C, and a lengthy blank run was carried out to ensure that there was no background contamination.

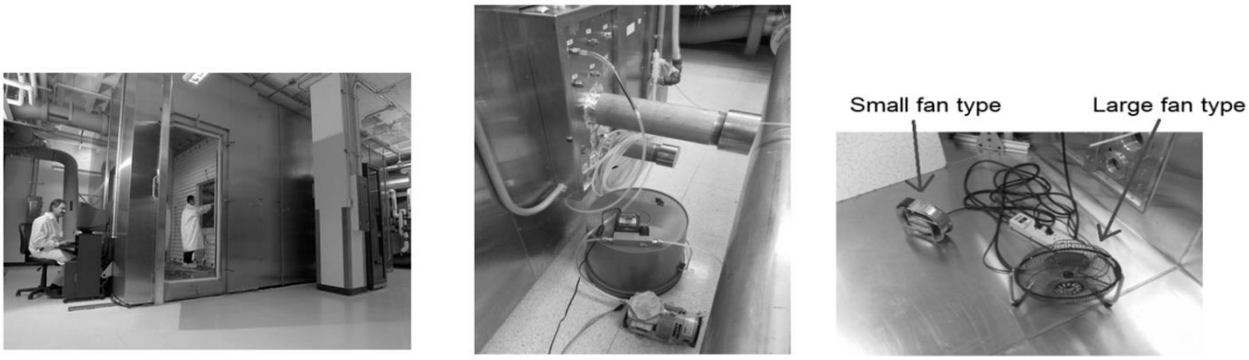

(a) (b) (c)

Figure D.2: Experimental setup for large chamber experiments. (a) photo of the large environmental chamber; (b) air sampling setup; and (c) mixing fans.

Chemical Analysis of Phthalates. Phthalate samples collected by solvent extraction were analysed by a GC-MS system (Agilent 5890 GC- 5973MS). The GC-MS was equipped with a 15 m × 0.25 mm DB-5HT column and operated at splitless mode with an injection temperature of 250 °C and transfer line temperature of 310 °C. The temperature program was 100 °C hold for 5 min, ramp 10 °C/min for 30 min to a temperature of 325 °C. For air samples, phthalates collected by the Tenax TA sorbent tubes were desorbed by a thermal desorber (TD) (Turbomatrix 650 ATD) and analyzed by a GC-MS system (Agilent 7890A GC- 5975MS). Before analysis, 5 µL solution of D_4-DEHP (2 µg/mL) in methanol was injected into the Tenax tubes as internal standard. The sorbent tubes were then desorbed for 30 min at 300 °C, with a He flow of 50 ml/min, and a cold trap temperature of minus 30 °C. Flash heating of the cold trap to 350 °C transferred the analyte through the valves at 250 °C and the transfer line at 250 °C to the

GC. The GC-MS had a constant pressure resulting in a flow rate of 1.6 ml/min at 80 °C, and was equipped with a 30 m × 0.25 mm DB-5MS column and operated at a 5:1 split injection. The temperature program was 80 °C, hold for 0.5 min, ramp 20 °C/min for 8.5 min, then ramp 30 °C/min for 2 min, and finally hold for 9 min. All analyses were performed in full scan mode and the extracted ions used for identification and quantification are summarized in Table D.2. It should be noted that DINP is mixtures of many isomers, and was detected as correspondingly broad peaks, which took about 1 min to elute. All tubes were analyzed in two successive desorptions to ensure complete desorption of both the tube and the TD-GC-MS system. The second desorption showed concentrations below the detection limit in all cases. A calibration standard was regularly run prior to each GC injection, and the variance was always below 5% for all injections.

Phthalate compounds	Abbrev.	CAS no.	MW (g/mol)	t_R (min)	Quantifying ion	Qualifier ions
Butyl benzyl phthalate	BBP	85-68-7	312.4	10.8	149	91, 206
Di(2-ethylhexyl) phthalate	DEHP	117-81-7	390.6	11.44	149	167, 279
Di(2-ethylhexyl) isophthalate	Iso-DEHP	137-89-3	390.6	12.50	149	261
Diisononyl phthalate	DINP	28553-12-0	418.6	11~12	293	149, 167
Di(2-ethylhexyl) phthalate-3,4,5,6-d_4	D_4-DEHP	93951-87-2	394.6	11.44	153	171, 283

Table D.2: GC-MS retention times (t_R), with quantifying and qualifier ions for phthalates.

Modeling of Phthalate Emissions in the Large Chamber. To further interpret the experimental results in the large chamber, we extended the SVOC emission model (Xu and Little, 2006; Xu et al., 2012) to predict phthalate concentrations in the large chamber, based on the knowledge of y_0 obtained in small-chamber measurements. Figure D.3 shows the schematic representation of the model. Phthalates are emitted from the vinyl flooring installed in the large chamber and sorbed onto interior surfaces of the

chamber, including chamber walls, ceiling, and the returning duct of the HVAC system. Considering that a high-efficiency particulate air filter was used to precondition the supply air to the chamber, we did not include particle dynamics in the model. We assumed that the air is well-mixed in the chamber with the use of large/small fans; therefore, the gas- and surface-phase concentrations of phthalates were assumed uniformly distributed. The accumulation of the gas-phase concentration of phthalates in the chamber obeys the following mass balance equation:

$$V\frac{dy(t)}{dt} = Q_r y_r(t) + E(t)A - \frac{dq(t)}{dt}A_s - Qy(t) - Q_r y(t) \quad (1)$$

where y ($\mu g/m^3$) is the bulk gas-phase concentration of phthalates in the chamber, V (m^3) is the interior volume of the chamber, Q_r (m^3/s) is the air flow rate through the return duct, y_r ($\mu g/m^3$) is the gas-phase concentration of phthalates from the return duct, E ($\mu g/m^2/h$) is the emission rate of phthalates from vinyl flooring, A (m^2) is the area of the vinyl flooring, q is the surface concentration ($\mu g/m^2$) of phthalates on interior chamber surfaces (i.e., walls and ceiling), A_s (m^2) is the area of the interior surfaces, and Q (m^3/s) is the fresh air flow rate. The emission rate can be expressed as

$$E(t) = h_m \cdot [y_0 - y\,(t)] \quad (2)$$

where h_m (m/s) is the convective mass-transfer coefficient near the source material, y_0 ($\mu g/m^3$) is the gas-phase phthalate concentration in the air immediately adjacent to the source materials, which was obtained in the small chamber experiment. The ratio of the concentration of a chemical on sorption surfaces (i.e., stainless steel surfaces of chamber walls and ceiling) to its concentration in the gas phase is equal to the surface/air partition coefficient, K_s (m), or

$$K_s = q(t)/y_s(t) \quad (3)$$

where y_s (μg/m^3) is the gas-phase concentration immediately adjacent to the sorption surface. Assuming a boundary layer exists adjacent to the sorption surfaces, the amount of phthalates accumulated on the surface is equal to the total mass transferred through the boundary layer from the gas phase, or

$$\frac{dq(t)}{dt} = h_s[y(t) - y_s(t)] \tag{4}$$

where h_s (m/s) is the convective mass-transfer coefficient near the sorption surface. Because the air was assumed well-mixed in the chamber, the value of h_s equals that of h_m.

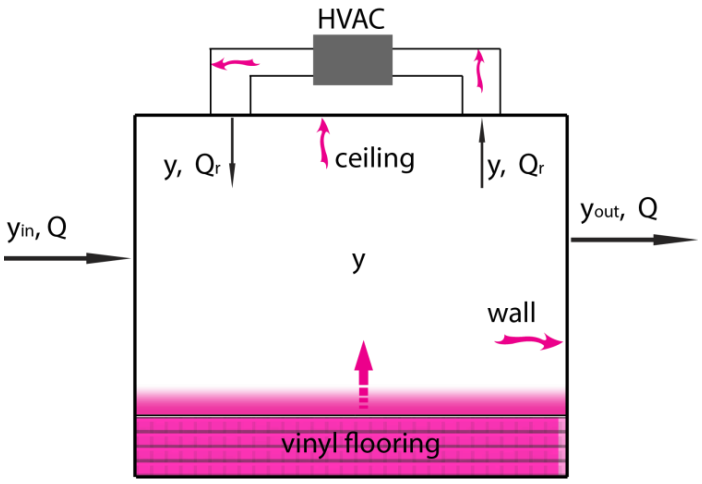

Figure D.3: Schematic representation of vinyl flooring in the large experimental chamber. HVAC = heating, ventilation and air conditioning system.

Similarly, in the return duct of the HVAC system, the accumulation of gas-phase concentration of phthalates can be described as

$$V_r \frac{dy_r(t)}{dt} = Q_r y(t) - Q_r y_r(t) - K_s \frac{dy_r}{dt} A_{sr} \tag{5}$$

where V_r (m^3) is the total volume of the return duct, A_{sr} (m^2) is the interior surface area of the duct. Because the air velocity across the interior surface of the return duct is high, we assumed instant sorption equilibrium between the gas- and surface-phase concentrations of phthalates within the duct.

RESULTS AND DISCUSSION

Measurements of Phthalate in Vinyl Flooring. The content of phthalates in vinyl flooring samples was measured and is listed in Table D.3. The background level of phthalates in blank was less than 0.2 % of the content of the samples. Phthalate concentration in these flooring samples ranges between 4 % and 22 % by weight. The vinyl flooring (sample 5), which had the highest phthalate concentration and contained DINP and DEHP, was selected and used in the following chamber studies.

	Phthalate concentration (mg/mg)				
	ISO-DEHP	DEHP	BBP	DINP	Total
Sample #1	0.03		0.05		0.08
Sample #2	0.09		0.08		0.17
Sample #3		0.11			0.13
Sample #4			0.04		0.04
Sample #5		**0.02**		**0.20**	**0.22**
Sample #6		0.004		0.05	0.05

Table D.3: Content of phthalates in vinyl flooring samples.

Small Chamber Experiment. Figure D.4 shows the gas-phase concentration of phthalates obtained in the small chamber experiments. In all tests, the phthalate concentration in a blank chamber was less than 5% of the highest measured concentrations in the sample chamber with vinyl flooring, indicating no contamination occurred during the measurements. The experimental conditions were constant over the entire test period. Each data point in Figure D.4 represents the mean value of

concentrations in triplicate measurements with error bars representing the standard deviation. At the temperature of 25 ºC, the concentration of DINP and DEHP increased and reached steady state in about three days. In the improved chamber design (Liang and Xu 2014a), the ratio of emission surface to sorption surface was high, the mass loss of phthalates onto sampling pathways was avoided, and the velocity field inside the chamber was optimized to enhance air mixing. Therefore, the build-up of phthalates in the gas phase occurred much faster and the time to reach steady state was significantly reduced, compared to the previous studies of DEHP emission in FLEC and in a special chamber, in which it took about 150 and 30 days, respectively (Clausen et al. 2004; Xu et al. 2012). In addition, the steady-state concentration of DINP is approximately 20 times higher than that of DEHP, primarily related to its high material-phase concentration in vinyl flooring (Table D.3).

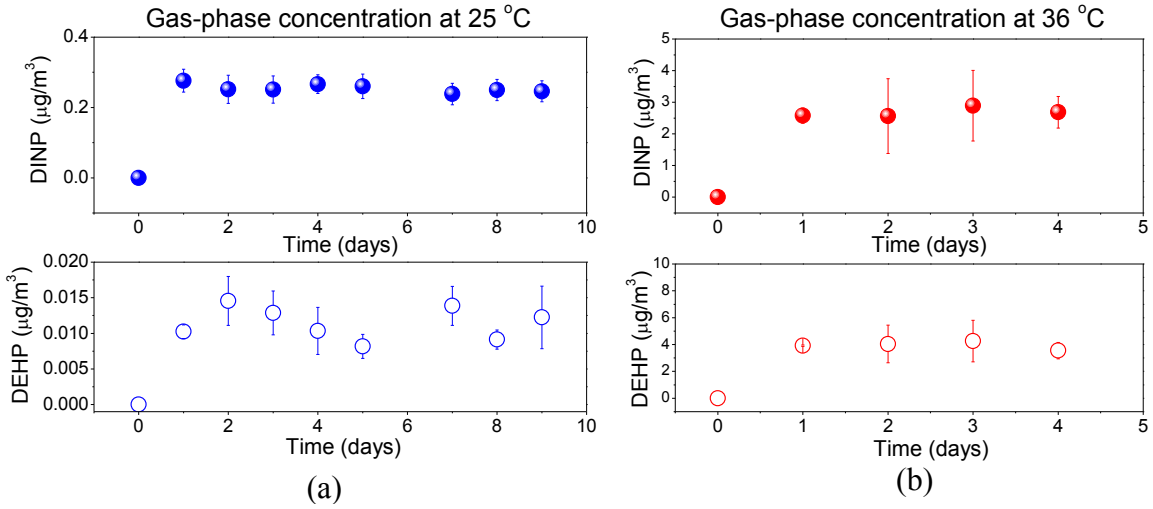

Figure D.4: Gas-phase concentration of DINP and DEHP measured in the small chamber experiments at two different temperatures. (a) 25 ºC and (b) 36 ºC.

Temperature had a strong influence on phthalate emissions. When the temperature was increased from 25 to 36 ºC, the steady-state air concentration of phthalates in the chamber increased 10 and 80 times for DINP and DEHP, respectively. The specific emission rate (SER) can be estimated based on the gas-phase concentration, chamber air change rate, the surface area of emission source, and the chamber's volume (Clausen et al. 2004). A 10 ºC increase in temperature (from 25 to 36 ºC) resulted in significant increase in SER. For DINP, the SER increased by 10 times, from 0.11 ± 0.01 to 1.1 ± 0.06 μg/m^2/h, while for DEHP, the value increased from 0.005 ± 0.001 to 1.6 ± 0.1 μg/m^2/h, which is about 300-fold. Based on the steady-state concentration (y_{ss}) that was measured in the small emission chamber, we can determine the value of y_0 (the gas-phase concentration of phthalates in equilibrium with the material phase) for the tested vinyl flooring sample at the two different temperatures, using the following equation (Liang and Xu 2014a):

$$y_0 = \frac{y_{ss} \cdot Q}{h_m \cdot A} + y_{ss} \quad (6)$$

where Q is the air flow rate of the chamber (m^3/s), A is the area of emission surfaces (m^2), and h_m (m/s) is the convective mass-transfer coefficient near the emission surface. The value of h_m at 25 ºC was measured by Liang and Xu (2014a) for the conditions of the test chamber and it was corrected to the temperature of 36 ºC (Liang and Xu 2014b). The obtained y_0 values are 0.43 μg/m^3 at 25 ºC and 4.31 μg/m^3 at 36 ºC for DINP and 0.02 μg/m^3 at 25 ºC and 6.35 μg/m^3 at 36 ºC for DEHP.

Large Chamber Experiment. Figure D.5 shows the measured phthalate concentrations in the large chamber over a period of a month, and the concentration trends for DINP and DEHP are similar. The estimated uncertainty associated with each

data point was included in the supporting information (SI). The measured gas-phase concentrations of DINP and DEHP in the large chamber experiment have a larger uncertainty than the small chamber experiment, reflecting the increased difficulty in full-scale chamber study of phthalates.

In the first experimental phase, the concentration of DINP and DEHP slowly increased and had not reached steady state at the end of the first phase, although a fast concentration build-up was expected at such a high temperature. The result suggested that surface sorption onto interior surfaces of the chamber (e.g., chamber wall and inner surface of HVAC air duct) could still be strong at 36 ºC for those SVOC compounds, which increased the time for the gas-phase concentration to become stable. Consistent with the lower area/volume ratio (Table D.1), the gas-phase concentrations of DINP and DEHP at 36 ºC were about three times lower in the large chamber experiment than in the small chamber experiment (Figures D.3 and D.4). Nevertheless, the SERs observed in the large chamber (DINP: 2.7 µg/m^2/h and DEHP: 3.2 µg/m^2/h) were consistent at an order of magnitude with those obtained in the small chamber experiment at 36 ºC.

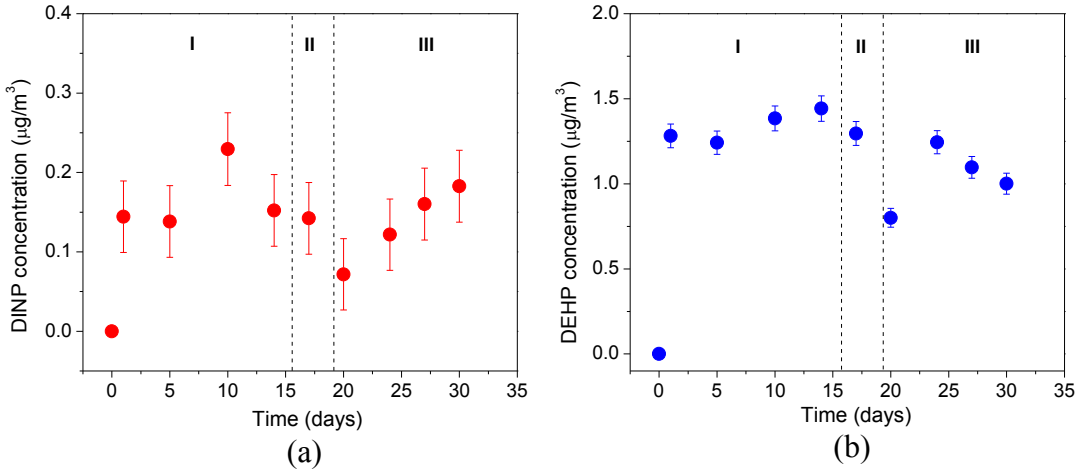

Figure D.5: Gas-phase concentration phthalates measured in the large chamber experiments with Roman numerals indicating experimental phases. (a) DINP and (b) DEHP.

From the first to the second phase, when a large fan was replaced with a small fan, the velocity across the vinyl flooring sample was reduced by half (Table D.1). As a result, the mass transfer coefficient above the vinyl flooring surface declined, which further caused a decrease of the emission rate, and thus the gas-phase concentrations of DINP and DEHP in the large chamber reduced slightly on day 16. When the third phase was initiated, the temperature of the chamber was reduced to 25 ºC. The concentrations of phthalates dropped instantly and steeply at the beginning, due to the significantly reduced emission from the vinyl flooring (Figure D.5a). However, the concentration did not decrease as quickly thereafter, which is possibly related to desorption of phthalates from the internal surfaces of the chamber as the gas-phase concentration decreased.

Modeling of Phthalate Emissions in the Large Chamber. To further interpret the experimental results in the large chamber, we extended the SVOC emission model (Xu and Little 2006; Xu et al. 2012) to predict phthalate concentrations in the large chamber, based on the y_0 value obtained in the small-chamber measurements. The sorption partition coefficients between gas and stainless steel surface (K_s) for DINP and DEHP at 25 ºC were obtained from previous small chamber measurements (Liang and Xu 2014a). Clausen et al. (2012) measured the adsorption of DEHP to stainless steel chamber surface at 35 ºC using FLEC, and their K_s value was used in the current study. For DINP at 36 ºC, K_s was estimated based on the correlation developed by Liang and Xu (2014a) using vapor pressure, and the vapor pressure of DINP at 36 ºC was calculated using the Clausius-Clapeyron equation, with equation constants as described by Cousins et al. (2003). As shown in Figure D.6, numerical simulation was then used to obtain the overall mass transfer coefficient (h_m), and only the data obtained for DEHP were used to obtain this parameter. The determined value of h_m for DEHP was then corrected for DINP based on the air diffusivity differences (Liang and Xu 2014a). The model

parameters for the large chamber are summarized in Table D.S2. As we expected, K_s increased and y_0 decreased with the decrease of temperature, and the value of h_m reduced when the large fan was replaced by the small fan.

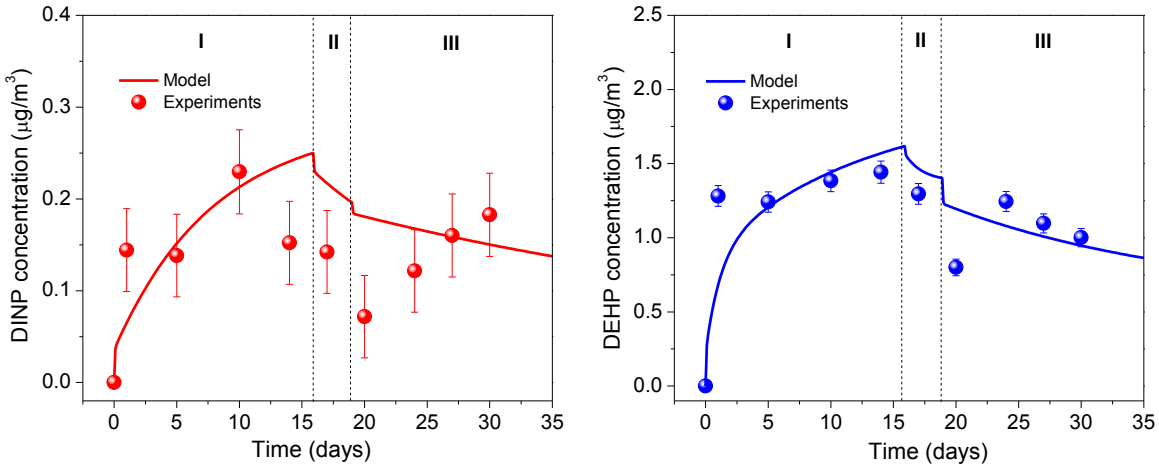

Figure D.6: Comparison of fitted gas-phase concentration with data measured in the large experimental chamber. (a) DINP and (b) DEHP.

Reasonable agreement was obtained between the gas-phase concentrations of DEHP and DINP calculated by the model and the experimental data. The difference might be related to uncertainty in the measured chemical concentrations as well as other environmental parameters. For example, we did not collect duplicate samples in the large chamber experiment, which may reduce the reliability of the data. DINP and DEHP showed opposite concentration trends during the third experimental phase. It is difficult to determine whether the slight increase of DINP concentration was due to the uncertainty of measurements. In addition, air samples in the large chamber experiment were collected by sorbent tubes via long Teflon tubing. The mass loss of phthalates onto sampling pathways might result in underestimations of the real gas-phase concentration in the large chamber. Furthermore, the difference between model prediction and

experimental data may also be related to the nonuniform distribution of the gas- and surface-phase phthalates in the large chamber. We measured the air velocity above the vinyl flooring during the experiment to obtain the mass transfer coefficient (h_m) using correlation equations (Axley 1991). But use of the estimated h_m value resulted in even worse model prediction, indicating that the mass transfer coefficient above the emission surface might not be equal to that above the sorption surfaces. Therefore, we used the set of DEHP data to obtain a lumped parameter, the fitted h_m, which could result in uncertainty in model prediction.

Using the model developed, we analyzed the amount of phthalates emitted from the source or adsorbed on interior chamber surfaces during each phase of the large chamber experiment. As listed in Table D.S3, strong emission and sorption happened in phase one for both DEHP and DINP. The amount of phthalates emitted was reduced in phase two due to the use of a smaller fan and the short time duration of phase two. At the beginning of phase three, there was a steep drop of phthalate concentrations, primarily due to significantly reduced emission from the vinyl flooring. During phase three, there was no emission of DEHP, because the gas-phase concentration in the chamber (y) was higher than the y_0 value (Equation 2). In contrast, desorption of DINP (5.36 mg) and DEHP (3.04 mg) from the interior chamber surfaces was significant, which is the reason for the slow decrease in the gas-phase concentration thereafter.

We further investigated the influence of temperature, air mixing, and ACH on the emission of DEHP in the large chamber using the validated model. As shown in Figure D.7a, it takes over 500 days for the gas-phase concentration of DEHP to reach steady state in the large chamber at the temperature of 25 ºC. In the design of the large chamber experiment, the selection of 36 ºC helped to speed up the concentration build-up. However, the model simulation shows that it still takes about 50 days for the DEHP

concentration to become stable at the temperature of 36 ºC. The effect of ACH on reducing DEHP concentration is more obvious at 36 ºC than at 25 ºC, because DEHP behaves more like a VOC compound at a higher temperature. Air mixing (i.e., air velocity) above the emission surface plays an important role on the fate of DEHP in the second phase of the experiment. As shown in Figure D.7b, the gas-phase concentration of DEHP dropped significantly with a decrease in velocity and h_m close to the vinyl flooring surface. If the third experimental phase was continued, it would take about 1000 days for the gas-phase concentration of DEHP to reach a steady-state level close to that in the small chamber experiment, indicating the persistence of the SVOC compound. During the process, an increase of ACH would only have a limited effect on reducing DEHP concentration; in contrast, the use of all fresh air (ACH=5/h) would result an instant and steep concentration drop, because the amount of DEHP desorbed from the interior surfaces of HVAC duct can be excluded from the chamber system.

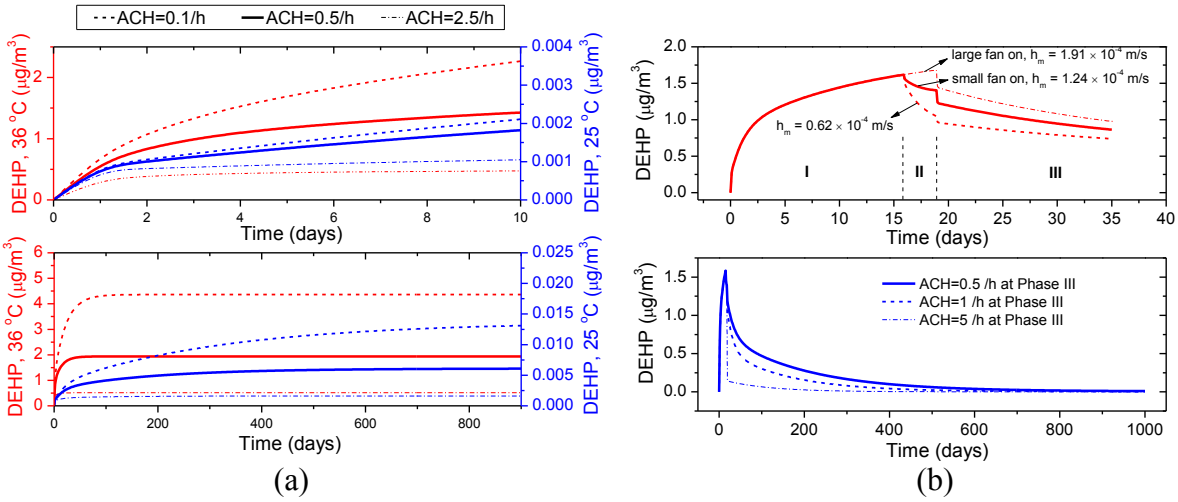

Figure D.7: (a) Influence of temperature and air change rate (ACH) on DEHP gas-phase concentration in the large experimental chamber; and (b) influence of air mixing on DEHP emission in Phase II and the effect of ACH on DEHP concentration in Phase III of the large chamber experiments.

CONCLUSIONS

This study investigated phthalate emissions from vinyl flooring in a large-scale chamber, which is the first study of its kind. Vinyl flooring with high DINP and DEHP content was selected and their emissions were characterized in small chambers at two different temperatures. The values obtained for the dominant emission parameter, gas-phase concentration of phthalates in equilibrium with the material phase (y_0), were 0.43 $\mu g/m^3$ at 25 ºC and 4.31 $\mu g/m^3$ at 36 ºC for DINP and 0.02 $\mu g/m^3$ at 25 ºC and 6.35 $\mu g/m^3$ at 36 ºC for DEHP. Large-scale chamber experiments were then conducted using the same type of vinyl flooring, and the concentrations of DINP and DEHP showed similar trends during three experimental phases. The gas-phase concentrations of DINP and DEHP at 36 ºC were about three times lower in the large chamber than in the small chamber, which is consistent with its lower area/volume ratio. In the second phase, when a large fan was replaced with a small fan, the gas-phase concentrations of DINP and DEHP in the large chamber reduced slightly, due to the decrease in the mass transfer coefficient and emission rate. During the last experimental phase, when the temperature of the chamber was reduced to 25 ºC, phthalate concentrations dropped instantly and steeply due to the significantly reduced y_0 values and emissions. However, they did not decrease as quickly thereafter because of the desorption of phthalates from the internal surfaces of the chamber. A fundamental mechanistic model was developed, with data on emission characteristics obtained in small chamber measurements, to interpret the experimental results in the large chamber. Reasonable agreement between model prediction and experimental data was obtained. Further model simulations show that temperature and air mixing above the source material have important effects on the fate of phthalates, while the impact of the air change rate (ACH) is not significant.

Along with several paths for future inquiry, there were some limitations in the current study. A large chamber study on emissions of SVOCs such as phthalates is difficult, and there are potential uncertainties associated with the measured concentration of phthalates as well as other environmental parameters. We did not collect duplicate samples in the large chamber experiment, which may reduce the reliability of the data. Additionally, the mass loss of phthalates onto sampling pathways might result in underestimation of phthalate concentrations. We made several simplifying assumptions in the model, and as such, much remains to be done to confirm the overall modeling approach. For example, we assumed that the air was well-mixed in the chamber and thus the gas- and surface-phase concentrations of phthalates were uniformly distributed. However, a recent study (Wang et al. 2011) showed that the distribution of SVOCs in indoor environments was strongly related to the flow field of the room. Airborne particles were not included in our experiments and modeling in this study. Given that they may facilitate the transport of SVOCs, further research is needed to examine the partition relationship between gas- and particle-phase phthalates as well as the sorption kinetics via small chamber experiments, and the influence of dynamic gas/particle interaction on the fate and transport of phthalate in large-scale chambers.

ACKNOWLEDGEMENTS

Financial support was provided by the National Science Foundation (NSF) (CBET-1150713 and CBET- 1066642) and American Society of Heating, Refrigerating and Air Conditioning Engineers (ASHRAE) (Grant-In-Aid and NIA Awards).

SUPPORTING INFORMATION

Estimation of concentration uncertainty in large chamber experiment. All the phthalate samples in this study were collected using Tenax TA sorbent tubes, with two tubes connecting in series to monitor any breakthrough of phthalates onto the sorbent; and the backup tubes showed concentrations below the detection limit in all cases. Limited by experimental conditions, no duplicate sample trains were collected in the large chamber experiment. The overall uncertainty for analytical procedure was calculated from the first rule of combination (square root of the sums of squares) of each uncertainty using Equation S1 and was listed in Table D.S1.

$$\mu_c(C_A) = C_A\sqrt{\left(\frac{\mu_{sp}}{V}\right)^2 + \left(\frac{\mu_{pc}}{C_A}\right)^2 + \left(\frac{\mu_{cc}}{C_A}\right)^2} \quad \text{(S1)}$$

where $\mu_C(C_A)$ = the combined mass concentration uncertainty for a phthalate, C_A = the mass concentration for a phthalate [$\mu g/m^3$], μ_{sp} = the uncertainty associated with the sample processing [μl], V = volume [μl], μ_{pc} = uncertainty associated with the preparation of the calibration solutions [$\mu g/m^3$], and μ_{cc} = uncertainty associated with the calibration check [$\mu g/m^3$].

DINP $\mu g/m^3$	uncertainty $\mu g/m^3$	DEHP $\mu g/m^3$	uncertainty $\mu g/m^3$
0.14431	0.045124	1.28174	0.069658
0.13826	0.045091	1.24146	0.068379
0.22951	0.045732	1.38431	0.072986
0.15222	0.045169	1.4425	0.074917
0.14222	0.045112	1.29576	0.070106
0.07174	0.044821	0.80035	0.055786
0.12167	0.045008	1.24458	0.068478
0.16021	0.045217	1.09688	0.063944
0.18271	0.045365	1.00083	0.061147

Table D.S1: Uncertainty associated with phthalate concentrations measured in the large chamber experiment.

Parameters	Unit	Values	References
Chamber volume (V)	m^3	54.4	measured
Ventilation rate (Q)	m^3/s	0.00755	measured
Return air flow rate (Q_r)	m^3/s	0.068	measured
Return duct length (L_r)	m	5	estimated
Return duct radius (R_r)	m	0.5	estimated
Inner surface area of return duct (A_{sr})	m^2	15.7	estimated
Emission area (A)	m^2	17.8	measured
Characteristic length (L)	m	4.9	measured
Adsorptive surface area (A_s)	m^2	52.02	measured
Velocity across the source (large fan)	m/s	2.4	measured
Velocity across the source (small fan)	m/s	1.01	measured
y_0 for DINP at 25 °C	$\mu g/m^3$	0.43	measured
y_0 for DINP at 36 °C	$\mu g/m^3$	4.31	measured
y_0 for DEHP at 25 °C	$\mu g/m^3$	0.02	measured
y_0 for DEHP at 36 °C	$\mu g/m^3$	6.35	measured
K_s for DINP at 25 °C	m	2100	measured
K_s for DINP at 36 °C	m	370	estimated
K_s for DEHP at 25 °C	m	1500	measured
K_s for DEHP at 36 °C	m	100	measured
h_m for DEHP at 36 °C with large fan on	m/s	1.91×10^{-4}	model fitted
h_m for DEHP at 36 °C with small fan on	m/s	1.24×10^{-4}	model fitted
h_m for DEHP at 25 °C with large fan on	m/s	1.93×10^{-4}	temperature corrected
h_m for DINP at 36 °C with large fan on	m/s	1.83×10^{-4}	diffusivity corrected
h_m for DINP at 36 °C with small fan on	m/s	1.19×10^{-4}	diffusivity corrected
h_m for DINP at 25 °C with large fan on	m/s	1.86×10^{-4}	diffusivity corrected

Table D.S2: Model parameters for DINP and DEHP emissions in the large chamber.

		Emitted (mg)	Adsorbed onto surfaces (mg)
DEHP	phase 1	22.73	8.96
	phase 2	2.69	0.23
	phase 3	0	-5.36
DINP	phase 1	17.20	6.99
	phase 2	2.09	0.99
	phase 3	0.18	-3.04

Table D.S3: Estimated mass emitted or adsorbed in the large chamber experiment.

Appendix E

Paper 5. Indoor Residential Fate Model of Phthalate Plasticizers

Yirui Liang, Chenyang Bi and Ying Xu
(In preparation for *Environmental Science & Technology*)

ABSTRACT

Particle dynamics (penetration, deposition, and resuspension) are possibly important for the fate of phthalate plasticizers in residential environments. Settled dust on indoor surfaces may serve as significant media in transporting phthalates from their sources to sinks. In this study, we develop a residential fate model to elucidate the mechanisms of phthalates transport and their distribution among the gas phase, airborne particles, interior surfaces and settled dust in indoor environment. This dynamic mass-balance model considers various environmental media (air, particulate matter, settled dust, vinyl flooring, wood floor, carpet, furniture, ceiling and walls) and associates particle dynamics as a core part of transporting phthalates from source to sink. Three size fractions of particles with different transport properties and indoor activities (vacuuming and cooking) are included. To validate the model, we conduct independent field experiments in a test house preinstalled with vinyl flooring that contains benzyl butyl phthalate (BBP). We monitor BBP concentrations in air, dust and interior surfaces and the model predictions of BBP are of the same order of magnitude as measured values. We conduct sensitivity analysis on model input parameters to identify the critical parameters that control the transport mechanisms of indoor phthalates. We extend the model to a three-compartment environment for bis(2-ethylhexyl) phthalate (DEHP) with different outdoor particle levels and the model results show significant difference of DEHP concentrations and emission rates, indicating the importance of particles and/or dust for enhancing the transport of indoor phthalates. To investigate the buffer effect of indoor surfaces (e.g. carpet) as secondary sources, we run the model with no DEHP

source input after a period of time and DEHP is proved to present in the environment for a long time thereafter.

INTRODUCTION

Phthalates have been produced and used as plasticizers to enhance the flexibility of rigid polyvinyl chloride (PVC) products. Because of their low volatility, these chemicals are classified as Semi-Volatile Organic Compounds (SVOCs). Phthalates can be found in a wide range of consumer products such as floor and wall covering, children's toys, electrical cable insulation, clothing, car interior trim (Uhde et al., 2001; Clausen et al., 2004; Bornehag et al., 2005; Xu et al., 2009), in which their concentration often ranges from percent to tens-of-percent by weight (Clausen et al., 2004; Xu and Little et al., 2006; Weschler and Nazaroff, 2008; Chen et al., 2009; Stapleton et al., 2009). Slow emissions of phthalates from source materials usually occurs due to the fact that they are not chemically bound to the polymer matrix; as a result, phthalates are among the most abundant SVOCs in indoor environments (Bernehag et al., 2005; Clausen et al., 2012; Rudel et al., 2009). Recent reviews on the health effects of phthalate esters suggest that exposure to phthalates may result in profound and irreversible changes in male reproductive system (Latini et al., 2006), increase prenatal mortality, and cause asthma, allergies and airway deceases in children (Bornehag et al., 2004; Kolarik et al., 2008; Larsson et al., 2009; Bornehag and Nanberg, 2010). Therefore, U.S. and E.U have restricted the use of several phthalates in children's articles because of the emerging concerns on the potential health effects of these compounds (Scott, 2005). As a result, the use of phthalates in PVC products are changing rapidly, with the trend of manufacturers substituting high molecular weight phthalates, for low molecular weight ones (ECPI 2009). More recently, some phthalate alternatives, such as

di(2-ethylhexyl) adipate (DEHA) and diisononyl cyclohexane-1,2-dicarboxylate (DINCH), have emerged but with very limited toxicology information. These compounds share similar chemical structure and properties with that of phthalate esters, comparable levels of emissions and concentrations may be expected in indoor environments (Schossler et al. 2011).

There is an urgent need to develop suitable approaches to reduce the concentrations of indoor phthalates and their alternatives. To achieve this, we must understand the characteristics of the fate and transport of these compounds in our environments. Models of SVOCs have been developed as useful tools to elucidate the behaviors of SVOCs in indoor environments. Bennett and Furtaw (2004) proposed a fugacity-based model to study pesticides concentrations in different media after applying indoors and successfully characterized the fate of pesticides in the home. Later on, Zhang et al. (2009) extended Bennett and Furtaw's model to a multimedia indoor model and described the fate and behavior of Polybrominated diphenyl ethers (PBDEs) in office rooms. Based on previous experiments (Clausen et al., 2004), Xu and Little (2006) developed a SVOC emission model showing that the emissions of SVOCs are subject to "external" control (partitioning from the material into the gas phase, convective mass transfer through the boundary layer, and strong sorption onto interior surfaces including particles and dust). Xu et al. (2009 and 2010) further extended this model to predict human exposures to DEHP emitted from vinyl flooring in a realistic residential environment using the data collected from CTEPP to establish surfaces/air DEHP partition isotherms for dust and other interior surfaces.

Particles have a great influence on the fate and transport of indoor phthalates. Because gas-particle sorption and desorption kinetics are sufficiently rapid (Benning et al. 2012; Odum et al. 1994; Weschler et al. 2008), airborne particles become important

carriers that accelerate the transport of phthalates from their original source to other indoor surfaces through deposition, resuspension, and advection of air. Liu et al. (2010) investigated the influence of aerosol particles on airborne DEHP concentration by applying a variable particle source to the indoor environment. Shi and Zhao (2012) included gas-particle sorption kinetics to predict indoor concentrations of polycyclic aromatic hydrocarbons (PAHs), and found that the model performed better than use of the typical assumption of linear instantaneous gas-particle partitioning. Liu et al. (2013) further showed that the size distribution of particles is critical to the timescale that is required for gas-particle partitioning to reach equilibrium. Recently, Liu et al. (2014) found that indoor concentrations of particle-associated SVOCs are affected by several factors including the gas/particle-partition coefficients of the SVOC, the residence time of the particles and the mass transfer coefficients around particles. Although these modeling studies (Liu et al. 2010, 2013 and 2014; Shi and Zhao, 2012) acknowledged the importance of gas-particle partitioning on the fate of indoor SVOCs, the actual role of particles in the transport of indoor SVOCs has not been fully characterized. Particle deposition and resuspension may result in a redistribution of SVOCs among the gas, particle, and surface phases near the source and sink surfaces, and thereby significantly influence the rate of SVOC emission from and sorption to those surfaces. Clausen et al. (2004) conducted small chamber studies and discovered that dust layer on a vinyl flooring sample increased the emission rate of DEHP by increasing the external concentration gradient above the surface. Similarly, a recent theoretical study (Liu et al. 2012) found that SVOC flux between air and indoor surfaces was significantly enhanced in the presence of particles. Currently no model exists for accurately characterizing the effect of particle dynamics on SVOC emission and sorption as well as the subsequent impacts on the fate and transport of indoor SVOCs. Furthermore, none of the fate and

transport model developed for SVOCs has been strictly validated, though most of them have compared their predicted airborne concentrations with field campaign data. In addition, phthalates (including both gas- and particle-phase phthalates) can accumulate in porous materials such as carpet and subsequently re-emitted into indoor environments. These materials can act as buffers for indoor phthalates, modulating and prolonging their presence in the environment (Zhang et al. 2009). Therefore, to accurately characterize the fate and transport of phthalates in indoor environments, it is necessary to include those porous materials.

The goal of this research is to provide a full mechanistic understanding of emission and transport for phthalates in indoor environments. Our specific objectives are to (1) develop a novel indoor fate and transport model for phthalates with consideration of particle dynamics and its effects on emission and sorption; (2) conduct field measurements in a test house to validate and refine the model; (3) investigate the influences of various environmental factors on the fate and transport of phthalates in indoor environments.

METHODS AND MATERIALS

Model Description. The indoor residential fate model of phthalate plasticizers is a dynamic mass-balance model. This model considers airborne phthalates with input from indoor sources, resuspended particles, and desorption from interior surfaces. Losses occur through air advection, particle deposition, dust removal, and phthalate transport to surfaces. As shown in Figure E.1, phthalates are emitted from vinyl flooring in a residential environment, the gas-phase phthalate is adsorbed onto interior surfaces, including walls, ceiling, wood floor, furniture, windows, tile, ceramic fixtures, and particles through partitioning mechanisms. Particle deposition and resuspension that may

further accelerate the mass transfer between sources and sinks are included in this model. In addition to adsorptive partitioning to interior surfaces, phthalates may also diffuse into porous materials (e.g. carpet) and sorb within the materials. Over time, such processes may establish important reservoirs and is thus included in the model.

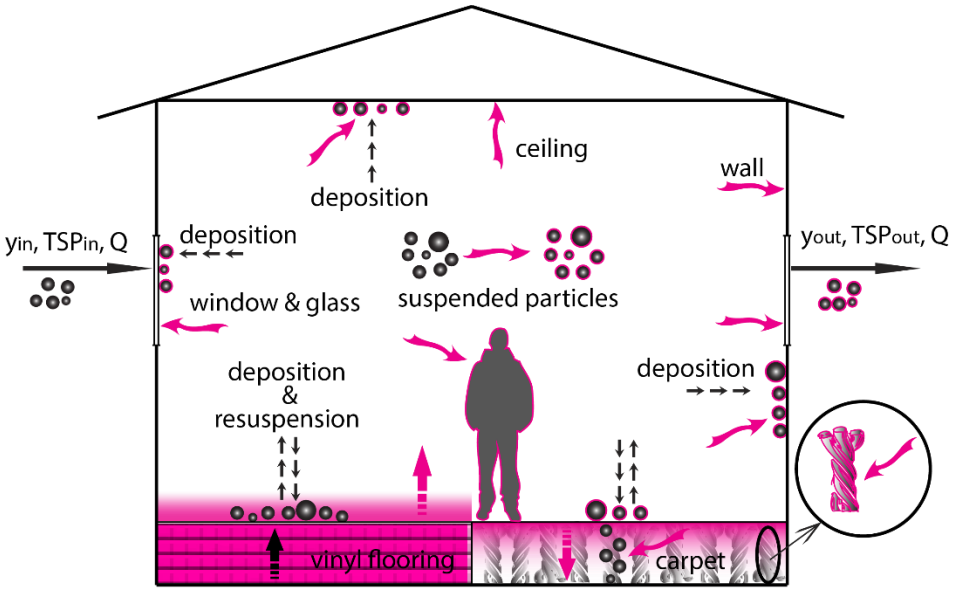

Figure E.1: Illustration of the residential environment.

The mass (particle and phthalates) in the room is defined by a set of differential equations accounting for all gain and loss processes including mass exchanges with outdoors. The source of total suspended particles (TSP) includes outdoor particles, indoor source and resuspension while the loss of TSP is caused by ventilation and deposition. The accumulation of TSP in the environment obeys the following mass balance equation:

$$V\frac{dTSP}{dt} = QP_pTSP_{in} - QTSP - v_dTSPA_s + RMA_s - v_dTSPA_0 + RM_0A_0 + S \quad (1)$$

where V (m^3) is the volume of the room, TSP ($\mu g/m^3$) is the TSP concentration in the room, TSP_{in} ($\mu g/m^3$) is the outdoor TSP concentration, P_p is the size-specific particle penetration factor, Q (m^3/h) is the ventilation rate of the room, v_d (m/h) is the size-dependent particle deposition velocity to interior surfaces, R (h^{-1}) is the particle resuspension rate for settled dust on the surface, M ($\mu g/m^2$) is the dust loading on interior surface (non-source surface), M_0 ($\mu g/m^2$) is the dust loading on vinyl flooring (source surface), A_s (m^2) is the surface area of interior surface (non-source surface), A_0 (m^2) is the surface area of vinyl flooring (source surface), and S ($\mu g/h$) is the generation rate of particles from sources in this room. Following Equation (1), the mass loading on interior surfaces and/or vinyl flooring is controlled by particle deposition and resuspension from the surface, as described by

$$\frac{dM}{dt} = v_d TSP - RM \tag{2}$$

where M (($\mu g/m^2$) can be the dust loading on either non-source surface or that on vinyl flooring.

The accumulation of phthalates in the environment obeys the following mass balance equation:

$$V\frac{dy}{dt} + V\frac{dF}{dt} = Q(y_{in} + F_{in}) - Q(y + F) - v_d F A_s - h_m A_s\left(y - y_{surf}\right) + RMP_{dust}A_s + h_{m0}(y_0 - y)A_0 + RM_0P_{dust,0}A_0 \tag{3}$$

where y ($\mu g/m^3$) is the gas-phase phthalate concentration in the room, F ($\mu g/m^3$) is the particle-phase phthalate concentration in the room, y_{in} ($\mu g/m^3$) is the outdoor gas-phase phthalate concentration, F_{in} ($\mu g/m^3$) is the outdoor particle-phase phthalate concentration, h_m (m/h) is the mass transfer coefficient through the boundary layer above the adsorptive surfaces, y_{surf} ($\mu g/m^2$) is the gas-phase phthalate concentration in the layer immediately adjacent to the adsorptive surfaces, P_{dust} ($\mu g/g$) is the mass fraction of phthalates in

settled dust on adsorptive surfaces, $P_{dust,0}$ (μg/g) is the phthalate mass fraction in settled dust on vinyl flooring, h_{m0} (m/h) is the mass transfer coefficient through the boundary layer above the source surface, y_0 (μg/m^3) is the gas-phase phthalate concentration in the layer immediately adjacent to the source material, and A_0 (m^2) is the emission surface area. In Equation 3, the sources of airborne DEHP include emission, ventilation and particle resuspension, while the loss is through particle deposition and partitioning to interior surfaces and settled dust.

Liu et al. (2013) found that for SVOCs with volatility between that of pyrene and DEHP, instantaneous equilibrium can be assumed for relatively small particles (with diameter less than 10 μm). The diameter of most indoor particles falls in the range of 0.01 to 10 μm. Therefore, in this model, an instantaneous equilibrium is adopted to describe the partition relationship between the gas-phase and particle-phase phthalate concentrations with a partition coefficient, K_p (Weschler et al. 2008):

$$F = K_p \cdot TSP \cdot y \tag{4}$$

Recent study (Liang and Xu, 2014a) on phthalate emissions from vinyl materials indicates that the gas-phase phthalate concentration in equilibrium with material-phase (y_0) is constant at a certain temperature. Without the presence of dust on the surface, the amount of phthalate emitted from source material will be equal to the gas-phase phthalate transferred through the boundary layer from the bulk air. However, particle deposition complicates the problem. Settled dust on vinyl material serves as a sink to which gas-phase phthalate may strongly absorb, resulting an increased emission rate from source material. Therefore the emission rate of phthalates from the source material can be expressed as

$$E = h_{m0}(y_0 - y) + v_d TSP\left(P_{dust,0} - K_p y\right) \tag{5}$$

where E (μg/m^2/h) is the emission rate of phthalate from source materials. In Equation (5), the difference of $P_{dust,0}$ and $K_p y$ (the second term on the right hand side) represents the amount of phthalate required to saturate the dust deposited on source material. In other words, when suspended particles with adsorbed phthalate on their surfaces deposited onto source material, they reached a new equilibrium with gas-phase phthalate concentration immediately above the material, y_0; and the difference of phthalate amount was compensated by emission from the source.

With reference to Figure E.2, for any impermeable surface (such as wood floor, furniture, ceiling, walls, glass and windows), a boundary layer is assumed to exist above the surface, and the partition process between the gas-phase and surface-phase phthalate concentrations can be described by

$$\frac{dC_{surf}}{dt} = h_m(y - y_{surf}) \tag{6}$$

where C_{surf} (μg/m^2) is the surface-phase phthalate concentration.

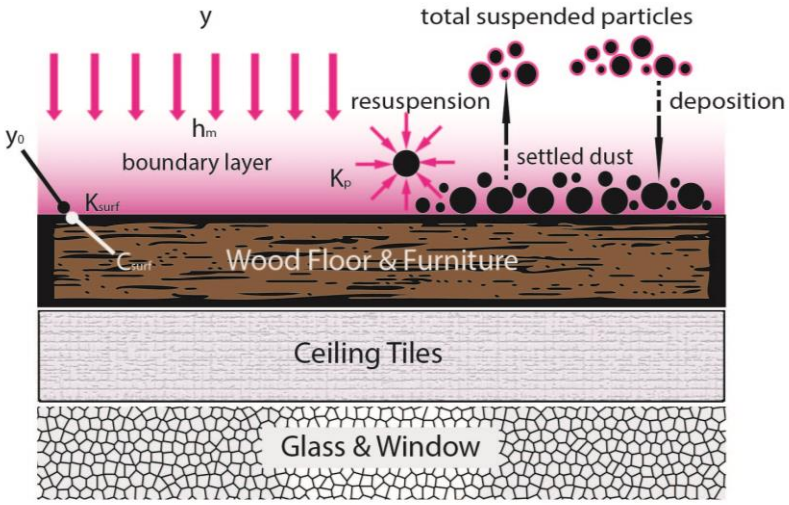

Figure E.2: Schematic of sorption process of phthalates onto impermeable interior surfaces.

The gas-phase phthalate concentration in the boundary layer above the adsorptive surface is also linearly related to the surface-phase concentration with an air/surface partition coefficient, K_s:

$$C_{surf} = K_s y_{surf} \quad (7)$$

Settled dust on adsorptive surfaces is possibly an important media of transporting indoor phthalates. In this model, one of our major focuses is to characterize the mass fraction of phthalates on settled dust on interior surfaces. In Equation (2), we referred the phthalate concentration on settled dust to as the mass fraction, P_{dust} (μg/g). The deposition of TSP with adsorbed phthalates is the source of phthalate mass fraction and particle resuspension from the adsorptive surfaces is the loss. Therefore, we present the accumulation of phthalate mass fraction on settled dust on adsorptive surfaces as following:

$$M \frac{dP_{dust}}{dt} = v_d F - RMP_{dust} \quad (8)$$

We extend our thoughts of phthalate mass fraction to settled dust on source surface (i.e. vinyl flooring). The difference between source surface and adsorptive surface is that y_0 above the source surface is assumed to be constant for phthalates at all times. Therefore phthalate mass fraction on settled dust on source surface can be simply expressed as

$$P_{dust,0} = K_p y_0 \quad (9)$$

With millions of fibers per square meter woven tightly into a textile backing, carpet may, therefore, serve as a significant reservoir for both phthalates and settled dust. As shown in Figure E.3, phthalates are transferred from indoor air into carpet in gas and physically adsorbed phases. The approach used in this model is consistent with previously developed models for sorption of Volatile Organic Compounds (VOCs) to

porous building materials (Haghighat et al. 2005; Xiong et al. 2008; Deng et al. 2009). The governing equation describing transient diffusion through carpet pores and sorption onto carpet fibers and settled dust is

$$\left[\varepsilon + (1-\varepsilon)K_{ca} + K_p \frac{M_{ca}}{L}\right]\frac{\partial C_g}{\partial t} = [(\varepsilon D_a + (1-\varepsilon)D_s K_{ca})]\frac{\partial^2 C_g}{\partial x^2} \quad (10)$$

where ε is the porosity of carpet, K_{ca} is the gas/fiber partition coefficient of phthalate, M_{ca} (μg/m^2) is the dust loading on carpet, L (m) is the thickness of the carpet, C_g (μg/m^3) is the gas-phase phthalate concentration in the carpet as a function of time and depth of the carpet, D_s (m^2/h) is the phthalate diffusion coefficient in carpet fibers, and D_a (m^2/h) is the phthalate diffusion coefficient in air. Considering that diffusion coefficient in solid is five orders of magnitude less than in air and thus insignificant, we use $D_s \sim 1\times 10^{-10}$ m^2/h as a representative value, based on C_{12}-C_{15} alkanes in vinyl flooring (Cox et al., 2001). We assume that the dust distributes homogeneously in carpet and therefore M_{ca}/L (μg/m^3) yields the average dust concentration in carpet.

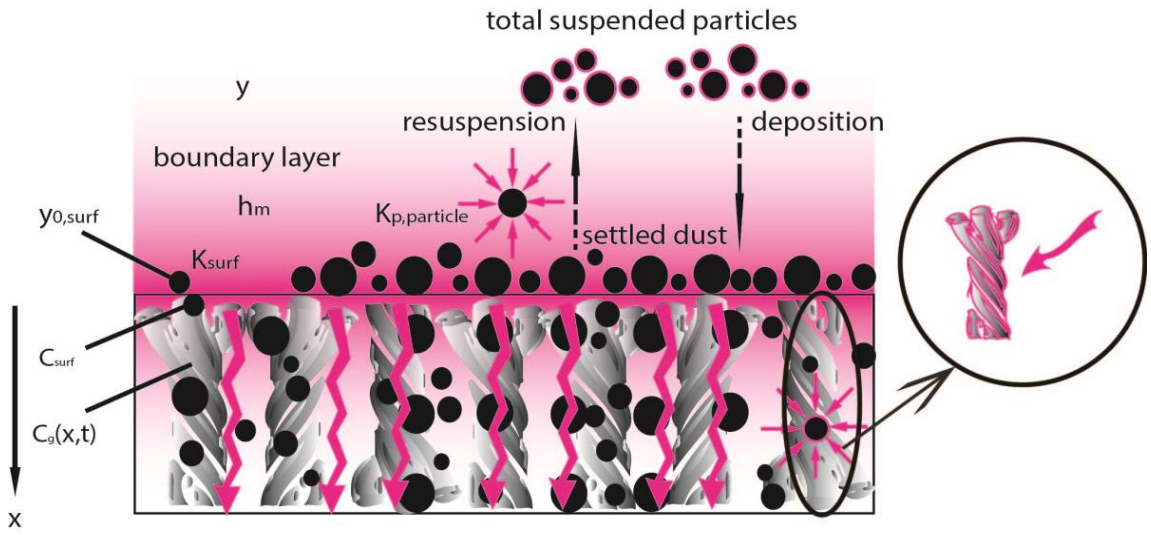

Figure E.3: Schematic of sorption process of phthalates in carpet.

Model Verification. We applied this model to a case study that was conducted in a test house at the University of Texas at Austin (UTest House) in Austin, TX. The UTest House consists of three bedrooms, two bath room, a kitchen and a living room. The house was preinstalled with vinyl flooring which contains approximately 10% of BBP by weight (determined in the laboratory). The field measurements were conducted in the living room with environmental parameters (temperature, relative humidity, and total suspended particles) monitored in real time. Air concentrations of BBP were measured periodically. On a monthly basis, dust (i.e. molding and floor dust) and surface wipe samples (i.e. window, wood cabinet door, and cloth) were also collected from selected locations.

Polyurethane foam (PUF) cartridge (22 × 100 mm size, 1-section, 76 mm sorbent) connected with low volume pumps (A.P. BUCK Inc.) was used for air sampling in the UTest House. Each PUF was housed with a glass fiber filter (SKC Inc.) and stored in a temperature controlled fridge prior to use. The sampling time was set as 48 hours with a sampling flow rate of 3 L/min calibrated by a bubble flow calibrator (A.P. BUCK Inc.). Dust samples were collected with a vacuum cleaner (Eureka) into a 26 – 60 mm cellulose extraction thimble (Whatman Inc.). The mass of each dust sample was set as 0.2 g with 10 – 15 min vacuum cleaning. Surface samples were collected by wiping designated surface area (30 × 30 cm) with gauze pads (Fisher Scientific). Each marked surface area was wiped three times with three pre-cleaned gauze pads. These gauze pads were then transferred and stored in a beaker inside a glass jar with PTFE lid for future analysis.

The samples collected by PUF, dust and gauze pads were ultrasonically extracted with hexane as the solvent. The extracts were condensed through rotary evaporation and nitrogen blow to a final solution of approximately 100 μl (1 ml for dust samples). The volume of the solution was calculated through its weight and the density of hexane (0.672

g/ml in this study). Condensed solutions with collected chemicals were analyzed on a GC (Agilent 7890A) – FID system with a DB-5HT column. The GC oven temperature was programed from 120°C for 2 min, ramp 12°C/min for 15 min, hold 3 min, then ramp 20°C/min for min, hold 2 min.

Model parameters that approximate the UTest House configuration (including room geometry and interior surface areas) were measured or estimated. We set the target phthalate of the model as BBP, with the input value of y_0 as 2.71 $\mu g/m^3$. This value was determined experimentally in a stainless steel small-chamber, with reference to a previous chamber study (Liang and Xu, 2014a). The temperature and air change rate in the house were monitored during the measurements, and the measured data were directly used as input values. We were unable to measure the air velocity above interior surfaces of UTest House during the experiment because the velocities were very low and beyond the detection limit of our apparatus. Huang et al. (2004) measured the air velocity in a typical house in the U.S. with a range of 0.01 – 0.16 m/s. Considering that UTest House remained unoccupied and the fans were turned on at a very low frequency during the measurements, we used the minimum value of 0.01 m/s above interior surfaces to calculated mass transfer coefficients with correlation equations (Axley, 1991). We obtained input values of sorption isotherms for BBP on different surfaces from experimental data. In the model, we considered suspended particles with three size fractions: $PM_{2.5}$, $PM_{2.5\text{-}10}$ and $PM_{10\text{-}30}$, and the concentrations were measured in UTest House as of 3.06, 0.7, and 0 $\mu g/m^3$, respectively. Size-dependent particle deposition velocities and resuspension rates were obtained from the literature. The air/particle partition coefficient used in the model was estimated based on octanol/air partition coefficient (Cousins and Mackay, 2000; Weschler et al., 2008). A list of all input parameters of the UTest House simulation can be found in the Supporting Information.

We compared modeled and measured BBP concentrations in the air, dust and interior surfaces.

Uncertainty Analysis. Using the case for UTest House, we conducted a sensitivity analysis to identify the critical parameters for the fate and transport of BBP in the test house, and then further estimated the uncertainties associated with the model's prediction. We found that parameters affecting source strength including the gas-phase concentration immediately adjacent to the vinyl flooring, y_0, the area of the flooring, and the mass transfer coefficient across source surface (h_m) are important for the emissions of BBP as well as its concentrations in all environmental media. Partition coefficient between the gas and particle phase (K_p) is also very important. The total airborne concentration of BBP, the extent to which the emission can be enhanced when particles deposited on the flooring, the sorption rate of BBP gas to different interior surfaces, and the overall concentration of BBP on those surfaces are all strongly determined by the value of K_p. In addition, parameters that influence TSP level and/or dust loading on interior surfaces, such as particle deposition velocity and resuspension rate and air change rate of the house, also have meaningful impacts. Finally, we conducted Monte Carlo analysis, the method that we have successfully applied previously (Xu et al., 2010), to account for uncertainty associated with these critical model parameters. Because the parameters affecting source strength (i.e., y_0, A, h_m) were either measured strictly in the laboratory or calculated based on measurements, they were not included in the uncertainty analysis. As shown in Table E.1, we developed ranges in the selected model parameters from data presented in other studies or obtained directly from the literature. We used simple uniform distributions because of the relative paucity of data, even though this may overestimate uncertainty.

Variable		Minimum	Maximum
Particle/air partition coefficient (K_p, $m^3/\mu g$)[a]		7.15×10^{-4}	2.10×10^{-3}
	$PM_{2.5}$	2.31×10^{-2}	1.20×10^{0}
Particle deposition velocity (v_d, m/h)[b]	$PM_{2.5-10}$	9.77×10^{-1}	1.55×10^{1}
	PM_{10-30}	4.28×10^{1}	4.28×10^{1}
	$PM_{2.5}$	0	18
Particle resuspension rate ($R \times 10^6$, 1/h)[c]	$PM_{2.5-10}$	0	83
	PM_{10-30}	0	340
Air change rate (1/h)[d]		0.404	0.718

a. Calculated using Equation (6) based on measurements in Cousins and Mackay (2000).
b. Lai, 2002.
c. Thatcher, 1995.
d. Obtained from experimental data.

Table E.1: Parameter ranges used in uncertainty analysis.

Three-compartment Model. Using DEHP in vinyl flooring as an illustrative example, we extended the one room model to predict DEHP emissions after installation of vinyl flooring in a more realistic family residence and investigate the impacts of environmental conditions on the transport of indoor DEHP. As shown in Figure E.4, DEHP is emitted from vinyl flooring to the air in a typical residence that we divided into three compartments: kitchen, bathroom and main house. Modeling on emission, sorption, and particle dynamics are similar as the one room model. We obtained the infiltration/exfiltration rates and ventilation rates between rooms from measurements conducted by Wilkes et al. (1992) in a five-room house. We estimated the interior surface area of furnishing and materials using typical surface/volume ratios for American houses established by Hodgson et al. (2005). The model input values of outdoor TSP level are listed in Table E.2, where we considered typical urban region in the U.S. and the city of Beijing in China as two sites, with the former as the base case. The air velocity across interior surfaces was set to 0.15 m/s (Xu et al., 2009), which was used to estimate the mass transfer coefficients through the boundary layer adjacent to surfaces based on

correlation equations (Axley, 1991). Gas-particle partition coefficient (K_p) for DEHP was estimated from its K_{OA} value using the methods discussed in previous studies (Cousins and Mackay, 2000; Weschler et al., 2008). Sorption isotherms for gas-phase DEHP on various indoor surfaces were obtained from estimations in previous studies (Xu et al., 2009). Detailed information on the mass balance equations and input parameters are available in Supporting Information.

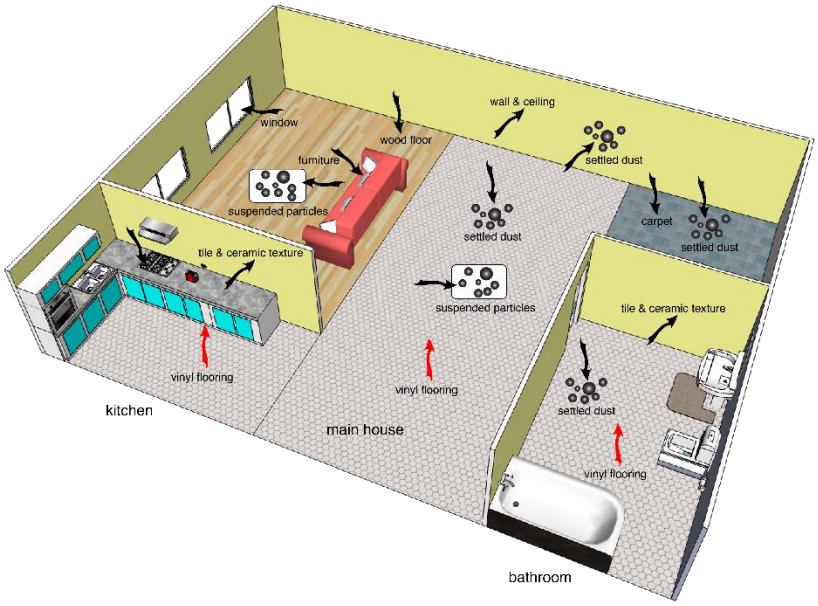

Figure E.4: Illustration of the three-compartment residential environment.

size fraction	Penetration factor [a]	v_d [b]	R × 10^6 [c]	outdoor mass concentration	
µm		m h^{-1}	1 h^{-1}	µg/m^3	
				Urban U.S. [d]	Beijing, China [e]
0-2.5	0.85	0.11	12.21	43	86.5
2.5-10	0.3	4.9	71.65	17	63.5
10-30	0	42.8	380	~	40.1

e. Obtained from Long et al. 2001.
f. Obtained from Lai, 2002.
g. Obtained from Thatcher, 1995.
h. Obtained from Riley et al. 2002.
i. Obtained from Hao and Wang, 2005.

Table E.2: Parameters of particle dynamics of the three-compartment residential model.

RESULTS AND DISCUSSION

Model Validation and Uncertainty Analysis. The model was used to estimate BBP emission and transport after vinyl flooring was installed in a residence. The total airborne concentration of BBP reached steady state fast compared to a previous model study of DEHP (Xu et al. 2010). The steep initial rise occurred because the rate at which it is emitted from the vinyl flooring is initially faster than the rate at which it is taken up by the interior surface sinks. The major BBP source identified in the UTesthouse is the vinyl flooring, which has been in installed in the house for over 5 years. Therefore, we assumed that the concentrations of BBP in air and dust phases have reached steady state. The measured data were used to perform initial validation of the fate and transport model of phthalates. As shown in Figure E.5, there are good agreement between model predictions and field measurements. Using the model, we further found that there is no significant difference between the gas and total airborne concentrations of BBP. Because the relatively small gas-particle partition coefficient of BBP, only a small fraction of the airborne mass is bound to particle phase, with the majority present in the gas-phase. The very low TSP concentration (<4 $\mu g/m^3$) in the UTest house strengthened the effect. We also compared the concentration of BBP in floor dust (dust accumulated on vinyl flooring) and non-floor dust (dust accumulated on non-source surfaces). Both model simulation and field measurements showed that the mass of BBP in floor dust (2823 to 3518 μg/g) is approximately 20 times higher than in non-floor dust (140 to 203 μg/g). This significant difference indicated that settled dust on source materials may absorb a great amount of phthalates from the gas layer immediately adjacent to the source. The agreement between predicted dust concentration of BBP and measured data further validated the critical part of the model on simulating phthalate redistribution between gas, particle, and surface phases close to interior source and sink surfaces.

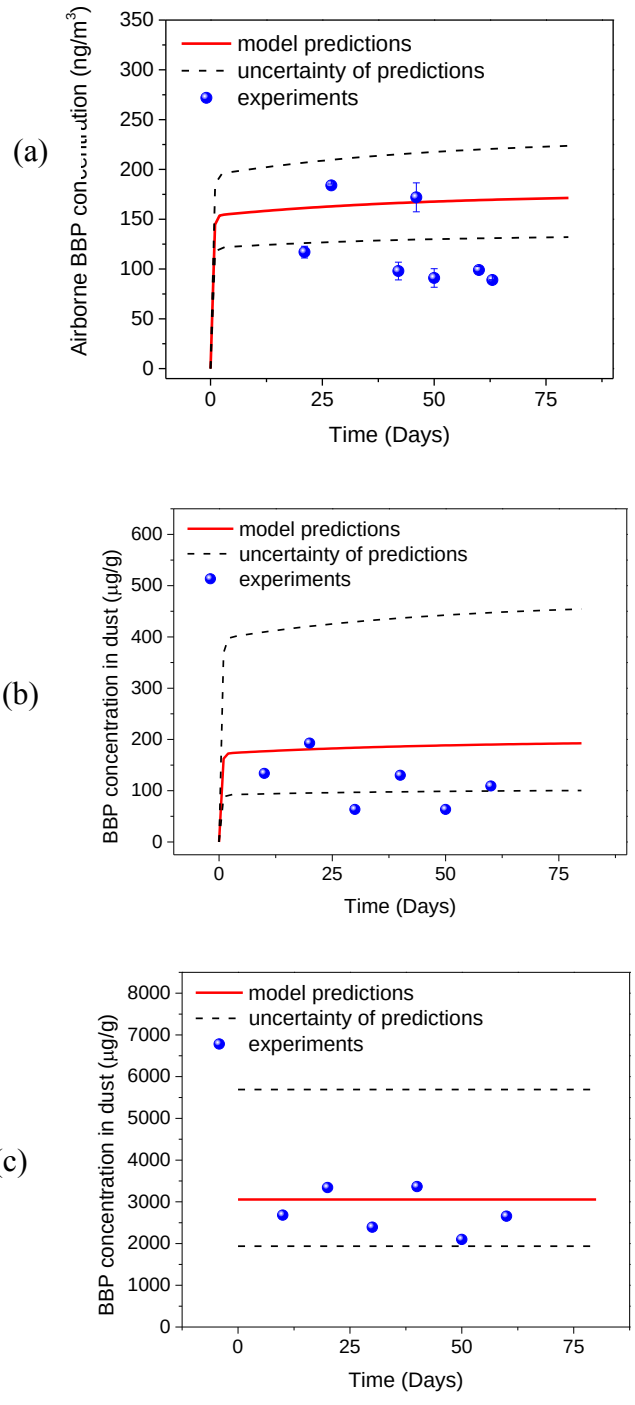

Figure E.5: a) Comparison of airborne BBP concentration between model results and experimental data; b) comparison of BBP mass fraction on floor and non-floor dust between model results and experimental data.

Three-compartment Residential Model. The gas-phase and total airborne concentrations of DEHP in each compartment were estimated, as shown in Figure E.6a. The three compartments reached steady state within about two years. Compared with the other two compartments, the main house had the lowest gas-phase concentration because of the larger ratio of sorption surface area to emission surface area. The predicted steady-state total airborne concentration of DEHP in the main house was consistent with measured data in recent field campaigns in the United States and Europe. The gas-phase concentration of DEHP in each compartment was about two times lower than that in the particle phase, due to the large partition coefficient between gas and particle phases (K_p). In addition to the gas-phase concentration, Figure E.6b shows that DEHP mass fraction in floor dust (dust on source surface) is over an order of magnitude higher compared to that in non-floor dust. The results suggested that particles deposited on source and sink surfaces should be separated when conducting field campaigns to measure SVOC concentrations in dust samples. Although the predicted steady-state DEHP concentration in non-floor dust agreed well with measured data in the literature, caution should be taken when interpreting this comparison, because the value of K_p may significantly influence the predicted result.

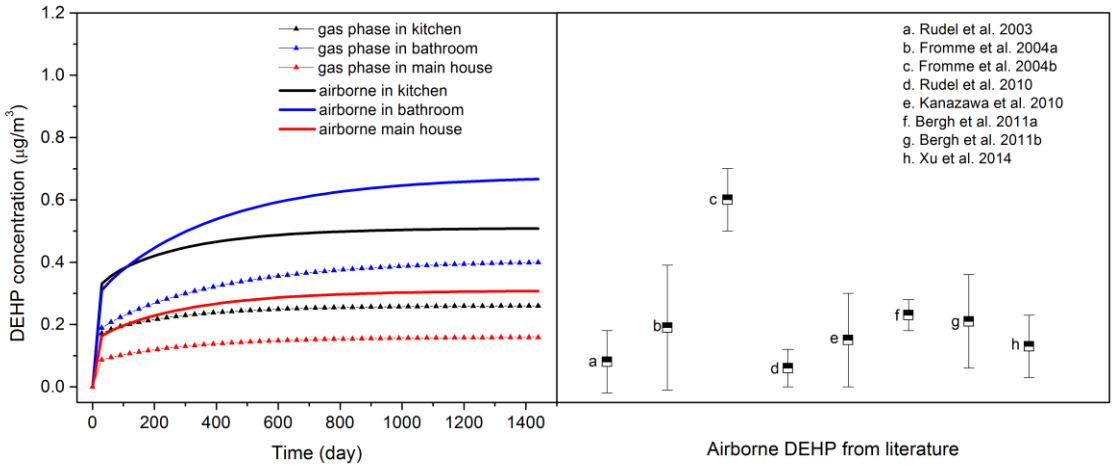

(a)

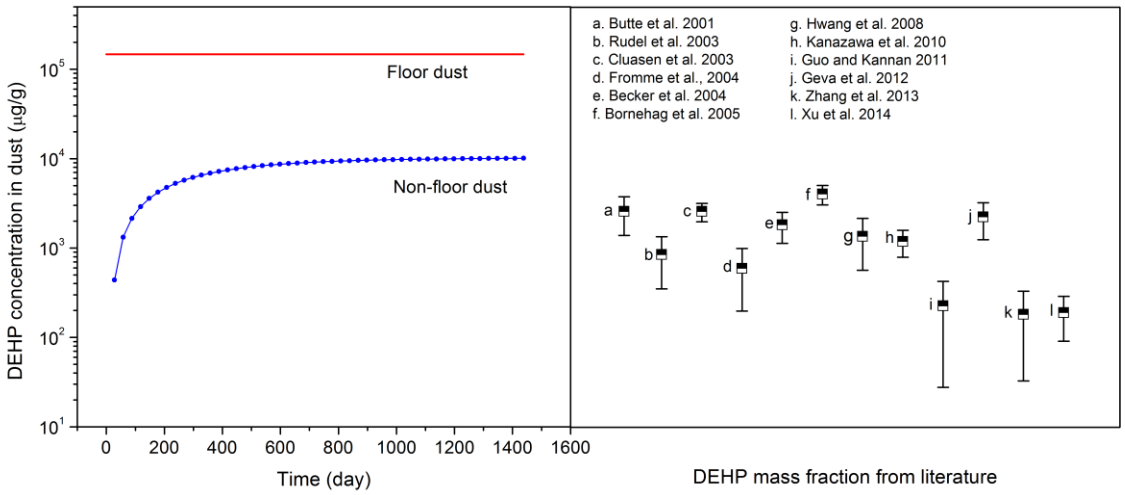

(b)

Figure E.6: (a) Gas-phase and airborne DEHP in different compartments with comparison to values reported in the literature; (b) DEHP mass fraction on non-floor dust and floor dust with comparison to values reported in the literature.

We further examined the surface-phase concentrations of DEHP on wood floor and carpet in the main house (see details in the SI). The surface concentration was calculated as the sum of two parts: the amount of gas-phase DEHP adsorbed onto the

surface and that of particle bound DEHP deposited on the surface. For both wood floor and carpet, the former level is higher than the latter, indicating the important contribution of particles to the DEHP surface concentration. In addition, we found that the impact of particle to DEHP surface concentration was reduced for vertical surfaces such as walls, due to the small particle deposition velocity. Carpet was found to be a unique significant sink surface for SVOCs. Because of its fiber structure and porous property, carpet had enormous effective surface area for gas-phase DEHP to adsorb on. Particles also deposited deeply into the material, which greatly increased the dust-bounded DEHP concentration in carpet. Using this new model, we are able to dynamically predict phthalate concentrations in different environmental media including gas, suspended particle, deposited dust, as well as a wide range of interior surfaces such as wood floor, carpet, furniture, walls and ceiling. The knowledge will further help us to understand and assess human exposures to phthalates via inhalation, dermal absorption and dust ingestion.

The Influences of Environmental Conditions on the Fate of Indoor Phthalates. We investigated the influence of outdoor TSP level on indoor phthalate concentrations by comparing the case of Beijing, China to the base case of typical urban area in the U.S. As listed in Table E.2, the outdoor particle concentration in Beijing, China is considerably higher than that in typical urban areas in the U.S., which resulted in a higher indoor TSP level in Beijing. As shown in Figure E.7a, the predicted airborne DEHP concentration was higher while the gas-phase DEHP concentration was lower in Beijing. We should also note that the difference between airborne and gas-phase DEHP is more prominent in Beijing than that in urban areas in the U.S. With more suspended particles in the environment, more gas-phase DEHP was emitted from the source and then adsorbed to particle phase. Therefore, a lower gas-phase concentration and a higher

particle-phase concentration were resulted. Overall, the total airborne DEHP concentration increased with the increase of indoor TSP level. In addition, a high indoor TSP level also means a high dust loading on interior surfaces, and those settled dust on the source surface can resuspend back into the air, increasing the total airborne DEHP concentration.

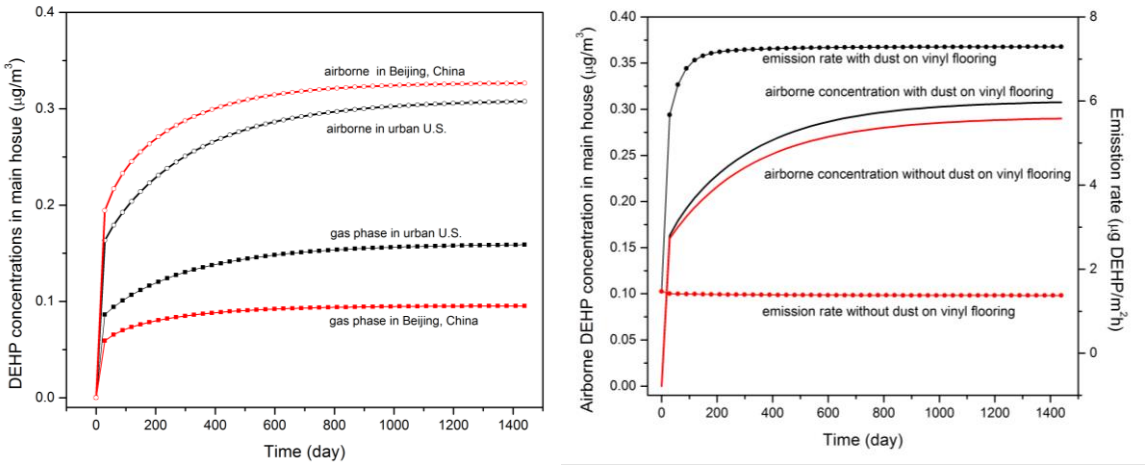

(a) (b)

Figure E.7: (a) Influence of outdoor TSP level on DEHP concentrations; (b) Influence of settled dust on DEHP emission rate from vinyl flooring.

We investigated the influence of settled dust on DEHP emissions. We calculated the emission rate and total airborne concentration of DEHP under two scenarios: 1) there is settled dust on vinyl flooring, and 2) no dust present on vinyl flooring. As shown in Figure E.7b, although the airborne DEHP concentrations in the two scenarios are close to each other, DEHP emission rate from vinyl flooring with settled dust is about four times higher than that without dust presence on the surface. Equation (5) shows that DEHP emission rate is determined by both the gas-phase mass transfer and sorption onto settled dust, the latter is proved to account more for the emissions from the source material. The

slight increase of airborne DEHP concentration is possibly due to particle resuspension from vinyl flooring as an important source. If we look into the increase of emission rate caused by settled dust, we can conclude that approximately 80% of emitted DEHP from the source was captured by settled dust, though this increase may be change when the dust loading on the source surface varies. Previous fundamental study (Liu et al. 2012) on the influence of aerosols on enhancing SVOC flux between air and indoor surfaces showed that DEHP emission rate can be significantly increased with particle mediation, which agreed well with our model results.

Figure E.8 shows the influence of ventilation rate on DEHP emissions. Increasing ventilation rate generally reduces the airborne DEHP concentration in the environment. However, this dilution effect can be compensated in three ways: 1) air velocity across source materials is increased with the increasing of ventilation rate, resulting a higher mass-transfer coefficient; 2) more outdoor TSP is introduced indoors, which sorbs more DEHP and increases the airborne concentration; and 3) increased level of dust loading on source surface enhances its emission rate. The compensation effect of particle mediation is subject to increase when outdoor TSP level is higher and/or gas/particle partition coefficient is higher. Note that the model predictions underestimate the increase of DEHP emission rates in both cases because we did not consider the change of mass transfer coefficient caused by the increase of ventilation rate. Although the difference of airborne DEHP concentration between 0.5/h and 0.2/h in the U.S. case is very similar as that in the Beijing case (about 0.2 $\mu g/m^3$), the emission difference in Beijing almost quadruple that in U.S. In Equation (5), the emission rate is the sum of mass flux induced by gas-phase concentration difference and the sorption to settled dust. Figure E.7a showed that gas-phase DEHP concentration in Beijing is lower than that in urban U.S. due to the increased suspended particle concentration, as a result, the DEHP

concentration gradient is larger in the Beijing case. Moreover, a higher dust loading level on source surface results in a higher emission rate by sorbing more DEHP from the source. Together these two effects increase DEHP emission rate when ventilation rate increases.

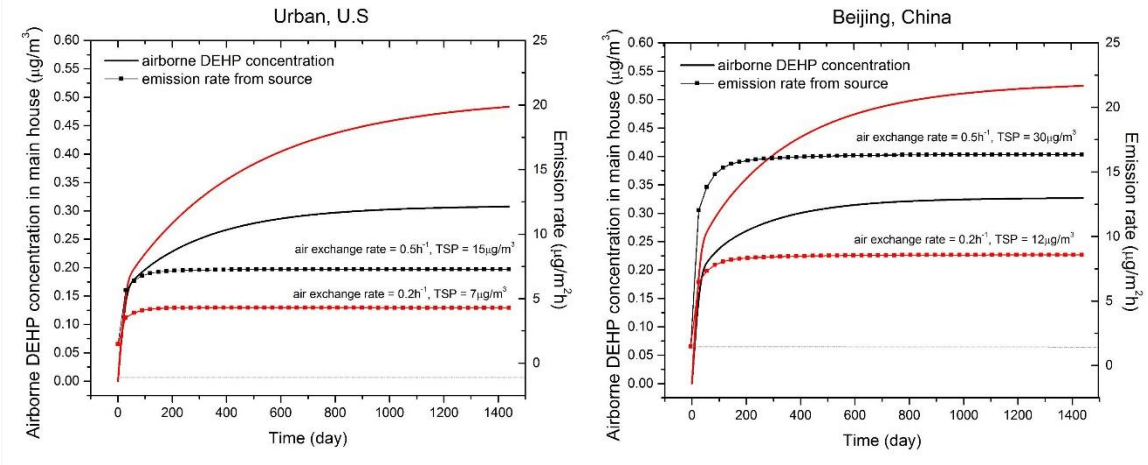

Figure E.8: Influence of air change rate on DEHP emission rate.

Finally, we examined the significance of carpet as in important adsorptive interior surface. In the model simulation, we removed the only source (vinyl flooring) from the main house after a period of time (2 years) and studied the change of concentrations in air and carpet thereafter. Figure E.9 shows a steep drop on airborne DEHP concentration after the vinyl flooring was removed from the residential home. However, the dramatic drop did not last thereafter and the total airborne concentration of DEHP started to decrease very slowly and was present at the levels above zero for years. We believed that the carpet including settled dust inside, which originally behaved as an indoor sink surface, became secondary source of DEHP after removal of the vinyl flooring. Furthermore, monthly cleaning activity was found to significantly reduce DEHP concentration of carpet, while its effect on the total airborne concentration is minor. In

addition, we investigated the influences of indoor activities such as cooking and cleaning on DEHP concentrations. Indoor TSP concentration increases steeply with a cooking event occurring in the kitchen, which resulted in a sudden increase of total airborne DEHP concentration and a reduction of gas-phase concentration. Change of the cleaning efficiency on different indoor surfaces will have a significant effect on the surface concentration of DEHP. With the increase of cleaning frequency or efficiency, the concentrations of DEHP in air and surfaces decreased greatly as shown in the SI.

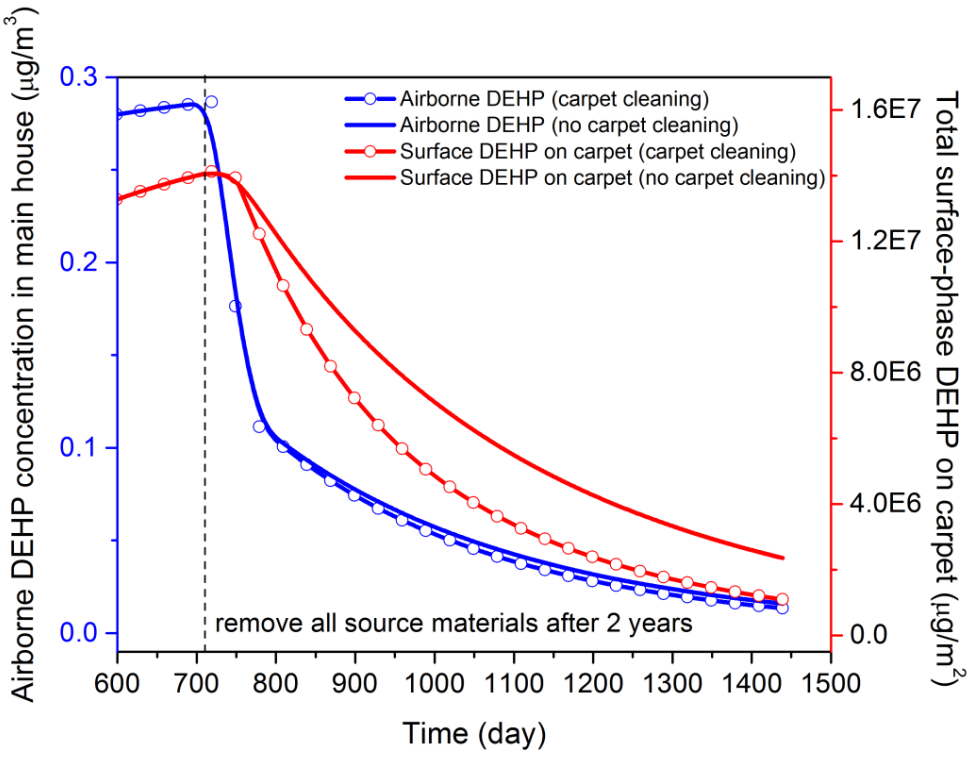

Figure E.9: Carpet as a secondary source after removing the original source material.

Collectively from these model predictions and comparisons, we can find the prominent importance of particle and/or dust as the indoor media of transporting

phthalates. To better understand the fate and transport of indoor SVOCs, we should focus on particle dynamics and their interactions with target compounds. A challenge is to better understand the partition effects and interactions between gas-phase, surface-phase, and dust-phase SVOC concentrations on interior surfaces. The case study results are on the same order of magnitude as measured results and field measurements results in the literature. The results can be improved if more accurate air/surface partition coefficient values can be estimated or experimentally determined. This model can be used for assessing exposures to indoor phthalates and other SVOCs if the input parameters can be determined.

ACKNOWLEDGMENTS

Financial support was provided by the National Science Foundation (NSF) (CBET-1150713 and CBET- 1066642).

SUPPORTING INFORMATION

Description of the Three-compartment Model

Particle and dust loading. Mass balance of the accumulation of TSP in kitchen:

$$V_k \frac{dTSP_k}{dt} = Q_{ok}P_pTSP_{in} - Q_{ko}TSP_k + Q_{ak}TSP_a - Q_{ka}TSP_k - \sum_i \left(v_d TSP_k A_{k_i} - RM_{k_i}A_{k_i}\right) + S_k(1)$$

Dust loading on i[th] surface in kitchen:

$$\frac{dM_{k_i}}{dt} = v_d TSP_k - RM_{k_i} \quad (2)$$

Mass balance of the accumulation of TSP in bathroom:

$$V_b \frac{dTSP_b}{dt} = Q_{ob}P_pTSP_{in} - Q_{kb}TSP_k + Q_{ab}TSP_a - Q_{ba}TSP_b - \sum_i \left(v_d TSP_b A_{b_i} - RM_{b_i}A_{b_i}\right) + S_b \quad (3)$$

Dust loading on i[th] surface in bathroom:

$$\frac{dM_{b_i}}{dt} = v_d TSP_b - RM_{b_i} \quad (4)$$

Mass balance of the accumulation of TSP in the main house:

$$V_a \frac{dTSP_a}{dt} = Q_{oa}P_pTSP_{in} - Q_{ao}TSP_a + Q_{ka}TSP_k - Q_{ka}TSP_a + Q_{ba}TSP_b - Q_{ab}TSP_a - \sum_i \left(v_d TSP_a A_{a_i} - RM_{a_i}A_{a_i}\right) + S_a \quad (5)$$

Dust loading on ith surface in the main house

$$\frac{dM_{a_i}}{dt} = v_d TSP_a - RM_{a_i} \quad (6)$$

Nomenclature

V_k	Volume of the kitchen (m^3)
V_b	Volume of the bathroom (m^3)
V_a	volume of the main house (m^3)
Q_{ok}	ventilation rate from outdoor to kitchen (m^3/h)
Q_{ko}	ventilation rate from kitchen to outdoor (m^3/h)
Q_{ka}	ventilation rate from kitchen to main house (m^3/h)
Q_{ak}	ventilation rate from main house to kitchen (m^3/h)
Q_{ob}	ventilation rate from outdoor to bathroom (m^3/h)
Q_{bo}	ventilation rate from bathroom to outdoor (m^3/h)
Q_{ab}	ventilation rate from main house to bathroom (m^3/h)
Q_{ba}	ventilation rate from bathroom to main house (m^3/h)
Q_{oa}	ventilation rate from outdoor to main house (m^3/h)
Q_{ao}	ventilation rate from main house to outdoor (m^3/h)
TSP_k	TSP concentration in kitchen ($\mu g/m^3$)
TSP_b	TSP concentration in bathroom
TSP_a	TSP concentration in main house
y_k	Gas-phase phthalate concentration in kitchen ($\mu g/m^3$)
y_b	Gas-phase phthalate concentration in bathroom ($\mu g/m^3$)
y_a	Gas-phase phthalate concentration in main house ($\mu g/m^3$)
F_k	Particle-phase phthalate concentration in kitchen ($\mu g/m^3$)
F_b	Particle-phase phthalate concentration in bathroom ($\mu g/m^3$)
F_a	Pas-phase phthalate concentration in main house ($\mu g/m^3$)
P_p	The penetration coefficient of particles
y_0	Gas-phase phthalate concentration above source ($\mu g/m^3$)
A_{ki}	Surface area of i^{th} surface in kitchen (m^2)
A_{bi}	Surface area of i^{th} surface in bathroom (m^2)
A_{ai}	Surface area of i^{th} surface in main house (m^2)
K_{ki}	Air/surface partition coefficient on i^{th} surface in kitchen (m)
K_{bi}	Air/surface partition coefficient on i^{th} surface in bathroom (m)
K_{ai}	Air/surface partition coefficient on i^{th} surface in main house (m)
K_p	The gas/particle partition coefficient ($m^3/\mu g$)
A_{k0}	Surface area of VF in kitchen (m^2)
A_{b0}	Surface area of VF in bathroom (m^2)
A_{a0}	Surface area of VF in main hosue (m^2)
TSP_{in}	Outdoor TSP concentration ($\mu g/m^3$)
S_k	Particle source generation rate in kitchen ($\mu g/h$)
S_b	Particle source generation rate in bathroom ($\mu g/h$)
S_a	Particle source generation rate in main house ($\mu g/h$)
V_d	Particle deposition velocity (m/h)
R	Particle resuspension rate (1/h)
M_{ki}	Dust loading on i^{th} surface in kitchen ($\mu g/m^2$)
M_{bi}	Dust loading on i^{th} surface in bathroom ($\mu g/m^2$)
M_{ai}	Dust loading on i^{th} surface in main house ($\mu g/m^2$)
h_m	Mass transfer coefficient on adsorptive surface (m/h)
h_{m0}	Mass transfer coefficient on source surface (m/h)
$y_{surf,ki}$	Gas-phase phthalate concentration on i^{th} surface in kitchen ($\mu g/m^3$)
$y_{surf,bi}$	Gas-phase phthalate concentration on i^{th} surface in bathroom ($\mu g/m^3$)
$y_{surf,ai}$	Gas-phase phthalate concentration on i^{th} surface in main hosue ($\mu g/m^3$)
$C_{surf,ki}$	Surface-phase phthalate concentration on i^{th} surface in kitchen ($\mu g/m^2$)
$C_{surf,bi}$	Surface-phase phthalate concentration on i^{th} surface in bathroom ($\mu g/m^2$)
$C_{surf,ai}$	Surface-phase phthalate concentration on i^{th} surface in main house ($\mu g/m^2$)
$P_{dust,k0}$	Phthalate mass fraction in dust on VF in kitchen ($\mu g/g$)
$P_{dust,b0}$	Phthalate mass fraction in dust on VF in bathroom ($\mu g/g$)
$P_{dust,a0}$	Phthalate mass fraction in dust on VF in main house ($\mu g/g$)
$P_{dust,ki}$	Phthalate mass fraction in dust on on i^{th} surface in kitchen ($\mu g/g$)
$P_{dust,bi}$	Phthalate mass fraction in dust on on i^{th} surface in bathroom ($\mu g/g$)
$P_{dust,ai}$	Phthalate mass fraction in dust on on i^{th} surface in main house ($\mu g/g$)

Phthalate concentrations. The accumulation of phthalate concentrations in kitchen:

$$V_k \frac{dy_k}{dt} + V_k \frac{dF_k}{dt} = Q_{ok}(y_{in} + F_{in}) - Q_{ko}(y_k + F_k) - \sum_i \left(v_d F_k A_{k_i} + h_m A_{k_i}(y_k - y_{surf,ki}) - RM_{k_i} P_{dust,ki} A_{k_i}\right) \quad (7)$$

Partition relationship between the gas-phase and particle-phase phthalate concentrations in kitchen:

$$F_k = K_p \cdot TSP_k \cdot y_k \quad (8)$$

Emission rate of phthalate from vinyl flooring in kitchen:

$$E_k = h_{m0}(y_0 - y_k) + v_d TSP_k \left(P_{dust,k0} - K_p y_k\right) \quad (9)$$

Partition process between the gas-phase and surface-phase phthalate concentrations on ith surface in kitchen:

$$\frac{dC_{surf,ki}}{dt} = h_m\left(y_k - y_{surf,ki}\right) \quad (10)$$

$$C_{surf,ki} = K_{ki} y_{surf,ki} \quad (11)$$

Accumulation of phthalate mass fraction on settled dust on adsorptive surfaces on ith surface in kitchen:

$$M_k \frac{dP_{dust,ki}}{dt} = v_d F_k - RM_k P_{dust,ki} \quad (12)$$

Phthalate mass fraction on settled dust on vinyl flooring in kitchen:

$$P_{dust,k0} = K_p y_0 \quad (13)$$

The accumulation of phthalate concentrations in bathroom:

$$V_b \frac{dy_b}{dt} + V_b \frac{dF_b}{dt} = Q_{ob}(y_{in} + F_{in}) - Q_{bo}(y_k + F_k) - \sum_i \left(v_d F_b A_{b_i} + h_m A_{b_i}(y_b - y_{surf,bi}) - RM_{b_i} P_{dust,bi} A_{b_i}\right) \quad (14)$$

Partition relationship between the gas-phase and particle-phase phthalate concentrations in bathroom:

$$F_b = K_p \cdot TSP_b \cdot y_b \quad (15)$$

Emission rate of phthalate from vinyl flooring in bathroom:

$$E_b = h_{m0}(y_0 - y_b) + v_d TSP_b \left(P_{dust,b0} - K_p y_b\right) \quad (16)$$

Partition process between the gas-phase and surface-phase phthalate concentrations on ith surface in bathroom:

$$\frac{dC_{surf,bi}}{dt} = h_m(y_b - y_{surf,bi}) \quad (17)$$

$$C_{surf,bi} = K_{bi} y_{surf,bi} \quad (18)$$

Accumulation of phthalate mass fraction on settled dust on adsorptive surfaces on ith surface in bathroom:

$$M_b \frac{dP_{dust,bi}}{dt} = v_d F_b - RM_b P_{dust,bi} \quad (19)$$

Phthalate mass fraction on settled dust on vinyl flooring in bathroom:

$$P_{dust,b0} = K_p y_0 \quad (20)$$

The accumulation of phthalate concentrations in the main house:

$$V_a \frac{dy_a}{dt} + V_a \frac{dF_a}{dt}$$
$$= Q_{oa}(y_{in} + F_{in}) - Q_{ao}(y_a + F_a) + Q_{ka}(y_k + F_k) - Q_{ak}(y_a + F_a)$$
$$+ Q_{ba}(y_b + F_b) - Q_{ab}(y_a + F_a)$$
$$- \sum_i \left(v_d F_k A_{a_i} + h_m A_{a_i}(y_a - y_{surf,ai}) - RM_{a_i} P_{dust,ai} A_{a_i}\right) \quad (21)$$

Partition relationship between the gas-phase and particle-phase phthalate concentrations in the main house:

$$F_a = K_p \cdot TSP_a \cdot y_a \quad (22)$$

Emission rate of phthalate from vinyl flooring in the main house:

$$E_a = h_{m0}(y_0 - y_a) + v_d TSP_a\left(P_{dust,a0} - K_p y_a\right) \quad (23)$$

Partition process between the gas-phase and surface-phase phthalate concentrations on ith surface in the main house:

$$\frac{dC_{surf,ai}}{dt} = h_m\left(y_a - y_{surf,ai}\right) \quad (24)$$

$$C_{surf,ai} = K_{ai} y_{surf,ai} \quad (25)$$

Accumulation of phthalate mass fraction on settled dust on adsorptive surfaces on ith surface in the main house:

$$M_a \frac{dP_{dust,ai}}{dt} = v_d F_a - RM_a P_{dust,ai} \quad (26)$$

Phthalate mass fraction on settled dust on vinyl flooring in the main house:

$$P_{dust,a0} = K_p y_0 \quad (27)$$

Model Input Parameters

Compartment	Kitchen	Bathroom	Main house
Volume (m^3)	35	15	128
Flow rate (m^3/h)	Q_{ok} 12	Q_{ob} 1.1	Q_{oa} 65
	Q_{ko} 32	Q_{bo} 2.1	Q_{ao} 44
	Q_{ak} 44	Q_{ab} 14	
	Q_{ka} 24	Q_{ba} 13	
Surface area (m^2)			
Vinyl flooring	14.4	6.20	19.2
Ceiling	14	6	51.2
Walls	20	17.3	72.8
Carpet	-	-	35.8
Wood floor	-	-	32.0
Furniture	12.6	5.40	61.4
Windows and mirrors	1.75	1.05	5.12
Tile and fixtures	3.50	16.5	20.0

Abbreviations: a. main house; b, bathroom; k, kitchen; o, outside.

Table E.S1: Input parameters for the three-compartment residential house.

Variable	Units	Value	References
Concentration at equilibrium with material-phase (y_0)	$\mu g/m^3$	2.30	Liang and Xu (2014a)
Air/wall partition coefficient of DEHP (K_{wall})	m	2500	Xu et al. (2009)
Air/glass partition coefficient (K_{win})	m	3800	Xu et al. (2009)
Air/wood floor partition coefficient (K_{wf})	m	2500	Xu et al. (2009)
Air/furniture partition coefficient (K_{fur})	m	2500	Xu et al. (2009)
Air/carpet partition coefficient (K_{ca})	m	1700	Xu et al. (2009)
DEHP vapor pressure at 25 °C (V_p)	Pa	1.0×10^{-4}	Liang and Xu (2014a)
DEHP Octanol/air partition coefficient (K_{oa})		3.4×10^{10}	Cousins and Mackay (2000)
Air/particle partition coefficient (K_p)	$m^3/\mu g$	0.064	Weschler et al. (2008)
Air velocity above source material	m/s	0.15	Huang et al. (2004)
Air velocity above adsorptive surfaces	m/s	0.15	Huang et al. (2004)

Table E.S2: Input parameters for the three-compartment residential model.

Variable	Units	Value	References
Concentration at equilibrium with material-phase (y_0)	μg/m^3	2.71	measured
Source surface are (A_0)	m^2	88	measured
Room height (H)	m	2.27	measured
Room volume (V)	m^3	250	measured
Air change rate (Ach)	1/h	0.5437	measured
Volumetric flow rate (Q)	m^3/h	135.93	measured
Interior surface area (A_s)	m^2	200.9	measured
Surface area of plate (A_p)	m^2	0.8	measured
Air/plate partition coefficient of BBP (K_{plate})	m	76.05	measured
Surface area of window (A_{win})	m^2	5.4	measured
Surface area of mirror (A_{mi})	m^2	1.68	measured
Air/window partition coefficient (K_{win})	m	120.0	measured
Air/mirror partition coefficient (K_{mi})	m	79.78	measured
Indoor total suspended particle concentration (TSP)	μg/m^3	3.76	measured
BBP vapor pressure at 21 °C (V_p)	Pa	3.6×10^{-5}	Liang and Xu (2014a)
Octanol/air partition coefficient (K_{oa})		6.0×10^{8}	Cousins and Mackay (2000)
Air/particle partition coefficient (K_p)	m^3/μg	1.1×10^{-3}	Weschler et al. (2008)
Air velocity above source material	m/s	0.01	Huang et al. (2004)
Air velocity above adsorptive surfaces	m/s	0.15	Huang et al. (2004)

Table E.S3: Input parameters for the UTest House.

Case Study

Surface-phase BBP concentration in UTest House. We compared the model predictions of surface-phase BBP concentrations with measured values on different interior surfaces (including plate and mirror) and the results are shown in Figure E.S1. The surface-phase BBP measurements were completed after the UTest House has been built for years, which we believe was sufficient to reach equilibrium in the house. Our model, on the other hand, simulates the UTest House environment with zero initial values of BBP concentrations in air and other indoor media.

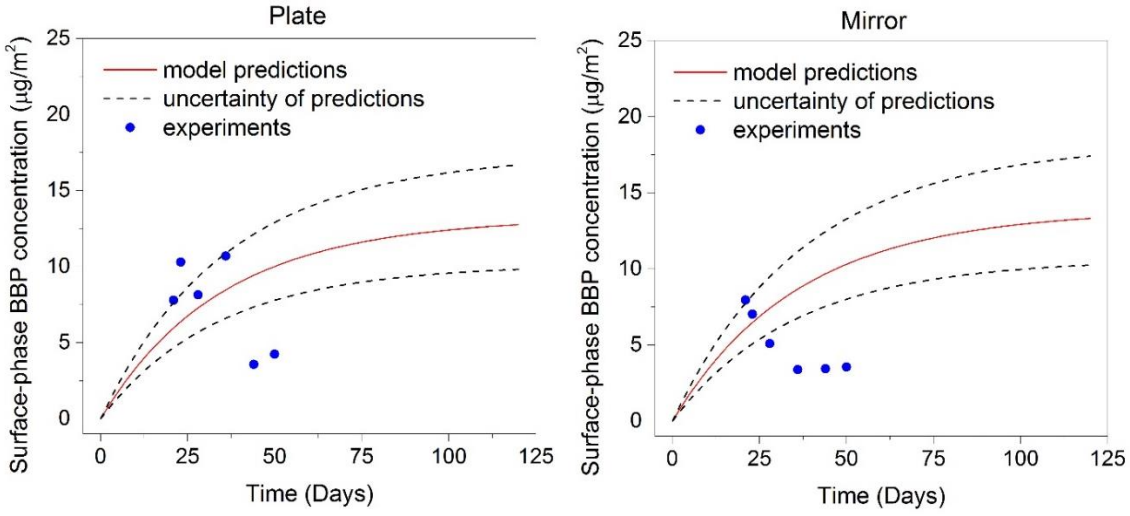

Figure E.S1: Comparison of surface-phase BBP concentrations on plate and mirror between model results and experimental data.

Three-compartment Residential Model.

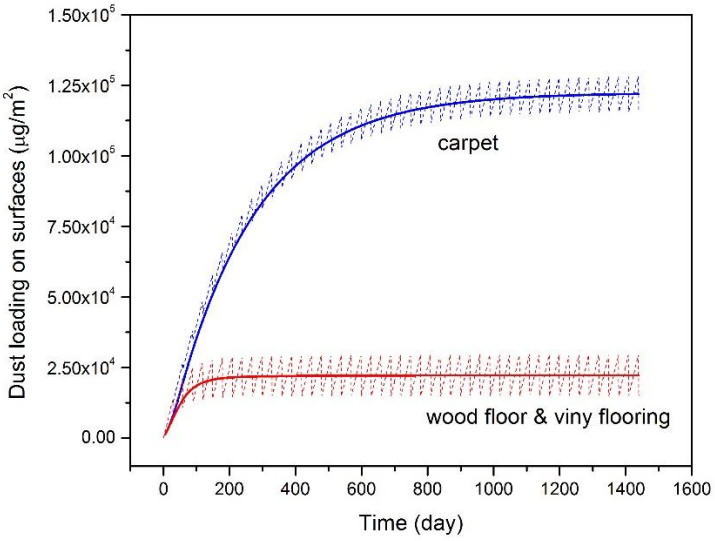

Figure E.S2: Dust loading on indoor surfaces.

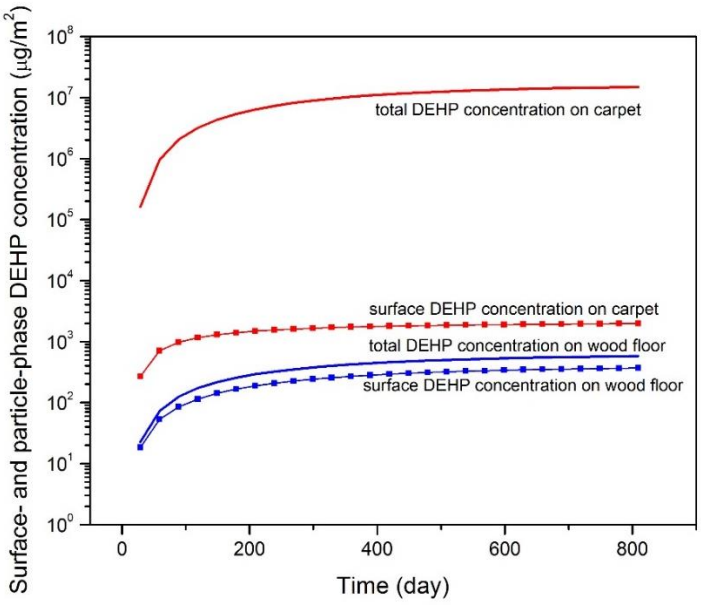

Figure E.S3: DEHP concentrations on wood floor and carpet.

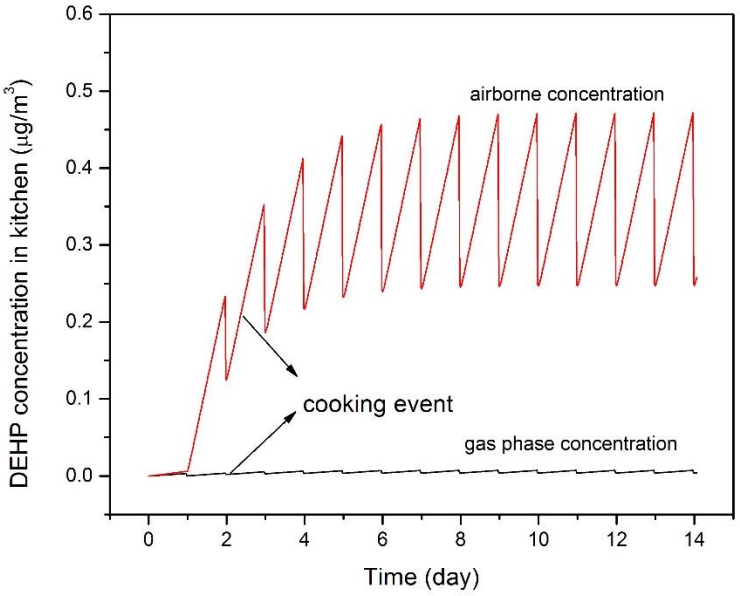

Figure E.S4: Influence of cooking on DEHP concentrations.

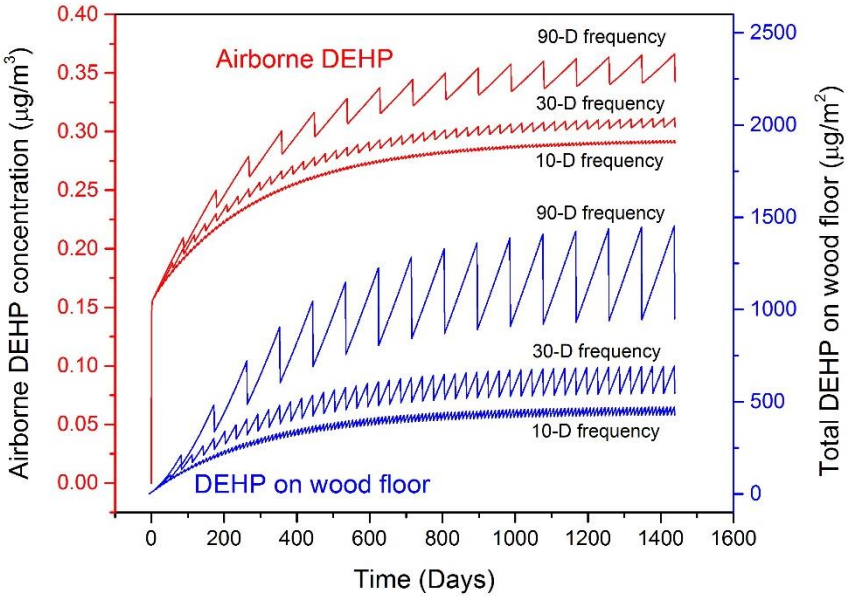

Figure E.S5: Influence of cleaning frequency on DEHP concentrations.

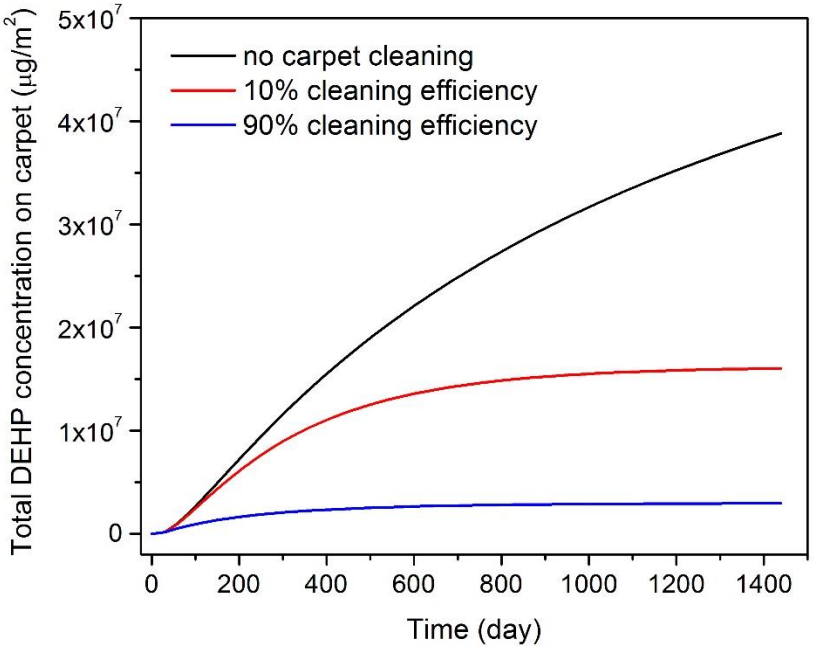

Figure E.S6: Influence of cleaning efficiency on DEHP concentrations on carpet.

References

Abb, M., Heinrich, T., Sorkau, E., Lorenz, W., 2009. Phthalates in house dust. Environment International 35, 965-970.

Adibi, J.J., Whyatt, R.M., Williams, P.L., Calafat, A.M., Camann, D., Herrick, R., Nelson, H., Bhat, H.K., Perera, F.A., Silva, M.J., Hauser, R., 2008. Characterization of phthalate exposure among pregnant women assessed by repeat air and urine samples. Environmental Health Perspectives 116, 467-473.

Adunola, A.O., 2014. Evaluation of urban residential thermal comfort in relation to indoor and outdoor air temperatures in Ibadan, Nigeria. Building and Environment 75, 190-205.

Afshari, A., Gunnarsen, L., Clausen, P.A., Hansen, V., 2004. Emission of phthalates from PVC and other materials. Indoor Air 14, 120-128.

Albert, O., Jegou, B., 2014. A critical assessment of the endocrine susceptibility of the human testis to phthalates from fetal life to adulthood. Human Reproduction Update 20, 231-249.

Alcock, R.E., MacGillivray, B.H., Busby, J.S., 2011. Understanding the mismatch between the demands of risk assessment and practice of scientists - The case of Deca-BDE. Environment International 37, 216-225.

Allen, J.G., McClean, M.D., Stapleton, H.M., Nelson, J.W., Webster, T.F., 2007. Personal exposure to Polybrominated Diphenyl Ethers (PBDEs) in residential indoor air. Environmental Science & Technology 41, 4574-4579.

Alshitawi, M., Awbi, H., Mahyuddin, N., 2009. Particulate matter mass concentration (PM10) under different ventilation methods in classrooms. International Journal of Ventilation 8, 93-108.

ASHRAE, 2004. Thermal environmental conditions for human occupancy, American Society of Heating, Refrigerating and Air-Conditioning Engineers (ASHRAE) Standard 55-2004.

BASF, Physical-chemical proterties of di-(2-ethylhexyl)adipate (DEHA), 2013b. Available at: http://www.weichmacher.basf.com/portal/load/fid247471/Plast_DOA_e_09_13.pdf. (Sep. 24, 2014).

BASF, Physical-chemical proterties of diisononyl cyclohexane-1,2-dicarboxylate, 2013a. Available at: http://www.plasticizers.basf.com/portal/load/fid247503/Hex_DINCH_e_09_13.pdf. (Sep. 24, 2014).

Becker, K., Seiwert, M., Angerer, J., Heger, W., Koch, H.M., Nagorka, R., Rosskamp, E., Schluter, C., Seifert, B., Ullrich, D., 2004. DEHP metabolites in urine of children

and DEHP in house dust. International Journal of Hygiene and Environmental Health 207, 409-417.

Becker, K., Seiwert, M., Kaus, S., Krause, C., Schultz, C., Seifert, B., 2002. German environmental survey 1998 (GerES III): pesticides and other pollutants in house dust, Proceedings of the 9th International Conference on Indoor Air Quality and Climate, pp. 883-887.

Bennett, D.H., Furtaw, E.J., 2004. Fugacity-based indoor residential pesticide fate model (vol 38, pg 2142, 2004). Environmental Science & Technology 38, 4912-4912.

Benning, J.L., Liu, Z., Tiwari, A., Little, J.C., Marr, L.C., 2013. Characterizing Gas-Particle Interactions of Phthalate Plasticizer Emitted from Vinyl Flooring. Environmental Science & Technology 47, 2696-2703.

Bergh, C., Aberg, K.M., Svartengren, M., Emenius, G., Ostman, C., 2011a. Organophosphate and phthalate esters in indoor air: a comparison between multi-storey buildings with high and low prevalence of sick building symptoms. Journal of Environmental Monitoring 13, 2001-2009.

Bergh, C., Torgrip, R., Emenius, G., Ostman, C., 2011b. Organophosphate and phthalate esters in air and settled dust - a multi-location indoor study. Indoor Air 21, 67-76.

Birnbaum, L.S., Staskal, D.F., Diliberto, J.J., 2003. Health effects of polybrominated dibenzo-p-dioxins (PBDDs) and dibenzofurans (PBDFs). Environment International 29, 855-860.

Boor, B.E., Jarnstrom, H., Novoselac, A., Xu, Y., 2014a. Infant Exposure to Emissions of Volatile Organic Compounds from Crib Mattresses. Environmental Science & Technology 48, 3541-3549.

Boor, B.E., Liang, Y., Crain, N., Xu, Y., 2014b. Identification of Plasticizers and Flame Retardants in Infant Crib Mattresses, Environmental Science & Technology Letters.

Bornehag, C.G., Lundgren, B., Weschler, C.J., Sigsgaard, T., Hagerhed-Engman, L., Sundell, J., 2005. Phthalates in indoor dust and their association with building characteristics. Environmental Health Perspectives 113, 1399-1404.

Bornehag, C.G., Nanberg, E., 2010. Phthalate exposure and asthma in children. International Journal of Andrology 33, 333-345.

Bornehag, C.G., Sundell, J., Weschler, C.J., Sigsgaard, T., Lundgren, B., Hasselgren, M., Hagerhed-Engman, L., 2004. The association between asthma and allergic symptoms in children and phthalates in house dust: A nested case-control study. Environmental Health Perspectives 112, 1393-1397.

Butte, W., Hoffmann, W., Hostrup, O., Schmidt, A., Walker, G., 2001. Endocrine disrupting chemicals in house dust: results of a representative monitoring. Gefahrstoffe Reinhaltung Der Luft 61, 19-23.

Butte, W., Hostrup, O., Walker, G., 2008. Phthalate im Hausstaub und in der Luft: assoziationen und mögliche quellen in wohnräumen. Gefahrstoffe Reinhalt Luft [in German] 68, 79-81.

Cadogan, D.F., Howick, C.J., 1996. Plasticizers, Kirk-Othmer encyclopedia of chimical technology, 4th ed. John Wiley and Sons, New York, NY, pp. 258-290.

Calafat, A.M., McKee, R.H., 2006. Integrating biomonitoring exposure data into the risk assessment process: Phthalates diethyl phthalate and di(2-ethylhexyl) phthalate as a case study. Environmental Health Perspectives 114, 1783-1789.

Clausen, P.A., Hansen, V., Gunnarsen, L., Afshari, A., Wolkoff, P., 2004. Emission of Di-2-ethylhexyl phthalate from PVC flooring into air and uptake in dust: Emission and sorption experiments in FLEC and CLIMPAQ. Environmental Science & Technology 38, 2531-2537.

Clausen, P.A., Lindeberg Bille, R.L., Nilsson, T., Hansen, V., Svensmark, B., Bøwadt, S., 2003. Simultaneous extraction of di(2-ethylhexyl) phthalate and nonionic surfactants from house dust: Concentrations in floor dust from 15 Danish schools. Journal of Chromatography A 986, 179-190.

Clausen, P.A., Liu, Z., Kofoed-Sorensen, V., Little, J., Wolkoff, P., 2012. Influence of Temperature on the Emission of Di-(2-ethylhexyl)phthalate (DEHP) from PVC Flooring in the Emission Cell FLEC. Environmental Science & Technology 46, 909-915.

Clausen, P.A., Liu, Z., Xu, Y., Kofoed-Sorensen, V., Little, J.C., 2010. Influence of air flow rate on emission of DEHP from vinyl flooring in the emission cell FLEC: Measurements and CFD simulation. Atmospheric Environment 44, 2760-2766.

Clausen, P.A., Xu, Y., Kofoed-Sorensen, V., Little, J.C., Wolkoff, P., 2007. The influence of humidity on the emission of di-(2-ethylhexyl) phthalate (DEHP) from vinyl flooring in the emission cell "FLEC". Atmospheric Environment 41, 3217-3224.

Corsi, R., Crain, N., Fardal, J., Little, J., Xu, Y., 2007. Determination of Sorption Parameters for 36 VOC/Material Combinations, Final EPA Report.

Cousins, I., Mackay, D., Parkerton, T., 2003. Physical-Chemical Properties and Evaluative Fate Modelling of Phthalate Esters, in: Staples, C. (Ed.), Series Anthropogenic Compounds. Springer Berlin Heidelberg, pp. 57-84.

Cox, S.S., Little, J.C., Hodgson, A.T., 2001. Measuring concentrations of volatile organic compounds in vinyl flooring. Journal of the Air & Waste Management Association 51, 1195-1201.

Cox, S.S., Little, J.C., Hodgson, A.T., 2002. Predicting the emission rate of volatile organic compounds from vinyl flooring. Environmental Science & Technology 36, 709-714.

Darnerud, P.O., 2003. Toxic effects of brominated flame retardants in man and in wildlife. Environment International 29, 841-853.

Deng, Q., Yang, X., Zhang, J., 2009. Study on a new correlation between diffusion coefficient and temperature in porous building materials. Atmospheric Environment 43, 2080-2083.

Dobruskin, V.K., Effect of Chemical Composition on Enthalpy of Evaporation and Equilibrium Vapor Pressure. Available at: http://arxiv.org/abs/1004.3400v1. (Sep 24, 2014).

Ekelund, M., Azhdar, B., Gedde, U.W., 2010. Evaporative loss kinetics of di(2-ethylhexyl)phthalate (DEHP) from pristine DEHP and plasticized PVC. Polymer Degradation and Stability 95, 1789-1793.

Ekelund, M., Azhdar, B., Hedenqvist, M.S., Gedde, U.W., 2008. Long-term performance of poly(vinyl chloride) cables, Part 2: Migration of plasticizer. Polymer Degradation and Stability 93, 1704-1710.

Engel, S.M., Wolff, M.S., 2013. Causal Inference Considerations for Endocrine Disruptor Research in Children's Health. Annual Review of Public Health, Vol 34, 139-158.

EPA, U.S., Integrated Risk Information System (IRIS), Available at: http://www.epa.gov/iris/ (Sep. 24, 2014).

EPA, U.S., 2005. A Pilot Study of Children's Total Exposure to Persistent Pesticides and Other Persistent Organic Pollutants (CTEPP).

Frederiksen, H., Aksglaede, L., Sorensen, K., Skakkebaek, N.E., Juul, A., Andersson, A.M., 2011. Urinary excretion of phthalate metabolites in 129 healthy Danish children and adolescents: Estimation of daily phthalate intake. Environmental Research 111, 656-663.

Frederiksen, M., Vorkamp, K., Thomsen, M., Knudsen, L.E., 2009. Human internal and external exposure to PBDEs - A review of levels and sources. International Journal of Hygiene and Environmental Health 212, 109-134.

French, L.J., Camilleri, M.J., Isaacs, N.P., Pollard, A.R., 2007. Temperatures and heating energy in New Zealand houses from a nationally representative study—HEEP. Energy and Buildings 39, 770-782.

Fromme, H., Lahrz, T., Piloty, M., Gebhart, H., Oddoy, A., Ruden, H., 2004. Occurrence of phthalates and musk fragrances in indoor air and dust from apartments and kindergartens in Berlin (Germany). Indoor Air 14, 188-195.

Fujii, M., Shinohara, N., Lim, A., Otake, T., Kumagai, K., Yanagisawa, Y., 2003. A study on emission of phthalate esters from plastic materials using a passive flux sampler. Atmospheric Environment 37, 5495-5504.

Gevao, B., Al-Ghadban, A.N., Bahloul, M., Uddin, S., Zafar, J., 2013. Phthalates in indoor dust in Kuwait: implications for non-dietary human exposure. Indoor Air 23, 126-133.

Gobble, C., Chickos, J., Verevkin, S.P., 2014. Vapor Pressures and Vaporization Enthalpies of a Series of Dialkyl Phthalates by Correlation Gas Chromatography. Journal of Chemical & Engineering Data 59, 1353-1365.

Gouin, T., Harner, T., 2003. Modelling the environmental fate of the polybrominated diphenyl ethers. Environment International 29, 717-724.

Gearhart, J., Posselt, H., 2014. Toxic At Any Speed: Chemicals in Cars and the Need for Safe Alternatives, http://www.ecocenter.org/healthy-stuff/toxic-any-speed-chemicals-cars-and-need-safe-alternatives.

Guo, Y., Kannan, K., 2011. Comparative Assessment of Human Exposure to Phthalate Esters from House Dust in China and the United States. Environmental Science & Technology 45, 3788-3794.

Haghighat, F., Hongyu, H., Chang-Seo, L., 2005. Modeling Approaches for Indoor Air VOC Emissions from Dry Building Materials--A Review. ASHRAE Transactions 111, 635-645.

Haghighat, F., Lee, C.S., Ghaly, W.S., 2002. Measurement of diffusion coefficients of VOCs for building materials: review and development of a calculation procedure. Indoor Air 12, 81-91.

Hansen, J.S., Larsen, S.T., Poulsen, L.K., Nielsen, G.D., 2007. Adjuvant effects of inhaled mono-2-ethylhexyl phthalate in BALB/cJ mice. Toxicology 232, 79-88.

Hao, J.M., Wang, L.T., 2005. Improving urban air quality in China: Beijing case study. Journal of the Air & Waste Management Association 55, 1298-1305.

Harrad, S., Hazrati, S., Ibarra, C., 2006. Concentrations of polychlorinated biphenyls in indoor air and polybrominated diphenyl ethers in indoor air and dust in Birmingham, United Kingdom: Implications for human exposure. Environmental Science & Technology 40, 4633-4638.

Hawkes, S.J., 1995. Raoults Law is a Deception. Journal of Chemical Education 72, 204-205.

Heudorf, U., Mersch-Sundermann, V., Angerer, E., 2007. Phthalates: Toxicology and exposure. International Journal of Hygiene and Environmental Health 210, 623-634.

Hodgson, A.T., Shendell, D.G., Fisk, W.J., Apte, M.G., 2004. Comparison of predicted and derived measures of volatile organic compounds inside four new relocatable classrooms. Indoor Air 14, 135-144.

Howard, P.H., Banerjee, S., Robillard, K.H., 1985. Meaasurement of Water Solubilities, Octanol Water Partition-coefficients and Vapor-pressures of Commercial Phthalate-esters. Environmental Toxicology and Chemistry 4, 653-661.

Hsu, N.Y., Lee, C.C., Wang, J.Y., Li, Y.C., Chang, H.W., Chen, C.Y., Bornehag, C.G., Wu, P.C., Sundell, J., Su, H.J., 2012. Predicted risk of childhood allergy, asthma, and reported symptoms using measured phthalate exposure in dust and urine. Indoor Air 22, 186-199.

Huang, J.M., Chen, Q., Ribot, B., Rivoalen, H., 2004. Modeling contaminant exposure in a single-family house. Indoor and Built Environment 13, 5-19.

Huang, P.C., Liou, S.H., Ho, I.K., Chiang, H.C., Huang, H.I., Wang, S.L., 2012. Phthalates Exposure and Endocrinal Effects: An Epidemiological Review. Journal of Food and Drug Analysis 20, 719-733.

Hunt, D.R.G., Gidman, M.I., 1982. A national field survey of house temperatures. Building and Environment 17, 107-124.

Hwang, H.-M., Park, E.-K., Young, T.M., Hammock, B.D., 2008. Occurrence of endocrine-disrupting chemicals in indoor dust. Science of The Total Environment 404, 26-35.

Jaakkola, J.J.K., Ieromnimon, A., Jaakkola, M.S., 2006. Interior surface materials and asthma in adults: A population-based incident case-control study. American Journal of Epidemiology 164, 742-749.

Jaakkola, J.J.K., Knight, T.L., 2008. The role of exposure to phthalates from polyvinyl chloride products in the development of asthma and allergies: A systematic review and meta-analysis. Environmental Health Perspectives 116, 845-853.

Jaakkola, J.J.K., Oie, L., Nafstad, P., Botten, G., Samuelsen, S.O., Magnus, P., 1999. Interior surface materials in the home and the development of bronchial obstruction in young children in Oslo, Norway. American Journal of Public Health 89, 188-192.

Jaakkola, J.J.K., Parise, H., Kislitsin, V., Lebedeva, N.I., Spengler, J.D., 2004. Asthma, wheezing, and allergies in Russian schoolchildren in relation to new surface materials in the home. American Journal of Public Health 94, 560-562.

Jurewicz, J., Polanska, K., Hanke, W., 2013. Exposure to widespread environmental toxicants and children's cognitive development and behavioral problems. International Journal of Occupational Medicine and Environmental Health 26, 185-204.

Kanazawa, A., Saito, I., Araki, A., Takeda, M., Ma, M., Saijo, Y., Kishi, R., 2010. Association between indoor exposure to semi-volatile organic compounds and building-related symptoms among the occupants of residential dwellings. Indoor Air 20, 72-84.

Kato, T., Tada-Oikawa, S., Takahashi, K., Saito, K., Wang, L., Nishio, A., Hakamada-Taguchi, R., Kawanishi, S., Kuribayashi, K., 2006. Endocrine disruptors that deplete glutathione levels in APC promote Th2 polarization in mice leading to the exacerbation of airway inflammation. European Journal of Immunology 36, 1199-1209.

Kawamura, A., Kim, H., Tanabe, S., Yuka, I., 2011. Emission rate measurement of semi-volatile organic compounds (SVOC) from building materials with Micro chamber, The 12th International Conference on Indoor AIr Quality and Climate, Austin, TX.

Kay, V.R., Chambers, C., Foster, W.G., 2013. Reproductive and developmental effects of phthalate diesters in females. Critical Reviews in Toxicology 43, 200-219.

Kersten, W., Reich, T., 2003. Schwerfluchtige organische umweltchemikalien in Hamburger hausstäben. Gefahrstoffe Reinhaltung Der Luft [in German] 63, 85-91.

Koch, H.M., Drexler, H., Angerer, J., 2003. An estimation of the daily intake of di(2-ethylhexyl)phthalate (DEHP) and other phthalates in the general population. International Journal of Hygiene and Environmental Health 206, 77-83.

Kolarik, B., Bornehag, C.G., Naydenov, K., Sundell, J., Stavova, P., Nielsen, O.F., 2008. The concentrations of phthalates in settled dust in Bulgarian homes in relation to building characteristic and cleaning habits in the family. Atmospheric Environment 42, 8553-8559.

Kumar, D., Little, J., 2003. Single-layer model to predict the source/sink behavior of diffusion-controlled building materials. Environmental Science & Technology 37, 3821-3827.

Lagercrantz, L., Famula, B., Sundell, J., 2005. Nitric oxide in exhaled and aspirated nasal air as an objective measure of human response to isopropanol oxidation products and pthtalate esters in indoor air.

Lai, A.C.K., 2002. Particle deposition indoors: a review. Indoor Air 12, 211-214.

Langer, S., Weschler, C.J., Fischer, A., Beko, G., Toftum, J., Clausen, G., 2010. Phthalate and PAH concentrations in dust collected from Danish homes and daycare centers. Atmospheric Environment 44, 2294-2301.

Long, C.M., Suh, H.H., Catalano, P.J., Koutrakis, P., 2001. Using time- and size-resolved particulate data to quantify indoor penetration and deposition behavior. Environmental Science & Technology 35, 2089-2099.

Larsen, S.T., Hansen, J.S., Hammer, M., Alarie, Y., Nielsen, G.D., 2004. Effects of mono-2-ethylhexyl phthalate on the respiratory tract in BALB/c mice. Human & Experimental Toxicology 23, 537-545.

Larsen, S.T., Hansen, J.S., Hansen, E.W., Clausen, P.A., Nielsen, G.D., 2007. Airway inflammation and adjuvant effect after repeated airborne exposures to di-(2-ethylhexyl)phthalate and ovalbumin in BALB/c mice. Toxicology 235, 119-129.

Latini, G., Del Vecchio, A., Massaro, M., Verrotti, A., De Felice, C., 2006. Phthalate exposure and male infertility. Toxicology 226, 90-98.

Laverge, J., Novoselac, A., Corsi, R., Janssens, A., 2013. Experimental assessment of exposure to gaseous pollutants from mattresses and pillows while asleep. Building and Environment 59, 203-210.

Legler, J., Brouwer, A., 2003. Are brominated flame retardants endocrine disruptors? Environment International 29, 879-885.

Letcher, T.M., Naicker, P.K., 2004. Determination of vapor pressures using gas chromatography. Journal of Chromatography A 1037, 107-114.

Liang, Y., Xu, Y., 2014b. Emission of Phthalates and Phthalate Alternatives from Vinyl Flooring and Crib Mattress Covers: The Influence of Temperature. Environmental Science & Technology.

Liang, Y., Xu, Y., 2014a. Improved Method for Measuring and Characterizing Phthalate Emissions from Building Materials and Its Application to Exposure Assessment. Environmental Science & Technology 48, 4475-4484.

Liang, Y., Xu, Y., 2014c. The Influence of Surface Sorption and Air Flow Rate on Phthalate Emissions from Vinyl Flooring: Measurement and Modeling. Atmospheric Environment.

Little, J.C., Hodgson, A.T., Gadgil, A.J., 1994. Modeling Emissions of Volative Organic-compounds from New Carpets. Atmospheric Environment 28, 227-234.

Little, J.C., Weschler, C.J., Nazaroff, W.W., Liu, Z., Hubal, E.A.C., 2012. Rapid Methods to Estimate Potential Exposure to Semivolatile Organic Compounds in the Indoor Environment. Environmental Science & Technology 46, 11171-11178.

Liu, C., Morrison, G.C., Zhang, Y.P., 2012. Role of aerosols in enhancing SVOC flux between air and indoor surfaces and its influence on exposure. Atmospheric Environment 55, 347-356.

Liu, C., Shi, S.S., Weschler, C., Zhao, B., Zhang, Y.P., 2013. Analysis of the Dynamic Interaction Between SVOCs and Airborne Particles. Aerosol Science and Technology 47, 125-136.

Liu, C., Zhang, Y., Benning, J.L., Little, J.C., 2014a. The effect of ventilation on indoor exposure to semivolatile organic compounds. Indoor Air, n/a-n/a.

Liu, C., Zhang, Y., Weschler, C.J., 2014b. The impact of mass transfer limitations on size distributions of particle associated SVOCs in outdoor and indoor environments. Science of The Total Environment 497–498, 401-411.

Liu, C., Zhao, B., Zhang, Y., 2010. The influence of aerosol dynamics on indoor exposure to airborne DEHP. Atmospheric Environment 44, 1952-1959.

Liu, X., Guo, Z., Roache, N.F., 2014c. Experimental method development for estimating solid-phase diffusion coefficients and material/air partition coefficients of SVOCs. Atmospheric Environment 89, 76-84.

Lyman, W.J., Reehl, W.F., Rosenblatt, D.H., 1990. Handbook of chemical property estimation methods: environmental behavior of organic compounds. American Chemistry Society, Washington, DC.

Mathworks, T., Pitfalls in Fitting Nonlinear Models by Transforming to Linearity. Available at: http://www.mathworks.com/help/stats/pitfalls-in-fitting-nonlinear-models-by-transforming-to-linearity.html. (Sep 24, 2014).

Matsumoto, M., Hirata-Koizumi, M., Ema, M., 2008. Potential adverse effects of phthalic acid esters on human health: A review of recent studies on reproduction. Regulatory Toxicology and Pharmacology 50, 37-49.

McKee, R.H., Butala, J.H., David, R.M., Gans, G., 2004. NTP center for the evaluation of risks to human reproduction reports on phthalates: addressing the data gaps. Reproductive Toxicology 18, 1-22.

Meeker, J.D., Johnson, P.I., Camann, D., Hauser, R., 2009. Polybrominated diphenyl ether (PBDE) concentrations in house dust are related to hormone levels in men. Science of the Total Environment 407, 3425-3429.

Meerts, I., van Zanden, J.J., Luijks, E.A.C., van Leeuwen-Bol, I., Marsh, G., Jakobsson, E., Bergman, A., Brouwer, A., 2000. Potent competitive interactions of some brominated flame retardants and related compounds with human transthyretin in vitro. Toxicological Sciences 56, 95-104.

Nagorka, R., Scheller, C., Ullrich, D., 2005. Weichmacher im Hausstaub. Gefahrstoffe Reinhalt Luft [in German] 115, 484-491.

Nazaroff, W., Weschler, C.J., Little, J.C., Hubal, E.A.C., 2012. Intake to Production Ratio: A Measure of Exposure Intimacy for Manufactured Chemicals. Environmental Health Perspectives 120, 1678-1683.

Nicholson, J.W., Royal Society of, C., 2006. The chemistry of polymers. Royal Society of Chemistry, Cambridge, UK.

North, M.L., Takaro, T.K., Diamond, M.L., Ellis, A.K., 2014. Effects of phthalates on the development and expression of allergic disease and asthma. Ann. Allergy Asthma Immunol. 112, 496-502.

Odum, J.R., Yu, J., Kamens, R.M., 1994. Modeling the Mass Transfer of Semivolatile Organics in Combustion Aerosols. Environmental Science & Technology 28, 2278-2285.

Oie, L., Hersoug, L.G., Madsen, J.O., 1997. Residential exposure to plasticizers and its possible role in the pathogenesis of asthma. Environmental Health Perspectives 105, 972-978.

Otake, T., Yoshinaga, J., Yanagisawa, Y., 2004. Exposure to phthalate esters from indoor environment. Journal of Exposure Analysis and Environmental Epidemiology 14, 524-528.

Park, J.S., She, J.W., Holden, A., Sharp, M., Gephartg, R., Souders-Mason, G., Zhang, V., Chow, J., Leslie, B., Hooper, K., 2011. High Postnatal Exposures to Polybrominated Diphenyl Ethers (PBDEs) and Polychlorinated Biphenyls (PCBs) via Breast Milk in California: Does BDE-209 Transfer to Breast Milk? Environmental Science & Technology 45, 4579-4585.

Pei, X.Q., Song, M., Guo, M., Mo, F.F., Shen, X.Y., 2013. Concentration and risk assessment of phthalates present in indoor air from newly decorated apartments. Atmospheric Environment 68, 17-23.

Raja, I.A., Nicol, J.F., McCartney, K.J., Humphreys, M.A., 2001. Thermal comfort: use of controls in naturally ventilated buildings. Energy and Buildings 33, 235-244.

Rim, D., Novoselac, A., 2009. Transport of particulate and gaseous pollutants in the vicinity of a human body. Building and Environment 44, 1840-1849.

Ritter, L., Arbucklet, T.E., 2007. Can exposure characterization explain concurrence of discordance between toxicology and epidemiology? Toxicological Sciences 97, 241-252.

Rudel, R.A., Camann, D.E., Spengler, J.D., Korn, L.R., Brody, J.G., 2003. Phthalates, alkylphenols, pesticides, polybrominated diphenyl ethers, and other endocrine-disrupting compounds in indoor air and dust. Environmental Science & Technology 37, 4543-4553.

Rudel, R.A., Dodson, R.E., Perovich, L.J., Morello-Frosch, R., Camann, D.E., Zuniga, M.M., Yau, A.Y., Just, A.C., Brody, J.G., 2010. Semivolatile Endocrine-Disrupting Compounds in Paired Indoor and Outdoor Air in Two Northern California Communities. Environmental Science & Technology 44, 6583-6590.

Rudel, R.A., Perovich, L.J., 2009. Endocrine disrupting chemicals in indoor and outdoor air. Atmospheric Environment 43, 170-181.

Santillo, D., Labunska, I., Fairley, M., Johnston, P., 2003. Hazardous chemicals in house dusts as indicators of chemical exposure in the home, Greenpeace Research Laboratories Technical Note 02/2003 (GRL-TN-02-2003).

Schossler, P., Schripp, T., Salthammer, T., Bahadir, M., 2011. Beyond phthalates: Gas phase concentrations and modeled gas/particle distribution of modern plasticizers. Science of the Total Environment 409, 4031-4038.

Schripp, T., Salthammer, T., Fauck, C., Bekö, G., Weschler, C.J., 2014. Latex paint as a delivery vehicle for diethylphthalate and di-n-butylphthalate: Predictable boundary layer concentrations and emission rates. Science of the Total Environment 494, 299-305.

Schwarzenbach, R.P., Gschwend, P.M., Imboden, D.M., 2003. Environmental organic chemistry. Wiley-Interscience.

Shi, S., Zhao, B., 2012. Comparison of the predicted concentration of outdoor originated indoor polycyclic aromatic hydrocarbons between a kinetic partition model and a linear instantaneous model for gas–particle partition. Atmospheric Environment 59, 93-101.

Silva, M.J.B., D. B., Reidy, J. A.; Malek, N. A.; Hodge, C. C.; Caudill, S. P.; Brock, J. W.; Needham, L. L. and Calafat, A. M., 2004. Urinary Levels of Seven Phthalate Metabolites in the U.S. Population from the National Health and Nutrition Examination Survey (NHANES) 1999–2000. Environmental Health Perspectives 112.

Smits, A.J., Dussauge, J.P., 2006. Turbulent Shear Layers in Supersonic Flow. Springer.

Stapleton, H.M., Harner, T., Shoeib, M., Keller, J.M., Schantz, M.M., Leigh, S.D., Wise, S.A., 2006. Determination of polybrominated diphenyl ethers in indoor dust standard reference materials. Analytical and Bioanalytical Chemistry 384, 791-800.

Thatcher, T.L., Layton, D.W., 1995. Deposition, resuspension, and penetration of particles within a residence. Atmospheric Environment 29, 1487-1497.

Thuresson, K., Bjorklund, J.A., de Wit, C.A., 2012. Tri-decabrominated diphenyl ethers and hexabromocyclododecane in indoor air and dust from Stockholm microenvironments 1: Levels and profiles. Science of the Total Environment 414, 713-721.

U.S. Consumer Production Safety Commission (CPSC), 2008. Consumer Product Safety Improvement Act (CPSIA) of 2008, Bethesda, Maryland.

Vonderheide, A.P., Mueller, K.E., Meija, J., Welsh, G.L., 2008. Polybrominated diphenyl ethers: Causes for concern and knowledge gaps regarding environmental distribution, fate and toxicity. Science of the Total Environment 400, 425-436.

Vorkamp, K., Thomsen, M., Frederiksen, M., Pedersen, M., Knudsen, L.E., 2011. Polybrominated diphenyl ethers (PBDEs) in the indoor environment and associations with prenatal exposure. Environment International 37, 1-10.

Wang, X.K., Xu, Y., Liu, G., 2011. A study of phthalate concentration distribution in indoor environment, Indoor Air, Austin, TX.

Wensing, M., Uhde, E., Salthammer, T., 2005. Plastics additives in the indoor environment - flame retardants and plasticizers. Science of the Total Environment 339, 19-40.

Weschler, C.J., 2003. Indoor/outdoor connections exemplified by processes that depend on an organic compound's saturation vapor pressure. Atmospheric Environment 37, 5455-5465.

Weschler, C.J., 2009. Changes in indoor pollutants since the 1950s. Atmospheric Environment 43, 153-169.

Weschler, C.J., Nazaroff, W.W., 2008. Semivolatile organic compounds in indoor environments. Atmospheric Environment 42, 9018-9040.

Weschler, C.J., Nazaroff, W.W., 2010. SVOC partitioning between the gas phase and settled dust indoors. Atmospheric Environment 44, 3609-3620.

Weschler, C.J., Nazaroff, W.W., 2013. Dermal Uptake of Organic Vapors Commonly Found in Indoor Air. Environmental Science & Technology 48, 1230-1237.

Weschler, C.J., Salthammer, T., Fromme, H., 2008. Partitioning of phthalates among the gas phase, airborne particles and settled dust in indoor environments. Atmospheric Environment 42, 1449-1460.

Wilkes, C.R., Small, M.J., Andelman, J.B., Giardino, N.J., Marshall, J., 1992. Inhalation exposure model for volatile chemicals from indoor uses of water. Atmospheric Environment. Part A. General Topics 26, 2227-2236.

Wilson, N.K., Chuang, J.C., Lyu, C., 2001. Levels of persistent organic pollutants in several child day care centers. Journal of Exposure Analysis and Environmental Epidemiology 11, 449-458.

Wilson, N.K., Chuang, J.C., Lyu, C., Menton, R., Morgan, M.K., 2003. Aggregate exposures of nine preschool children to persistent organic pollutants at day care and at home. Journal of Exposure Analysis & Environmental Epidemiology 13, 187.

Wilson, V.S., Lambright, C., Furr, J., Ostby, J., Wood, C., Held, G., Gray, L.E., 2004. Phthalate ester-induced gubernacular lesions are associated with reduced insl3 gene expression in the fetal rat testis. Toxicology Letters 146, 207-215.

Xiong, J., Zhang, Y., Wang, X., Chang, D., 2008. Macro–meso two-scale model for predicting the VOC diffusion coefficients and emission characteristics of porous building materials. Atmospheric Environment 42, 5278-5290.

Xiong, J.Y., Huang, S.D., Zhang, Y.P., 2012. A Novel Method for Measuring the Diffusion, Partition and Convective Mass Transfer Coefficients of Formaldehyde and VOC in Building Materials. Plos One 7.

Xu, X., Culligan, P.J., Taylor, J.E., 2014a. Energy Saving Alignment Strategy: Achieving energy efficiency in urban buildings by matching occupant temperature preferences with a building's indoor thermal environment. Applied Energy 123, 209-219.

Xu, Y., Hubal, E.A.C., Clausen, P.A., Little, J.C., 2009. Predicting Residential Exposure to Phthalate Plasticizer Emitted from Vinyl Flooring: A Mechanistic Analysis. Environmental Science & Technology 43, 2374-2380.

Xu, Y., Hubal, E.A.C., Little, J.C., 2010. Predicting Residential Exposure to Phthalate Plasticizer Emitted from Vinyl Flooring: Sensitivity, Uncertainty, and Implications for Biomonitoring. Environmental Health Perspectives 118, 253-258.

Xu, Y., Liang, Y., 2011. Indoor Residential Fate Model of Phthalate Plasticizers, Proceedings of the 10th International Conference of Healthy Buildings, Brisbane, Australia.

Xu, Y., Liang, Y., Urquidi, J.R., Siegel, J.A., 2014b. Phthalates and polybrominated diphenyl ethers in retail stores. Atmospheric Environment 87, 53-64.

Xu, Y., Little, J.C., 2006. Predicting emissions of SVOCs from polymeric materials and their interaction with airborne particles. Environmental Science & Technology 40, 456-461.

Xu, Y., Liu, Z., Park, J., Clausen, P.A., Benning, J.L., Little, J.C., 2012. Measuring and Predicting the Emission Rate of Phthalate Plasticizer from Vinyl Flooring in a Specially-Designed Chamber. Environmental Science & Technology 46, 12534-12541.

Xu, Y., Zhang, Y.P., 2003. An improved mass transfer based model for analyzing VOC emissions from building materials. Atmospheric Environment 37, 2497-2505.

Yang, G.T., Qiao, Y.K., Li, B., Yang, J.W., Liu, D.D., Yao, H.C., Xu, D.Q., Yang, X., 2008. Adjuvant effect of di-(2-ethylhexyl) phthalate on asthma-like pathological changes in ovalbumin-immunised rats. Food and Agricultural Immunology 19, 351-362.

Zhang, Q., Lu, X.M., Zhang, X.L., Sun, Y.G., Zhu, D.M., Wang, B.L., Zhao, R.Z., Zhang, Z.D., 2013. Levels of phthalate esters in settled house dust from urban dwellings with young children in Nanjing, China. Atmospheric Environment 69, 258-264.

Zhang, X.M., Diamond, M.L., Ibarra, C., Harrad, S., 2009. Multimedia Modeling of Polybrominated Diphenyl Ether Emissions and Fate Indoors. Environmental Science & Technology 43, 2845-2850.

Zhang, Y.P., Yang, R., Xu, Q.J., Mo, J.H., 2007. Characteristics of photocatalytic oxidation of toluene, benzene, and their mixture. Journal of the Air & Waste Management Association 57, 94-101.

Zhao, D.Y., Little, J.C., Cox, S.S., 2004. Characterizing polyurethane foam as a sink for or source of volatile organic compounds in indoor air. Journal of Environmental Engineering-Asce 130, 983-989.

Zuraimi, M.S., Roulet, C.A., Tham, K.W., Sekhar, S.C., David Cheong, K.W., Wong, N.H., Lee, K.H., 2006. A comparative study of VOCs in Singapore and European office buildings. Building and Environment 41, 316-329.

Vita

Yirui Liang was born in Hunan Province, China. He obtained his Bachelor of Engineering degree in the School of Architecture from Tsinghua University in June 2009. He entered graduate school in 2009, receiving his Master of Science degree in Architectural Engineering in 2010 from the University of Texas at Austin.

Permanent email: liangyirui AT gmail DOT com

This dissertation was typed by Yirui Liang.